AD699198

FOREIGN TECHNOLOGY DIVISION

HEAT TRANSFER AND RESISTANCE IN THE LAMINAR
FLOW OF LIQUIDS IN TUBES

By

B. S. Petukhov

D D C
JAN 21 1970
D

279

EDITED TRANSLATION

HEAT TRANSFER AND RESISTANCE IN THE LAMINAR FLOW OF
LIQUIDS IN TUBES

By: B. S. Petukhov

English Pages: 244 - 521

Source: Teploobmen i Soprotivleniye Pri Laminarnom
Techenii Zhidkosti V Trubakh (Heat Transfer
and Resistance in the Laminar Flow of Liquids in
Tubes). 1967, 1-411

Translated Under: F33657-68-D-0865-P002

DISCLAIMER NOTICE
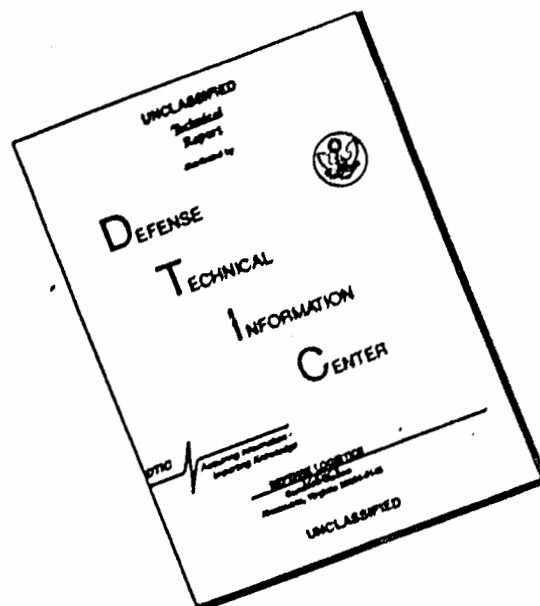
THIS DOCUMENT IS BEST QUALITY AVAILABLE. THE COPY FURNISHED TO DTIC CONTAINED A SIGNIFICANT NUMBER OF PAGES WHICH DO NOT REPRODUCE LEGIBLY.

Chapter 10

INFLUENCE OF HEAT CONDUCTION ALONG AXIS ON HEAT EXCHANGE IN TUBES

10-1. PRELIMINARY REMARKS

In heat-exchange problems for tubes, we ordinarily assume that the change in heat-flux density caused by heat conduction along the axis is small in comparison with the radial variation. In other words, we neglect heat transferred by conduction in the axial direction. In most cases, this assumption is justified in practice. It can lead to significant errors, however, if the number Pe (x/d) is small (see §6-1). Such conditions are encountered, for example, for heat exchange with a flow of liquid metals (since Pr is small, Pe is also small) and for ordinary liquids in direct proximity to the entrance (x/d small). Thus determination of heat exchange with allowance for heat conduction near the axis is of both theoretical and practical interest.

Neglect of axial heat conduction significantly simplifies determination of heat exchange, since here the sole mechanism for transfer of heat along the axis is convective. Thus any "thermal disturbance" appearing in the flow can only move downstream with the velocity at which the fluid moves. Here the temperature field in a certain flow section will depend on the temperature fields (and the velocity fields) in the preceding sections alone. If we allow for the heat conduction caused by the axial temperature gradients, then the "thermal disturbance" will not only be carried along by the moving fluid, but will also propagate upstream. Under these conditions, naturally, the temperature field in the given flow section will depend on the temperature fields in both preceding and succeeding sections.

This feature of heat-exchange processes considered with allowance for axial heat conduction substantially complicates the calculations, since it is necessary to allow for the relationships among heat-exchange processes in different parts of the tube: the stilling segment, heating segment, and exit segment (i.e., the segment following the heating portion). Here the stilling segment will not be isothermal. Owing to upstream transport of heat by conduction, a nonuniform temperature field appears in the stilling segment; it is connected with the temperature field in the heating segment. Thus only a few heat-exchange problems can be solved with allowance for axial heat conduction.

10-2. LIMITING NUSSELT NUMBER IN ROUND AND FLAT TUBES

Let us consider the heat-exchange process far from the entrance in the heating segment of a tube, allowing for axial heat conduction for two types of boundary conditions: constant wall temperature (t_s = const) and constant heat-flux density at the wall (q_s = const).

Since the heat-exchange process is investigated far from the tube entrance, i.e., for large X, the boundary conditions at the entrance cross section will naturally be eliminated. If we assume that the tube extends to infinity, there will also be no boundary conditions specified at the exit cross section. All remaining conditions are the same as in §§6-1 and 8-1.

Taking the foregoing conditions into account, with allowance for heat conduction along the axis, we can write the energy equation for the flow in a round tube as follows:

$$\frac{\partial^2 \theta}{\partial R^2} + \frac{1}{R}\frac{\partial \theta}{\partial R} + \frac{1}{Pe^2}\frac{\partial^2 \theta}{\partial X^2} = (1-R^2)\frac{\partial \theta}{\partial X}. \qquad (10\text{-}1)$$

where

$$R = \frac{r}{r_0}; \quad Y = \frac{2}{Pe}\cdot\frac{x}{d}; \quad Pe = \frac{\bar{w}d}{a}$$

As we can see from (10-1), here the temperature depends not only on R and X, but also on Pe, which appears together with a term allowing for the heat conduction along the axis. When Pe → ∞, this term vanishes and (10-1) goes over to (6-2).

1. We first investigate heat exchange in a round tube when t_s = const, a case considered by D.L. Labuntsov [1] and others [2]. Here it is convenient to replace t by the temperature $\vartheta = t - t_c$. This substitution does not change (10-1). The boundary condition at the wall has the form

$$\vartheta = 0 \text{ for } R = 1. \qquad (10\text{-}2)$$

We seek a particular solution for ϑ in the form

$$\vartheta = A\varphi(R)\exp(-\beta X).$$

Substituting this expression into (10-1), we obtain

$$\varphi''(R) + \frac{1}{R}\varphi'(R) + \left[\beta(1-R^2) + \left(\frac{\beta}{Pe}\right)^2\right]\varphi(R) = 0.$$

As usual, we represent the function $\varphi(R)$ as an infinite power series:

$$\varphi(R) = \sum_{m=0}^{\infty} b_m R^m.$$

Determining the series coefficients from the preceding equation,

we obtain the recursion relationships

$$b_0 = 1,$$

$$b_2 = -b_0 \frac{1 + \left(\frac{\beta}{Pe}\right)^2}{2^2},$$

$$b_4 = -b_2 \frac{1 + \left(\frac{\beta}{Pe}\right)^2}{4^2} + b_0 \frac{\beta}{4^2},$$

$$\cdots \cdots \cdots \cdots \cdots \cdots$$

$$b_m = -b_{m-2} \frac{1 + \left(\frac{\beta}{Pe}\right)^2}{m^2} + b_{m-4} \frac{\beta}{m^2},$$

where m takes on even values (0, 2, 4 ...).

From boundary condition (10-2) it follows that $\psi(1) = 0$; satisfying this condition, we obtain a relationship for determining the eigenvalues β_i:

$$\sum_{m=0}^{\infty} b_m (\beta_i Pe) = 0.$$

This equation has an infinity of roots, i.e., there is an infinitely increasing sequence of eigenvalues $\beta_i(Pe)$ $(i = 1, 2, 3 ...)$ corresponding to the eigenfunctions $\psi_i(R, Pe)$.

Thus the general solution of the problem has the form

$$\theta = \sum_{i=1}^{\infty} A_i \psi_i(R, Pe) \exp[-\beta_i(Pe) X]. \tag{10-3}$$

It is clear from the structure of (10-3) that in the heat-exchange problem, when t_s = const and allowance is made for axial heat conduction, temperature-field stabilization will also set in . Thus when X is sufficiently large, the temperature distribution will be described by the first term of Series (10-3), while the local Nu number, determined in the usual manner, will cease to depend on tube length.

The limiting value of Nu is

$$Nu_{\infty} = -\frac{2}{\bar{\theta}} \left(\frac{\partial \theta}{\partial R}\right)_{R=1} = 2 \frac{\psi'_1(1, Pe)}{\bar{\psi}_1(Pe)}. \tag{10-4}$$

Here $\bar{\theta} = 4 \int_0^1 \theta(1 - R^2) R \, dR$ is the mean mass temperature of the fluid in the given cross section; $\bar{\psi}_1(Pe)$ is the value of the function $\psi_1(R, Pe)$, averaged in accordance with the same law.

TABLE 10-1

Value of Nu_∞ for Round Tube with t_s = const

Pe	1.0	3.16	10	31.6	100 и более 1
β_1	2.045	4.625	6.75	7.28	7.315
Nu_∞	4.04	3.86	3.74	3.68	3.66

1) or more.

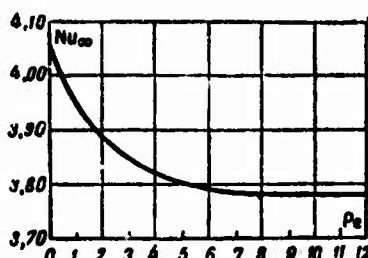Fig. 10-1. Dependence of Nu_∞ =
= $\alpha_\infty h/\lambda$ on Pe = $\bar{w}h/a$ for a flat
tube with t_s = const.

It follows from (10-4) that when we allow for the axial heat
conduction, the limiting value of Nu_∞ for our problem will depend
on Pe. This relationship has been determined elsewhere [1] by cal-
culation of β_1 and Nu_∞ for various values of Pe. The results are
shown in Table 10-1.

A different method has been used to estimate the limiting
values of Nu_∞ for a flat tube with constant wall temperature [3].
Figure 10-1 shows the computational results.

For both round and flat tubes, Nu_∞ increases as Pe decreases.
The reason is that as the contribution of axial heat conduction
increases as compared with that of convective transfer, the tempe-
rature profiles become more and more filled, and the temperature
gradient at the wall increases more rapidly than the mean mass
temperature of the fluid.

2. Let us now look at the case of heat exchange when q_s =
= const [1]. Here, as in the similar case considered earlier (see
§8-1), we introduce the excess temperature $\vartheta_1 = t - t_*$, where

$$t_* = t_{-\infty} + \frac{q_c d}{\lambda}\left(2X + \frac{1}{2}R^2 - \frac{1}{8}R^4 - \frac{7}{48}\right)$$

is the known particular solution of Eq. (8-2) for the region of
stabilized heat exchange; $t_{-\infty}$ is the constant fluid temperature
in the stilling segment far from the entrance to the heating segment

(i.e., for $X \to -\infty$), where axial heat conduction no longer has any influence.

Since $t_g(X, R)$ is also a particular solution of (10-1), after making the substitution $t = \vartheta_1 + t_g$, we have

$$\frac{\partial^2 \vartheta_1}{\partial R^2} + \frac{1}{R} \cdot \frac{\partial \vartheta_1}{\partial R} + \frac{1}{Pe^2} \cdot \frac{\partial^2 \vartheta_1}{\partial X^2} = (1 - R^2) \frac{\partial \vartheta_1}{\partial X}. \tag{10-5}$$

This equation must be solved under the boundary condition

$$\left(\frac{\partial \vartheta_1}{\partial R}\right)_{R=1} = 0,$$

corresponding to q_g = const (see §8-1).

A solution can be obtained by the same method as for the case in which t_g = const. Analysis of the solution shows that the heat-exchange process will become stabilized sufficiently far from the entrance. Then the expression for the temperature field will have the form

$$t = t_{-\infty} + \frac{q_c d}{\lambda}\left(4 \frac{1}{Pe} \cdot \frac{x}{d} + \frac{1}{2} R^2 - \frac{1}{8} R^4 - \frac{7}{48}\right) + C, \tag{10-6}$$

i.e., it differs from the expression for t_g only in the constant C.
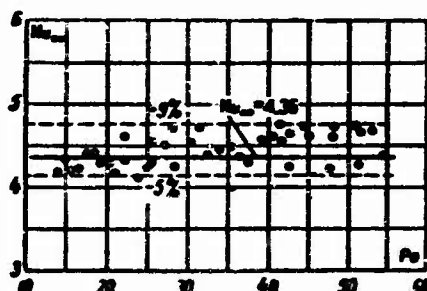
Fig. 10-2. Comparison of theoretical value of Nu_∞ with experimental heat-transfer data for mercury flowing in a round tube.

The constant C characterizes the additional temperature rise in the fluid and the wall in the region of stabilized heat exchange caused by heat supplied by conduction along the axis. The value of C can be found from an expression following from the energy-balance equation:

$$\int_0^{r_0} \lambda \frac{\partial t}{\partial x} 2\pi r \, dr = \pi r_0^2 c_p \rho \bar{w} C,$$

from which we have

$$C = \frac{4}{Pe^2} \int_0^1 \frac{\partial t}{\partial X} R \, dR = \frac{4}{Pe^2} \cdot \frac{q_c d}{\lambda}.$$

The mean mass temperature of the fluid in the thermal-stabilization region is

$$\bar{t} = 4\int_0^1 t(1 - R^2)\, R\, dR = t_{-\infty} + \frac{q_c d}{\lambda}\left(4\,\frac{1}{Pe}\cdot\frac{x}{d} + \frac{4}{Pe^2}\right); \qquad (10\text{-}7)$$

the temperature head is

$$t_c - \bar{t} = \frac{11}{48}\cdot\frac{q_c d}{\lambda}$$

and the limiting Nusselt number is

$$Nu_\infty = \frac{q_c d}{(t_c - \bar{t})\lambda} = \frac{48}{11} = 4.36.$$

Thus when we allow for axial heat conduction, the limiting value of Nu_∞ in the heat-exchange problem with q_s = const will remain the same as before (see §8-1), i.e., equal to 4.36. Again as before, the fluid and wall temperatures in the region of stabilized heat exchange will vary linearly along the tube length, but they will be greater in absolute value by an amount C.

Figure 10-2 compares the theoretical value of Nu_∞ with experimental data on heat exchange for mercury flowing in a round tube; the values were obtained at the Moscow Power Institute [4, 5]. The measurements were carried out at a distance of $(18\text{-}43)d$ from the entrance to the heating section for an Re range between 600 and 2300 at q_s = const. As we can see, within experimental accuracy, we find good agreement between the theoretical and experimental values of Nu_∞.[1]

10-3. NUMERICAL METHOD FOR DETERMINING HEAT EXCHANGE IN TUBES WITH ALLOWANCE FOR HEAT CONDUCTION ALONG THE AXIS

Considerable difficulties are involved in applying analytic methods to determination of heat exchange in the thermal initial segment of a tube with allowance for heat conduction along the axis. Numerical methods are more effective in solving such problems.
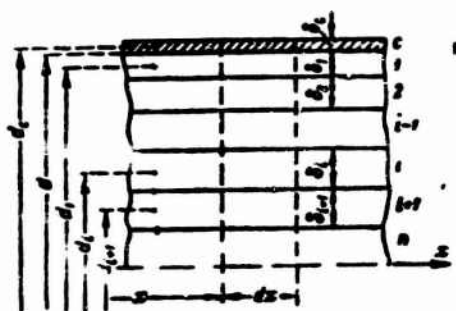
Fig. 10-3. Derivation of heat-balance equations.

Let us look briefly at one such method, the method of straight lines, as applied to heat exchange in a round tube (including the thermal initial segment) (see [8]). The method consists in replacing the continuous radial temperature variation by a step variation; here the temperature distribution over the length remains continuous. With such an approach, the partial differential equation describing the continuous temperature field in the

- 248a -

fluid flow is replaced by a system of ordinary differential equations that are easily solvable.

Let us consider steady heat exchange in a round tube, assuming that the physical properties of the fluid are constant, that the flow is stabilized, and (for simplicity) that the heat of friction can be neglected. We divide the tube along the radius into several coaxial cylindrical layers, whose thicknesses δ_i need not be identical in the general case (Fig. 10-3). The tube wall can be treated as one layer. The heat flow produced along the axis by conduction and convection is computed on the assumption that the fluid temperature and velocity do not vary radially within each layer, but equal the mean values for the given layer. Consequently, the heat flow through the cross section of layer i in the x axis direction is

$$Q_i = -\lambda \frac{dt_i}{dx} s_i + G_i c_p t_i. \qquad (10\text{-}8)$$

where t_i is the fluid temperature in the given cross section of layer i; s_i is the cross-sectional area of layer i; λ and c_p are the thermal-conductivity coefficient and specific isobaric heat capacity of the fluid; G_i is the rate at which the fluid flows through the cross section of layer i.

On the assumption that the temperature at the middle of each layer equals the mean temperature of the fluid in this layer, we write an expression from the heat flow from layer i into layer $i + 1$ for a segment with length dx; it has the form

$$dQ_{i,i+1} = \frac{\lambda(t_i - t_{i+1})}{\frac{1}{2}(\delta_i + \delta_{i+1})} \pi d_{i,i+1} dx, \qquad (10\text{-}9)$$

where $d_{i,i+1} = \frac{1}{2}(d_i + d_{i+1})$; d_i and d_{i+1} are the diameters corresponding to the centers of layers i and $i + 1$.

We use (10-8) and (10-9) to set up the heat-balance equation for a length element of each layer. For the first layer (next to the wall), we obtain

$$\lambda \frac{d^2 t_1}{dx^2} s_1 - G_1 c_p \frac{dt_1}{dx} + q_l - \frac{2\pi d_{1,2}\lambda}{\delta_1 + \delta_2}(t_1 - t_2) = 0. \qquad (10\text{-}10)$$

where q_l is the heat flux at the wall, referred to unit length of tube. If we are given $q_s(x)$, the distribution at the wall of the heat-flux density along the tube length, then $q_l = \pi d q_c$, where d is the inside diameter of the tube.

If we are given the wall-temperature distribution $t_s(x)$, then

$$q_l = \frac{2\pi d_{0,1}\lambda}{\delta_1}(t_c - t_1).$$

where $d_{0,1} = \frac{1}{2}(d + d_1)$.

For any of the remaining layers (other than the first), the heat-balance equation will have the form

$$a\frac{\partial t_i}{\partial r}s_i - Gc_p\frac{dt_i}{dz} + \frac{2\pi\lambda_{i-1,i}\lambda}{\delta_{i-1}+\delta_i}(t_{i-1}-t_i) - \frac{2\pi\lambda_{i,i+1}\lambda}{\delta_i+\delta_{i+1}}(t_i-t_{i+1})=0. \quad (10\text{-}11)$$

Then in virtue of the axial symmetry of the temperature field, the last term in (10-11) will vanish for the last layer.

We thus obtain n second-order ordinary differential equations, which allow for the boundary conditions at the wall. We solve this system to find the temperature variation as a function of z for each layer, to within constant values. The constants are found from the boundary conditions at the entrance and exit of the tube (or at infinity).

After the equations describing the temperature field have been found, it is not difficult to determine the local heat-transfer coefficient. Thus when $q_s(z)$ is given at the inside wall surface,

$$\alpha = \frac{q_s}{t_s - \bar{t}}.$$

The wall temperature is

$$t_s = t_1 + \frac{q_s\delta_1}{\lambda}.$$

If we are given the distribution $t_s(z)$ at the inside wall surface, then

$$\alpha = \frac{\lambda(t_s - t_1)}{\delta_1(t_s - \bar{t})}.$$

The mean mass temperature of the fluid is determined in the usual manner.

The approximate method presented here will be more effective the fewer the number of layers required to attain the necessary accuracy. Estimates obtained by comparing the results of computations by the approximate method with exact solutions for certain problems have shown that the error does not exceed 1-2% even for division into four layers.

10-4. HEAT EXCHANGE IN ROUND AND FLAT TUBES

Let us use the method of the preceding section to investigate heat exchange in a round tube (including the thermal initial segment) with allowance for axial heat conduction [8]. For simplicity, we shall assume that the tube wall is infinitely thin. Let the stilling segment ($-\infty < x < 0$) be heat-insulated, and let a constant heat-flux density q_s or constant wall temperature t_s be maintained at the surface of the heating segment ($0 < x < \infty$). For $x = -\infty$, the fluid temperature in the stilling segment is constant and equal t_∞. All other conditions are the same as in §§6-1 and 8-1.

2. We first consider heat exchange for q_s = const. We divide the tube cross section into four layers: $\delta_1 = \delta_2 = r_0/6$ and $\delta_3 = \delta_4 = r_0/3$, and set up the heat-balance equations for each layer; this yields the following system of differential equations:

$$
\left.
\begin{aligned}
a_1 \, Pe^{-2}\theta''_1 - b_1\theta'_1 + C_0 &= C_1(\theta_1 - \theta_2), \\
a_2 \, Pe^{-2}\theta''_2 - b_2\theta'_2 + C_1(\theta_1 - \theta_2) &= C_2(\theta_2 - \theta_3), \\
a_3 \, Pe^{-2}\theta''_3 - b_3\theta'_3 + C_2(\theta_2 - \theta_3) &= C_3(\theta_3 - \theta_4), \\
a_4 \, Pe^{-2}\theta''_4 - b_4\theta'_4 + C_3(\theta_3 - \theta_4) &= 0.
\end{aligned}
\right\}
\tag{10-12}
$$

Here $\theta = \dfrac{t - t_\infty}{q_s d/\lambda}$; a_i, b_i, C_0 and C_i $(i = 1, 2, 3 \text{ and } 4)$ are constants. The derivatives are taken with respect to the dimensionless coordinate $X = \dfrac{1}{Pe} \cdot \dfrac{x}{d}$, where $Pe = \dfrac{wd}{a}$. When $X < 0$ $C_0 = 0$, when $X > 0$ $C_0 = 1$.

A solution of System (10-12) is found for $X < 0$ and $X > 0$. The constants are found from the boundary conditions:

$$
\left.
\begin{aligned}
&\text{for } X = -\infty & \theta &= 0; \\
&\text{for } X = 0 & \theta_{X<0} &= \theta_{X>0}, \; \theta'_{X<0} = \theta'_{X>0}; \\
&\text{for } X = \infty & \theta' &= 4.
\end{aligned}
\right\}
\tag{10-13}
$$

The last boundary condition follows directly from Eq. (10-6)

By solving the problem, we obtain the following equations.
For the temperature field:
for $X > 0$

$$
\left.
\begin{aligned}
\theta_i &= 4X + \sum_{j=1}^{3} A_{ij} \exp(-s_j X) + A_{i4}; \\
\theta_i &= \sum_{j=1}^{4} B_{ij} \exp(\mu_j X).
\end{aligned}
\right\}
\tag{10-14}
$$

for $X < 0$

For the mean mass temperature of the fluid:
for $X > 0$

$$
\left.
\begin{aligned}
\bar{\theta} &= 4X + \sum_{j=1}^{3} C_j \exp(-s_j X) + C_4; \\
\bar{\theta} &= \sum_{j=1}^{4} D_j \exp(\mu_j X).
\end{aligned}
\right\}
\tag{10-15}
$$

for $X < 0$

For the local Nusselt number:

$$
\frac{1}{Nu} = \sum_{j=1}^{3} E_j \exp(-s_j X) + E_4.
\tag{10-16}
$$

Here $Nu = \alpha d/\lambda$; A_{ij}, B_{ij}, C_j, D_j, E_j, s_j and μ_j are constants that depend on Pe. Table 10-2 shows the values of the constants needed to determine $\bar{\theta}$ and Nu.

TABLE 10-2

Values of Constants in Eqs. (10-15) and (10-16)

Pe	1.0	2.5	10	45	P·	1.0	2.5	10	45
C_1	0.0132	0.0144	0.0058	−0.0004		−0.0069	−0.0077	−0.0118	−0.0292
C_2	0.0004	0.0006	−0.0003	−0.0066	E_6	0.2330	0.2330	0.2330	0.2330
C_3	0.0013	0.0014	0.0017	0.0020	ε_1	6.65	14.6	33.7	42.6
C_4	4.0083	0.6485	0.0461	0.0075	ε_2	10.3	23.5	64.2	105
D_1	4.0439	0.6814	0.0596	0.0029	ε_3	18.4	44.8	157	435
D_2	−0.0171	−0.0160	−0.0047	0.0000	μ_1	0.995	6.05	73.5	849
D_3	0.0000	0.0003	0.0008	−0.0011	μ_2	7.97	22.9	173	2000
D_4	−0.0012	−0.0011	−0.0008	0.0004	μ_3	11.8	32.7	222	2990
E_1	−0.0536	−0.0627	−0.0753	−0.0809	μ_4	19.1	49.3	236	3860
E_2	−0.0095	−0.0134	−0.0313	−0.0647					
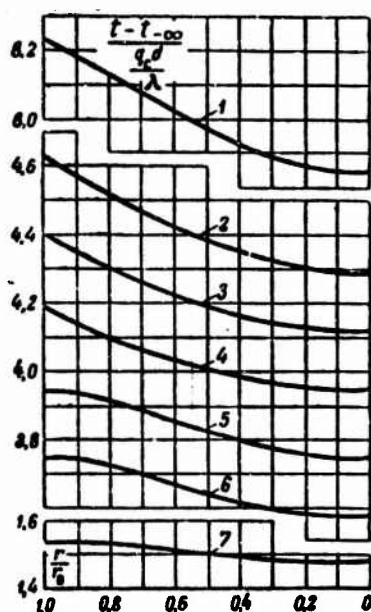
Fig. 10-4. Temperature distribution over flow cross section when Pe = 1 for various values of X.

$1 - X=1$; $2 - X=0.1$; $3 - X=0.05$ $4 - X=-0.001$; $5 - X=-0.05$; $6 - X=-0.1$; $7 - X=-1.0$.

Figure 10-4 shows the temperature distribution over the flow cross section for Pe = 1, computed from Eqs. (10-14). Owing to upstream heat conduction, the temperature field will not be uniform in the stilling segment, as the figure shows. Figure 10-5 shows the variation in $\bar{\theta}$ with length for various values of Pe.

re $\bar{\theta}$ is larger the smaller Pe. When Pe is small enough, a noticeable increase in $\bar{\theta}$ is found even in the stilling segment. As

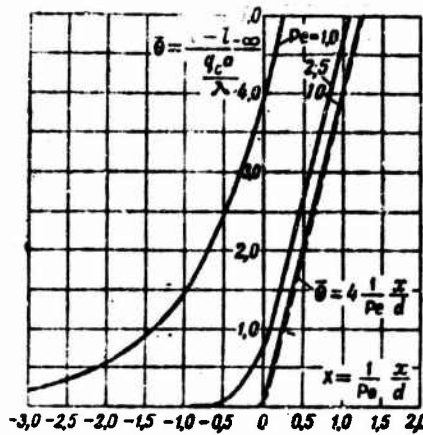Fig. 10-5. Dependence of $\bar{\theta}$ on X for a round tube with Pe - 1, 2.5, and 10 with (solid lines) and without (dashed line) allowance for axial heat conduction.

Pe increases, the mean fluid temperature approaches limiting values: $\bar{\theta} = 0$ for $X < 0$ and $\bar{\theta} = 4\frac{1}{Pe}\cdot\frac{x}{d}$ for $X > 0$, values corresponding to negligible change in the heat flux produced by axial heat conduction.

Figure 10-6 shows Nu as a function of X for various values of Pe in accordance with Eq. (10-16). The figure also shows a curve for the limiting case (Pe $\to$ ∞) corresponding to negligible influence of axial heat conduction. As the figure shows, the influence of axial heat conduction appears primarily as a reduction in Nu as Pe decreases at small X. Thus, for example, when $X = 0$, Nu has the following values:

$$Pe = 1,0; \quad 2,5; \quad 10; \quad 45;$$
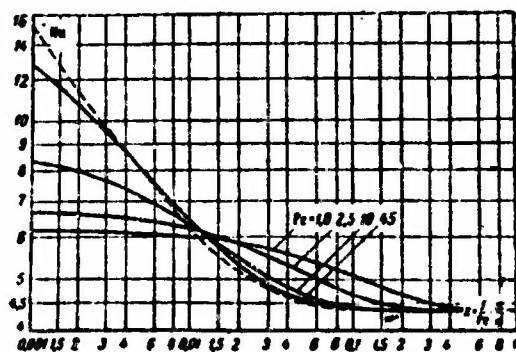$$Nu_{X=0} = 6,14; \quad 6,7; \quad 8,73; \quad 17,2.$$

Fig. 10-6. Dependence of Nu on X for round tube with Pe = 1, 2.5, 10, and 45 with (solid lines) and without (dashed line) allowance for axial heat conduction.

- 253 -

TABLE 10-3

Values of Reduced and Relative Lengths of
Thermal Initial Segment for Round Tube
with q_s = const

Pe	$\frac{1}{Pe}\frac{l_{н.т}}{d}$	$\frac{l_{н.т}}{d}$	Pe	$\frac{1}{Pe}\frac{l_{н.т}}{d}$	$\frac{l_{н.т}}{d}$
1.0	0.485	0.485	10	0.106	1.05
2.5	0.224	0.560	45	0.084	3.78

This result is understandable from the physical viewpoint, since the flow of heat out of the layer near the wall to the stilling segment causes a reduction in the temperature gradients at the wall. Moreover, the reduced length of the thermal initial segment $\left(\frac{1}{Pe}\frac{l_{н.т}}{d}\right)$ decreases as Pe increases, reaching a limit of 0.07. Here the relative length of the thermal initial segment increases. Table 10-3 shows the dimensionless lengths of the initial segment. They were computed on the basis of the condition that $X = \frac{1}{Pe}\frac{l_{н.т}}{d}$ when $Nu = 1.01 Nu_\infty$.

As we can see from (10-16), when $X \to \infty$, Nu approaches its limit

$$Nu_\infty = E_4^{-1} = 4.29,$$

which is only 1.6% below the limit $Nu_\infty = 4.36$ obtained from the exact calculations. To eliminate this difference, caused by the approximate nature of the numerical calculations, it is best to let the constant B_4 equal 11/48.

Thus, for the case under consideration, for small Pe, the axial heat conduction influences heat exchange only in the region of the thermal initial segment, whose length is relatively slight. This is particularly clear from Fig. 10-7, which shows the ratio of Nusselt numbers, computed with (Nu) and without (Nu_0) allowance for axial heat conduction. When $Pe \geq 50 \to X \geq 0.002$, the ratio $1.05 > \frac{Nu}{Nu_0} > 0.95$. We can say with confidence that when $Pe \geq 100$, the influence of axial heat conduction will be negligible.

If the tube wall has sufficient relative conductivity in the axial direction, which is characterized by $\left(1 - \frac{d^2}{d_s^2}\right)\frac{\lambda_s}{\lambda}$. d_s is the outside diameter of the tube and λ_s is the thermal-conductivity coefficient of the wall, this may have a significant influence on heat exchange in the initial segment. Figure 10-8 shows Nu as a function of X for $Pe = 10$ under the same conditions as in the preceding case, but with allowance for wall heat conduction in the axial direction.[3] The calculations were carried out for a value of

the parameter $\left(1-\frac{\xi}{s^2}\right)\frac{h}{k} \approx 0$ on the assumption that a constant heat-flux density is maintained at the outside wall surface, and that the wall thermal resistance is negligible in the radial directions.[6] As the figure shows, axial heat conduction in the wall has no influence on Nu_∞ or the length of the thermal initial segment, but it does substantially reduce heat transfer in the initial segment. This reduction in heat transfer is associated with removal of heat along the wall from the heating segment to the stilling segment. Figure 10-9 shows the variations in mean mass temperature of the fluid and temperature of the wall inside surface under the same conditions. Like fluid axial heat conduction, the wall heat conduction increases δ and θ_s

It is not difficult to obtain expressions for δ and θ_s in the region of stabilized heat exchange with allowance for axial heat conduction in the fluid and the wall; to do this, we add a term allowing for wall heat conduction to Eq. (10-7). As a result we obtain

$$\delta = \frac{\bar{t}-t_{\infty}}{q_s d/\lambda} = \frac{4}{k}\frac{z}{d} + \frac{4}{Pe}\left[1 + \frac{h}{\lambda}\left(\frac{\xi}{s^2}-1\right)\right] \qquad (10\text{-}17)$$

and

$$\theta_s = \frac{t_s-t_{\infty}}{q_s d/\lambda} = \frac{4}{k}\frac{z}{d} + \frac{4}{Pe}\left[1 + \frac{h}{\lambda}\left(\frac{\xi}{s^2}-1\right)\right] + \frac{11}{d} \qquad (10\text{-}18)$$

When the tube length $l \gg l_{n.t.}$, these equations can be used, with a certain degree of approximation, for all positive values of I.

3. Let us now consider the case of heat exchange in a round tube whose wall temperature is maintained constant and equal to t_s over the segment between $x=0$ to $x=\infty$; the wall is heat-insulated between $x=0$ to $x=-\infty$.

The results of computations carried out with the method and the conditions specified in §1 are shown in Figs. 10-10 and 10-11.[5] As we see, the variation in $\delta = \frac{\bar{t}-t_s}{t_{\infty}-t_s}$ along the tube length depends essentially on Pe. For small Pe, the temperature field in the stilling segment is nonuniform for a considerable distance from the $x = 0$ section. As Pe increases, however, the region of nonuniform temperature distribution contracts rapidly, and at Pe > 100, the temperature distribution over the length of the stilling segment (except for very small $|x|$) becomes nearly uniform. In the heating segment, δ varies more sharply along the length the greater Pe. In the thermal initial segment, Nu is significantly lower for small Pe than for large, as for the case in which q_s = const. The limiting value of Nu_∞ rises slightly as Pe decreases, as has been shown by a more rigorous theoretical analysis (see §10-2).

The data given show that for heat exchange in a round tube

with t_s = const, the axial heat conduction can be neglected if
$\sim \geq 100$, while $\frac{1}{Pe}\frac{x}{e} > 0.505$ (for Pe = 100, the axial heat conduction
has an effect only for a segment 0.5x long).

4. Let us consider heat exchange in a flat tube with an abrupt
change in wall temperature. Let the temperature of both walls be
t_{s1} when $-\infty < x < 0$, and t_{s2} when $0 < x < \infty$; here $t_{s1} \neq t_{s2}$. In contrast
to the same problem as considered in §6-2, here we allow for heat
transfer owing to axial conduction.[6]

Figure 10-12 shows the distribution of the dimensionless temp-
erature $\theta = \frac{t - t_{s2}}{t_{s1} - t_{s2}}$ over the tube cross section for values $X = -0.25$,
0, and +0.25 with Pe = 2 (here $X = \frac{1}{Pe}\frac{x}{e}$; $Pe = \frac{\bar{w}h}{e}$; h is the width of the
tube). The disagreement between the dashed curves for $\theta_{x<0} - \bar{\theta}_{x>0}$
at $X = 0$ is explained by the fact that a limited number of series
terms was used in the calculation. The center curve gives a quite
good idea as to the actual temperature distribution at $z = 0$. Fig-
ure 10-13 shows the way in which the mean mass temperature $\bar{\theta}$ varies
with the length for the same value of Pe. By hypothesis, when
$X \to -\infty$ $\theta = 1$, and when $X \to \infty$ $\theta = 0$. For all other values of X, when
Pe is small, the temperature field is nonuniform, and heat exchange
is observed under the specified boundary conditions; if heat flows
from the fluid to the wall when $X > 0$, it flows from the wall to the
fluid when $X < 0$. When Pe $\to \infty$, the influence of axial heat conduc-
tion becomes unimportant, and in the region $-\infty < X < 0$ $\theta = \bar{\theta} = 1$, i.e.,
this tube segment becomes an ordinary isothermal damping segment,
with no heat transfer.

$Nu = \frac{\alpha h}{\lambda}$ Figure 10-14 shows the variations in the local value of
with tube length for both $X > 0$ and $X < 0$. When $X \to 0$, both
$Nu_{x<0}$ and $Nu_{x>0}$ go to infinity, and this is associated with the in-
finite increase in the temperature gradient at the wall when $X \to 0$.
It is interesting to note that for the specified boundary conditions
(t_{s1} = const and t_{s2} = const), in contrast to the cases considered
in §§2 and 3, the axial heat conduction causes an increase in the
heat transfer in the thermal initial segment.
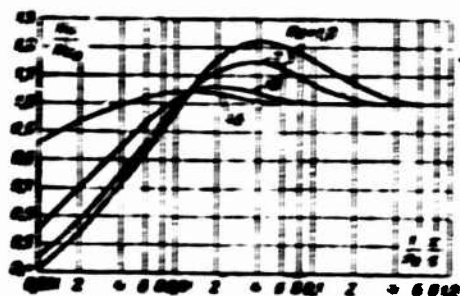
Fig. 10-7. Values of $\frac{Nu}{Nu_0} = f\left(\frac{1}{Pe}\frac{x}{e}\right)$
for various values of Pe.
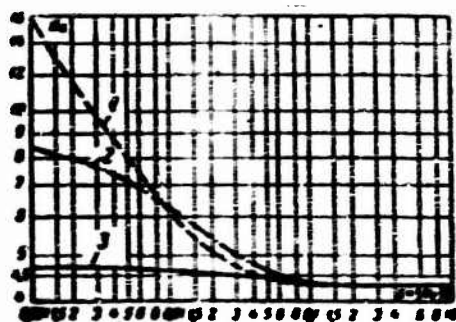
Fig. 10-8. Dependence of Nu as a function of X. 1) No allowance for axial heat conduction; 2) with allowance for fluid axial heat conduction at $Pe = 10$; 3) with allowance for axial heat conduction of fluid and wall with $Pe = 10$ and $\left(1 - \frac{d_i}{d}\right)\frac{\lambda_s}{\lambda} = 1$.
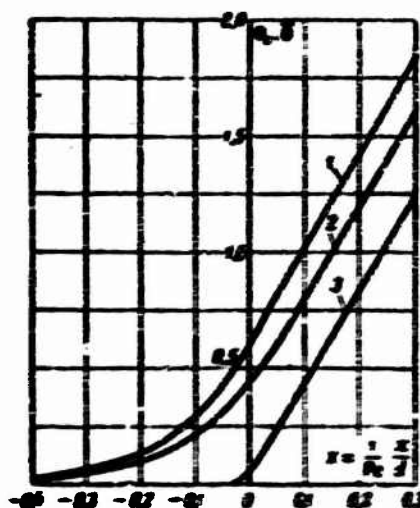
Fig. 10-9. Values of θ_s and $\bar{\theta}$ as functions of X with $Pe = 10$. 1) θ_s with allowance for axial heat conduction of fluid and wall; 2) $\bar{\theta}$ under the same conditions; 3) $\bar{\theta}$ with allowance for axial heat conduction of fluid alone.
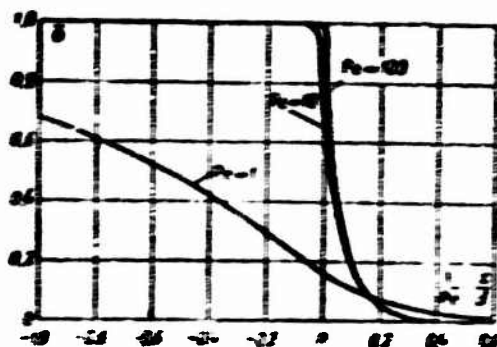
Fig. 10-10. Values of $\bar{\theta} = F\left(\frac{1}{Pe}\frac{x}{d}, Pe\right)$ for round tube at $t_s = $ const with allowance for axial heat conduction.

- 257 -
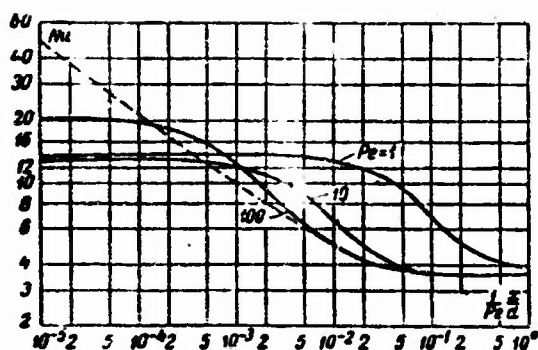
Fig. 10-11. Values of $Nu = i\left(\frac{1}{Pe} \cdot \frac{x}{d}, Pe\right)$ for round tube at t_s = const with (solid lines) and without (dashed line) allowance for axial heat conduction.
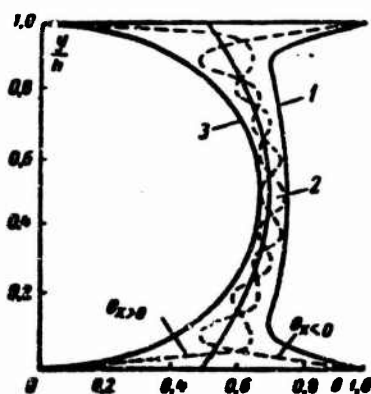
Fig. 10-12. Distribution of θ over cross section of flat tube under abrupt change in wall temperature (Pe = 2). 1) $X = -0.25$; 2) $X = 0$ (center curve); 3) $X = +0.25$.
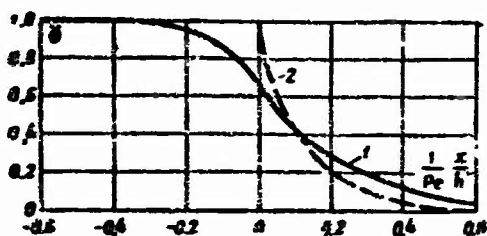
Fig. 10-13. Dependence of $\bar{\theta}$ or X under abrupt change in wall temperature in flat tube. 1) Pe = 2; 2) Pe → ∞.

- 256 -
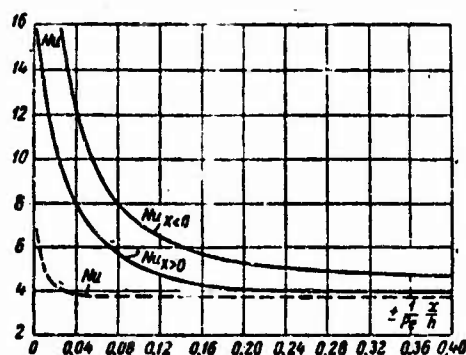
Fig. 10-14. Dependence of Nu on X under abrupt change in wall temperature for flat tube. Solid lines) Pe = 2; dashed line) Pe → ∞.

Analysis of heat exchange in tubes with allowance for axial heat conduction is simplified substantially if we assume that the fluid velocity is constant over a cross section (bar flow). It is appropriate to consider this question in Chapter 12, however, where we shall look at heat exchange in the hydrodynamic initial segment.

Manuscript Page No.	Footnotes
248a	[1]In contrast to the theory, experiments have been reported [6, 7] on heat transfer to liquid metals at low values of Pe in which a rapid increase in Nu_∞ was detected as Pe increases. It has been shown [4, 5] that these data are in error, since in design of the experiments and processing of the results there was no allowance for heat transferred by fluid and wall conduction in the direction of the tube axis.
249	[2]Equation (10-10) has been written on the assumption that the boundary condition is specified at the inside surface of the tube wall. Thus the process of heat conduction in the wall is neglected.
254	[3]With allowance for axial conduction along the tube, $$Nu = \frac{q_c d}{\lambda (t_s - \bar{t})},$$ where q_s is the heat-flux density at the inside wall surface and t_s is the temperature of this surface.
255	[4]The calculations were performed by V.V. Kirillov
255	[5]The calculations were performed by A.Ya. Yushin.

2S6 *The problem has been solved analytically by Agrawal
[9], but the computational results are shown only for
Ie = 2.

Manu- script Page No.	Transliterated Symbols
247	c = s = stenka = wall
254	H.T = n.t = termicheskiy nachal'nyy = thermal initial
254	H = n = naruzhnyy = outside

Chapter 11

HEAT EXCHANGE IN ROUND AND FLAT TUBES WITH BOUNDARY CONDITIONS OF THE THIRD KIND

11-1. PRELIMINARY REMARKS

In many heat-exchange systems, for example, in heat exchangers, the fluid flowing in the tube is cooled or heated by a medium (another fluid) that washes the tube from the outside. Strictly speaking, the determination of heat exchange for such systems would require solution of a conjugate problem, i.e., joint consideration of three temperature fields: in the fluid flowing within the tube, in the tube wall, and in the flow washing the outside of the tube. Significant difficulties are involved in the solution of such conjugate problems, however. To eliminate or reduce these difficulties, while not going too far from the actual conditions, we make certain assumptions. The first consists in the following: the temperature field at the wall is taken to be uniform, i.e., heat is transferred only in the direction normal to the wall surface, and heat conduction along the wall is negligibly small. Naturally, this assumption is more supportable the lower the axial temperature gradients in the wall as compared with the radial gradients. As the second assumption, we omit detailed consideration of the heat-exchange process in the flow washing the outside of the tube; instead, we specify boundary conditions of the third kind at the outside surface of the tube. This means that the local heat-flux density at the wall is taken to be proportional to the difference between the temperature t_{s1} of the outside wall surface and the temperature t_1 of the surrounding medium:

$$q_c = \alpha_1(t_{s1} - t_1).$$

where α_1 is the coefficient of heat transfer from the outside tube surface to the surrounding medium. We assume the values of t_1 and α_1 to be given. In the general case, α_1 is a function of the coordinates of the points on the outside tube surface. The calculations are usually carried out under the assumption that α_1 = const, however. Naturally, the results of such calculations will be closer to the actual case the better this assumption is satisfied.

Under steady-state conditions, q_s can be represented by the following relationships:

$$q_c = \alpha(\bar{t} - t_c) = K'(t_c - t_1) = K(\bar{t} - t_1). \tag{11-1}$$

where $\bar{t}$ and t_s are the mean mass temperature of the fluid and the temperature of the inside wall surface at the given tube cross section; α is the local coefficient of heat transfer from the fluid flowing in the tube to the inside wall surface; K' is the local coefficient of heat transfer from the inside surface of the wall to the surrounding medium; K is the local coefficient of heat transfer from the fluid flowing in the tube to the surrounding medium. The coefficients α, K', and K are associated by the relationship

$$\frac{1}{K} = \frac{1}{\alpha} + \frac{1}{K'}. \tag{11-2}$$

For a round tube,

$$\frac{1}{K'} = \frac{d}{2\lambda_c} \ln \frac{d_1}{d} + \frac{d}{\alpha_1 d_1};$$

for a flat tube (and tubes of any cross section, provided δ is substantially less than the cross-sectional dimensions)

$$\frac{1}{K'} = \frac{\delta}{\lambda_c} + \frac{1}{\alpha_1},$$

where d and d_1 are the tube inside and outside diameters; δ is the wall thickness; λ_s is the thermal-conductivity coefficient for the wall material.

Multiplying (11-2) by the fluid thermal-conductivity coefficient λ and dividing by d, we obtain

$$\frac{1}{Nu_K} = \frac{1}{Nu} + \frac{1}{Bi}. \tag{11-3}$$

Here

$Nu_K = \frac{\overline{K}d}{\lambda}$ is a number which we call the general Nusselt number;

$Nu = \frac{\alpha d}{\lambda}$ is the ordinary Nusselt number;

$Bi = \frac{K'd}{\lambda}$ is the Biot number.

For the problem of heat exchange under boundary conditions of the third kind, both Bi and the temperature t_1 of the surrounding medium are given; we do not know Nu_K, Nu, or the wall temperatures t_s and t_1. If $Bi \to \infty$, then $t_s \to t_1$ and $Nu_K = Nu$, i.e., the problem of heat exchange under boundary conditions of the third kind goes over to a problem with boundary conditions of the first kind.

11-2. HEAT EXCHANGE IN A ROUND TUBE WITH CONSTANT TEMPERATURE IN SURROUNDING MEDIUM

The problem of heat exchange in a round tube under boundary conditions of the third kind was first considered in a very general formulation (with allowance for axial heat conduction and

and ene·gy dissipa· ·. by L.S. ·ybenzon in 1922 [1]. ..e obtained
a solut..on in hypergeometric functions, but did not carry it all
the way through. In 1951, Lauvcrier [2] obtained a solution to this
problem independently of Leybenzon, but in a less general formula-
tion (neglecting axial heat conduction and energy dissipation). Un-
fortunat..ly, the hypergeometri. functions are not tabulated, which
hampers p··actical utilization of the results obtained. In the en-
suing discussion, therefore, we shall consider a solution of this
problem obtained in a form convenient for practical application.
This problem (Fig. 11-1) differs fromthe one considered in §6-1
only in the boundary conditions at the wall. Here the boundary con-
ditions at the inside wall surface have the form

$$-\lambda\left(\frac{\partial t}{\partial r}\right)_{r=r_\bullet}=K'(t_{r=r_\bullet}-t_1),$$

where K' and t_1 are constants.

Introducing the dimensionless variables

$$\theta=\frac{t-t_1}{t_\bullet-t_1}, \ X=\frac{2}{Pe}\cdot\frac{x}{d}, \ Pe=\frac{\bar{w}d}{a} \text{ and } R=\frac{r}{r_\bullet},$$

we write the energy equation and boundary conditions in the form

$$\frac{\partial^2\theta}{\partial R^2}+\frac{1}{R}\cdot\frac{\partial\theta}{\partial R}=(1-R^2)\frac{\partial\theta}{\partial X}; \tag{11-4}$$

$$\left(\frac{\partial\theta}{\partial R}\right)_{R=1}=-\frac{1}{2}Bi\,\theta_{R=1}; \ \left(\frac{\partial\theta}{\partial R}\right)_{R=0}=0; \tag{11-5}$$

$$\theta(0,\,R)=1. \tag{11-6}$$

A solution has been obtained for this problem by Schenk and
Dumore [3]; they used the ordinary method of separation of variables.
Letting

$$\theta=A\psi(R)\exp(-\varepsilon^2 X)$$

and substituting this expression into (11-4), we obtain

$$\psi''+\frac{1}{R}\psi'+\varepsilon^2(1-R^2)\psi=0. \tag{11-7}$$

The boundary conditions (11-5) for ψ are written as

$$\psi'(1)=-\frac{1}{2}Bi\,\psi(1), \ \psi'(0)=0. \tag{11-8}$$

A general solution of the problem, satisfying Eq. (11-7) and
Conditions (11-6) and (11-8), can be written as a series in eigen-
functions:

$$\theta(X,\,R)=\sum_{n=0}^{\infty}A_n\psi_n(R)\exp\left(-2\varepsilon_n^2\frac{1}{Pe}\cdot\frac{x}{d}\right). \tag{11-9}$$

whe··e ε, $(n=0,1,2\ldots)$ are the eigenvalues of System (11-7) and (11-8).

If ψ ?) is represented, as usual, as a power series of the
(6-10) type with coefficients b_{2n} that are the same as in the prob-
lem with t_s = const, and if Condition (11-8) is satisfied, we then
obtain the following equation for calculating the eigenvalues:

$$\sum_{n=0}^{\infty} 2n\theta_1 s^{2n} = - \ \mathrm{Bi} \sum_{n=0}^{\infty} b_{2n} s^{2n}.$$
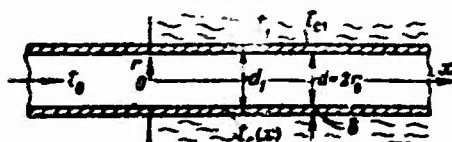
Fig. 11-1. On the problem of heat
transfer in a round tube, with
ambient medium at constant tempera-
ture.

TABLE 11-1

Values of Constants in Problem of Heat Exchange
in a Round Tube with Constant Temperature of Sur-
rounding Medium

n	Bi = 1				Bi = 4			
	ε_n	ε_n^2	A_n	B_n	ε_n	ε_n^2	A_n	B_n
0	1,2716	1,6170	1,120	0,994	2,0000	4,0000	1,295	0,953
1	5,2951	28,038	—0,171	0,005	5,7439	32,992	—0,447	0,036
2	9,3063	86,607	0,078	0,001	9,6450	93,026	0,246	0,006
n	Bi = 40				Bi = ∞			
	ε_n	ε_n^2	A_n	B_n	ε_n	ε_n^2	A_n	B_n
0	2,6069	6,7959	1,469	0,847	2,7044	7,3136	1,466	0,819
1	6,5096	42,377	—0,764	0,091	6,6790	44,609	—0,803	0,101
2	10,450	109,20	0,539	0,028	10,673	113,92	0,587	0,032
3	—	—	—	—	14,671	215,24	—0,475	0,015

The values of ε_n will now depend on the values of Bi. Table
11-1 gives the first three values of ε_n (n = 0, 1, and 2) for
Bi = 1, 4, 0, and ∞. The eigenvalues correspond to a series of
eigenfunctions whose values are given in Table 11-2 for the same
Bi. The coefficients A_n, computed from (6-16), are given in Table
11-1.

TABLE 11-2

Values of Functions $\psi(R)$ in Problem of Heat Exchange in Round Tube With Constant Temperature of Surrounding Medium

R	Bi = 1			Bi = 4			Bi = 40			Bi = ∞
	ϕ_0	ϕ_1	ϕ_2	ϕ_0	ϕ_1	ϕ_2	ϕ_0	ϕ_1	ϕ_2	
0.0	1.000	1.000	1.000	1.000	1.000	1.000	1.000	1.000	1.000	
0.1	0.996	0.931	0.795	0.993	0.919	0.781	0.983	0.897	0.746	
0.2	0.984	0.741	0.309	0.961	0.699	0.270	0.934	0.622	0.178	
0.3	0.965	0.472	−0.171	0.914	0.306	−0.213	0.856	0.303	−0.396	$\frac{1}{\text{См. табл.}}$
0.4	0.939	0.179	−0.407	0.852	0.079	−0.414	0.755	−0.076	−0.406	6-1
0.5	0.917	−0.066	−0.342	0.775	−0.157	−0....	0.636	−0.320	−0.180	
0.6	0.672	−0.305	−0.096	0.698	−0.363	−0.036	0.515	−0.429	0.131	
0.7	0.833	−0.402	0.150	0.613	−0.444	0.223	0.389	−0.448	0.332	
0.8	0.794	−0.472	.32	0.527	−0.446	0.350	0.272	−0.323	0.508	
0.9	0.754	−0.470	0.528	0.445	−0.399	0.356	0.153	−0.198	0....	
1.0	0.717	−0.451	0.372	0.366	−0.333	0.383	0.049	−0.063	0.871	

1) See Table 6-1.

Let us determine the temperature of the inside wall surface. In accordance with (11-9),

$$\theta_c = \frac{t_c - t_1}{t_0 - t_1} = \sum_{n=0}^{\infty} A_n \phi_n(1) \exp\left(-2\varepsilon_n^2 \frac{1}{Pe} \cdot \frac{x}{d}\right). \qquad (11\text{-}10)$$

The mean mass temperature of the fluid is

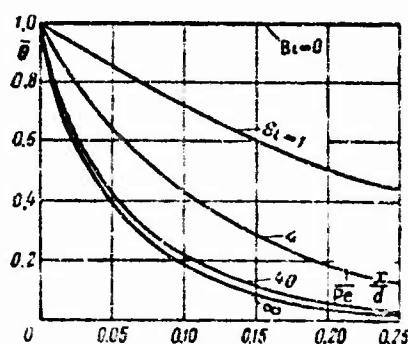$$\bar{\theta} = 4 \int_0^1 (1 - R^2)\, R\, dR.$$

Fig. 11-2. Variation in $\bar{\theta}$ along length of round tube for various values of Bi.

Substituting θ from (11-9) into this expression and integrating, we obtain

$$\bar{\theta} = \frac{\bar{t} - t_1}{t_0 - t_1} = \sum_{n=0}^{\infty} B_n \exp\left(-2\varepsilon_n^2 \frac{1}{Pe} \cdot \frac{x}{d}\right), \qquad (11\text{-}11)$$

- 26 -
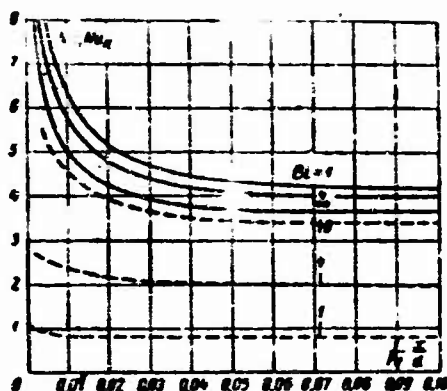
Fig. 11-3. Variation in Nu (so-
lid lines) and Nu_K (dashed line)
along length of round tube for
various values of Bi.

where B_n are constants whose values are given in Table 11-1. Figure
11-2 illustrates Relationship (11-11).

The local Nu_K number can be found either from the Fourier law
or from the heat-balance equation. Using the second method, we ob-
tain

$$K\,(\bar{t} - t_i)\,\pi d\,dx = -\frac{\pi d^2}{4}\,\overline{w\rho c_p}\,d\bar{t}_i.$$

from which we have

$$Nu_K = \frac{Kd}{\lambda} = -\frac{1}{2\bar{\theta}}\left(\frac{d\bar{\theta}}{dX}\right).$$

After substituting the value of $\bar{\theta}$ from (11-11) into this expres-
sion, we finally obtain

$$Nu_K = \frac{1}{2} \cdot \frac{\displaystyle\sum_{n=0}^{\infty} B_n \epsilon_n^2 \exp\left(-2\epsilon_n^2 \frac{1}{Pe} \cdot \frac{x}{d}\right)}{\displaystyle\sum_{n=0}^{\infty} B_n \exp\left(-2\epsilon_n^2 \frac{1}{Pe} \cdot \frac{x}{d}\right)}. \tag{11-12}$$

It is simplest to determine the local value of Nu from (11-3):

$$Nu = \frac{\alpha d}{\lambda} = \frac{Bi\,Nu_K}{Bi - Nu_K}. \tag{11-13}$$

Figure 11-13 shows the variation in Nu and Nu_K along the tube
length for various values of Bi.

When Bi → 0, i.e., for a thermally isolated flow, the fluid
temperature does not vary ($\theta = 1$), while $Nu_K = 0$ even though Nu is
finite.

- 266 -

When Bi $\to \infty$, the function $\varphi_n(1) \to 0$ (see Table 11-2), so that $t_s \to t_1 = $ const and $Nu_K \to Nu$; in other words, the problem of heat exchange with $t_1 = $ const reduces to the problem of heat exchange with $t_s = $ const. In practice, by Bi = 40, the value of Nu at $t_1 = $ const will differ by no more than 2% from its value at $t_s = $ const; thus for sufficiently large Bi we can use the equations for Nu with constant wall temperature (see §6-1). At the same time, for small Bi, this computational method may lead to significant error. For example, when Bi = 1, the error reaches 15-20%.
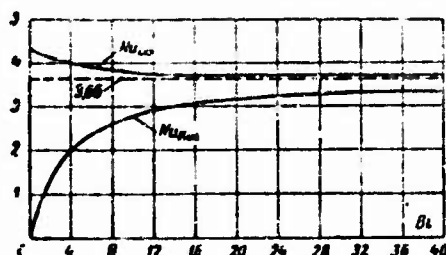
Fig. 11-4. Values of Nu_∞ and $Nu_{K\infty}$ for round tube as functions of Bi (solid lines); $Nu_{K\infty} = Nu_\infty = 3.66$ when Bi = ∞ (dashed line).

The limiting Nusselt numbers corresponding to values $X \to \infty$ will obviously be

$$Nu_{K\infty} = \frac{\epsilon_0^2}{2},$$
$$Nu_\infty = \frac{Bi\,\epsilon_0^2}{2Bi - \epsilon_0^2}. \qquad (11-14$$

They naturally depend on Bi. These relationships are illustrated in Fig. 11-4. As Bi varies from 0 to ∞, $Nu_{K\infty}$ varies from 0 to 3.66, while Nu_∞ changes by only 15%, approaching the same limit.

The length of the thermal initial segment for Nu and Nu_K is nearly independent of Bi, and has roughly the same value as when $t_s = $ const, i.e.,

$$\frac{l_{n,\tau}}{d} \approx (0.055 \div 0.065)\,Pe.$$

The mean Nusselt number over the length is

$$\overline{Nu}_K = \frac{\bar{K}d}{\lambda} = -\frac{1}{4}Pe\,\frac{d}{l}\ln\bar{\theta}_{x=l}, \qquad (11-15)$$

where $\bar{\theta}_{x=l}$ is the mean mass temperature of the fluid a distance l from the tube entrance, as determined from (11-11).

The mean heat-transfer coefficient $\bar{K}$, computed with the aid of

- 267 -

(11-15), refers to the mean logarithmic temperature head. In other words, the amount of heat transferred from the fluid flowing in the tube to the surrounding medium is determined by the equations

$$Q_c = \overline{K} \overline{\Delta t}_n \pi dl,$$

where

$$\overline{\Delta t}_n = \frac{t_0 - \overline{t}_{x=l}}{\ln \dfrac{t_0 - t_1}{t_{x=l} - t_1}}.$$

For small values of reduced length, the series in Eqs. (11-9)-(11-12) converge very slowly. Moreover, for such values of X, good results are given (when t_s = const) by the approximate Leveque solution (see §6-3). Thus it is of interest to consider a solution based on the same assumptions as the Leveque solution, but with boundary conditions of the third kind. Such a solution has been obtained for the case $\alpha_1 \to \infty$ [4]. In other words, we consider the problem of heat exchange in the thermal initial segment with allowance for the finite thickness of the tube wall; a constant temperature t_{s1} is maintained at the outside surface of the tube. Then the temperature t_s of the inside wall surface will vary with the length. The following expressions are obtained for this temperature and the local Nu_K number:

$$\frac{t_c - t_0}{t_{c_1} - t_0} = \sum_{n=1}^{\infty} (-1)^{n+1} \frac{\left[\eta \left(\frac{1}{\text{Pe}} \cdot \frac{x}{d}\right)^{1/3}\right]^n}{\Gamma\left(1 + \frac{n}{3}\right)}; \qquad (11\text{-}16)$$

$$\text{Nu}_K = \frac{Kd}{\lambda} = 2\tilde{\lambda} \left\{ 1 + \sum_{n=1}^{\infty} (-1)^n \frac{\left[\eta \left(\frac{1}{\text{Pe}} \cdot \frac{x}{d}\right)^{1/3}\right]^n}{\Gamma\left(2 + \frac{n}{3}\right)} \right\}, \qquad (11\text{-}17)$$

where t_0 is the fluid temperature at the tube entrance;

Γ is a gamma function; $\text{Pe} = \overline{w} d/a$;

K is the coefficient of heat transfer from the fluid flowing in the tube to the outside wall surface, referred to the temperature difference $t_{s1} - t_0$;

$$\eta = \tilde{\lambda} \frac{9^{1/3} \Gamma\left(\frac{4}{3}\right)}{\Gamma\left(\frac{2}{3}\right)}; \quad \tilde{\lambda} = \frac{\lambda_c}{\lambda \ln \dfrac{d_1}{d}}.$$

Figures 11-5 and 11-6 show the distributions with length for the temperature of the inside wall and Nu_K for various values of the parameter λ.

The results obtained in this section show that for boundary conditions of the third kind, α depends on λ_s, δ, and α_1. This is explained by the fact that as these quantities vary, the tempera-
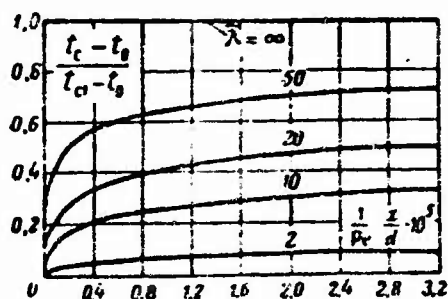
Fig. 11-5. Variation in temperature of inside wall surface along tube length for various values of the parameter $\tilde{\lambda}$.
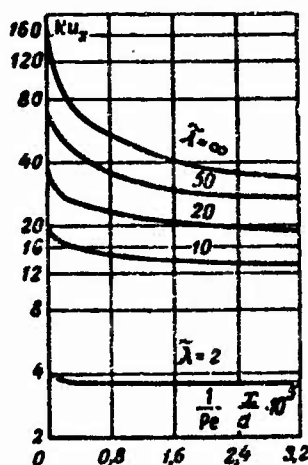
Fig. 11-6. Variation in Nu_K along tube length for various values of the parameter $\tilde{\lambda}$.

ture distribution at the inside tube surface changes, while the nature of the distribution of t_s in turn influences α. We observed this influence in §6-5 in considering heat transfer when wall temperature varies with the length.

11-3. HEAT EXCHANGE IN A FLAT TUBE WHEN THE SURROUNDING MEDIUM IS AT CONSTANT TEMPERATURE

The problem of heat exchange in a flat tube with symmetric heating and constant temperature of the external medium (the remaining conditions are the same as for the problem with t_s = const, see §6-2) reduces to solution of the equation

$$\frac{\partial^2 \Theta}{\partial Y^2} = \frac{3}{8}(1 - Y^2)\frac{\partial \Theta}{\partial X} \tag{11-18}$$

under the boundary conditions

$$\left(\frac{\partial\theta}{\partial Y}\right)_{Y=1}=-\frac{1}{2}\,\mathrm{Bi}\,\vartheta_{Y=1};\ \left(\frac{\partial\theta}{\partial Y}\right)_{Y=0}=0;\Big\}$$
$$\theta(0,\ Y)=1. \qquad (11\text{-}19)$$

TABLE 11-3

Values of Constants in
Problem of Heat Exchange
in Flat Tube with Constant
Temperature of Surrounding
Medium

Fig. 11-7. Values of $\mathrm{Nu}_{K\infty}$
for flat tube (solid lines)
and round tube (dashed lines)
as a function of Bi.

n	ε_n	ε_n^2	A_n	B_n
		Bi = 2		
0	1.0000	1.0000	1.088	0.990
1	4.6562	21.680	−0.117	0.008
2	8.5618	73.304	0.038	0.001
		Bi = 20		
0	1.5518	2.4081	1.183	0.936
1	5.3976	29.134	−0.266	0.043
2	9.3025	86.536	0.132	0.011
		Bi = ∞		
0	1.6816	2.8278	1.201	0.914
1	5.6699	32.148	−0.292	0.053
2	9.6678	93.466	0.153	0.015

Here we let

$$\theta=\frac{t-t_1}{t_0-t_1};\ \ X=\frac{1}{\mathrm{Pe}}\cdot\frac{x}{h};\ \ Y=\frac{y}{r_0};$$

$$\mathrm{Pe}=\frac{\overline{w}h}{a};\ \ \mathrm{Bi}=\frac{K'h}{\lambda};$$

$h = 2r_0$ is the distance between the tube walls.

The solution obtained in [5] by separation of variables has
the form

$$\theta(X,\ Y)=\sum_{n=0}^{\infty}A_n\psi_n(Y)\exp\left(-\frac{8}{3}\,\varepsilon_n^2\,\frac{1}{\mathrm{Pe}}\cdot\frac{x}{h}\right). \qquad (11\text{-}20)$$

The eigenvalues ε_n and the coefficients A_n are given in Table
11-3, and the eigenfunctions $\psi_n(Y)$ are shown in Table 11-4 for two
values of Bi.

The mean mass temperature of the fluid in a given cross sec-
tion is

$$\overline{\theta}=\frac{\overline{t}-t_1}{t_0-t_1}=\sum_{n=0}^{\infty}B_n\exp\left(-\frac{8}{3}\,\varepsilon_n^2\,\frac{1}{\mathrm{Pe}}\cdot\frac{x}{h}\right), \qquad (11\text{-}21)$$

where the B_n are constants that depend on Bi (see Table 11-3).

From the heat-balance equation, we determine the coefficient of heat transfer K from the fluid flowing in the tube to the surrounding medium (see §11-2); we then use Eq. (11-21) to obtain an expression for the overall Nusselt number (local value):

$$Nu_K = \frac{Kh}{\lambda} = \frac{4}{3} \cdot \frac{\sum_{n=0}^{\infty} B_n \epsilon_n^2 \exp\left(-\frac{8}{3} \cdot \frac{1}{Pe} \cdot \frac{x}{h}\right)}{\sum_{n=0}^{\infty} B_n \exp\left(-\frac{8}{3} \cdot \frac{1}{Pe} \cdot \frac{x}{h}\right)}. \qquad (11-22)$$

TABLE 11-4

Values of Functions $\psi n(Y)$ in Problem of Heat Exchange in Flat Tube with Constant Temperature of Surrounding Medium

Y	Bi = 2			Bi = 20			Bi → ∞
	ψ_0	ψ_1	ψ_2	ψ_0	ψ_1	ψ_2	
0,0	1,000	1,000	1,000	1,0000	1,000	1,000	
0,1	0,995	0,894	0,656	0,988	0,858	0,598	1
0,2	0,980	0,599	−0,137	0,954	0,475	−0,282	См. табл.
0,3	0,957	0,182	−0,843	0,986	−0,039	−0,948	6-3
0,4	0,923	−0,272	−1,021	0,818	−0,544	−0,920	
0,5	0,884	−0,678	−0,602	0,725	−0,922	−0,259	
0,6	0,835	−0,977	0,140	0,618	−1,102	0,572	
0,7	0,783	−1,143	0,829	0,502	−1,081	1,114	
0,8	0,726	−1,186	1,229	0,380	−0,902	1,189	
0,9	0,667	−1,135	1,318	0,254	−0,627	0,902	
1,0	0,607	−1,039	1,226	0,127	−0,316	0,460	

1) See Table 6-3.

The local value of $Nu = \alpha h/\lambda$ is found from (11-3).

Letting X approach ∞, we find the limiting Nusselt numbers:

$$Nu_{K\infty} = \frac{4}{3} \epsilon_0^2. \qquad (11-23)$$

$$Nu_{\infty} = \frac{Bi \, \epsilon_0^2}{\frac{3}{4} Bi - \epsilon_0^2}. \qquad (11-24)$$

For a flat tube with $t_1 = $ const, the length of the thermal initial segment is nearly independent of Bi, and has roughly the same value as for a round tube, i.e., $l_{\text{н.т}}/d \approx 0,06\, Pe$.

The nature of the variations in $\bar{\theta}$, Nu_K, and Nu along the tube length are the same as for a round tube (see §11-2). When $Bi \to \infty$, we arrive at the problem of heat exchange in a flat tube with $t_s = $ const (see §6-2). Figure 11-7 shows $Nu_{K\infty}$ as a function of Bi. As Bi varies from 0 to ∞, $Nu_{K\infty}$ varies from 0 to 3.77. We note that in this range of Bi values, Nu_{∞} varies by a total of 7%, decreasing

s Bi increases. For comparison, the same figure shows analogous ~lationships for a round tube.

For this case, the average value of the Nusselt number over the length equals

$$\overline{\mathrm{Nu}}_K = \frac{\overline{K}d}{\lambda} = -\frac{1}{2}\,\mathrm{Pe}\,\frac{h}{l}\,\ln\overline{\theta}_{x=l},\qquad(11\text{-}25)$$

where $\overline{K}$ is the length-averaged value of the coefficient of heat transfer between the fluid flowing in the tube and the surrounding medium, referred to the mean logarithmic temperature head.

11-4. HEAT EXCHANGE IN A FLAT TUBE WITH ONE WALL HEAT-INSULATED AND AN EXTERNAL MEDIUM WITH CONSTANT TEMPERATURE AT THE OTHER WALL

This problem is analogous to that considered in §6-4, with the difference that here there is assumed to be an external medium with constant temperature at one of the walls (t_1 = const rather than t_s = const). As before, the other wall is heat-insulated.

TABLE 11-5

Values of Constants in Problem of Heat Exchange in Flat Tube with One Wall Heat-Insulated and with an External Medium Having Constant Temperature at the Other Wall

n	ε_n	ε_n^2	A_n	B_n
		Bi = 2		
0	2,5991	6,7553	1,104	0,980
1	10,0898	101,804	0,276	0,016
		Bi = 10		
0	3,4537	11,9280	1,86	0,937
		Bi = ∞		
0	3,8187	14,5825	2,176	0,896
1	11,8972	141,5434	1,427	0,061
2	19,9248	397,0051	1,20	0,018

TABLE 11-6

Values of eigenfunctions $\psi_n(Y)$ in Problem of Heat Exchange in Flat Tube With one wall Heat-Insulated and an External Medium with Constant Temperature at the Other Wall

Y	Bi = 2		Bi = 10	Bi = ∞
	ψ_0	ψ_1	ψ_0	
0	0,5000	0,5000	0,1000	1)
0,1	0,5994	0,5912	0,1997	См. табл.
0,2	0,6952	0,6286	0,2972	6-8
0,3	0,7834	0,5662	0,3889	
0,4	0,8606	0,3866	0,4709	
0,5	0,9240	0,1158	0,5396	
0,6	0,9719	—0,1836	0,5923	
0,7	1,0041	—0,4403	0,6282	
0,8	1,0223	—0,6068	0,6486	
0,9	1,0295	—0,6778	0,6567	
1,0	1,0306	—0,6889	0,6580	

1) see Table 6-8.

Equation (6-61), as well as the first and third boundary conditions of (6-62), will be valid in this case, provided we replace t_s by t_1 in the expression for θ. In place of the second boundary condition of (6-62), we have the condition

$$\left(\frac{\partial\theta}{\partial Y}\right)_{Y=0} = \mathrm{Bi}\,\theta_{Y=0}.$$

 ~~re Y = " (the origin is shifted to the wall through which heat is exchanged).

The solution of this problem [6] has the form

$$\theta = \sum_{n=0}^{\infty} A_n \psi_n(Y) \exp\left(-\frac{1}{6} \epsilon_n^2 \frac{1}{Pe} \cdot \frac{x}{h}\right). \tag{11-26}$$

The mean mass temperature of the fluid is

$$\bar{\theta} = \sum_{n=0}^{\infty} B_n \exp\left(-\frac{1}{6} \epsilon_n^2 \frac{1}{Pe} \cdot \frac{x}{h}\right). \tag{11-27}$$

Tables 11-5 and 11-6 give values of the constants ϵ_n, A_n, B_n, and the eigenfunctions $\psi_n(Y)$ as functions of Bi.

The local value of the general Nusselt number is

$$Nu_K = \frac{Kh}{\lambda} = \frac{1}{6} \cdot \frac{\displaystyle\sum_{n=0}^{\infty} B_n \epsilon_n^2 \exp\left(-\frac{1}{6} \epsilon_n^2 \frac{1}{Pe} \cdot \frac{x}{h}\right)}{\displaystyle\sum_{n=0}^{\infty} B_n \exp\left(-\frac{1}{6} \epsilon_n^2 \frac{1}{Pe} \cdot \frac{x}{h}\right)}, \tag{11-28}$$

where K is the local coefficient of heat transfer from the fluid flowing in the tube to the surrounding medium.

The local value $Nu = \alpha h / \lambda$ is found from (11-13).

The limiting Nusselt numbers are

$$Nu_{K\infty} = \frac{\epsilon_0^2}{6}, \tag{11-29}$$

$$Nu_{\infty} = \frac{Bi \, \epsilon_0^2}{6 \, Bi - \epsilon_0^2}. \tag{11-30}$$
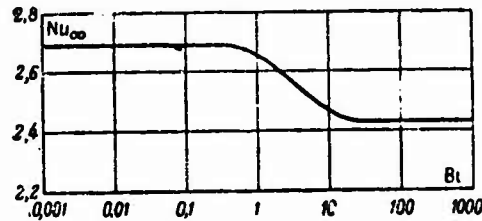
Fig. 11-8. Dependence of Nu_{∞} on Bi for flat tube with heating on one side.

As Bi varies from 0 to ∞, $Nu_{K\infty}$ varies from 0 to 2.43, and Nu_{∞} varies from 2.692 to 2.43. Figure 11-8 illustrates the dependence of Nu_{∞} on Bi. A substantial change in Nu_{∞} is found only within the relatively narrow range in Bi values between 0.6 and 10.

The length of thermal initial segment for a flat tube with heating on one side has the same value for t_1 = const as for t_s = const, i.e., $l_{n.t}/h = 0.21 Pe$.

The mean value of the general Nusselt number is

$$\overline{Nu}_\kappa = \frac{\overline{K}h}{\lambda} = -Pe \frac{h}{l} \ln \overline{\theta}_{x=l}. \qquad (11\text{-}31)$$

where $\overline{K}$ is the length-averaged coefficient of heat transfer between the fluid flowing in the tube and the surrounding medium.

Manuscript Page No.	Transliterated Symbols
261	c = s = stenka = wall
266	н.т = n.t = thermicheskiy nachal'nyy = thermal initial
266	л = 1 = logarifmicheskiy = logarithmic

Chapter 12

HEAT EXCHANGE IN THE HYDRODYNAMIC INITIAL SEGMENT OF ROUND AND FLAT TUBES

12-1. PRELIMINARY REMARKS

In the preceding chapters, we studied heat exchange for stabilized flow. In this case, if ρ and μ are constant, the velocity profile is parabolic over the entire length of the heat-exchange segment. Such a flow is realized in practice, when the heat-exchange segment is preceded by a sufficiently long stilling segment, along which the parabolic velocity profile is formed. In many heat-exchange devices, the tube fluid entrance coincides with the initial heat-exchange segment; such devices are often made from short tubes over which a parabolic velocity profile cannot form, or within which the formation process occupies a significant portion of the tube. In such case, the heat-exchange process takes place in the hydrodynamic initial segment, i.e., the velocity profile changes along the length of the tube. This problem is also of particular interest since laminar flow is maintained even for Re $\gg$ Re$_{kr}$ over a

certain portion of the length of the hydrodynamic initial segment. Thus, for example, under favorable entrance conditions, laminar flow is maintained up to Re $= 10^5$. Naturally, as Re increases, the length of the segment occupied by the laminar boundary layer is reduced.

The flow field in the initial segment can be divided into the dynamic boundary layer and the flow core. As we move away from the entrance, the thickness δ of the boundary layer increases, while the core section contracts, until the boundary layer fills the entire tube cross section at $x = l_{n.g}$ (Fig. 12-1). Beginning at this distance, the velocity profile ceases to vary with the length (see §5-4). The same scheme can be applied to the temperature field in the thermal initial segment. If Pe is sufficiently great, we can distinguish in the flow between a thermal boundary layer whose temperature varies along the normal to the wall, and an isothermal core whose temperature equals the temperature of the fluid at the entrance. The thickness Δ of the thermal boundary layer increases with distance from the entrance, while the section of the isothermal core contracts (Fig. 12-1). At a distance $x = l_{n.t}$ from the entrance, the boundary layer reaches the tube axis, and the isothermal core vanishes. As x increases further, the temperature at any point in the flow, even near the axis, will vary both radially and longitudinally.
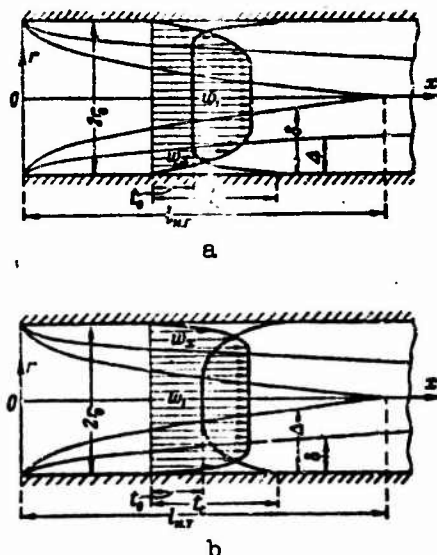
Fig. 12-1. Development of dyna-
mic and thermal boundary layers
in initial tube segment. a)
$\Delta < \delta$; b) $\Delta > \delta$.

Depending on Pr, the thickness of the thermal boundary layer
may be either greater (Pr < 1) or less (Pr > 1) than the thickness
of the dynamic boundary layer. When Pr = 1, these thicknesses will
be roughly the same.

The reduced lengths $\frac{1}{Pe}\cdot\frac{l_{\text{н.т}}}{d}$ and $\frac{1}{Re}\cdot\frac{l_{\text{н.г}}}{d}$ of the thermal and hydrodynamic
initial segments have roughly the same numerical values (in any case,
they are of the same order of magnitude). Equating these quantities,
we have

$$l_{\text{н.т}} \approx \Pr l_{\text{н.г}}.$$

Depending on the value of Pr, we can have three characteristic
cases Pr $\gg$ 1, $l_{\text{н.т}} \gg l_{\text{н.г}}$; 2) Pr $\ll$ 1, $l_{\text{н.т}} \ll l_{\text{н.г}}$ and 3) Pr $\approx$ 1; $l_{\text{н.т}} \approx l_{\text{н.г}}$. In the first case,
the velocity profile will be nearly parabolic over almost the entire
length of the thermal initial segment. Consequently, if the tube
length $l \geqslant l_{\text{н.т}}$, the heat transfer can be determined with a certain de-
gree of approximation from the equations for hydrodynamically stab-
ilized flow.

In the second case, when the velocity profile at the entrance
is uniform, the velocity profile will be nearly uniform over the
entire length of the thermal initial segment. If $l \leqslant l_{\text{н.т}}$, in this case,
then, with a certain error, the heat exchange can be determined on
the basis of the bar-flow model, i.e., we assume that the fluid
flow resembles the motion of a continuous solid bar, all points of
which have exactly the same velocity with respect to the stationary
walls. Naturally, if $l \leqslant l_{\text{н.г}}$, we can use the bar-flow model regardless
the value of Pr. In any case, such a scheme is useful for estimat-

ing the upper limit for heat transfer near the tube entrance (see §12-2).

In all cases other than 1 and 2, allowance must be made for the change in velocity profile with length when heat-exchange calculations are carried out.

12-2. HEAT EXCHANGE IN BAR FLOW

Let us consider heat exchange in round and flat tubes during bar flow, i.e., we assume $w_x = w_0 = $ const. Let the temperature of the fluid at the entrance and the wall temperature be constant and equal to t_0 and t_s, respectively, and let all remaining conditions be the same as in the corresponding problems of heat exchange during flow with a parabolic velocity profile (see §§6-1 and 6-2).

For a round tube, the energy equation and the boundary conditions will have the form

$$
\left.
\begin{aligned}
&\frac{\partial^2 \theta}{\partial R^2} + \frac{1}{R} \cdot \frac{\partial \theta}{\partial R} = \frac{\partial \theta}{\partial X}, \\
&\text{for } X = 0 \text{ and } 0 \leqslant R < 1 \quad \theta = 1, \\
&\text{for } X \geqslant 0 \text{ and } R = 1 \quad \theta = 0,
\end{aligned}
\right\}
\tag{12-1}
$$

where

$$
\theta = \frac{t - t_c}{t_0 - t_c}; \quad R = \frac{r}{r_0}; \quad X = \frac{4}{\text{Pe}} \cdot \frac{x}{d}; \quad \text{Pe} = \frac{w_0 d}{a}.
$$

From the mathematical viewpoint, this problem is identical to the problem of heat conduction in a long cylinder under unsteady conditions and boundary conditions of the first type. The solution methods for such problems are well known [1]. The solution of Problem (12-1), i.e., the expression for the temperature field in the fluid flow has the form

$$
\theta = \sum_{n=1}^{\infty} \frac{2}{\varepsilon_n J_1(\varepsilon_n)} J_0(\varepsilon_n R) \exp(-\varepsilon_n^2 X).
\tag{12-2}
$$

where the ε_n are the sequential roots of a zero-order Bessel function of the first kind, J_0; the roots have the following numerical values:

n	1	2	3	4	5	6
ε_n	2.4048	5.5201	8.6537	11.7915	14.9309	18.0711

where J_1 is a first-order Bessel function of the first kind.

The mean mass temperature of the fluid is

$$
\overline{\theta} = 2 \int_0^1 \theta R \, dR = \sum_{n=1}^{\infty} \frac{4}{\varepsilon_n^2} \exp(-\varepsilon_n^2 X).
\tag{12-3}
$$

The local Nusselt number is found from the equation

$$Nu=\frac{\alpha d}{\lambda}=-\frac{2}{\bar{\theta}}\left(\frac{\partial\theta}{\partial R}\right)_{R=1}.$$

Substituting in θ and $\bar{\theta}$ from (12-2) and (12-3), we find

$$Nu=\frac{\sum_{n=1}^{\infty}\exp(-\varepsilon_n^2 X)}{\sum_{n=1}^{\infty}\frac{1}{\varepsilon_n^2}\exp(-\varepsilon_n^2 X)}. \tag{12-4}$$

The limiting Nusselt number is

$$Nu_\infty=\varepsilon_1^2=5{,}783.$$

The length of the thermal initial segment is

$$\frac{l_{n.\tau}}{d}=0{,}0466Pe.$$

Figure 12-2 compares the Nu relationships in a round tube for bar flow and for flow having parabolic velocity profile. The difference is extremely significant. In accordance with what was said in §12-1, curve 1 corresponds to Pr = 0 and curve 3 to Pr → ∞. The relationships for finite values of Pr should lie between these curves.

For heat exchange in a flat tube, the energy equation and boundary conditions have the form

$$\left.\begin{array}{l}\dfrac{\partial^2\theta}{\partial Y^2}=\dfrac{\partial\theta}{\partial X},\\[2mm]\text{for } X=0 \text{ and } 0<Y<1 \ \ \theta=1,\\[2mm]\text{for } X\geqslant 0 \text{ and } Y=1 \ \ \theta=0,\end{array}\right\} \tag{12-5}$$

where $Y=\frac{y}{r_0}$; $X=\frac{4}{Pe}\cdot\frac{x}{h}$; $Pe=\frac{w_0 h}{a}$; $h=2r_0$ is the distance between the walls.

This problem is identical to the problem of unsteady heat conduction in an infinite plate under boundary conditions of the first kind. The solution has the form

$$\theta=\sum_{n=0}^{\infty}\frac{2}{\varepsilon_n\sin\varepsilon_n}\cos(\varepsilon_n Y)\exp(-\varepsilon_n^2 X), \tag{12-6}$$

where $\varepsilon_n=(2n+1)\frac{\pi}{2}$, $n=0, 1, 2\ldots$

The mean mass temperature of the fluid is

$$\bar{\theta}=\int_0^1\theta\,dY=\sum_{n=0}^{\infty}\frac{2}{\varepsilon_n^2}\exp(-\varepsilon_n^2 X). \tag{12-7}$$

The local Nusselt number is

$$Nu = \frac{\alpha h}{\lambda} = \frac{2 \sum\limits_{n=0}^{r} \exp(-\varepsilon_n^2 X)}{\sum\limits_{n=0}^{r} \frac{1}{\varepsilon_n^2} \exp(-\varepsilon_n^2 X)}. \qquad (12\text{-}8)$$

The limiting Nusselt number and the length of the thermal initial segment are

$$Nu_\infty = 2\varepsilon_0^2 = 4.935,$$

$$\frac{l_{n.r}}{h} = 0.0584 Pe.$$

The solution of Problem (12-5) can be represented in terms of the function erfc x [1], which is convenient for analysis when X is small.

2. Solutions have been given in §1 for two elementary heat-ex-change problems in bar flow. Many more such problems can be considered. If we neglect the influence of axial heat conduction, then the energy equation for bar flow reduces to the Fourier heat-conduction equation. There are well-developed methods for solving the heat-con-duction equation; solutions are also known for numerous problems of unsteady heat conduction. Under appropriate boundary conditions, these solutions are easily employed to determine heat exchange for bar flow. In particular, we can obtain heat-exchange equations for flows in tubes of different shapes (circular, flat, rectangular, etc.), under different boundary conditions at the wall (of the first, se-cond, or third kinds), and for a nonuniform temperature distribu-tion over the entrance cross section. Thus, for example, heat-exchange calculations have been carried out for the initial segments of flat and rectangular tubes under boundary conditions of the first kind for uniform and nonuniform temperature fields at the entrance [2, 3, 4].[1] Naturally, these results can only be used for quantitative es-timates of heat transfer if the tube length $l \ll l_{n.r}$.
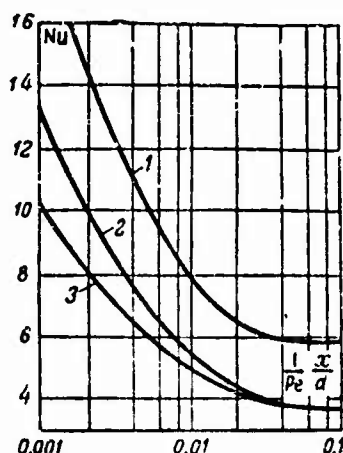

Fig. 12-2. Values of $Nu = f\left(\frac{1}{Pe} \cdot \frac{x}{d}\right)$ for round tube with $t_s = $ const.
1) Bar flow; 2) flow with variation in velocity profile along length, Pr = 0.7; 3) flow with parabolic velocity profile.

3. As we have already noted in §12-1, when Pr << 1 (for liquid metals, for example), $l_{H.T} \ll l_{H.\Gamma}$ and, consequently, we can use the bar-flow model to determine heat exchange in the thermal initial segment. Under these conditions, however, Pr is usually fairly small, so that it is necessary to consider the axial heat conduction.

Some problems of heat exchange during bar flow in round and flat tubes have been considered with allowance for axial heat conduction [5, 6]. In [5], solutions were obtained for two types of boundary conditions: a) with constant entrance temperature and constant temperature of surrounding medium (t_s = const in the special case); b) for a step variation in the temperature of the surrounding medium (step variation in t_s in the special case). In [6], the calculations were performed for an arbitrary change in q_s over the heating segment, and q_s = 0 for the stilling and exit segments.

Figures 12-3 and 12-4, taken from [5], give an idea as to the influence of axial heat conduction on heat exchange in a round tube and on the length of the thermal initial segment for t_0 = const and t_s = const. In these and other cases considered in [5], axial heat conduction had a substantial influence only within the thermal initial segment for values Pe < 100. The limiting value of Nu_∞ does not depend on Pe, and has the same value as was found earlier without regard to axial heat conduction (Nu_∞ = 5.783, see paragraph 1 of this section).

4. The bar-flow model can also be used to determine heat exchange for motion in tubes of free-flowing materials consisting of fine particles [7, 8, 9]. Observations show that when such a material moves as a continuous flow in a vertical tube under its own weight, the layer of particles experiencing deceleration at the wall is negligible. Thus the assumption that the velocity is constant over the cross section and the length is quite well satisfied.[2]
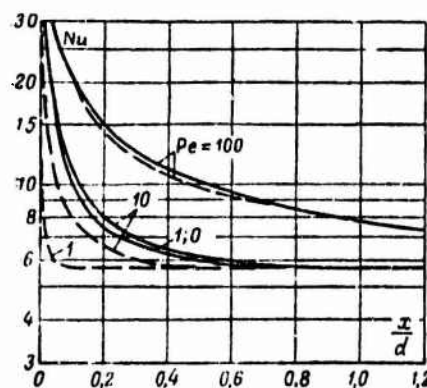

Fig. 12-3. Values of $Nu = f\left(\frac{x}{d}, Pe\right)$ for bar flow in a round tube with (solid lines) and without (dashed lines) allowance for axial heat conduction.
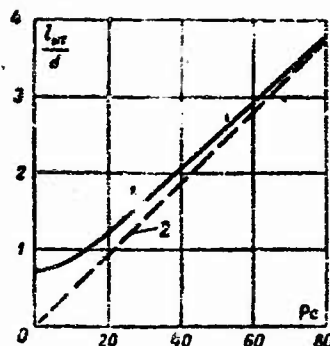
Fig. 12-4. Dependence of $l_{n.t}/d$
on Pe for ba. motion in round
tube. 1) With allowance for ax-
ial heat conduction; 2) with no
such allowance.

5. Utilization of the bar-flow model considerably simplifies
the analysis of heat-exchange processes. Thus such an approach is
often used to analyze complex heat-exchange processes even when
the condition requiring that the velocity be constant over the cross
section is not necessarily satisfied. Although such computations
give a qualitatively correct picture of the process, the quanti-
tative results may differ substantially from the actual values of
heat transfer (see, for example, Fig. 12-2).

12-3. HEAT EXCHANGE UNDER BOUNDARY CONDITIONS OF THE FIRST TYPE
WHEN VELOCITY PROFILE VARIES WITH LENGTH

A theoretical analysis has been given for heat exchange in
the hydrodynamic initial segments of round and flat tubes for uni-
formly distributed velocity and temperature at the entrance and
constant wall temperature [10-14]. In all these studies, the phy-
sical properties of the fluid were assumed to be constant, while
energy dissipation and axial heat conduction were neglected. An
experimental study of heat transfer near the entrance to a tube
has been reported in [15].

1. Let us first consider heat exchange in a round tube. Figure
12-2 (curve 2) shows the results of heat-transfer calculations,
based on published data [10, 11], for Pr = 0.7. A numerical method
was used, and the change in velocity profile was taken into account
by means of Eq. (5-33).[3] As we might expect, heat transfer is con-
siderably greater near the entrance than for stabilized flow (curve
3). This is explained by the fact that the velocity profile is so
full in the hydrodynamic initial segment as compared with the velo-
city profile far from the entrance; in addition, the transverse
velocity components present also play a certain role.

Stephan [12] has carried out a more complete investigation
into heat exchange in a round tube when the velocity profile var-
ies with the length. In the region of low reduced-length values,
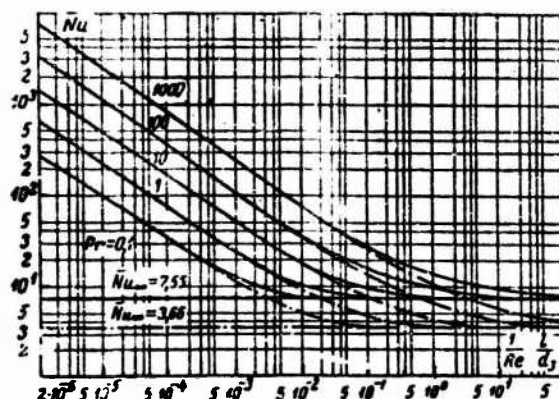where the thicknesses of the dynamic and thermal boundary layers

[3]/294   - 281 -

Fig. 12-5. Values of $\overline{Nu} = f\left(\frac{1}{Re} \cdot \frac{l}{d_a}, Pr\right)$ in hydrodynamic initial segment of round (dash-dot lines) and flat (solid lines) tubes at t_s = const.

are small, he used exact methods of boundary-layer theory for the calculations. In regions of large reduced-length values, where the velocity profile is nearly parabolic, he constructed approximate solutions for the temperature fields, resembling the solutions for stabilized flow, but with constants depending on Pr. Interpolation was used where these conditions are not satisfied.

Figure 12-5 shows the calculated results for Pr between 0.1 and 1000. The axis of ordinates shows $\overline{Nu} = \overline{\alpha} d_e/\lambda$, where $\overline{\alpha}$ is the length-averaged heat-transfer coefficient for the segment between $x = 0$ and $x = l$, referred to the mean logarithmic temperature head on this segment. The axis of abscissas shows the reduced length $\frac{1}{Re} \cdot \frac{l}{d_o}$, where $Re = w_o d_o/\nu$ [*]. For both round and flat tubes, heat transfer near the entrance is described, in approximation, by the equation for a plate in a longitudinal flow:

$$\frac{\overline{\alpha} l}{\lambda} = 0.664 \left(\frac{w_o l}{\nu}\right)^{1/2} Pr^{1/3},$$

in our notation,

$$\overline{Nu} = 0.664 \left(\frac{1}{Re} \cdot \frac{l}{d_o}\right)^{-1/2} Pr^{1/3} \quad [5] \tag{12-9}$$

This result is not surprising, since the boundary-layer thicknesses are small near the entrance, and the flow and heat-exchange conditions are independent of the shape and dimensions of the tube cross section, being close to the conditions for a plate in a longitudinal flow.[6] Far from the entrance, the velocity profiles are very nearly parabolic, and $\overline{Nu}$ becomes constant when $l > l_{n.t}$, having a value of 3.66 for a round tube and 7.54 for a flat tube.

The computational results for heat transfer in the hydrodynamic initial segment can be represented, approximately, as
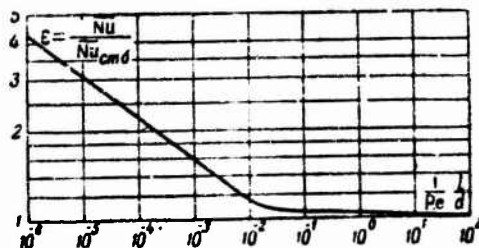
Fig. 12-6. Increase in heat
transfer in hydrodynamic ini-
tial segment of round tube for
t_s = const.

$$\varepsilon = \frac{\overline{Nu}}{\overline{Nu}_{cT6}} = f\left(\frac{1}{Re} \cdot \frac{x}{d_3}\right),$$

where Nu_{stb} is the length-averaged Nusselt number over the segment
between $x = 0$ and $x = l$ for stabilized flow (see Chapter 6). Figure
12-6 shows this relationship for a round tube. The values of $\overline{Nu}$ are
taken from Fig. 12-5, while the values of $\overline{Nu}_{stb}$ are computed from
Eqs. (6-26a) (following preliminary integration over the length)
and (6-29).

For heat exchange in a round tube, the relationship between
ε and the reduced lengt' ·.n be described to within about $\pm 5\%$ by
the equation

$$\varepsilon = \frac{\overline{Nu}}{\overline{Nu}_{cT6}} = 0,60\left(\frac{1}{Re} \cdot \frac{l}{d}\right)^{-1/7}\left(1 + 2,5\frac{1}{Re} \cdot \frac{l}{d}\right),\qquad (12\text{-}10)$$

which is valid for $\frac{1}{Re} \cdot \frac{l}{d} < 0,1.$

Equation (12-10) is in good agreement with experimental data
[15] (for $\mu_s/\mu_{zh} = 1$), but it does not allow for the way in which
heat exchange is influenced by changes in the fluid physical pro-
perties with temperature. For liquids, we need only consider the
influence of variable viscosity. Analysis of experimental data on
heat exchange for a flow of type MC oil (see §7-5), including
measurements in the hydrodynamic initial segment, shows that it
is possible to allow for the influence of variable viscosity by
means of the ratio $(\mu_s/\mu_{zh})^{-0.14}$, which has been used earlier for
the region of developed flow. This is quite clear from Fig. 12-7,
which shows experimental data for a wide range of μ_s/μ_{zh}. Thus if
we include the correction ε in (7-84), we obtain an equation that
will be valid for the entire flow region in the thermal initial
segment (including that portion over which the velocity profile
develops):

$$\overline{Nu} = 1,55\varepsilon\left(\frac{1}{Pe} \cdot \frac{l}{d}\right)^{-1/3}\left(\frac{\mu_c}{\mu_{\text{ж}}}\right)^{-0,14},\qquad (12\text{-}11)$$

where ε is found from the curve of Fig. 12-6 or from Eq. (12-10)

- 283 -

(or $\frac{1}{Re}\cdot\frac{l}{d}<0,1$). The computational method with Eq. (12-11) and it s limits of applicability are the same as for (7-84).[7]
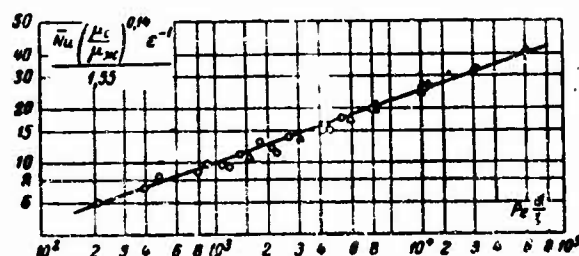
Fig. 12-7. Comparison of Eq. (12-11) with experimental data on heat exchange for flow of type MC oil.

$$\Delta - \frac{\mu_c}{\mu_{\text{ж}}} = 0,095 - 1; \quad O - \frac{\mu_c}{\mu_{\text{ж}}} = 1 - 670.$$
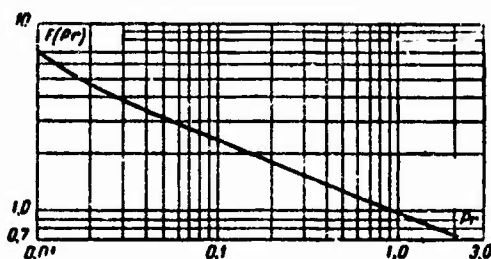
Fig. 12-8. The function $F(Pr)$.

2. The same method used for a round tube was employed by ephan to determine heat exchange in the hydrodynamic initial gment of a flat tube [12]. His results are illustrated in Fig. 12-5. Similar calculations, but employing approximate methods of boundary-layer theory, were carried out by Sparrow [13]. The com-utational results for $\frac{1}{Pe}\cdot\frac{l}{d_\bullet}<0,01$ can be described by the equation

$$\overline{Nu}=\frac{0,664}{F(Pr)}\left(\frac{1}{Re}\cdot\frac{l}{d_\bullet}\right)^{-1/2}\sqrt{1+C\left(\frac{1}{Re}\cdot\frac{l}{d_\bullet}\right)^n},\qquad(12\text{-}12)$$

where

$$\overline{Nu}=\frac{\bar{a}d_\bullet}{\lambda};\quad Re=\frac{w_0 d_\bullet}{v};$$

$$Pe=\frac{w_0 d_\bullet}{a};\quad d_\circ=2h.$$

For s $0,01 \leqslant Pr \leqslant 2$ the function $F(Pr)$ is found from the curve f Fig. 12-8, $C = 7.3$ and $n = \frac{1}{2}$; for $Pr > 2$, the function $F(Pr)=Pr^{-1/3}$, $C = 6,27$ and $n = \frac{4}{9}$.

The values of $\overline{Nu}$ found from the curves of Fig. 12-5 and Eq.

(12-12) agree to within 10-15%; this is apparently connected with the approximate nature of the calculations in [13].

12-4. HEAT EXCHANGE UNDER BOUNDARY CONDITIONS OF THE SECOND KIND WHEN THE VELOCITY PROFILE CHANGES WITH LENGTH

Let us investigate heat exchange in a round tube with a uniform distribution of velocity and temperature at the entrance and constant heat-flux density at the wall. We assume that the physical properties of the fluid are constant, and that energy dissipation is negligible; we also ignore heat-flux variations caused by axial heat conduction. The solution of this problem was given in [16].

Allowing for these conditions, we write the energy equation as

$$w_x \frac{\partial t}{\partial x} + w_r \frac{\partial t}{\partial r} = a \frac{1}{r} \cdot \frac{\partial}{\partial r} \left(r \frac{\partial t}{\partial r} \right). \qquad (12\text{-}13)$$

The temperature boundary conditions are

$$\left. \begin{array}{l} \text{for } x = 0 \text{ and } 0 \leqslant r < r_0, \ t = t_0, \\ \text{for } x \geqslant 0 \text{ and } r = r_0, \ \dfrac{\partial t}{\partial r} = \dfrac{q_c}{\lambda}. \end{array} \right\} \qquad (12\text{-}14)$$

Remembering that we shall later make use of the approximate method of boundary-layer theory, we apply Eq. (12-13) to the region of the thermal boundary layer. Transforming the left side with the aid of the equation of continuity, we obtain

$$\frac{\partial (w_x \vartheta)}{\partial x} + \frac{1}{r} \cdot \frac{\partial (w_r \vartheta r)}{\partial r} = a \frac{1}{r} \cdot \frac{\partial}{\partial r} \left(r \frac{\partial t}{\partial r} \right). \qquad (12\text{-}15)$$

where $\vartheta = t - t_0$; t_0 is the fluid temperature at the entrance.

We multiply this equation by $r\,dr$, and integrate it over the thickness Δ of the thermal boundary layer, i.e., between $(r_0 - \Delta)$ and r_0:

$$\int\limits_{(r_0 - \Delta)}^{r_0} \frac{\partial (w_x \vartheta)}{\partial x} r\, dr + w_r \vartheta r \Big|_{r_0 - \Delta}^{r_0} = ar \frac{\partial \vartheta}{\partial r} \Big|_{r_0 - \Delta}^{r_0}.$$

The second term on the left side equals zero, since $(w_r)_{r=r_0} = 0$ and $\vartheta_{r=r_0 - \Delta} = 0$. The right side equals

$$ar \frac{\partial \vartheta}{\partial r} \Big|_{r_0 - \Delta}^{r_0} = ar_0 \left(\frac{\partial \vartheta}{\partial r} \right)_{r=r_0} = \frac{r_0}{\rho c_p} q_c,$$

since

$$\left(\frac{\partial \vartheta}{\partial r} \right)_{r=r_0 - \Delta} = 0.$$

Changing the sequence of differentiation and integration in the first term on the left side of the equation, we arrive at the relationship

- 285 -

$$\frac{d}{dx} \int_{r_0-\Delta}^{r_0} w_x \theta r \, dr = \frac{r_0}{\kappa_p} q_1. \qquad (12\text{-}16)$$

Integrating (12-16) between $x = 0$ and x, and going over to dimensionless variables, we obtain integral relationships of the following form:

If $\Delta \leq \delta$, then

$$\int_{1-\Delta}^{1} W_x \theta R \, dR = 4 \frac{1}{Pe} \cdot \frac{x}{d}; \qquad (12\text{-}17)$$

if $\Delta > \delta$, then

$$\int_{1-\tilde{\delta}}^{1} W_x \theta R \, dR + \int_{1-\tilde{\Delta}}^{1-\tilde{\delta}} W_1 \theta R \, dR = 4 \frac{1}{Pe} \cdot \frac{x}{d}. \qquad (12\text{-}17a)$$

where

$$\tilde{\Delta} = \frac{\Delta}{r_0}; \quad \tilde{\delta} = \frac{\delta}{r_0};$$

$$R = \frac{r}{r_0}; \quad W_x = \frac{w_x}{w_0}; \quad W_1 = \frac{w_1}{w_0};$$

$$\theta = \frac{(t - t_0)\lambda}{q c r_0}; \quad Pe = \frac{w_0 2 r_0}{a};$$

Here Δ and δ are the thicknesses of the thermal and hydrodynamic boundary layers; w_0 and w_1 are the velocities of the fluid at the entrance and in the flow core (i.e., at the external boundary of the boundary layer).

To use Relationships (12-17) and (12-17a), we must know the $W_x(R)$ and $\theta(R)$ distributions over the boundary-layer thickness.

The velocity distribution over the cross section of the dynamic boundary layer is described by the equation

$$W_x = W_1 \left[2 \frac{1-R}{\tilde{\delta}} - \frac{(1-R)^2}{\tilde{\delta}^2} \right] \quad (1 - \tilde{\delta} < R < 1). \qquad (5\text{-}25)$$

and the velocity in the core by the equation

$$W_1 = \frac{6}{6 - 4\tilde{\delta} + \tilde{\delta}^2} \quad (0 < R < 1 - \tilde{\delta}). \qquad (5\text{-}26)$$

The dimensionless thickness $\tilde{\delta}$ of the dynamic boundary layer can be computed from Eq. (5-29) or with the aid of one of the equations for $W(X, R)$ given in §5-4. We use Eq. (5-33). Letting $R = 0$ in this equation, we obtain $W_1 = f\left(\frac{1}{Re} \cdot \frac{x}{d}\right)$ (see Fig. 5-11). With this relationship and (5-26), it is easy to compute $\tilde{\delta}$ for various values of $\frac{1}{Re} \cdot \frac{x}{d}$. The results of this computation are shown in Table 12-1.

Equations (5-25) and (5-26), together with Table 12-1, com-

TABLE 12-1

Value of $\tilde{\delta}$ as function of $\dfrac{1}{Re}\cdot\dfrac{x}{d}$

$\dfrac{1}{Re}\cdot\dfrac{x}{d}$	$\tilde{\delta}=\dfrac{\delta}{r_0}$
$8.35\cdot10^{-6}$	0.1
$3.95\cdot10^{-4}$	0.2
$9.75\cdot10^{-4}$	0.3
$2.00\cdot10^{-3}$	0.4
$3.53\cdot10^{-3}$	0.5
$5.8\cdot10^{-3}$	0.6
$9.18\cdot10^{-3}$	0.7
$1.46\cdot10^{-2}$	0.8
$2.51\cdot10^{-2}$	0.9
$6.43\cdot10^{-2}$	0.99

pletely deter ι $\exists$ the velocity distribution in the hydrodynamic initial segment. With an increase in $\dfrac{1}{Re}\cdot\dfrac{x}{d}$ $\tilde{\delta}\to1$, $W_r\to 2$ and $W_x\to2(1-R^2)$, i.e., the velocity distribution in the initial segment goes over to the parabolic profile for stabilized flow.

The function selected for $\theta(R)$ must, first, satisfy the following boundary conditions at the external boundary of the thermal boundary layer and at the wall:

$$\theta_{R=1-\tilde{\Delta}}=0, \quad \left(\frac{\partial\theta}{\partial R}\right)_{R=1-\tilde{\Delta}}=0, \\ \left(\frac{\partial\theta}{\partial R}\right)_{R=1}=1, \quad \left(\frac{\partial^2\theta}{\partial R^2}\right)_{R=1}=-1, \qquad (12\text{-}18)$$

(this last condition follows from the energy equation at $R=1$) and, second, when $\tilde{\Delta}=1$ it must go over to the familiar expression for the temperature field in the case of stabilized heat exchange:

$$t-t'_0=\frac{q_c r_0}{\lambda}\left[\left(\frac{r}{r_0}\right)^2-\frac{1}{4}\left(\frac{r}{r_0}\right)^4\right], \qquad (12\text{-}19)$$

where t'_0 is the temperature on the tube axis (for $\tilde{\Delta}<1$ $t'_0=t_0$.

This last condition is unconditionally valid if $\tilde{\Delta}\leqslant\tilde{\delta}$ If $\tilde{\Delta}>\tilde{\delta}$, however, it will not be satisfied, strictly speaking since the velocity profile will then cease to be parabolic. On the assumption that this difference is not great, we take (12-19) to be valid in approximation for $\tilde{\Delta}>\tilde{\delta}$ as well.

In first approximation, we can use (12-19) as the unknown function in the thermal-boundary-layer region at the initial tube segment; we then replace r_0 by $\Delta(x)$. The quantity $r/r_0 = 1 - y/r_0$ must be replaced by $1-\frac{y}{\Delta}=1-\frac{r_0}{\Delta}+\frac{r}{\Delta}$. As a result, we obtain the expression

$$\theta=\tilde{\Delta}\left[\left(1-\frac{1}{\tilde{\Delta}}+\frac{R}{\tilde{\Delta}}\right)^2-\frac{1}{4}\left(1-\frac{1}{\tilde{\Delta}}+\frac{R}{\tilde{\Delta}}\right)^4\right].$$

which satisfies all of the conditions formulated. Calculations carried out by means of this equation show, however, that it does not satisfactorily describe the temperature distribution over the boundary-layer cross section. Significantly better results can be obtained if we add a term containing the logarithmic to this equation.[8] Thus we finally represent the function $\theta(R)$ in the form

$$\theta=\tilde{\Delta}\left[\xi^2-\frac{1}{4}\xi^4+(1-\tilde{\Delta})(\xi\ln\xi)^2\right], \qquad (12\text{-}20)$$

where $\xi=1-\frac{1}{\tilde{\Delta}}+\frac{R}{\tilde{\Delta}}$

This function also satisfies all the conditions indicated above. It still contains an unknown quantity, the dimensionless thickness $\tilde{\Delta}(x)$ of the thermal boundary layer.

To determine $\tilde{l}$, we substitute the value of $W_x(R)$, found from (5-25) and (5-26) into integral relationship (12-17), together with the value of $\Theta(R)$ from (12-20). After integration we obtain

$$\frac{6\tilde{\Delta}^2}{(6-4\tilde{\delta}+\tilde{\delta}^2)\tilde{\delta}}\left[\frac{3}{20}-\frac{13}{420}(1+2\tilde{\delta})\frac{\tilde{\Delta}}{\tilde{\delta}}+\frac{53}{3360}\cdot\frac{\tilde{\Delta}^2}{\tilde{\delta}^2}\right]+$$

$$+\frac{6\tilde{\Delta}^2}{6-4\tilde{\delta}+\tilde{\delta}^2}\left\{(1-\tilde{\Delta})^2\left[\frac{2}{27}\left(2\frac{\tilde{\Delta}}{\tilde{\delta}}-\frac{\tilde{\Delta}^2}{\tilde{\delta}^2}\right)-\right.\right.$$

$$-\frac{2}{32}\cdot\frac{\tilde{\Delta}}{\tilde{\delta}}\left(1-\frac{\tilde{\Delta}}{\tilde{\delta}}\right)+\frac{2}{125}\cdot\frac{\tilde{\Delta}^2}{\tilde{\delta}^2}\right]+(1-\tilde{\Delta})\tilde{\Delta}\left[\frac{1}{32}\cdot\frac{\tilde{\Delta}}{\tilde{\delta}}\left(2-\frac{\tilde{\Delta}}{\tilde{\delta}}\right)-\right.$$

$$\left.\left.-\frac{4}{125}\cdot\frac{\tilde{\Delta}}{\tilde{\delta}}\left(1-\frac{\tilde{\Delta}}{\tilde{\delta}}\right)+\frac{1}{108}\cdot\frac{\tilde{\Delta}^2}{\tilde{\delta}^2}\right]\right\}=4\frac{1}{Pe}\cdot\frac{x}{d}. \qquad (12\text{-}21)$$

Equation (12-21) is valid for the case in which $\tilde{\Delta}<\tilde{\delta}$. Using integral relationship (12-17a), we can without difficulty obtain an analogous equation for $\tilde{\Delta}>\tilde{\delta}$.

Since we know the relationship between $\tilde{\delta}$ and $\frac{1}{Re}\cdot\frac{x}{d}$, we can use (12-21) to determine the thickness $\tilde{\Delta}$ of the thermal boundary layer as a function of $\frac{1}{Pe}\cdot\frac{x}{d}$ and Pr; we can then determine the temperature field and heat-transfer coefficient.

By definition, the local heat-transfer coefficient equals

$$\alpha=\frac{q_c}{t_c-\bar{t}}.$$

For the case in which $\tilde{\Delta}<1$ (here $t_0'=t_0$), we can represent $t_s-\bar{t}$ as

$$t_c-\bar{t}=(t_c-t_0')-(\bar{t}-t_0). \qquad (12\text{-}22)$$

When $R=1$, we obtain the following expression from (12-20):

$$t_c-t_0'=t_c-t_0=\frac{3}{8}\cdot\frac{q_c d}{\lambda}\tilde{\Delta}.$$

It follows from the heat balance that

$$\bar{t}-t_0=\frac{2q_c x}{w_0 c_p r_0}=4\frac{q_c d}{\lambda}\cdot\frac{1}{Pe}\cdot\frac{x}{d}.$$

Thus when $\tilde{\Delta}<1$, the expression for the local Nu number will have the form

$$Nu=\frac{\alpha d}{\lambda}=\frac{1}{\frac{3}{8}\tilde{\Delta}-4\frac{1}{Pe}\cdot\frac{x}{d}}. \qquad (12\text{-}23)$$

This expression is valid both for $\tilde{\Delta}<\tilde{\delta}$ and for $\tilde{\Delta}>\tilde{\delta}$.

Beginning with the reduced-length value for which $\tilde{\Delta}$ becomes unity, we must distinguish two cases: $\Delta<\delta$ and $\Delta>\delta$.

- 288 -

In the first case $(\tilde{\Delta} \leqslant \tilde{\delta})$, velocity-profile stabilization terminates before, or at the same time as, temperature-profile stabilization. Thus as soon as Δ becomes unity, stabilization of the heat-exchange process occurs and Nu takes on the constant (limiting) value

$$Nu_\infty = \frac{1}{\frac{3}{8} - 4 \frac{1}{Pe} \cdot \frac{l_{\text{s.т}}}{d}}.$$

If we let $\tilde{\delta} = 1$ and $\tilde{\Delta} = 1$, we can find the reduced length of the thermal initial segment from (12-21); it equals $\frac{1}{Pe} \cdot \frac{l_{\text{s.т}}}{d} = 0{,}0365$. Consequently, $Nu_\infty = 4.36$, which corresponds to the previous results.

In the second case $(\tilde{\Delta} > \tilde{\delta})$, the velocity profile will change even after $\tilde{\Delta}$ has become equal to unity. Thus the heat-exchange process is stabilized only in the tube cross section at which the velocity profile has become stabilized. We cannot use Eq. (12-22) for the segment over which $\Delta = 1$, and $\delta < 1$, since $t_0' \neq t_0$. For this segment, we can determine $t_s - \bar{t}$ from the relationship

$$t_c - \bar{t} = \frac{2}{w_c r_0^2} \left[\int_0^{r_0 - \delta} (t_c - t) w_s r \, dr + \int_{r_0 - \delta}^{r_0} (t_c - t) w_x r \, dr \right].$$

When $\tilde{\Delta} = 1$, Eq. (12-20) goes over to (12-19). Using (12-19), (5-25) and (5-26), we find $t_s - \bar{t}$ and then Nu. As a result, we have

$$Nu = \frac{6 - 4\tilde{\delta} + \tilde{\delta}^2}{1 - \frac{1}{2}\tilde{\delta}^2 + \frac{1}{10}\tilde{\delta}^3 + \frac{3}{20}\tilde{\delta}^4 - \frac{1}{14}\tilde{\delta}^5 + \frac{1}{112}\tilde{\delta}^6}. \qquad (12\text{-}24)$$

When $\tilde{\delta} = 1$, $Nu = Nu_\infty = 4.36$. Here the length of the thermal initial segment corresponds to the length of the hydrodynamic initial segment, and it can be found from Table 12-1 as the value of the argument for which $\tilde{\delta} = 0{,}99$.

$$\frac{1}{Re} \cdot \frac{l_{\text{н.т}}}{d} \approx 0{,}064, \text{ or } \frac{1}{Pe} \cdot \frac{l_{\text{н.т}}}{d} \approx \frac{0{,}064}{Pr}.$$

The values of Nu have been computed in the $10^{-7} < \frac{1}{Pe} \cdot \frac{x}{d} < 10^{-1}$ range for $Pr = 0.7$, 1, 10, 100, 1000 and ∞. The computational results are shown in Fig. 12-9. As we might expect, for the same value of $\frac{1}{Pe} \cdot \frac{x}{d}$, Nu will be larger the smaller Pr.

The curve for $Pr \to \infty$ represents a limit, and corresponds to parabolic distribution of the velocity over the entire tube length. This curve coincides with the exact solution (8-13), with the exception of a narrow region of values of $\frac{1}{Pe} \cdot \frac{x}{d}$ (from $2 \cdot 10^{-2}$ to $7 \cdot 10^{-2}$), where the difference amounts to -5%.

For small values of $\frac{1}{Pe} \cdot \frac{x}{d}$, when the velocity profile is parabolic it is not difficult to obtain an asymptotic expression for Nu. In this case $\tilde{\Delta} \ll 1$ and $\tilde{\delta} = 1$, Eq. (12-21) takes the form

$$2\tilde{\Delta}' \cdot \frac{3}{20} + 2\left(\frac{1}{2\tilde{r}} - \frac{2}{3\tilde{z}}\right)\tilde{\Delta}' = 4\frac{1}{Pe} \cdot \frac{x}{d},$$

i.e.,

$$\tilde{\Delta}' = 8{,}5\frac{1}{Pe} \cdot \frac{x}{d}.$$

Determining $\tilde{\Delta}$ from this, we substitute it into (12-23); neglecting $4\frac{1}{Pe} \cdot \frac{x}{d}$, which is small in comparison with $\frac{3}{8}\tilde{\Delta}$, we obtain

$$Nu = 1{,}31\left(\frac{1}{Pe} \cdot \frac{x}{d}\right)^{-1/3}, \qquad (12\text{-}25)$$

which is in very good agreement with Eq. (8-14).
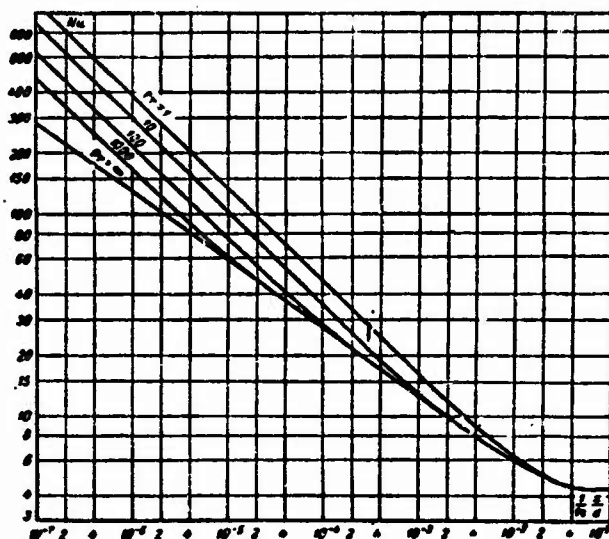
Fig. 12-9. Value of Nu in initial
segment of round tube when velocity
profile varies along the length, q_s =
= const.

When $\frac{1}{Re} \cdot \frac{x}{d}$ is small, i.e., near the tube entrance, where the boundary-layer thicknesses are small, we can obtain another asymptotic expression for Nu. When $\tilde{\delta} \ll 1$ and $\tilde{\Delta} \ll 1$, Expression (12-21) takes the form

$$\frac{\tilde{r}_1}{\tilde{\delta}}\left(0{,}2355 - 0{,}0265\frac{\tilde{\Delta}}{\tilde{\delta}}\right) = 4\frac{1}{Pe} \cdot \frac{x}{d}.$$

The computational results whos that the ratio $\tilde{\Delta}/\tilde{\delta}$ depends basically just on Pr, while when $0{,}7 \leqslant Pr \leqslant 1000$ and $\frac{1}{Re} \cdot \frac{x}{d} \leqslant 4 \cdot 10^{-4}$ (or $10 \leqslant Pr \leqslant 1000$ and $\frac{1}{Re} \cdot \frac{x}{d} \leqslant 2 \cdot 1$), it is described by the equation

$$\frac{\tilde{\Delta}}{\tilde{\delta}} = 0{,}54\,Pr^{-1/3}.$$

Substituting this value into the preceding equation, we find

- 290 -

$$0.54 \tilde{\Lambda}^+ Pr^{-1/3} (0.2355 - 0.043 \, Pr^{-1/3}) = 4 \frac{1}{Pe} \cdot \frac{x}{d}.$$

Since the second term in parentheses is small as compared with the first, we take an approximate estimate, letting $Pr = 1$. We then obtain

$$\tilde{\Delta} = 5.80 \left(\frac{1}{Pe} \cdot \frac{x}{d} \right)^{1/2} Pr^{1/6}.$$

Substituting this expression into (12-23) and neglecting $4 \frac{1}{Pe} \cdot \frac{x}{d}$ since it is so small, we obtain

$$Nu = 0.46 \left(\frac{1}{Re} \cdot \frac{x}{d} \right)^{-1/2} Pr^{1/3}. \tag{12-26}$$

This equation coincides exactly with the equation for local heat transfer for a plate in a longitudinal flow when $q_s = $ const [17]. Thus for the case in which $t_s = $ const as well, heat transfer near the entrance is described in approximation by the flat-plate relationship, for $q_s = $ const.

Fig. 12-10. Increase in heat transfer in hydrodynamic initial segment of round tube at $q_s = $ const. Curve) Equation (12-27); circles) experimental data.
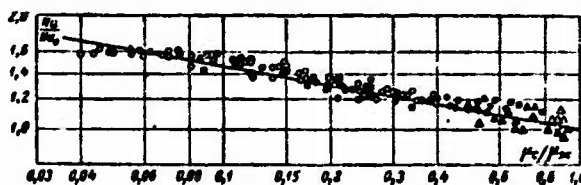
Fig. 12-11. Ratio Nu/Nu_0 as function of μ_s/μ_{zh} for type BM-4 oil (circles) and water (triangles). Empty circles correspond to developed flow and black circles to the hydrodynamic initial segment.

The following interpolation equation can be recommended for the entire region of values of $1/Re \cdot x/d$, corresponding to the hydrodynamic initial segment (with the exception of very small values):

$$\frac{Nu}{Nu_{stb}} = 0.35 \left(\frac{1}{Re} \cdot \frac{x}{d} \right)^{-1/6} \left[1 + 2.85 \left(\frac{1}{Re} \cdot \frac{x}{d} \right)^{0.42} \right]. \tag{12-27}$$

where Nu_{stb} is the Nusselt number for stabilized flow with $q_s = $ const (see §8-1). This equation describes the computational results within the $10^{-4} \leqslant \frac{1}{Re} \cdot \frac{x}{d} \leqslant 0.064$ and $0.7 \leqslant Pr \leqslant 1000$ ranges to within about 6%. For values of $\frac{1}{Re} \cdot \frac{x}{d} > 0.064$, the velocity profile becomes

- 291 -

parabolic and, consequently, Nu = Nu_{stb}. Equation (12-27) is compared with experimental data [18] in Fig. 12-10. Here only data for water at low temperature heads are plotted [$t_s - \bar{t}$ = (2-10)°C] so as to minimize the influence of the temperature dependence of physical properties. It can be seen that the calculated and experimental data are in satisfactory agreement The spread that is present in the experimental points is evidently associated with the difficulties of experimentation at low temperature heads.

Experimental data for water and type BM-4 oil, covering the hydrodynamic initial segment and the region of developed flow (see §9-1, paragraph 2) were used to allow for the influence of variable viscosity on heat exchange in flow of liquids in the presence of large temperature gradients. These data are shown in Fig. 12-11 as the relationships between Nu/Nu_0 and μ_s/μ_{zh}, where Nu is the Nusselt number found experimentally, and Nu_0 is computed from Eq. (12-27) (i.e., for constant physical properties). We can see that

$$\frac{Nu}{Nu_0} \approx \left(\frac{\mu_c}{\mu_{\text{m}}}\right)^{-1/8}$$

not only for developed flow, but also in the hydrodynamic initial segment. Using Relationship (8-15) for Nu_{stb}, we arrive at the equation

$$Nu = 1.31\varepsilon\left(\frac{1}{Pe}\cdot\frac{x}{d}\right)^{-1/3}\left(1+2\frac{1}{Pe}\cdot\frac{x}{d}\right)\left(\frac{\mu_c}{\mu_{\text{m}}}\right)^{-1/8}, \qquad (12\text{-}28)$$

where

$$\varepsilon = 0.35\left(\frac{1}{Re}\cdot\frac{x}{d}\right)^{-1/6}\left[1+2.85\left(\frac{1}{Re}\cdot\frac{x}{d}\right)^{0.42}\right].$$
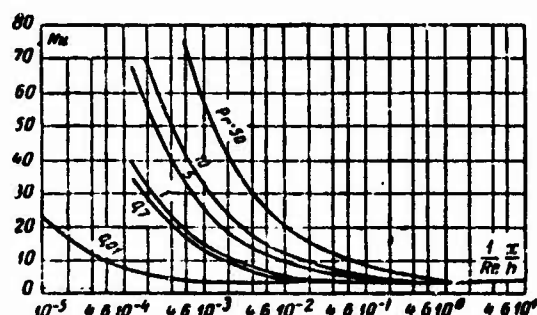

Fig. 12-12. Heat transfer in hydrodynamic initial segment of flat tube for q_s = const.

The heat-transfer coefficient in (12-28) refers to the local temperature head $t_s - \bar{t}$, while the physical properties of the liquid in the expressions for Nu, Pe, and Re are chosen at $t = \frac{1}{2}(t_c + \bar{t})$.

Equation (12-28) encompasses the entire flow region in the thermal initial segment, including the portion over which the velocity profile is formed. In the rest of the region, (12-28) is used, like (9-19) for developed flow (see §9-1, paragraph 2).

The dependence of ρ, c_p, μ, and λ on T must be taken into account for gas flowing at high temperature gradients. The heat transfer and resistance in this case can be determined by numerical integration of the system of energy, motion, and continuity equations, written in approximation for the boundary layer. Such calculations have been carried out, for example, in [19] for helium flowing in a round tube with uniform distribution of velocity and temperature at the entrance, and constant heat-flux density at the wall. The calculations show that if the physical properties in the expressions for Nu and ξ are selected for a mean mass temperature $\overline{T}$ of the gas, then in the hydrodynamic initial segment (which coincides with the thermal initial segment in this case), Nu will depend little on q_s (or $T_s/\overline{T}$); at the same time, ξ varies quite sharply. Thus, for example, when the parameter $q_s d/T_0\lambda_0$ changes from 0 to 27, Nu changes by 5-10%, while ξ increases by roughly a factor of 2 (here λ_0 is the thermal-conductivity coefficient of the gas or the entrance temperature T_0).

2. Siegel and Sparrow [20] have solved the problem of heat exchange in a flat tube with uniform velocity and temperature distribution at the entrance and constant and identical heat-flux densities at the two walls. The solution was obtained by the same method and under the same basic assumptions as in paragraph 1. The final results are shown in Fig. 12-12 as the dependence of Nu on $\frac{1}{Re}\cdot\frac{x}{h}$ and Pr. Here $Nu = \alpha h/\lambda$ and $Re = w_0 h/\nu$ (h is the distance between the walls).

Heat exchange in the hydrodynamic initial segment of a flat tube for constant heat-flux density at one wall, with the other wall heat-insulated, has been considered in [21]. The values of $Nu = \alpha d_9/\lambda$ at the heated wall and the adiabatic temperature $\theta_{a.s} = \frac{t_{a.c} - \overline{t}}{q_s d_9/\lambda}$ at the heat-insulated wall are given in Table 12-2.

TABLE 12-2

Values of Nu at Heated Wall and $\theta_{a.s}$ at Heat-Insulated Wall of Flat Tube with Uniform Velocity Profile at Entrance

$\frac{1}{Pr}\cdot\frac{x}{d_9}$	Pr = 10		Pr = 0.7		Pr = 0.01	
	Nu	$\theta_{a.c}$	Nu	$\theta_{a.c}$	Nu	$\theta_{a.c}$
0,00010	40,4	—0,000200	52,8	—0,000200	—	—0,000200
0,0010	15,56	—0,00200	18,50	—0,00200	24,2	—0,00200
0,0025	11,46	—0,00500	12,60	—0,00500	15,8	—0,00500
0,0050	9,20	—0,0100	9,62	—0,0100	11,7	—0,0100
0,010	7,49	—0,0199	7,68	—0,0200	8,80	—0,0200
0,025	6,09	—0,0433	6,13	—0,0433	6,48	—0,0480
0,050	5,55	—0,0589	5,55	—0,0589	5,77	—0,0655
0,10	5,40	—0,0639	5,40	—0,0639	5,53	—0,0680
0,25	5,39	—0,0643	5,39	—0,0643	5,47	—0,0660
∞	5,39	—0,0643	5,39	—0,0643	5,39	—0,0643

A cer*ain generalization of the integral method for determining t'* boundary layer in the initial tube segment has been given in [22]. In this generalized form, tne method can also be used to determine heat exchange in prismatic tubes. The calculations are only carried out for a flat tube, however. They agree well with the data of Fig. 12-12.

Manu-script Page No.	Footnotes

279   [1]In these studies, an attempt was made to allow for the influence of convective heat transfer along the normal to the wall (i.e., for the term $w, \frac{\partial t}{\partial y}$, missing from the heat-conduction equation) as well as for the influence of the deviation of the actual velocity profile from the uniform profile. For this purpose, a correction is introduced into the initial heat-conduction equation in the form of a constant factor. The value of this correction is found later by comparing the solution to the problem of a plate in a longitudinal bar flow with the known exact solution of this problem.

280   [2]We note that in such calculations, the physical properties of the free-flowing material (ρ, λ, a) for a state of motion, or for the so-called limiting shear. These properties differ from the properties of the material when stationary.

281   [3]In [11], in contrast to [10], the heat-transfer calculat*ons take into account the transverse velocity component, which makes it possible to refine the data of [10] by as much as 15%. Figure 12-2 shows the data of [11].

282   [4]In addition to the round-tube data, Fig. 12-5 gives the same author's data for a flat tube. Thus the equivalent diameter is taken as the characteristic dimension.

.*.   [5]In the equation for the plate, $\bar{\alpha}$ is referred to the initial temperature head, and in Eq. (12-9) to the mean logarithmic head. The difference is slight for small x, however.

282   [6]This is so provided the mean radius of curvature for the section perimeter substantially exceeds the boundary-layer thickness. K.D. Voskresenskiy has called attention to this fact.

*84   [7]Equation (12-11) refers to the case in which the tube fluid entrance coincides with the initial heated segment. If there is an unheated segment of length $l' < l_{n.g}$, then

we can use (12-11) with a certain degree of approximation, substituting the sum $l' + l$ in place of l in the equation for $\frac{1}{Re} \cdot \frac{l}{d}$. If $l' \geq l_{n.g}$, then Eq. (7-84) is valid or, what is the same thing, (12-11) with $\varepsilon = 1$.

287   'We can see that the function $\Theta(R)$ must contain the logarithm by analyzing the energy equation, using the method of successive approximations.

Manuscript Page No.	Transliterated Symbols
275	кр = kr = kriticheskiy = critical
275	н.г = n.g = nachal'nyy gidrodinamicheskiy = hydrodynamic initial
275	н.т = n.t = nachal'nyy thermicheskiy = thermal initial
	с = s = stenka = wall
282	э = e = ekvivalentnyy = equivalent
283	стб = stb = stabilizorovannyy = stabilized
283	ж = zh = zhidkost' = fluid, liquid
293	a.c = a.s = adiabaticheskiya stenka = adiabatic wall

Chapter 13

HEAT EXCHANGE IN TUBES OF ANNULAR CROSS SECTION

13-1. HEAT EXCHANGE UNDER BOUNDARY CONDITIONS OF THE FIRST KIND WITH STABILIZED FLOW

Technology makes wide use of heat-exchange equipment in which a fluid moves within an annular tube formed by two coaxial cylinders, with heat exchanged through one or both walls of the annular tube. Examples are exchangers of the "tube-in-tube," Field-tube, and similar types.

Heat exchange calculations for annular tubes can be carried out by the same method used for round or flat tubes (see Chapters 6 and 8). The computations are more complex, however, since an additional parameter appears in the form of the ratio of the radii of the inner and outer tubes. Quite diverse boundary conditions at the walls can also occur for annular tubes.

1. Let us first consider the case of fully developed (stabilized) flow and heat exchange when one wall is at constant temperature and the other is heat-insulated. We assume that the physical properties of the fluid are constant, and ignore heat conduction along the axis and the heat of friction. We use the method of successive approximations (iterations) developed by Reichardt [1], and subsequently applied in [2, 3] to problems of heat exchange with laminar flow in tubes. The method is based on utilization of two relationships connecting the temperature distribution and distribution of heat-flux density over the tube cross section. We first set up these relationships for the case in which a constant temperature t_{s1} is set up at the inside tube wall (Fig. 13-1), while the outside wall is heat-insulated, i.e., $\left(\frac{t}{\partial r}\right)_{r=r_2}=0$.

For hydrodynamic stabilization of the flow, heat is transported normal to the wall solely by conduction. Thus we can write the ratio of the heat-flux densities at an arbitrary point and at the wall in the following form:

$$\frac{q}{q_{r_1}} = \frac{\frac{\partial t}{\partial r}}{\left(\frac{\partial t}{\partial r}\right)_{r=r_1}}.$$

Integrating this expression, we find

$$\frac{t-t_{c_1}}{\left(\frac{\partial t}{\partial r}\right)_{r=r_1}} = \int_{r_1}^{r} \frac{q}{q_{c_1}}\, dr; \quad \frac{t_{c_2}-t_{c_1}}{\left(\frac{\partial t}{\partial r}\right)_{r=r_1}} = \int_{r_1}^{r_2} \frac{q}{q_{c_1}}\, dr.$$

Dividing the **first integral by the second,** we obtain the first relationship in which we are interested:
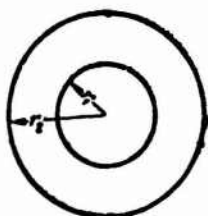
Fig. 13-1.
The Problem
of heat ex-
change in
an annular
tube.

$$\theta = \frac{\displaystyle\int_{R_1}^{R} \frac{q}{q_c}\, dR}{\displaystyle\int_{R_1}^{1} \frac{q}{q_{c_1}}\, dR}, \qquad (13\text{-}1)$$

where

$$\theta = \frac{t-t_{c_1}}{t_{c_2}-t_{c_1}}; \quad R = \frac{r}{r_2};$$
$$R_1 = \frac{r_1}{r_2} \text{ and } R_2 = \frac{r_2}{r_2} = 1.$$

To obtain the second relationship, we make use of the energy equation

$$w_x \frac{\partial \vartheta}{\partial x} = a\, \frac{1}{r}\cdot\frac{\partial}{\partial r}\left(r\, \frac{\partial \vartheta}{\partial r}\right),$$

where $\vartheta = t - t_{c_1}$. Replacing $\partial\vartheta/\partial r$ by $-q/\lambda$ in the equation, we multiply it by $r\, dr$ and integrate between r and r_2, making allowance for the fact that $q_{s2} = 0$. As a result we obtain

$$q = \frac{1}{r}\, \rho c_p \int_{r}^{r_2} \frac{\partial \vartheta}{\partial x} w_x r\, dr$$

and, accordingly,

$$q_{0_1} = \frac{1}{r_1}\, \rho c_p \int_{r_1}^{r_2} \frac{\partial \vartheta}{\partial x} w_x r\, dr.$$

For thermal stabilization with $t_s = $ const, the fluid temperature along the axis will vary exponentially, i.e., $\vartheta \sim \exp(-\text{const}\, x)$.[1] From this we have directly that $\frac{\partial \vartheta}{\partial x} \sim \vartheta$. Thus in the expression for q/q_{s1}, found on the basis of the relationships given above, we can substitute ϑ for $\partial\vartheta/\partial x$. As a result we obtain the second relationship,

$$\frac{q}{q_{c_1}} = \frac{R_1}{R}\, \frac{\displaystyle\int_{R}^{1} \vartheta W_x R\, dR}{\displaystyle\int_{R_1}^{1} \vartheta W_x R\, dR}, \qquad (13\text{-}2)$$

where $W_x = \frac{w_x}{w}$.

It is also simple to obtain relationships similar to (13-1) and (13-2) for the case in which the temperature t_{s2} of the outside wall is maintained constant, while the inside wall is heat-insulated ($q_{s1} = 0$). They have the form

$$\theta = \frac{t - t_{c2}}{t_{c1} - t_{c2}} = \frac{\int_1^R \frac{q}{q_{c2}} \, dR}{\int_1^{R_1} \frac{q}{q_{c2}} \, dR}; \tag{13-3}$$

$$\frac{q}{q_{c2}} = \frac{1}{R} \cdot \frac{\int_{R_1}^R \theta W_x R \, dR}{\int_{R_1}^1 \theta W_x R \, dR}. \tag{13-4}$$

In (13-2) and (13-4), the velocity is a known function of R (see §5-2):

$$W_x = 2 \frac{(1 - R^2) \ln R_1 - (1 - R_1^2) \ln R}{(1 + R_1^2) \ln R_1 + (1 - R_1^2)}. \tag{13-5}$$

The following procedure is used to determine the heat exchange by the iteration method.

A suitable function for determining the heat-flux density is specified in first approximation. This function must evidently satisfy the boundary conditions at the inside and outside walls. We can take a linear relationship, for example:

for a tube with internal heating,

$$\left(\frac{q}{q_{c1}} \right)_1 = \frac{1 - R}{1 - R_1};$$

for a tube with external heating

$$\left(\frac{q}{q_{c2}} \right)_1 = \frac{R - R_1}{1 - R_1}.$$

Substituting these expressions into (13-1) and (13-3), we find the first approximation for the temperature distribution θ_I. Substituting θ_I into (13-2) and (13-4), we find the second approximation for the distribution of heat-flux density $\left(\frac{q}{q_{c1}} \right)_{II}$ or $\left(\frac{q}{q_{c2}} \right)_{II}$. We next determine the second-approximation temperature distribution θ_{II}, etc. The process is repeated until the last approximations are in sufficiently good agreement with the preceding ones.

..... the temperature field has been found, there is no difficulty in determining the limiting values of Nu_∞. If we take the equivalent diameter $d_s = 2(r_2 - r_1)$, as the characteristic dimension, we obtain the following expressions for Nu_∞ at the inside and outside walls with nonsymmetric heating (i.e., with heating of just the in-

side or just the outside wall):

$$\mathrm{Nu}_{\text{в∞0}} = \frac{\alpha_{\text{в0}}d_э}{\lambda} = \frac{2(1-R_1)}{\bar{\theta}}\left(\frac{d\theta}{dR}\right)_{R=R_1}{}^2,$$

$$\mathrm{Nu}_{\text{н∞0}} = \frac{\alpha_{\text{н0}}d_э}{\lambda} = -\frac{2(1-R_1)}{\bar{\theta}}\left(\frac{d\theta}{dR}\right)_{R=1},$$

where $\bar{\theta}$ is the dimensionless mean mass temperature of the fluid.

Fig. 13-2. Distribution of heat-flux density (a) and temperature (b) over width of annular tube heated (cooled) from within, for various values of r_1/r_2. 1) Inside wall; 2) outside wall.

In isolated cases, the iteration method can be used for analytic determination of heat exchange. Thus, for example, in third approximation, the following results are obtained for a round tube:[3]

$$\frac{q}{q_{ст}} = \frac{40}{21}R\left(\frac{11}{6} - \frac{29}{12}R^2 + \frac{3}{2}R^4 - \frac{11}{24}R^6 + \frac{1}{15}R^8\right),$$

$$\theta = \frac{800}{819}\left(\frac{819}{800} - \frac{11}{6}R^2 + \frac{29}{24}R^4 - \frac{1}{2}R^6 + \frac{11}{90}R^8 - \frac{1}{75}R^{10}\right),$$

$$\bar{\theta} = 0,558 \text{ and } \mathrm{Nu}_\infty = 3,678.$$

This value of Nu_∞ differs by only 0.5% from the value found by exact calculation $(\mathrm{Nu}_\infty = 3,658)$.

Since the expression for W_x is so complex, calculations for annular tubes can only be carried out by a numerical method. Figures 13-2, 13-3, and 13-4 show the results of a numerical calculation Figure 13-2 shows the distributions of heat-flux density and temperature over the width of an annular tube with internal heating for various values of r_1/r_2. Figure 13-3 also gives data for a tube with external heating. It is noteworthy that the curves for the relative heat-flux density in the externally heated tube have a maximum, which is greater in magnitude and the farther away from the outside wall the smaller r_1/r_2.
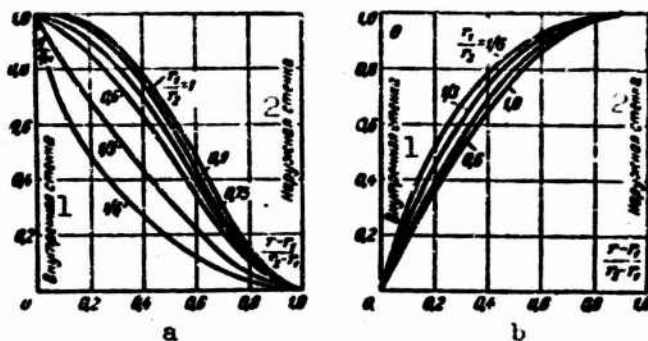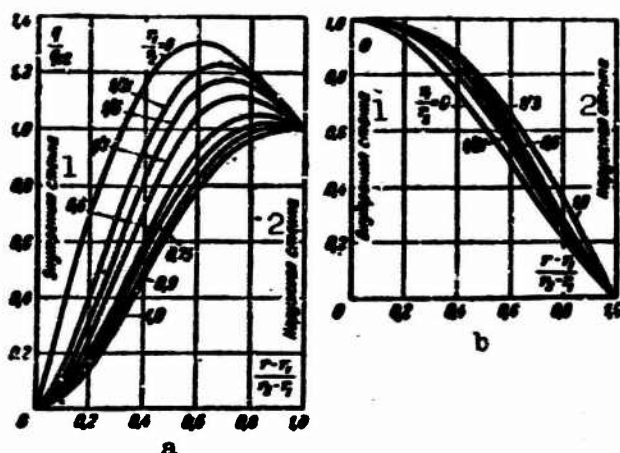
Fig. 13-3. Distributions of heat-flux density (a) and temperature (b) over width of annular tube heated (cooled) externally, for various values of r_1/r_2. 1) Inside wall; 2) outside wall.
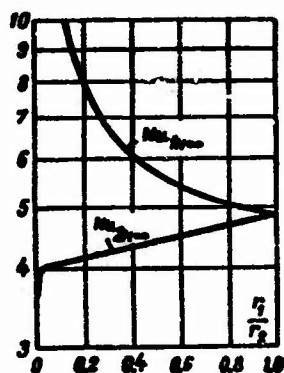
Fig. 13-4. Limiting values of Nu in annular tubes with internal and external heating.

TABLE 13-1

Limiting Values of Nusselt Numbers in Annular Tubes with Internal ($Nu_{1\infty}$) and External ($Nu_{2\infty}$) Heating at t_s = const

r_1/r_2	$Nu_{1\infty}$	$Nu_{2\infty}$
1.0	4,860	4,860
0.9	4,955	4,761
0.75	5.143	4,630
0.60	5.422	4,503
1/3	6,549	4,289
1/6	8,709	4,163
1/21	—	4,049
1/101	—	3,977
0	—	3,658

Values for the quantities $Nu_{1\infty}$ and $Nu_{2\infty}$ are given in Table 13-1, while their dependences on r_1/r_2 are given in Fig. 13-4. When $r_1/r_2 = 1$, the annular tube degenerates into a flat tube and $Nu_{1\infty} = Nu_{2\infty} = 4,86$, which corresponds to the value obtained in §6-4 for a flat tube heated on one side (if we consider that d_e = = 2h). As we might expect, as r_1/r_2 decreases, the Nusselt number for an internally heated annular tube rises rapidly, approaching infinity in the limit when $r_1/r_2 \rightarrow 0$. For an externally heated annular tube, the Nusselt number decreases; it is only for very small r_1/r_2 that it approaches the value of 3.66 for a round tube. This indicates that the flow characteristic of an annular tube is

maintained even when r_1/r_2 is small.

Interpolation equations have been published for $Nu_{1\infty}$ and $\overline{Nu}_{2\infty}$ [3]:

$$Nu_{1\infty} = 3.96 + 0.9\left(\frac{r_1}{r_2}\right)^{-0.06},\tag{13-6}$$

$$Nu_{2\infty} = 4.03\exp\left(0.185\frac{r_1}{r_2}\right).\tag{13-7}$$

The first is valid when $\frac{r_1}{r_2} \geqslant 0.2$ and describes the calculated data to within 0.5%; the second holds for $\frac{r_1}{r_2} \geqslant 0.15$, and is accurate to within 0.2%.

So far as we know, no quantitative estimates have been given for the convergence and accuracy of the iteration method considered. Design practice has shown however, that the method is good convergence after a few approximations. Thus, for example, even in unfavorable cases, the differences in Nu_∞ for the third and fourth approximations is always less than 0.5%. Comparing the results of calculations using this method with certain exact solutions, we see that the method is accurate enough. Thus, for example, for a round tube Nu_∞ coincides with the exact value by the fourth approximation.

2. Let us now consider heat exchange in an annular tube, including the thermal initial segment. As before, we assume the flow to be stabilized, and keep the same conditions and assumptions as in Paragraph 1. Let the temperature be uniformly distributed at the entrance to the heated segment, let the temperature of the inside wall be constant (t_{s1} = const), and let the outside wall be heat-insulated ($q_{s2} \approx 0$).

The problem reduces to solution of the energy equation

$$W_x\frac{\partial\theta}{\partial X} = \frac{\partial^2\theta}{\partial\tilde{R}^2} + \frac{1}{\tilde{R}}\cdot\frac{\partial\theta}{\partial\tilde{R}}\tag{13-8}$$

under the boundary conditions

$$\left.\begin{array}{l}\text{for } X=0 \text{ and } \tilde{R}_1 < \tilde{R} < \tilde{R}_2, \ \theta=1, \\ \text{for } X \geqslant 0 \text{ and } \tilde{R}=\tilde{R}_1, \ \theta=0, \\ \text{for } X \geqslant 0 \text{ and } \tilde{R}=\tilde{R}_2, \ \frac{\partial\theta}{\partial\tilde{R}}=0.\end{array}\right\}\tag{13-9}$$

Here we let

$$\theta = \frac{t-t_{c1}}{t_0-t_{c1}}; \quad X = \frac{4}{Pe}\cdot\frac{x}{d_0};$$

$$Pe = \frac{wd_0}{a}; \quad \tilde{R} = \frac{r}{r_2-r_1} = \frac{2r}{d_0}; \quad d_0 = 2(r_2-r_1).$$

The velocity W_x is specified by Eq. (13-5). The solution obtained to this problem in [4] by separation of variables has the

form

$$\theta = \sum_{n=0}^{\infty} A_n \psi_n(\tilde{R}) \exp(-\epsilon_n^2 X). \qquad (13\text{-}10)$$

where ϵ_n, $\psi_n(\tilde{R})$ are the eigenvalues and eigenfunctions of the problem,

$$\left. \begin{array}{l} \dfrac{d^2\psi}{d\tilde{R}^2} + \dfrac{1}{\tilde{R}} \cdot \dfrac{d\psi}{d\tilde{R}} + \epsilon_n^2 W_x \psi = 0, \\[2mm] \text{for } \tilde{R} = \tilde{R}_1, \quad \psi = 0, \\[2mm] \text{for } \tilde{R} = \tilde{R}_2, \quad \dfrac{d\psi}{d\tilde{R}} = 0. \end{array} \right\} \qquad (13\text{-}11)$$

The constants

$$A_n = \frac{\displaystyle\int_{\tilde{R}_1}^{\tilde{R}_2} \psi_n \tilde{R} W_x \, d\tilde{R}}{\displaystyle\int_{\tilde{R}_1}^{\tilde{R}_2} \psi_n^2 \tilde{R} W_x \, d\tilde{R}}.$$

By definition, the Nusselt number at the inside wall equals

$$Nu_{1s} = \frac{\alpha_1 d_e}{\lambda} = 2 \frac{\left(\dfrac{\partial \theta}{\partial R}\right)_{\tilde{R}=\tilde{R}_1}}{\bar{\theta}},$$

where $\bar{\theta}$ is the mean mass temperature of the fluid,

$$\bar{\theta} = \frac{\displaystyle\int_{r_1}^{r_2} \theta w_x 2\pi r \, dr}{w\pi(r_2^2 - r_1^2)} = \frac{2}{2\tilde{R}_1 + 1} \int_{\tilde{R}_1}^{\tilde{R}_2} \theta w_x \tilde{R} \, d\tilde{R}.$$

TABLE 13-2

Eigenvalues and Constants in Problem of Heat Exchange in Annular Tube with t_{s1} = const and q_{s2} = = 0

n	$\tilde{R}_1 = 0.2;\ R_1 = 1/6$		$\tilde{R}_1 = 0.5;\ R_1 = 1/3$		$\tilde{R}_1 = 1.0;\ R_1 = 1/2$		$\tilde{R}_1 = 2.0;\ R_1 = 2/3$		$\tilde{R}_1 = 20;\ R_1 = 20/21$	
	ϵ_n	B_n	ϵ_n	B_n	ϵ_n	B_n	ϵ_n	B_n	ϵ_n	B_n
0	1.124054	0.8197293	1.282161	1.543650	1.383003	2.651176	1.456400	4.838529	1.546883	44.0721
1	4.583686	0.3641899	4.704137	0.8017342	4.767710	1.522857	4.807803	2.956504	4.851740	28.65708
2	7.800738	0.2911149	7.881437	0.6568992	8.052764	1.250903	8.030105	2.456434	8.100898	23.94991
3	11.04763	0.2554909	11.33549	0.5815754	11.32103	1.118297	11.36689	2.186097	11.40302	21.34054
4	14.28304	0.2338140	14.48151	0.5324162	14.58304	1.035015	14.63466	2.005779	14.67321	19.59566
5	17.45278	0.2185746	17.73927	0.4966860	17.84195	0.9574833	17.90112	1.876619	17.94215	18.31187
6	20.64929	0.2041237	20.96365	0.4690400	21.09910	0.9045479	21.16606	1.770727	21.21035	17.31062
7	23.84175	0.1941389	24.20056	0.4467082	24.35514	0.8618086	24.43017	1.687354	24.47810	16.49814
8	27.03685	0.1858733	27.43748	0.4281261	27.61044	0.8261867	27.69372	1.617808	27.74554	15.82019
9	30.22899	0.1788674	30.67373	0.4123141	30.86523	0.7958158	30.95689	1.558519	31.01279	15.24163

Using (13-10), we find
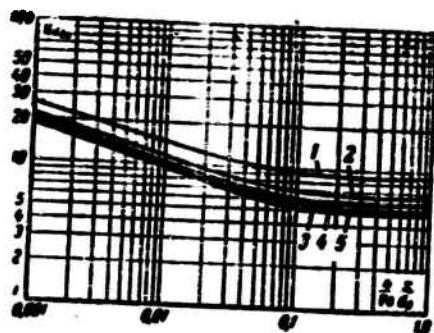
Fig. 13-5. Values of Nu_{1n} in annular tube with t_{s1} = const and q_{s2} = 0. 1) R_1 = 0.2; 2) R_1 = 0.5; 3) R_1 = 1.0; 4) R_1 = 2.0 5) flat tube.

$$Nu_{1H} = \frac{2\tilde{R}_1 + 1}{R_1} \cdot \frac{\sum\limits_{n=0}^{\infty} B_n \exp(-\varepsilon_n^2 X)}{\sum\limits_{n=0}^{\infty} \frac{B_n}{\varepsilon_n^2} \exp(-\varepsilon_n^2 X)}, \qquad (13\text{-}12)$$

where

$$B_n = A_n \psi'_n(\tilde{R}_1).$$

For $X \to \infty$,

$$Nu_{1H} = Nu_{1H\infty} = \left(2 + \frac{1}{\tilde{R}_1}\right)\varepsilon_0^2. \qquad (13\text{-}13)$$

Table 13-2 shows the eigenvalues ε_n and the constants B_n for several values of $\tilde{R}_1$. Figure 13-5 shows Nu_{1n} as a function of X for five values of R_1. The curve for $R_1 = 20$ nearly coincides with the corresponding curve for a flat tube with heating on one side. The approximate $Nu_{1H\infty}$ values given in Table 13-1 are very close to the exact values, which can be found from Eq. (13-13).

3. If we know a solution of the problem for t_{s1} = const, we can then use the Duhamel principle (see §6-5) to obtain an expression for Nu when the temperature of the inside wall varies continuously along the length. Thus, for example, if the temperature of the inside wall varies linearly, $t_{s1} = t_0 +$ const x, then

$$Nu_{1H} = \frac{2\tilde{R}_1 + 1}{2} \cdot \frac{\sum\limits_{n=0}^{\infty} \frac{B_n}{\varepsilon_n^2}[1 - \exp(-\varepsilon_n^2 X)]}{\sum\limits_{n=0}^{\infty} \frac{B_n}{\varepsilon_n^4}[1 - \exp(-\varepsilon_n^2 X)]}. \qquad (13\text{-}14)$$

- 303 -

Here the eigenvalues and constants are the same as for paragraph 2 (Table 13-2).

13-2. HEAT EXCHANGE UNDER BOUNDARY CONDITIONS OF THE SECOND KIND WITH STABILIZED FLOW

1. We first analyze the limiting case of stabilized heat exchange in an annular tube, assuming that the physical properties are constant, the velocity profile is developed, and the heat of friction is negligible. Let the constant values q_{s1} and q_{s2} of heat-flux densities be given at the inside and outside walls; $q_{s1} \neq q_{s2}$. A solution of this problem has been published in [5].

The condition for stabilization of the heat-exchange process over the length can be represented by the relationship

$$\frac{\partial}{\partial x}\left(\frac{t_c - t}{t_c - \bar{t}}\right) = 0,$$

from which we find that the heat-transfer coefficient at both walls,

$$a = \frac{q_c}{t_c - \bar{t}} = \lambda\left[\frac{\partial}{\partial n}\left(\frac{t_c - t}{t_c - \bar{t}}\right)\right]_{n=0}$$

also varies with the length. Here t_s and q_s represent t_{s1} and q_{s1} or t_{s2} and q_{s2}, while n is the normal to the wall surface, directed toward the fluid.[5]

Where q_{c1} and q_{c2}, a_1 and a_2 are constant over the length, the above relationships yield

$$\frac{dt_c}{dx} = \frac{d\bar{t}}{dx} = \frac{\partial t}{\partial x}.$$

The mean mass temperature of the fluid is found from the heat-balance equation

$$\bar{t} = \frac{2(q_{c1}r_1 + q_{c2}r_2)}{\rho c_p \bar{w}(r_2^2 - r_1^2)}x + t_0, \tag{13-15}$$

where t_0 is the temperature of the fluid at the entrance.

Taking (13-15) into account, we arrive at the relationship

$$\frac{\partial t}{\partial x} = \frac{dt_c}{dx} = \frac{d\bar{t}}{dx} = \frac{2(q_{c1}r_1 + q_{c2}r_2)}{\rho c_p \bar{w}(r_2^2 - r_1^2)}. \tag{13-16}$$

Using this relationship, we can write the energy equation as

$$CW_x R = \frac{\partial}{\partial R}\left(R\frac{\partial t}{\partial R}\right), \tag{13-17}$$

where

$$C = \frac{2(q_{c1}r_1 + q_{c2}r_2)r_2^2}{\lambda(r_2^2 - r_1^2)}; \quad W_x = \frac{w_x}{\bar{w}}; \quad R = \frac{r}{r_2}.$$

We integrate (13-17) between R_1 and R, allowing for the fact that $\left(R\frac{d t}{dR}\right)_{R=R_1} = -\frac{q_{c_1}r_1}{\lambda}$. As a result, we obtain

$$\frac{dt}{dR} = \frac{1}{R}\left[C\int_{R_1}^{R} W_z R\, dR - \frac{q_{c_1}r_1}{\lambda}\right]. \qquad (13\text{-}18a)$$

If we integrate (13-17) between $R_2 = 1$ and R, and allow for the fact that $\left(R\frac{dt}{dR}\right)_{R=R_2} = \frac{q_{c_2}r_2}{\lambda}$, we then obtain an expression analogous to the preceding one:

$$\frac{dt}{dR} = \frac{1}{R}\left[C\int_{R_2=1}^{R} W_z R\, dR + \frac{q_{c_2}r_2}{\lambda}\right]. \qquad (13\text{-}18b)$$

Integrating (13-18a) between R_1 and R, we find

$$t - t_{c_1} = C\int_{R_1}^{R}\frac{1}{R}\left(\int_{R_1}^{R} W_z R\, dR\right) dR - \frac{q_{c_1}r_1}{\lambda}\ln\frac{R}{R_1}.$$

Substituting the value of the constant C and introducing the dimensionless temperature

$$\theta = \frac{(t - t_{c_1})\lambda}{q_{c_1}r_1 + q_{c_2}r_2},$$

we finally obtain

$$\theta = \frac{2}{1 - R_1^2}\int_{R_1}^{R}\frac{1}{R}\left(\int_{R_2}^{R} W_z R\, dR\right) dR - P\ln\frac{R}{R_1}, \qquad (13\text{-}19)$$

where $P = \dfrac{q_{c_1}r_1}{q_{c_1}r_1 + q_{c_2}r_2} = \dfrac{1}{1 + \frac{q_{c_2}r_2}{q_{c_1}r_1}}$.

Thus determination of the temperature field reduces to evaluation of an integral.

Equation (13-5) describes the velocity distribution in an annular tube. Substituting this expression into (13-19) and integrating, we obtain an equation for the temperature field:

$$\theta = \frac{1}{D}\left[(1+z)(R^2 - R_1^2) - \frac{1}{4}(R^4 - R_1^4) - z(R^2\ln R + R_1^2\ln R_1) - \right.$$
$$\left. - (z + R_1^2)R_1^2\ln\frac{R}{R_1}\right] - P\ln\frac{R}{R_1}, \qquad (13\text{-}20)$$

where $z = \dfrac{1 - R_1^2}{\ln R_1}$; $D = (1 - R_1^2)(1 + R_1^2 + z)$.

Figure 13-6 shows this relationship for $R_1 = 0.75$. The $P=0$ curve corresponds to delivery of heat to the outside wall alone $(q_{c_1}=0)$, and the $P=1$ curve to the inside wall alone $(q_{c_2}=0)$. The $P=0.5$ curve corresponds to identical supply (or removal) of heat at both walls $(q_{c_1}r_1 = q_{c_2}r_2)$. The curves for $P < 0$ correspond to the case in which $q_{c_1} < 0$ and $q_{c_2} > 0$ or $q_{c_1} > 0$ and $q_{c_2} < 0$, here $|q_{c_2}r_2| > |q_{c_1}r_1|$. Finally, the curves for
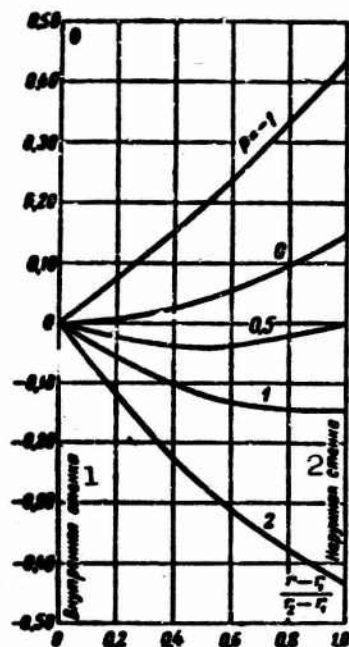
Fig. 13-6. Distribu-
tion of temperature
over cross section of
annular tube with
$r_1/r_2 = 0.75$. 1) Inside
wall; 2) outside wall.
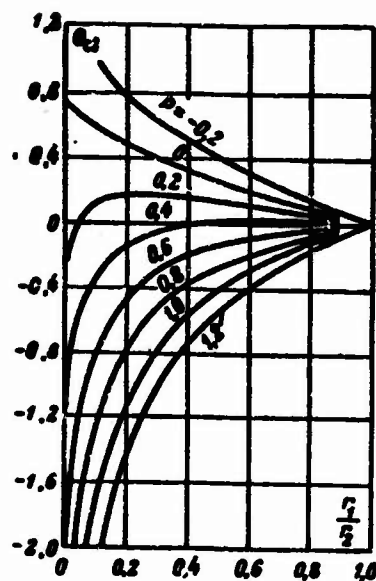
Fig. 13-7. Dimension-
less difference in
temperatures of outside
and inside walls of an-
nular tube.

$P > 1$ correspond to the case in which $q_{c1} > 0$ and $q_{c2} < 0$ or $q_{c1} < 0$ and $q_{c2} > 0$; here $|q_{c1}r_1| > |q_{c2}r_2|$.

Letting $R_1 = 0$ and $q_{s1} = 0$ in (13-20), we arrive at the equation for the temperature field in a round tube (see §8-1):[6]

$$\theta = \frac{t - t_{r=0}}{\frac{q_c r_2}{\lambda}} = R^2 - \frac{1}{4}R^4.$$

Letting $R = 1$ in (13-20), we obtain an expression for the dimensionless difference in the temperatures of the outside and inside walls of an annular tube:

$$\theta_{c2} = \frac{(t_{c2} - t_{c1})\lambda}{q_{c1}r_1 + q_{c2}r_2} = \frac{1}{D}\left\{(1 - R_1^2)\left[\frac{3}{4}(1 + R_1^2) + z\right] + \right.$$
$$\left. + R_1^2 \ln R_1 (R_1^2 + z) + (\ln R_1)[1 - R_1^2(R_1^2 + z) + z]P\right\}.$$

We note that this equation was obtained first by Jacob and Rees [6] by a different method. Figure 13-7, taken from [7], shows θ_{s2} as a function of R_1 for various values of the parameter P. The point at which $\theta_{s2} = 0.75$ when $R_1 = 0$ and $P = 0$ corresponds to the limiting case, where the annular tube degenerates to a round tube.

In all other cases, when $R_1 \to 0$ $\theta_{c2} \to \pm \infty$, since transmission of a finite amount of heat by an infinitely thin filament requires infinitely large temperature gradients.

To determine the heat-transfer coefficients α_1 and α_2 at the inside and outside walls, we consider the expression for the mean mass temperature of the fluid,

$$\bar{t} = \frac{\int_{r_1}^{r_2} t w_x \, 2\pi r \, dr}{\pi (r_2^2 - r_1^2)} = \frac{2}{1 - R_1^2} \int_{R_1}^{1} t W_x R \, dR.$$

Taking the integral on the right side by parts, we obtain

$$\bar{t} = \frac{2}{1 - R_1^2} \left[\left(t \int_{R_2=1}^{R} W_x R \, dR \right) \Big|_{R_1}^{1} - \int_{R_1}^{1} \left(\int_{R_2=1}^{R} W_x R \, dR \right) dt \right] =$$

$$= \frac{1}{1 - R_1^2} \left[2t_{c_1} \int_{R_1}^{1} W_x R \, dR - 2 \int_{R_1}^{1} \left(\int_{R_2=1}^{R} W_x R \, dR \right) dt \right].$$

Since $\dfrac{2}{1 - R_1^2} \displaystyle\int_{R_1}^{1} W_x R \, dR = 1$, we have

$$t_{c_1} - \bar{t} = \frac{2}{1 - R_1^2} \int_{R_1}^{1} \left(\int_{R_2=1}^{R} W_x R \, dR \right) dt.$$

Proceeding in like manner, we find the second relationship

$$t_{c_2} - \bar{t} = \frac{2}{1 - R_1^2} \int_{R_1}^{1} \left(\int_{R_1}^{R} W_x R \, dR \right) dt.$$

Substituting dt from (13-18b) into the first expression, and the value from (13-18a) into the second expression, we have

$$\left. \begin{aligned} t_{c_1} - \bar{t} &= \frac{2}{1 - R_1^2} \int_{R_1}^{1} \frac{1}{R} \left[C \left(\int_{R}^{1} W_x R \, dR \right)^2 - \frac{q_{c2} r_2}{\lambda} \int_{R}^{1} W_x R \, dR \right] dR; \\ t_{c_2} - \bar{t} &= \frac{2}{1 - R_1^2} \int_{R_1}^{1} \frac{1}{R} \left[C \left(\int_{R_1}^{R} W_x R \, dR \right)^2 - \frac{q_{c1} r_1}{\lambda} \int_{R_1}^{R} W_x R \, dR \right] dR. \end{aligned} \right\} \quad (13\text{-}21)$$

We divide the first equation by q_{s1} and the second by q_{s2}; we also multiply both equations by λ and divide by $d_c = 2(r_2 - r_1)$. After substitution of the value of C into the resulting relationships and certain manipulations, we arrive at the final expressions for the Nusselt numbers at the inside and outside walls of an annular tube:

$$\frac{1}{Nu_{1\infty}}=\frac{1}{(1-R_1^2)(1-R_1)}\left[\frac{2\left(\frac{q_{c2}}{q_{c1}}+R_1\right)}{1-R_1^2}\int_{R_1}^1\frac{1}{R}\left(\int_R^1 W_x R\,dR\right)^2 dR-\right.$$
$$\left.-\frac{q_{c1}}{q_{c2}}\int_{R_1}^1\frac{1}{R}\left(\int_R^1 W_x R\,dR\right)dR\right];$$

$$\frac{1}{Nu_{2\infty}}=\frac{1}{(1-R_1^2)(1-R_1)}\left[\frac{2\left(\frac{q_{c1}}{q_{c2}}R_1+1\right)}{1-R_1^2}\int_{R_1}^1\frac{1}{R}\left(\int_{R_1}^R W_x R\,dR\right)^2 dR-\right.$$
$$\left.-\frac{q_{c1}}{q_{c2}}R_1\int_{R_1}^1\frac{1}{R}\left(\int_{R_1}^R W_x R\,dR\right)dR\right].$$

(13-22)

Here

$$Nu_{1\infty}=\frac{\alpha_1 d_0}{\lambda}=\frac{q_{c1}2(r_2-r_1)}{(t_{c1}-\bar{t})\lambda};$$

$$Nu_{2\infty}=\frac{\alpha_2 d_0}{\lambda}=\frac{q_{c2}2(r_2-r_1)}{(t_{c2}-\bar{t})\lambda}.$$

It is easy to obtain equations for Nu_∞ in round and flat tubes from (13-22) as special cases.

For a round tube $(R_1 = 0)$, letting $\alpha_2 = \alpha$ and $2r_2 = d$, we find the following expression from the second equation:

$$\frac{1}{Nu_\infty}=\frac{\lambda}{\alpha d}=2\int_0^1\frac{1}{R}\left(\int_0^R W_x R\,dR\right)^2 dR.$$

(13-23)

This expression is known as the Lyon integral [8]. If we make the substitution $W_x=2(1-R^2)$, we then find $Nu_\infty = 48/11$, corresponding to the value found earlier (see §8-1).

For a flat tube, $R=R_1=1;\ 1-R_1=\frac{r_2-r_1}{r_1}=\frac{h}{r_1}$, where h is the tube width. If, in addition, we introduce the coordinate $Y = y/h$, i.e., the dimensionless distance between the inside wall and the point under consideration, Eq. (13-22) will take the form

$$\frac{1}{Nu_{1\infty}}=\frac{1}{2}\left(\frac{q_{c2}}{q_{c1}}+1\right)\int_0^1\left(\int_Y^1 W_x\,dY\right)^2 dY-\frac{1}{2}\cdot\frac{q_{c2}}{q_{c1}}\int_0^1\left(\int_Y^1 W_x\,dY\right)dY;$$
$$\frac{1}{Nu_{2\infty}}=\frac{1}{2}\left(\frac{q_{c1}}{q_{c2}}+1\right)\int_0^1\left(\int_0^Y W_x\,dY\right)^2 dY-\frac{1}{2}\cdot\frac{q_{c1}}{q_{c2}}\int_0^1\left(\int_0^Y W_x\,dY\right)dY.$$

(13-24)

Substituting in $W_x=6(Y-Y^2)$, we obtain expressions for $Nu_{1\infty}$ and $Nu_{2\infty}$ that coincide with the previously derived equations (8-43).

Returning to determination of heat exchange in annular tubes, we substitute Expression (13-5) for the velocity profile in an annular tube into (13-22). After integration we find

$$\frac{1}{Nu_{1\infty}} = \frac{1}{(1-R_1^2)(1-R_1)}\left[\frac{8\left(\frac{q_{c2}}{q_{c1}}+R_1\right)B_1}{(1-R_1^2)A^2} - 2\frac{q_{c2}}{q_{c1}}\cdot\frac{B_1}{A}\right]. \qquad (13\text{-}25)$$

where

$$A = 1 + R_1^2 + \frac{1-R_1^2}{\ln R_1};$$

$$B_1 = b_1 + \frac{b_2}{\ln R_1} + \frac{b_3}{(\ln R_1)^2} - \frac{1}{16}\ln R_1;$$

$$b_1 = -\frac{73}{384} + \frac{1}{8}R_1^2 + \frac{3}{32}R_1^4 - \frac{11}{384}R_1^8;$$

$$b_2 = -\frac{31}{144} + \frac{29}{72}R_1^2 - \frac{3}{32}R_1^4 - \frac{23}{144}R_1^6 + \frac{19}{288}R_1^8;$$

$$b_3 = -\frac{11}{128} + \frac{19}{64}R_1^2 - \frac{3}{8}R_1^4 + \frac{13}{64}R_1^6 - \frac{5}{128}R_1^8;$$

$$B_2 = -\frac{7}{16} + \frac{1}{4}R_1^2 + \frac{3}{16}R_1^4 - \frac{1}{\ln R_1}\left(\frac{1}{4} - \frac{1}{2}R_1^2 + \frac{1}{4}R_1^4\right) - \frac{1}{4}\ln R_1.$$

The equation for $Nu_{2\infty}$ is easily found from the equation for $Nu_{1\infty}$ if in the latter we replace R_1 by $1/R_1$ and q_{c2}/q_{c1} by q_{c1}/q_{c2}.

Since the energy equation and the boundary conditions are linear in the temperature, the temperature field for $q_{c1} \neq q_{c2} \neq 0$ can be represented as the result of superposition of the two fields for the two limiting cases of nonsymmetric heating:

a) the case in which $q_{s1} = 0$; here $t_{c1} = t'_{a.c1}$, $t_{c2} = t'_{c2}$ and $\bar{t} = \bar{t}'$;

b) the case in which $q_{s2} = 0$; here $t_{c2} = t_{a.c2}$, $t_{c1} = t''_{c1}$ and $\bar{t} = \bar{t}''$.

Using our definitions, we can then write

$$\left.\begin{array}{l} t_{c1} - \bar{t} = (t''_{c1} - \bar{t}'') + (t_{a.c1} - \bar{t}'); \\ t_{c2} - \bar{t} = (t'_{c2} - \bar{t}') + (t_{a.c2} - \bar{t}''). \end{array}\right\} \qquad (13\text{-}26)$$

In this case, the relationships will differ from the equations (13-21) given above.

Dividing the first relationship by q_{s1} and the second by q_{s2} and going over to Nusselt numbers, we obtain

$$\left.\begin{array}{l} Nu_{1\infty} = \dfrac{Nu_{1H\infty}}{1 + Nu_{1H\infty}\theta_{a.c1}\dfrac{q_{c2}}{q_{c1}}}, \\[3ex] Nu_{2\infty} = \dfrac{Nu_{2H\infty}}{1 + Nu_{2H\infty}\theta_{a.c2}\dfrac{q_{c1}}{q_{c2}}}, \end{array}\right\} \qquad (13\text{-}27)$$

where

$$Nu_{1n\infty} = \frac{q_{s1}d_0}{(t''_{c1} - \bar{t}'')\lambda}; \quad Nu_{2n\infty} = \frac{q_{s2}d_0}{(t''_{c2} - \bar{t}'')\lambda};$$

$$\theta_{a.c_1} = \frac{t_{ac_1} - \bar{t}''}{\frac{q_{s0}d_0}{\lambda}} \quad \text{and} \quad \theta_{a.c_2} = \frac{t_{ac_2} - \bar{t}''}{\frac{q_{s0}d_0}{\lambda}}$$

are the Nusselt numbers and adiabatic wall temperatures (i.e., the temperatures of the heat-insulated walls) with nonsymmetric heating, when $q_{s1} = 0$ or $q_{s2} = 0$.

Naturally, relationships such as (13-26) and (13-27) are valid not only for fully developed flow and heat exchange, but also for more general cases.
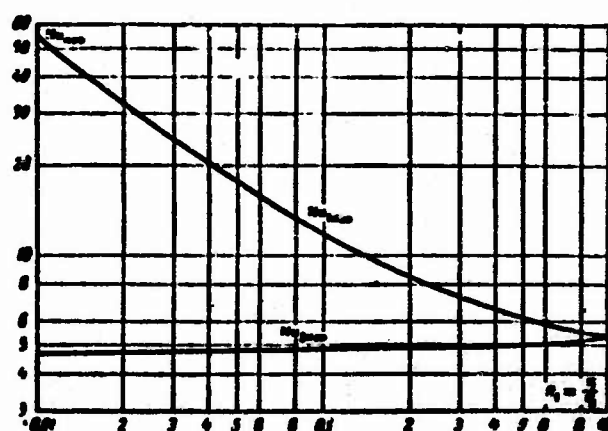

Fig. 13-8. Values of $Nu_{1n\infty}$ and $Nu_{2n\infty}$ for nonsymmetric heating as a function of R_1.
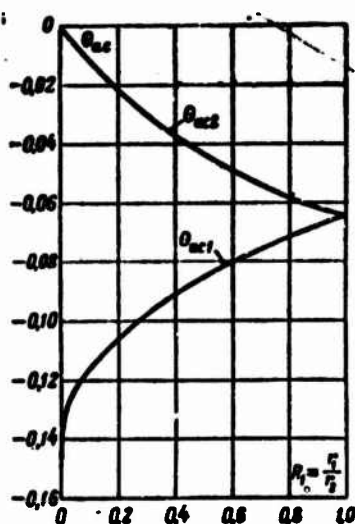

Fig. 13-9. Values of θ_{as1} and θ_{as2} as functions of R_1.

- 310 -

TABLE 13-3

Values of $Nu_{1\infty}$, $Nu_{2\infty}$, $\theta_{a.c1}$ and $\theta_{a.c2}$ in Annular Tubes with Nonsymmetric Heating

$R_1 = \frac{r_1}{r_2}$	$Nu_{1\infty}$	$Nu_{2\infty}$	$\theta_{a.c1}$	$\theta_{a.c2}$
0	∞	4.36	−0.1458	0
0.01	54.02	4.69	−0.1308	−0.001307
0.04	20.51	4.78	−0.1241	−0.004962
0.1	11.90	4.83	−0.1162	−0.01161
0.2	8.49	4.89	−0.1061	−0.02132
0.4	6.58	5.00	−0.09146	−0.03694
0.6	5.91	5.12	−0.08007	−0.04867
1.0	5.38	5.38	−0.06428	−0.06428

By the symmetry conditions, $Nu_{1\infty} = Nu_{2\infty}$ and $\theta_{a.c1} = \theta_{a.c2}$ for a flat tube. For annular tubes, $Nu_{1\infty}$, $Nu_{2\infty}$, $\theta_{a.c1}$ and $\theta_{a.c2}$ are functions of R_1 alone. It is not difficult to establish the specific form of these functions from (13-25) for $Nu_{1\infty}$ and the analogous equation for $Nu_{2\infty}$, or directly from (13-21). Table 13-3 and Figs. 13-8 and 13-9 give their values as a function of R_1.[8]

Figures 13-10 and 13-11 show $Nu_{1\infty}$ and $Nu_{2\infty}$ as functions of R_1 for various relationships between the heat-flux densities at the wall. The nature of the functions is easily understood if we look at Eqs. (13-27). If $Nu_{1\infty}\theta_{a.c1}\frac{q_{c2}}{q_{c1}} > -1$, then $Nu_{1\infty} > 0$; if this quantity takes on values less than −1, however, then $Nu_{1\infty}$ will become negative. This means that when q_{s1} is positive, the temperature head $\Delta t = t_{c_1} - \bar{t}$ is negative ($t_{c_1} < \bar{t}$). For $Nu_{1\infty}\theta_{a.c1} \times \frac{q_{c2}}{q_{c1}} \to -1$, $Nu_{1\infty} \to \pm\infty$. This occurs since $\Delta t \to 0$ for finite values of q_{s1} and q_{s2} (positive or negative). It is also clear that when $\frac{q_{c2}}{q_{c1}} < 0$, $Nu_{1\infty}$ will always be positive. Naturally, this analysis also applies to $Nu_{2\infty}$. As we can see from the curves, there is a substantial difference between the way in which $Nu_{1\infty}$ and $Nu_{2\infty}$ depend on R_1. In particular, when $R_1 \to 0$, $Nu_{1\infty} \to -\frac{48}{7} \cdot \frac{q_{c1}}{q_{c2}}$; and $Nu_{2\infty} \to \frac{48}{11}$.

To conclude, we note that (13-19), (13-21), and (13-22) are valid for any axisymmetric velocity profile. Thus, for example, they can be used without difficulty to determine heat exchange for bar flow, i.e., with $W_x = 1$.

2. Let us consider heat exchange in the thermal initial segment of an annular tube, on the assumption that the temperature is uniformly distributed at the entrance to the heated segment, the heat-flux density at the inside wall is constant (q_{s1} = const), and the outside wall is heat-insulated ($q_{s2} = 0$). All other conditions are the same as in paragraph 1.
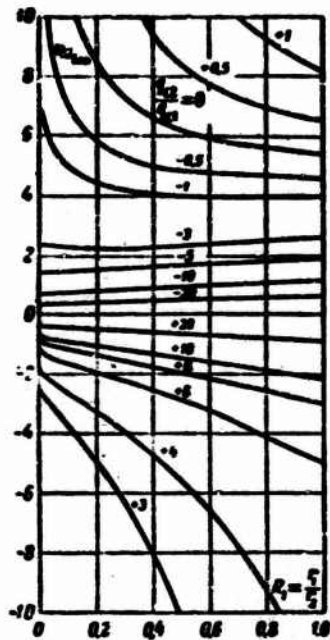
Fig. 13-10. Dependence
of $Nu_{1\infty}$ on R_1 for var-
ious values of q_{s2}/q_{s1}.
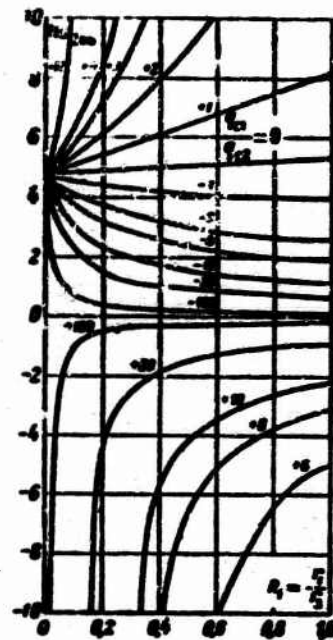
Fig. 13-11. Dependence
of $Nu_{2\infty}$ as a function
of R_1 for various values
of q_{s1}/q_{s2}.

In this case, it is convenient to represent the dimension-
less temperature as

$$\theta = \frac{t - t_0}{\frac{q_{c1}d_0}{\lambda}},$$

while the general solution of the problem is divided into two parts:

$$\theta = \theta_s + \theta_1,$$

where θ_s is the solution found in paragraph 1 for the stabilized
temperature field; θ_1 is an additional function for the thermal
initial segment, which vanishes when X is sufficiently large.

The stabilized temperature field is described by Eq. (13-20).
When $q_{s2} = 0$, it can be written as

$$\frac{t_0 - t_{c1}}{\frac{q_{c1}d_0}{\lambda}} = \frac{R_1}{2(1 - R_1)} F(R),$$

where $F(R)$ is the right side of (13-20) when $P = 1$.

For the segment where thermal stabilization occurs, by defini-
tion

$$\frac{t_{c1} - \bar{t}}{\frac{q_{c1}d_0}{\lambda}} = \frac{1}{Nu_{1\infty}}.$$

- 312 -

When $q_{s2} = 0$, Eq. (13-15) yields

$$\frac{\bar{t}-t_0}{\frac{q_{s1}d_0}{\lambda}}=\frac{R_1}{1+R_1}\cdot\frac{4}{Pe}\cdot\frac{x}{d_0}.$$

Adding the three preceding equations term-by-term, we obtain

$$\theta_0=\frac{t_0-t_b}{\frac{q_{s1}d_0}{\lambda}}=\frac{\tilde{R}_1}{2+\tilde{R}_1}X+G(\tilde{R}).\qquad(13\text{-}28)$$

where

$$X=\frac{4}{Pe}\cdot\frac{x}{d_0};\ Pe=\frac{\bar{w}d_0}{a};\ \tilde{R}=\frac{r}{r_2-r_1}=\frac{2r}{d_0};$$

$$G(\tilde{R})=\frac{R_1}{2(1-R_1)}F(\tilde{R})+\frac{1}{Nu_{1\infty}}$$

is a certain function of $\tilde{R}$ (or R). When $\tilde{R}=\tilde{R}_1$, $F(R)=F(R_1)=0$ and $G(\tilde{R}_1)=G_1=Nu_{1\infty}^{-1}$.

The solution for θ_1 can be constructed in exactly the same manner as for a round tube (see §8-1). It has the following form [4]:

$$\theta_1=\sum_{n=0}^{\infty}A_n\psi_n(\tilde{R})\exp(-\epsilon_n^2 X).\qquad(13\text{-}29)$$

The eigenvalues ϵ_n and eigenfunction ψ_n are found from the equation and the boundary conditions

$$\left.\begin{array}{l}\dfrac{d^2\psi}{d\tilde{R}^2}+\dfrac{1}{\tilde{R}}\cdot\dfrac{d\psi}{d\tilde{R}}+\epsilon^2 W_x\psi=0,\\[2mm]\dfrac{d\psi}{d\tilde{R}}=0\ \text{for}\ \tilde{R}=\tilde{R}_1\ \text{and}\ \tilde{R}=\tilde{R}_2.\end{array}\right\}\qquad(13\text{-}30)$$

The constants A_n are determined from the relationship

$$A_n=-\frac{\displaystyle\int_{\tilde{R}_1}^{\tilde{R}_2}G\psi_n\tilde{R}W_x\,d\tilde{R}}{\displaystyle\int_{\tilde{R}_1}^{\tilde{R}_2}\psi_n^2\,\tilde{R}W_x\,d\tilde{R}}.$$

The Nusselt number at the inside wall is

$$Nu_{1H}=\frac{\alpha_1 d_0}{\lambda}=\frac{1}{G_1\left[1-\displaystyle\sum_{n=0}^{\infty}A_n\exp(-\epsilon_n^2 X)\right]}.\qquad(13\text{-}31)$$

When $X\to\infty$,

$$Nu_{1H}=G_1^{-1}=Nu_{1H\infty}.$$

TABLE 13-4

Eigenvalues and Constants for Problem of Heat Exchange in Annular Tube with q_{s1} = const and q_{s2} = 0

n	$\tilde{R}_1 = 0.2;\ G_1 = 9.1084?$		$\tilde{R}_1 = 0.5;\ G_1 = 0.14336$		$\tilde{R}_1 = 1.0;\ G_1 = 0.16178$		$\tilde{R}_1 = 20;\ G_1 = 0.18145$	
	ε_n	A_n	ε_n	A_n	ε_n	A_n	ε_n	A_n
0	3.73734	0.354737	3.72849	0.4024391	3.710150	0.4243079	3.625802	0.4450448
1	6.96990	0.1456844	6.965235	0.1403154	6.994183	0.1496772	7.001240	0.1490632
2	10.15002	0.08324779	10.23638	0.08121473	10.25972	0.07956408	10.28435	0.07796080
3	13.33630	0.05509405	13.46328	0.05217145	13.51925	0.05065061	13.50034	0.04987633
4	16.52106	0.03963310	16.69850	0.03682774	16.77621	0.03539772	16.83312	0.03391540
5	19.70083	0.00029991	19.93290	0.02762987	20.03179	0.02640702	20.10357	0.02519036
6	22.89124	0.02391886	23.16845	0.02163319	23.28635	0.02068747	23.37320	0.01926512
7	26.07971	0.01950039	26.40055	0.01748174	26.54078	0.01658108	26.64210	0.01570465
8	29.26843	0.01625300	29.63410	0.01447512	29.79465	0.01369226	29.91052	0.01283694
9	32.44630	0.01381129	32.86757	0.01221967	33.04830	0.01153905	33.17868	0.01087097
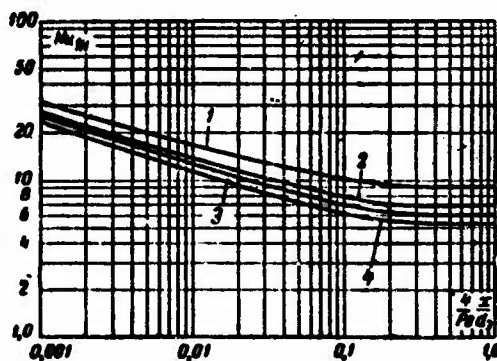
Fig. 13-12. Values of Nu_{1n} in annular tube with q_{s1} = const and q_{s2} = 0. 1) R_1 = 0.2; 2) R_1 = 0.5; 3) R_1 = 1.0; 4) flat tube.

Table 13-4 shows the eigenvalues and constants for several values of R_1. Figure 13-12 gives Nu_{1n} as a function of X for four values of R_1. The relationships for $\tilde{R}_1$ = 20 and a flat tube with heating on one side are very close.

3. If we know a solution for q_{s1} = const, we can then use the Duhamel principle (see §8-4) to obtain an expression for Nu when q_{s1} varies continuously with the length. Let us look at two examples.

Where q_{s1} varies linearly with the length and q_{s2} = 0,

$$\mathrm{Nu}_{1n} = \frac{1}{G_1\left\{1 - \displaystyle\sum_{n=0}^{\infty} \frac{A_n}{\varepsilon_n^2 X}\left[1 - \exp(-\varepsilon_n^2 X)\right]\right\}}.$$

TABLE 13-5

Constants in Problem of
Heat Exchange in Annular
Tube for q_{s1} = const and
q_{s2} = const, with $\tilde{R}_1 = 1.0$

n	$\phi_n(\tilde{R}_1)$	D_n	$D_n \psi_n(\tilde{R}_1)$
0	0.130840	0.452343	−0.111054
1	−0.126922	0.150120	0.037993
2	0.125173	0.077715	−0.019943
3	−0.124149	0.048511	0.012552
4	0.123466	0.033598	−0.0087411
5	−0.122972	0.024863	0.0064947
6	0.122595	0.019265	−0.0050478
7	−0.122296	0.015441	0.0040556
8	0.122052	0.012700	−0.0033423
9	−0.121847	0.010662	0.0028105

$G_1 = 0.161785; \quad G_2 = -0.042757;$
$H_1 = -0.0655143; \quad H_2 = 0.198548$

If the variation of q_{s1} over a segment of length l is governed by the law $q_{s1} = b + k \sin \frac{\pi x}{l}$ (b and k are constants), with $q_{s2} = 0$,

$$\mathrm{Nu}_{1n} = \frac{1 + K \sin \frac{\pi X}{L}}{G_1 \left[1 - \sum_{n=0}^{\infty} A_n \exp(-\varepsilon_n^2 X) + K \sin \frac{\pi X}{L} - K \sum_{n=0}^{\infty} \frac{A_n \frac{\pi}{L}}{\left(\frac{\pi}{L}\right)^2 + \varepsilon_n^4} \xi_n(X) \right]},$$

where

$$\xi_n(X) = \varepsilon_n^2 \cos \frac{\pi X}{L} + \frac{\pi}{L} \sin \frac{\pi X}{L} - \varepsilon_n^2 \exp(-\varepsilon_n^2 X);$$

$$K = \frac{k}{b}; \quad L = \frac{4}{\mathrm{Pe}} \cdot \frac{l}{d_o}.$$

The eigenvalues and constants are the same here as for q_{s1} = = const (Table 13-4).

4. If the heat-flux densities q_{s1} and q_{s2} at each wall are constant but not equal to one another, a solution can be obtained by superposing the temperature fields found for the cases in which just the inside or just the outside wall is heated. As we have already noted, this method can be used since the energy equation and the boundary conditions are linear. This method has been used in [4] to obtain expressions for the Nusselt numbers at the inside and outside walls:

$$Nu_1 = \cfrac{1}{G_1\left[1-\sum_{n=0}^{\infty}A_n\exp(-\varepsilon_n^2 X)\right]+\cfrac{q_{c2}}{q_{c1}}\left[H_1-\sum_{n=0}^{\infty}D_n\psi_n(\bar{R}_1)\exp(-\varepsilon_n^2 X)\right]},\quad (13\text{-}32)$$

$$Nu_2 = \cfrac{1}{\cfrac{q_{c1}}{q_{c2}}\left[G_2-\sum_{n=0}^{\infty}A_n\psi_n(\bar{R}_2)\exp(-\varepsilon_n^2 X)\right]+H_2\left[1-\sum_{n=0}^{\infty}D_n\exp(-\varepsilon_n^2 X)\right]},$$

$$(13\text{-}33)$$

where the ε_n are the same eigenvalues as in the problem considered in paragraph 2 (Table 13-4); A_n and $\psi_n(\bar{R})$ are constants and functions in the solution for the case in which just the inside wall is heated (see paragraph 2); D_n and $\varphi_n(\bar{R})$ are the constants and functions in the solution for the case in which just the outside wall is heated; $G(\bar{R})$ is a function allowing for the radial temperature distribution when there is thermal stabilization and just the inside wall is heated; $H(\bar{R})$ is th same, for the case in which just the outside wall is heated. The subscripts "1" and "2" indicate the values of G and H when $R=R_1$ and $R=R_2$. Unfortunately, the additional constants appearing in (13-32) and (13-33) have only been calculated for one value, $R_1 = 1$. They are given in Table 13-5.

When X is sufficiently large, Eqs. (13-32) and (13-33) reduce to Eqs. (13-27) for stabilized heat exchange. This clarifies the meaning of the constants: $G_1 = Nu_{1n\infty}^{-1}$; $H_1 = \Theta_{n.c1}$; $G_2 = \Theta_{n.c2}$ and $H_2 = Nu_{2n\infty}^{-1}$.

13-3. HEAT EXCHANGE UNDER BOUNDARY CONDITIONS OF THE SECOND KIND WHEN THE VELOCITY PROFILE VARIES ALONG THE LENGTH

So far, we have investigated heat exchange in annular tubes with fully developed (stabilized) flow. Here we shall consider the same problem, but under the condition that both the velocity and temperature distributions are uniform over the cross section at the entrance to the heated segment. Consequently, the velocity and temperature profiles will vary simultaneously with the length. Approximate calculations have been published for heat exchange under these conditions (the remaining conditions are the same as in
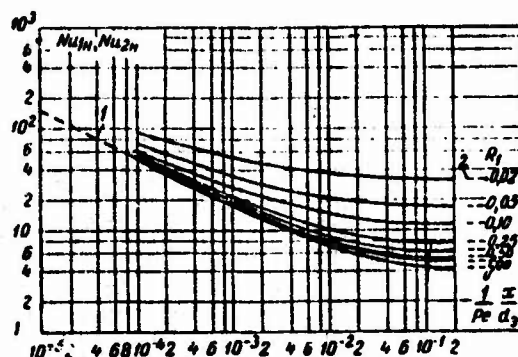

Fig. 13-13. Values of Nu_{1n} and Nu_{2n} in annular tube with $Pr = 0.7$ and various R_1. 1) Flat plate; 2) developed flow and heat exchange.

TABLE 13-5

Nusselt Numbers and Adiabatic Temperatures in Hydrodynamic Initial Segment of Annular Tube with Heating of Just the Inside or Just the Outside Wall

2. Обогрев внутренней стенки

$\frac{1}{Pe}\cdot\frac{x}{d_э}$	$R_1=0{,}02$ Pr=10 Nu$_{1н}$	Pr=10 $\Theta_{a,c2}$	Pr=0,7 Nu$_{1н}$	Pr=0,7 $\Theta_{a,c2}$	Pr=0,01 Nu$_{1н}$	Pr=0,01 $\Theta_{a,c2}$	$R_1=0{,}05$ Pr=0,7 Nu$_{1н}$	Pr=0,7 $\Theta_{a,c2}$	$R_1=0{,}10$ Pr=10 Nu$_{1н}$	Pr=10 $\Theta_{a,c2}$
0,00010	87,2	$-0{,}0_2784$	94,3	$-0{,}0_2784$	—	$-0{,}0_2784$	70,3	$-0{,}0_2191$	51,2	$-0{,}0_2364$
0,0010	54,2	$-0{,}0_2784$	53,5	$-0{,}0_2784$	—	$-0{,}0_2784$	34,0	$-0{,}0_2191$	25,3	$-0{,}0_2364$
0,0025	46,6	$-0{,}0_2196$	45,4	$-0{,}0_2196$	46,0	$-0{,}0_2196$	27,2	$-0{,}0_2176$	20,1	$-0{,}0_2909$
0,0050	41,9	$-0{,}0_2392$	41,0	$-0{,}0_2392$	40,5	$-0{,}0_2392$	23,7	$-0{,}0_2332$	17,1	$-0{,}00182$
0,010	38,1	$-0{,}0_2784$	37,4	$-0{,}0_2784$	36,3	$-0{,}0_2784$	21,2	$-0{,}00191$	14,9	$-0{,}00363$
0,025	34,6	$-0{,}00173$	34,4	$-0{,}00173$	32,4	$-0{,}00183$	19,1	$-0{,}00417$	12,9	$-0{,}00792$
0,050	33,1	$-0{,}00236$	33,1	$-0{,}00236$	32,1	$-0{,}00201$	18,1	$-0{,}00565$	12,13	$-0{,}0107$
0,10	32,7	$-0{,}00255$	32,7	$-0{,}00255$	32,2	$-0{,}00205$	17,8	$-0{,}00610$	11,92	$-0{,}0116$
0,25	32,7	$-0{,}00256$	32,7	$-0{,}00256$	32,3	$-0{,}00220$	17,8	$-0{,}00613$	11,91	$-0{,}0116$
∞	32,7	$-0{,}00256$	32,7	$-0{,}00256$	32,7	$-0{,}00256$	17,8	$-0{,}00613$	11,91	$-0{,}0116$

3. Обогрев наружной стенки

$\frac{1}{Pe}\cdot\frac{x}{d_э}$	$R_1=0{,}02$ Pr=10 Nu$_{2н}$	Pr=10 $\Theta_{a,c1}$	Pr=0,7 Nu$_{2н}$	Pr=0,7 $\Theta_{a,c1}$	Pr=0,01 Nu$_{2н}$	Pr=0,01 $\Theta_{a,c1}$	$R_1=0{,}05$ Pr=0,7 Nu$_{2н}$	Pr=0,7 $\Theta_{a,c1}$	$R_1=0{,}10$ Pr=10 Nu$_{2н}$	Pr=10 $\Theta_{a,c2}$
0,00010	39,6	$-0{,}0_2392$	52,2	$-0{,}0_2392$	—	$-0{,}0_2392$	52,3	$-0{,}0_2381$	39,7	$-0{,}0_2364$
0,0010	14,78	$-0{,}00392$	18,1	$-0{,}00392$	24,2	$-0{,}00392$	18,1	$-0{,}00381$	14,96	$-0{,}00364$
0,0025	10,49	$-0{,}00980$	12,27	$-0{,}00980$	15,9	$-0{,}00980$	12,30	$-0{,}00952$	10,64	$-0{,}00909$
0,0050	8,35	$-0{,}0191$	9,30	$-0{,}0196$	11,9	$-0{,}0196$	9,33	$-0{,}0191$	8,48	$-0{,}0182$
0,010	6,74	$-0{,}0391$	7,34	$-0{,}0392$	8,99	$-0{,}0392$	7,37	$-0{,}0381$	6,86	$-0{,}0363$
0,025	5,44	$-0{,}0863$	5,72	$-0{,}0843$	6,68	$-0{,}0940$	5,76	$-0{,}0833$	5,54	$-0{,}0792$
0,050	4,89	$-0{,}118$	5,02	$-0{,}0118$	5,97	$-0{,}125$	5,07	$-0{,}113$	4,98	$-0{,}107$
0,10	4,75	$-0{,}127$	4,77	$-0{,}127$	5,66	$-0{,}128$	4,83	$-0{,}122$	4,85	$-0{,}115$
0,25	4,73	$-0{,}128$	4,73	$-0{,}128$	5,42	$-0{,}128$	4,79	$-0{,}123$	4,83	$-0{,}116$
∞	4,73	$-0{,}128$	4,73	$-0{,}128$	4,73	$-0{,}128$	4,79	$-0{,}123$	4,83	$-0{,}116$

TABLE 13-6 CONTINUED

2 — Обогрев внутренней стенки

$\dfrac{1}{Pe}\cdot\dfrac{x}{d_v}$	$R_1=0.10$, Pr = 0.7		$R_1=0.10$, Pr = 0.01		$R_1=0.25$, Pr = 0.7		$R_1=0.50$, Pr = 10		$R_1=0.50$, Pr = 0.7		$R_1=0.50$, Pr = 0.01	
	$Nu_{1н}$	$\Theta_{а,с2}$	$Nu_{1н}$	$\Theta_{а,с2}$	$Nu_{1н}$	$\Theta_{а,с2}$	$Nu_{1н}$	$\Theta_{а,с2}$	$Nu_{1н}$	$\Theta_{а,с2}$	$Nu_{1н}$	$\Theta_{а,с2}$
0.00010	61.2	$-0{,}0_4364$	—	$-0{,}0_4364$	55.4	$-0{,}0_3800$	—	$-0{,}0_3133$	53.5	$-0{,}0_313$	—	$-0{,}0_3133$
0.0010	26.3	$-0{,}0_3364$	—	$-0{,}0_3364$	21.2	$-0{,}0_3800$	16.86	$-0{,}00133$	19.22	$-0{,}0013$	—	$-0{,}00133$
0.0025	20.1	$-0{,}0_3909$	21.7	$-0{,}0_3909$	15.20	$-0{,}00200$	12.60	$-0{,}0_3333$	13.46	$-0{,}0_3333$	—	$-0{,}0_3333$
0.0050	16.92	$-0{,}00182$	17.8	$-0{,}00182$	12.20	$-0{,}00400$	10.20	$-0{,}00667$	10.47	$-0{,}00667$	—	$-0{,}00667$
0.010	14.72	$-0{,}00364$	14.8	$-0{,}00364$	10.28	$-0{,}00800$	8.43	$-0{,}0133$	8.52	$-0{,}0133$	9.43	$-0{,}0133$
0.025	12.90	$-0{,}00792$	12.4	$-0{,}00780$	8.57	$-0{,}0173$	6.93	$-0{,}0289$	6.98	$-0{,}0289$	7.05	$-0{,}0289$
0.050	12.13	$-0{,}0107$	11.8	$-0{,}00955$	7.94	$-0{,}0235$	6.35	$-0{,}0392$	6.35	$-0{,}0392$	6.40	$-0{,}0392$
0.10	11.92	$-0{,}0116$	11.71	$-0{,}0102$	7.77	$-0{,}0254$	6.19	$-0{,}0425$	6.19	$-0{,}0425$	6.22	$-0{,}0425$
0.25	11.91	$-0{,}0116$	11.76	$-0{,}0106$	7.75	$-0{,}0255$	6.18	$-0{,}0428$	6.18	$-0{,}0428$	6.18	$-0{,}0428$
∞	11.91	$-0{,}0116$	11.91	$-0{,}0116$	7.75	$-0{,}0255$	6.18	$-0{,}0428$	6.18	$-0{,}0428$	6.18	$-0{,}0428$

3 — Обогрев наружной стенки

$\dfrac{1}{Pe}\cdot\dfrac{x}{d_v}$	$R_1=0.10$, Pr = 0.7		$R_1=0.10$, Pr = 0.01		$R_1=0.25$, Pr = 0.7		$R_1=0.50$, Pr = 10		$R_1=0.50$, Pr = 0.7		$R_1=0.50$, Pr = 0.01	
	$Nu_{2н}$	$\Theta_{а,с1}$	$Nu_{2н}$	$\Theta_{а,с1}$	$Nu_{2н}$	$\Theta_{а,с1}$	$Nu_{2н}$	$\Theta_{а,с1}$	$Nu_{2н}$	$\Theta_{а,с1}$	$Nu_{2н}$	$\Theta_{а,с1}$
0.00010	52.3	$-0{,}0_3364$	—	$-0{,}0_3364$	52.4	$-0{,}0_3364$	40.0	$-0{,}0_3267$	52.5	$-0{,}0_3267$	—	$-0{,}0_3267$
0.0010	18.1	$-0{,}0_3364$	24.2	$-0{,}0_3364$	18.2	$-0{,}0_3364$	15.14	$-0{,}00267$	18.3	$-0{,}00267$	24.2	$-0{,}00267$
0.0025	12.32	$-0{,}0_3909$	15.9	$-0{,}0_3909$	12.36	$-0{,}00909$	10.94	$-0{,}00667$	12.42	$-0{,}00667$	15.9	$-0{,}00667$
0.0050	9.35	$-0{,}0182$	11.9	$-0{,}0182$	9.38	$-0{,}0160$	8.75	$-0{,}0133$	9.45	$-0{,}0133$	11.8	$-0{,}0133$
0.010	7.39	$-0{,}0364$	8.96	$-0{,}0364$	7.43	$-0{,}0320$	7.09	$-0{,}0266$	7.50	$-0{,}0267$	8.90	$-0{,}0267$
0.025	5.78	$-0{,}0792$	6.65	$-0{,}0870$	5.83	$-0{,}0694$	5.74	$-0{,}0568$	5.91	$-0{,}0568$	6.59	$-0{,}0630$
0.050	5.10	$-0{,}107$	5.94	$-0{,}113$	5.16	$-0{,}0940$	5.20	$-0{,}0784$	5.27	$-0{,}0784$	5.88	$-0{,}0820$
0.10	4.87	$-0{,}116$	5.64	$-0{,}116$	4.93	$-0{,}102$	5.05	$-0{,}0851$	5.06	$-0{,}0851$	5.60	$-0{,}0855$
0.25	4.83	$-0{,}116$	5.43	$-0{,}116$	4.91	$-0{,}102$	5.04	$-0{,}0855$	5.04	$-0{,}0855$	5.14	$-0{,}0855$
∞	4.83	$-0{,}116$	4.83	$-0{,}116$	4.91	$-0{,}102$	5.04	$-0{,}0855$	5.04	$-0{,}0855$	5.44	$-0{,}0855$

1) Type of heating; 2) heating of inside wall; 3) heating of outside wall.

§13-2), with constant heat-flux density at one wall, the other being thermally insulated [10]. The computational method involves integrating the simplified energy equation, which makes it possible to find an approximate expression for the temperature profile that contains a certain unknown function of the x coordinate. This expression is then substituted into the integral energy equation. The unknown function is found by numerical integration. After this, the Nusselt numbers at the heated walls are determined, together with the adiabatic temperatures at the heat-insulated walls:

$$\text{Nu}_{1n} = \frac{q_{s1}d_o}{(t''_{s1}-\bar{t}'')\lambda} \quad \text{and} \quad \theta_{a.s2} = \frac{t_{a.s2}-\bar{t}''}{\frac{q_{s1}d_o}{\lambda}};$$

$$\text{Nu}_{2n} = \frac{q_{s2}d_o}{(t'_{s2}-\bar{t}')\lambda} \quad \text{and} \quad \theta_{a.s1} = \frac{t_{a.s1}-\bar{t}'}{\frac{q_{s2}d_o}{\lambda}},$$

where t''_{s1}, $\bar{t}''$, and $t_{a.s2}$ are the values of the temperatures t_{s1}, $\bar{t}$, and t_{s2} when $q_{s2} = 0$; t'_{s2}, $\bar{t}'$, and $t_{a.s1}$ are the values of the same temperatures for $q_{s1} = 0$.

For heating of just the inside wall, the calculations were carried out for several values of $R_1 = r_1/r_2$ (between 0.02 and 1), while for heating of just the outside wall values $R_1 = 0$ (round tube) and $R_1 = 1$ (flat tube with heating on one side) were used. Since the difference in the computational results for these limiting cases proved relatively small, interpolation was carried out within the interval between $R_1 = 0$ and $R_1 = 1$. Table 13-6 shows the computed results.[1] Figure 13-13 gives Nu_{1n} and Nu_{2n} as functions of $\frac{1}{\text{Pe}}\cdot\frac{x}{d_o}$ (here $\text{Pe}=\bar{w}d_o/a$) for $\text{Pr} = 0.7$ and various values of R_1. The curves located above the $R_1 = 1$ curve refer to heating of the inside surface, and the curves located below refer to heating of the outside surface. The dashed line on the left indicates the solution for a plate in a longitudinal flow; the dashed lines to the right show the solution for fully developed velocity and temperature profiles. The theoretical results are in satisfactory agreement with the experimental data obtained for air flowing in annular tubes with various ratios of radii [10].

The data given pertain to heating (cooling) of just the inside or just the outside wall. Using these data and a superposition method (see §13-2, paragraph 1), we have no difficulty in determining the Nusselt numbers at the two walls, provided constant heat-flux densities q_{s1} and q_{s2} are maintained at each wall. Here, as before, Relationships (13-26) are valid; with them, it is simple to obtain expressions resembling (13-27) for the Nusselt numbers with simultaneous heating of both walls:

$$\left.\begin{array}{l} \dfrac{1}{\text{Nu}_1} = \dfrac{1}{\text{Nu}_{1n}} + \dfrac{q_{s2}}{q_{s1}}\theta_{a.s1}, \\[2mm] \dfrac{1}{\text{Nu}_2} = \dfrac{1}{\text{Nu}_{2n}} + \dfrac{q_{s1}}{q_{s2}}\theta_{a.s2}, \end{array}\right\} \qquad (13\text{-}34)$$

where

$$\mathrm{Nu}_1 = \frac{q_{c1} d_{\ni}}{(t_{c_1} - \bar{t})\lambda} \quad \text{and} \quad \mathrm{Nu}_2 = \frac{q_{c2} d_{\ni}}{(t_{c_2} - \bar{t})\lambda};$$

here t_{s1}, t_{s2}, and $\bar{t}$ are the temperatures of the inside and outside walls and the mean mass temperature of the fluid with simultaneous heating of both walls.

Example. In an annular tube with $R_1 = 0.10$, let air move (Pr = = 0.7) at Re = 2000. The ratio $q_{s2}/q_{s1} = 2$. We are to determine Nu at both walls a distance $x/d_e = 7$ from the entrance.

The reduced distance from the entrance is

$$\frac{1}{Pe} \cdot \frac{x}{d_{\ni}} = \frac{7}{2\,000 \cdot 0.7} = 0,005.$$

Using Table 13-6 and the values $R_1 = 0,10$; $Pr = 0,7$ and $\frac{1}{Pe} \cdot \frac{x}{d_{\ni}} = 0,005$, we find $\mathrm{Nu}_{1\infty} = 16,92$; $\theta_{\text{a.c}_1} = -0,00182$; $\mathrm{Nu}_{2\infty} = 9,35$ and $\theta_{\text{a.c}_1} = -0,0182$. Using Eqs. (13-34), we have

$$\mathrm{Nu}_1 = \left(\frac{1}{16,92} - 2 \cdot 0,0182 \right)^{-1} = 44,0;$$

$$\mathrm{Nu}_2 = \left(\frac{1}{9,35} - \frac{1}{2} \cdot 0,00182 \right)^{-1} = 9,43.$$

Knowing Nu_1 and Nu_2 and using the heat balance to determine the mean mass temperature $\bar{t}$, we can easily calculate the wall temperature t_{s1} and t_{s2}.

13-4. INFLUENCE OF RADIATIVE HEAT TRANSFER

For a diathermal medium, the influence of radiative heat transfer on convective heat exchange is felt only by way of the boundary conditions.

If a certain temperature distribution, i.e., boundary conditions of the first kind, are specified at the inside and outside walls of an annular tube, then radiative and convective heat exchange will not influence one another, and they can be treated completely independently by the usual methods. Thus, for example, for a long tube with temperatures that are constant but not identical at the inside and outside walls, the heat flow produced by radiation from one wall to the other will be

$$Q = \sigma \varepsilon_{\text{np}} (T_{c_1}^4 - T_{c_1}^4) F,$$

where σ is the constant in the Stephan-Boltzmann law; ε_{pr} is the reduced system emissivity,

$$\frac{1}{\varepsilon_{\text{np}}} = \frac{1}{\varepsilon_1} + \frac{F_1}{F_2} \left(\frac{1}{\varepsilon_2} - 1 \right);$$

ε_1 and ε_2 are the emissivities of the inner and outer walls; F_1 and F_2 are the wall surfaces; and T_{s1} and T_{s2} are their absolute temperatures.

If the heat-flux densities are specified at the walls of the annular tube, for example as $q_{s1}(x)$ and $q_{s2}(x)$, i.e., if we are given boundary conditions of the second kind, then radiative heat transfer will introduce a substantial change in the boundary conditions. In the absence of radiation, the boundary conditions will have the form

$$-\left(\frac{\partial t}{\partial r}\right)_{r=r_1}=\frac{q_{c_1}}{\lambda}, \quad \left(\frac{\partial t}{\partial r}\right)_{r=r_2}=\frac{q_{c_2}}{\lambda},$$

while with simultaneous radiative and convective transport of energy, they have the form

$$-\left(\frac{\partial t}{\partial r}\right)_{r=r_1}=\frac{1}{\lambda}\left(q_{c_1}+E'_{nad}\varepsilon_1-E'_{c6}\right),$$

$$\left(\frac{\partial t}{\partial r}\right)_{r=r_2}=\frac{1}{\lambda}\left(q_{c_2}+E''_{nad}\varepsilon_1-E''_{c6}\right),$$

where E'_{nad} and E'_{c6}, E''_{nad} and E''_{c6} are the densities of the incident and intrinsic emissions at a given point on the tube inside and outside surfaces.

Radiative heat transfer may lead to a substantial change in the difference in the temperatures between individual elements of the inside tube surface as compared with the values for purely convective heat exchange, i.e., there will be a certain equalization of the inside-surface temperatures (for the same values of q_{s1} and q_{s2}). As far as we know, there has been no consideration given to the problem of heat exchange in annular tubes under boundary conditions of the second kind with allowance for radiation.

In practice, we often encounter the case in which one wall of an annular tube is heat-insulated (q_{s1} = 0 or q_{s2} = 0), while the temperature of the other wall is constant. In such cases, the heat-insulated wall delivers heat by radiation to the cooler wall (or receives heat from the hotter wall) through which heat is being transferred, while simultaneously receiving heat from the gas flow (or delivering heat to the flow) owing to convection. Since there is no resultant heat flow at the heat-insulated wall, the heat-flux densities produced at each point on its surface by convective and radiative heat exchange will be equal in absolute value but opposite in sign. There also is no known solution for this problem, but we can make an approximate evaluation of the influence of radiation in such a system. For example, let the inside wall be heat-insulated. We then can write the following approximate relationships to represent the heat balance for the insulated wall and the gas flow:

$$a_1(\bar{T} - T_{c_1}) = \sigma \varepsilon_{\text{пр}}(T^4_{c_1} - T^4_{c_2});$$

$$a_1(\bar{T} - T_{c_1})\pi d_1 + a_2(\bar{T} - T_{c_2})\pi d_2 = -\rho c_p \bar{w}\frac{d\bar{T}}{dx}\cdot\frac{\pi(d_2^2 - d_1^2)}{4}.$$

Assuming α_1, α_2, and T_{s2} to be known,[11] and solving these equations simultaneously (numerically or analytically), we can determine the variation in $\bar{T}$ and T_{s1} along the tube length, and can then calculate the heat flux at the outside wall owing to convection and radiation:

$$Q_2 = \int_0^l [a_2(\bar{T} - T_{c_2})\pi d_2 + \sigma \varepsilon_{\text{пр}}(T^4_{c_1} - T^4_{c_2})\pi d_1]\,dx.$$

It follows from these equations that radiation from the heat-insulated wall may substantially increase the heat flux at the wall through which heat is exchanged. This fact is often used to intensify heat exchange in tubes by placing a bar made from a material that is a good radiator within the tube. If the heat-flux density is specified at the tube wall, the presence of such a radiating bar makes it possible to reduce the wall temperature for the same value of q_{s2}.

Manuscript Page No.	Footnotes
297	[1]See, for example, §§6-1, 6-2, and 6-4. This will evidently also hold for an annular tube.
299	[2]The subscript "n" on Nu means that heating is "nonsymmetric," i.e., just one of the walls is heated.
299	[3]The calculations make use of Eqs. (13-3) and (13-4) with $R_1 = 0$. Here t_{s1} is interpreted as the temperature on the tube axis, while $\left(\frac{q}{q_{c2}}\right)_1 = R$.
301	[4]The new variable $\tilde{R}$ introduced here is associated with the variable R by the relationship $\tilde{R} = \frac{R}{1 - R_2}$.
304	[5]The directions of n and r coincide at the inside wall $\left(\frac{\partial}{\partial n} = \frac{\partial}{\partial r}\right)$, while they are opposite at the outside wall $\left(\frac{\partial}{\partial n} = -\frac{\partial}{\partial r}\right)$.
306	[6]At first glance, this transition to the limit may not appear to give correct results, since according to (13-5) the condition $w_x = 0$ is maintained on the axis. In this connection we note that the expression for the temperature

field [see (13-17) an (13-18)] does not contain just W_x, but $W_x R$. When $R = 0$, $W_x R$ vanishes regardless of the value of W_x on the axis.

309   [7]The subscript "a" means that the wall is adiabatic.

311   [8]Calculations have also been given in [9] for the special case of nonsymmetric heating; the results agree with ours.

311   [9]The way in which Nu_{1a} varies for small R_1 cannot be seen in Fig. 13-10 since the scale is too small.

319   [10]A table has been given in §12-4 (Table 12-2) for $R_1 = 1$ (flat tube).

322   [11]Approximate estimates for α_1 and α_2 can be obtained on the basis of the data given above for purely convective heat exchange.

Manuscript Page No.	Transliterated Symbols
296	c = s = stenka = wall
298	э = e = ekvivalentnyy = equivalent
299	н = n = nesimmetrichnyy = nonsymmetric
309	a.c = a.s = adiabaticheskaya stenka = adiabatic wall
320	пр = pr = privedennyy = reduced
321	над = pad = padayushchiy = incident
321	сб = sb = sobstvennyy = intrinsic

Chapter 14

HEAT EXCHANGE IN PRISMATIC, CYLINDRICAL, AND CURVED TUBES

14-1. PRELIMINARY REMARKS

Investigation of heat exchange for viscous flow in prismatic or cylindrical (but not round) tubes is of great interest from the viewpoint of designing compact heat-exchange systems. Compactness problems are very important for many heat-exchange plants, in particular for systems cooling nuclear reactors. Examples of compact systems are the regenerative rotating-head exchangers employed in boiler and gas-turbine plants. In such exchangers, the head forms a system of narrow channels of triangular or rectangular shape.

For a fluid flowing in prismatic tubes, the temperature field is three-dimensional; this significantly complicates research, and prevents the use of most of the analysis methods used earlier. Approximate methods (numerical or analytic) are ordinarily employed to determine temperature fields in prismatic tubes. The finite-difference method is used in particular, while recently variational methods and the associated Galerkin and Ritz methods have found employment. Elementary problems of heat exchange in tubes with cross sections that are not round (for example, for fully developed velocity and temperature fields) admit of exact solutions, by means of functions of a complex variable, for instance.

From the mathematical viewpoint, many problems of heat exchange in prismatic tubes are analogous to certain problems in elasticity theory. Both types of problem are described by differential equations of the same kind under identical or similar boundary conditions. This permits the familiar solutions obtained in the well-field of elasticity theory to be used directly, or after appropriate modification, for heat-exchange computations.

Owing to significant computational difficulties, problems of heat exchange in prismatic and cylindrical (nonround) tubes have still not received adequate development.

14-2. HEAT EXCHANGE IN PRISMATIC AND CYLINDRICAL TUBES UNDER BOUNDARY CONDITIONS OF THE FIRST KIND

1. Let us consider heat exchange in a tube with cross section in the form of an *equilateral triangle* with a uniformly distributed entrance temperature and constant wall temperature. We assume that the properties of the fluid are constant and that the flow is stabilized; then neglecting axial heat conduction and the heat of fric-
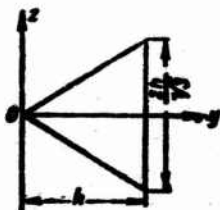
Fig. 14-1. The problem of heat
exchange in a triangular tube.

tion, we write the energy equation as

$$w_x \frac{\partial t}{\partial x} = a\left(\frac{\partial^2 t}{\partial y^2} + \frac{\partial^2 t}{\partial z^2}\right).$$

As usual, the x axis is directed along the tube axis; Fig.
14-1 shows the direction of the y and z axes.

Equation (5-17a) describes the velocity profile in a tube
with cross section in the form of an equilateral triangle. Sub-
stituting this expression into the energy equation and going
over to dimensionless variables, we obtain

$$\frac{\partial^2 \theta}{\partial Y^2} + \frac{\partial^2 \theta}{\partial Z^2} = 101,25\left[(Y-1)\left(Z^2 - \frac{1}{3}Y^2\right)\right]\frac{\partial \theta}{\partial X}. \qquad (14\text{-}1)$$

Here we let

$$\theta = \frac{t-t_c}{t_0-t_c}; \quad X = \frac{1}{Pe}\cdot\frac{x}{d_3}; \quad Pe = \frac{\bar{w}d_3}{a}; \quad Y = \frac{y}{h}; \quad Z = \frac{z}{h};$$

Where h is the altitude of the triangle, and $d_3 = \frac{4f}{s} = \frac{2}{3}h$ is the
equivalent diameter.

The boundary conditions have the form

$$\left.\begin{array}{l}\theta = 1 \text{ for } X = 0, \; 0 < Y < 1 \text{ and } -\frac{1}{\sqrt{3}}Y < Z < \frac{1}{\sqrt{3}}Y; \\[2mm] \theta = 0 \text{ for } X \geqslant 0, \; 0 < Y \leqslant 1 \text{ and } Z = \pm\frac{1}{\sqrt{3}}Y.\end{array}\right\} \qquad (14\text{-}2)$$

An approximate solution of this problem has been obtained by
V.K. Migay by the Galerkin method [1]. By the substitution

$$\theta(X, Y, Z) = AF(Y, Z)e^{-\epsilon X},$$

where A and ϵ are constants, Eq. (14-1) is reduced to the form

$$L(F) = \frac{\partial^2 F}{\partial Y^2} + \frac{\partial^2 F}{\partial Z^2} + \epsilon'\left[(Y-1)\left(Z^2 - \frac{1}{3}Y^2\right)\right]F = 0, \qquad (14\text{-}3)$$

where $\epsilon' = 101,25\epsilon$.

It follows from the second boundary condition of (14-2), that

$$F = 0 \text{ for } 0 < Y < 1 \text{ and } Z = \pm \frac{1}{\sqrt{3}} Y. \qquad (14\text{-}4)$$

The general solution of the problem can evidently be represented as the following series:

$$\theta = \sum_{n=1}^{\infty} A_n F_n(Y, Z) e^{-\epsilon_n X}. \qquad (14\text{-}5)$$

Thus the problem reduces to finding the eigenvalues ϵ_n and eigenfunctions F_n of (14-3) under the boundary condition (14-4).

Following the Galerkin method [2], we approximate the eigenfunctions by a polynomial that is even in Z:

$$F_n = B_1 \omega + B_2 \omega Z^2 + B_3 \omega Y + \dots = B_1 \varphi_1 + B_2 \varphi_2 + B_3 \varphi_3 + \dots + B_m \varphi_m, \qquad (14\text{-}6)$$

where $B_1, B_2, \dots, B_m$ are undetermined coefficients;

$$\omega = (Y - 1)\left(Z^2 - \frac{1}{3} Y^2\right); \; \varphi_1 = \omega; \; \varphi_2 = \omega Z^2, \text{ etc.}$$

The expression for F_n satisfies boundary conditions (14-14), since $\omega = 0$ on the boundary of the triangle.

If $F_n(Y, Z)$ is to be an approximate solution of (14-3), the condition requiring orthogonality of $L(F_n)$ with respect to all functions φ_i $(i=1, 2, \dots, m)$ must be satisfied:

$$\iint_f L(F_n) \varphi_i \, dY \, dZ = 0 \; (i = 1, 2, \dots, m). \qquad (14\text{-}7)$$

where the integral is taken over the region f bounded by the triangle perimeter.

Condition (14-7) leads to a linear system of algebraic equations in the unknown coefficients B_i; the coefficients can be determined from this condition. The eigenvalues are found from the condition for existence of a nontrivial solution to this equation system. As a result, we obtain expressions for the eigenfunctions that are accurate to within a constant factor, which is later found from the normalization condition:

$$\iint_f F_n^2 \omega \, dY \, dZ = 1. \qquad (14\text{-}8)$$

In first approximation, $F_{nI} = B_1 \omega$. In accordance with (14-7), we have

$$\int_0^1 dY \int_0^{Y/\sqrt{3}} \left(\frac{\partial^2 B_1 \omega}{\partial Y^2} + \frac{\partial^2 B_1 \omega}{\partial Z^2} + \epsilon' B_1 \omega^2\right) \omega \, dZ = 0.$$

Carrying out the calculations, we determine the value of the first eigenvalue in first approximation: $\epsilon_{11} = 11.4$.

In se ond approximation,

$$F_{n} = f \omega - B_2 \omega Z^2.$$

The System (14-7) is written as

$$\int_0^1 dY \int_0^1 \left(\frac{\partial^2 F_{nII}}{\partial Y^2} + \frac{\partial^2 F_{nII}}{\partial Z^2} + \epsilon' \phi F_{nII} \right) \omega \, dZ = 0,$$

$$\int_0^1 dY \int_0^{Y/Z} \left(\frac{\partial^2 F_{nII}}{\partial Y^2} + \frac{\partial^2 F_{nII}}{\partial Z^2} - \epsilon' \phi_n \right) \omega Z^2 \, dZ = 0.$$

After substitution and integration, we obtain the following system of algebraic equations:

$$B_1(0.1175\epsilon' - 13.333) + A_2(0.1975\epsilon' - 0.4235) = 0,$$

$$B_1(0.0565\epsilon' - 12.69) + B_2(0.0028\epsilon' - 1.905) = 0.$$

The first solution will be $B_1 = 0$, $B_2 = 0$. The second (nontrivial) solution is easily found by representing the equations in the form

$$B_1 = -B_2 \frac{\cdots}{\cdots},$$

$$B_1 = A_2 \frac{\cdots}{\cdots}.$$

Equating these expressions, we obtain a quadratic equation for ϵ'; solving it, we find two roots, which, respectively, equal ϵ_{III}. These roots also give the first and second eigenvalues in second approximation $\epsilon_{III} = 10.709$ and $\epsilon_{2II} = 87.53$.

Substituting the eigenvalues into one of the preceding equations, we find B_1 and B_2 (to within a constant factor). This is used in approximation, the first and second eigenfunctions F_{nII} which will be found in second approximation as obtain,

Thus,

$$F_{nIII} = B_{00} + B_{20} \omega Z^2 + B_{00} Y.$$

in third approximation, we use an analogous method to find $\epsilon_{III} = 10.705$ and $\epsilon_{2III} = 86.57$.

see that the difference in the values of ϵ_{1II} and ϵ_{1III} ... ~ .04%, while the difference is 1.1% for ϵ_{2II} and ϵ_{2III}. We thus can assure that the first and second eigenvalues ϵ_1 and ϵ_2 have been determined with sufficient accuracy.

The coefficients B_2 for the first eigenfunction (in third ap-

proximation) equal $B_1 = 0.1083C$, $B_2 = -0.4869C$ and $B_3 = 0.01997C$ where C is an unknown constant. Substituting these values into the expression for $F_{n III}$ and determining C by means of (14-8), we obtain the final expression for the first eigenfunction in third approximation:

$$F_1 = 247\omega - 1\,110\omega Z^2 + 45.5\omega Y.$$

We use a similar method to find the second eigenfunction:

$$F_2 = 152\omega - 11\,340\omega Z^2 + 31.6\omega Y.$$

To complete the calculations, we must still determine the constants A_n in (14-5). When $X = 0$, we have

$$1 = \sum_{n=1}^{n} A_n F_n.$$

Multiplying this equation by $F_k \omega dY dZ$, integrating over region f, and remembering that

$$\iint_f F_k F_n \omega dY dZ = \begin{cases} 0 \text{ for } k \neq n \\ 1 \text{ for } k = n, \end{cases}$$

we obtain

$$A_n = \iint_f F_n \omega dY dZ.$$
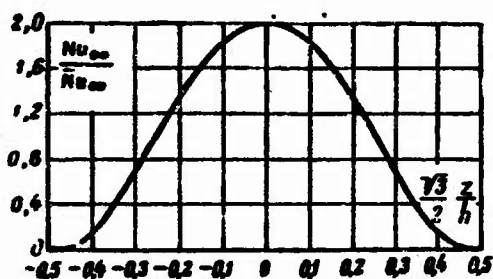
Fig. 14-2. Distribution of local values of Nu_∞ along side of triangular tube.

The calculations yield $A_1 = 0.103$, $A_2 = 0.0342$.

Rewriting (14-5) with allowance for the values found for the functions and constants, we obtain the following expression for the temperature field:

$$\Theta = (22.55\omega - 114.2\omega Z^2 + 4.69\omega Y)\exp(-10.705X) +$$
$$+ (5.2\omega - 388\omega Z^2 + 1.08\omega Y)\exp(-86.57X). \tag{14-9}$$

The mean mass temperature of the fluid in the given section is

$$\bar{\theta} = \frac{\bar{t} - t_c}{t_0 - t_c} = \frac{\iint_f \theta W_x \, dY \, dZ}{\iint_f W_x \, dY \, dZ},$$

where

$$W_x = \frac{w_x}{\bar{w}} = 45\omega \quad [\text{see (5-17a)}].$$

Performing the calculations, we find

$$\bar{\theta} = 0.827 \exp(-10.705X) + 0.0902 \exp(-86.57X). \tag{14-10}$$

The local Nusselt number is

$$\mathrm{Nu} = \frac{\alpha d_9}{\lambda} = -\frac{2}{3} \frac{1}{\bar{\theta}} \left(\frac{\partial \theta}{\partial Y}\right)_{Y=1}.$$

Using (14-9) and (14-10), we obtain

$$\mathrm{Nu} = \frac{\frac{2}{3}\left(Z^2 - \frac{1}{3}\right)[(114.2Z^2 - 30.24)\exp(-10.705X) + (6.28 - 388Z^2)\exp(-86.57X)]}{0.827 \exp(-10.705X) + 0.0902 \exp(-86.57X)}. \tag{14-11}$$

For $X \to \infty$, we find

$$\mathrm{Nu}_\infty = 0.806 \left(Z^2 - \frac{1}{3}\right)(114.2Z^2 - 30.24). \tag{14-12}$$

This equation yields the distribution of local values for the limiting Nu numbers over the side of a triangular tube. Figure 4-12 shows the ratio $\frac{\alpha_\infty}{\bar{\alpha}_\infty} = \frac{\mathrm{Nu}_\infty}{\overline{\mathrm{Nu}}_\infty}$ as a function of Z, where $\bar{\alpha}_\infty$ is the heat-transfer coefficient, averaged over the perimeter, and calculated from Eq. (14-12). At the center of each side, α_∞ has its maximum value, which is 2 times $\bar{\alpha}_\infty$. As we approach the corners, α_∞ drops, vanishing at the corners. This type of variation in α_∞ is dictated by the velocity profile; as we can see, for example, from Fig. 5-3, the velocity is considerably less near the corners than far from them.

Since Solution (14-9) is approximate, it contains a certain error; the derivatives of this expression with respect to Y and Z will contain still greater errors. Thus Eqs. (14-11) and (14-12), obtained by differentiating (14-9) with respect to Y, are inaccurate, and they should not be used to determine the mean Nusselt number $\overline{\mathrm{Nu}}$ over the perimeter. This is better done by means of Eq. (14-10). We then have

$$\overline{\mathrm{Nu}} = -\frac{1}{4} \cdot \frac{1}{\bar{\theta}} \cdot \frac{d\bar{\theta}}{dX} = \frac{2.213 \exp(-10.705X) + 1.952 \exp(-86.57X)}{0.827 \exp(-10.705X) + 0.0902 \exp(-86.57X)} \tag{14-13}$$

and

$$\overline{\mathrm{Nu}}_\infty = -\frac{\varepsilon_1}{4} = \frac{10.705}{4} = 2.68. \tag{14-14}$$

This value of $\overline{\mathrm{Nu}}_\infty$ is in satisfactory agreement with experimental data and other calculated estimates.[1]

Averaging $\overline{Nu}$ over the tube length, we find

$$\overline{\overline{Nu}} = \frac{\overline{\overline{a}}d_0}{\lambda} = \frac{1}{l}\int_0^l \overline{Nu}\,dx = -\frac{1}{4}\,Pe\,\frac{d_0}{l}\ln\overline{\theta}_{x=l}$$

or

$$\overline{\overline{Nu}} = -\frac{1}{4}\,Pe\,\frac{d_0}{l}\,\ln\left[0.827\exp\left(-\frac{10.705}{Pe}\frac{l}{d_0}\right) + \right.$$
$$\left. + 0.0902\exp\left(-\frac{86.57}{Pe}\cdot\frac{l}{d_0}\right)\right]. \qquad (14\text{-}15)$$

Figure 14-3 compares values of $\overline{\overline{Nu}}$, computed from (14-15), with experimental data [1] on heat transfer in triangular tubes. We can see that the calculated and experimental values are in satisfactory agreement.[2] The figure also shows a curve for a round tube. As we might expect, $\overline{\overline{Nu}}$ is lower for the triangular tube than for the round tube owing to the poor heat transfer at the corners. The equations derived here are valid for $\frac{1}{Pe}\cdot\frac{x}{d_0} > 0.01$ (they may not be accurate enough for smaller values).

2. Let us now analyze heat exchange in a *rectangular tube* with a uniformly distributed entrance temperature and constant wall tempe ture (the remaining conditions are the same as for paragraph 1). Here the energy equation and the boundary conditions have the form

$$W_x\frac{\partial\theta}{\partial X} = \frac{\partial^2\theta}{\partial Y^2} + \frac{\partial^2\theta}{\partial Z^2}, \qquad (14\text{-}16)$$

where W_x is determined by Eq. (5-16);

$$\left.\begin{array}{l}\theta = 1 \text{ for } X = 0,\ -B < Y < B,\ -H < Z < H;\\ \theta = 0 \text{ for } X > 0,\ Y = \pm B;\\ \theta = 0 \text{ for } X > 0,\ Z = \pm H,\end{array}\right\} \qquad (14\text{-}17)$$

where

$$\theta = \frac{t-t_0}{t_0 - t_s};\ \ Y = \frac{y}{d_0};\ \ Z = \frac{z}{d_0};\ \ B = \frac{b}{2d_0} = \frac{1+\frac{1}{\gamma}}{4};$$
$$H = \frac{h}{2d_0} = \frac{1+\gamma}{4};\ \ d_0 = \frac{4bh}{2(b+h)};$$

here $\gamma = h/b$ is the ratio of sides for the tube cross section.

Figure 14-4 shows the direction of the y and z axes. The remaining notation is the same as in paragraph 1.

An approximate solution has been obtained in [3, 4] by the Galerkin method. In [5], a numerical method was employed to find the limiting $\overline{Nu}_\infty$ numbers, averaged over the perimeter, while in [5a], $\overline{Nu}$ was found as a function of X. In principle, the solution is analogous to the one considered in paragraph 1, so that we shall only give the ultimate results. The mean mass temperature
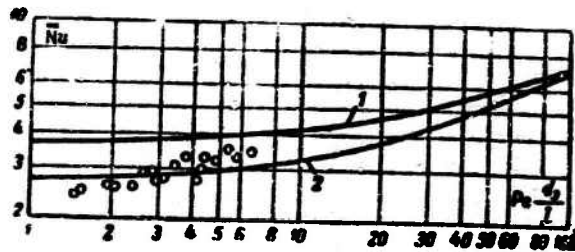
Fig. 14-3. $\overline{\overline{Nu}} = F\left(Pe\frac{d_e}{l}\right)$. 1) Calculations for round tube; 2) calculations for triangular tube; circles) Experimental data for triangular tube.
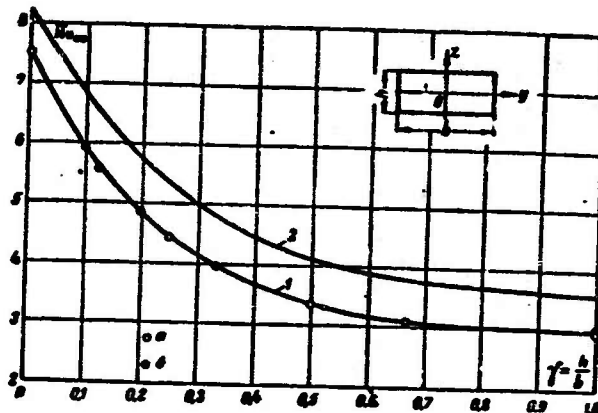

Fig. 14-4. Dependence of $\overline{Nu}_\infty$ on γ for rectangular tube. 1) t_s = const (a) Data of [3, 4]; b) data of [5]; 2) q_s = const along length and t_s = const along perimeter.

f the fluid is

$$\overline{\theta} = \frac{t - t_c}{t_0 - t_c} = \sum_{n=1}^{\infty} A_n \exp\left(-\beta_n \frac{1}{Pe} \cdot \frac{x}{d_e}\right). \qquad (14\text{-}18)$$

Table 14-1 shows the constants A_n and β_n as functions of the ratio of the cross-section sides.

With (14-18), it is not difficult to compute the Nusselt number averaged over the perimeter in a given section and to find its limiting value. The latter will obviously be

$$\overline{Nu}_\infty = \frac{\overline{a}_\infty d_e}{\lambda} = \frac{\beta_1}{4}. \qquad (14\text{-}19)$$

Figure 14-4 shows $\overline{Nu}_\infty$ as a function of γ on the basis of pub-

- 331 -

TABLE 14-1

Values of Constants in Problem of Heat Exchange in Rectangular Tube for t_s = const

$\gamma = \frac{a}{b}$	β_1	β_2	β_3	A_1	A_2	A_3
1 По данным [Л. 3]						
0.125	22.38	25.61	31.81	0.737	0.091	0.034
0.250	17.76	28.17	47.82	0.755	0.107	0.028
0.500	13.57	41.17	94.93	0.789	0.071	0.030
0.667	12.49	51.56	99.71	0.802	0.064	0.043
1.000	11.91	71.07	157.9	0.804	0.104	0.014
2 По данным [Л. 4]						
0.100	23.745	381	—	0.8	0.064	—
0.200	19.48	303	—	0.813	0.069	—
0.333	16.024	236	—	0.835	0.07	—
1.000	12.25	103.5	—	0.83	0.06	—

1) Data of [3]; 2) data of [4].

Fig. 14-5. Dependence of $\overline{\overline{Nu}}$ as function of $\frac{1}{Pe} \cdot \frac{l}{d_s}$ at values $\gamma = 1$, 1/2, and 1/8 for a rectangular tube with t_s = const.

lished data [3, 4] (curve 1). These data are in excellent agreement. They agree just as well with the results of numerical calculations [5]. When $\gamma = 0$, i.e., for a flat tube, $Nu_\infty = 7.54$, which agrees with the value found previously (see §6-2).

The Nusselt number, averaged over the perimeter and the length, and referred to the mean logarithmic temperature head, is

$$\overline{\overline{Nu}} = \frac{\overline{\overline{a}} d_s}{\lambda} = -\frac{1}{4} Pe \frac{d_s}{l} \ln \sum_{n=1}^{\infty} A_n \exp\left(-\beta_n \frac{1}{Pe} \cdot \frac{l}{d_s}\right). \qquad (14\text{-}20)$$

Figure 14-5 shows $\overline{\overline{Nu}}$ as a function of $\frac{1}{Pe} \cdot \frac{l}{d_s}$ for all values of γ on the basis of published data [4].

Owing to the approximate nature of the calculations, there is considerable divergence in the values of the constants A_1, A_2, and, in particular, β_2, as found from the data of [3, 4] (see Table 14-1). The discrepancy in $\overline{\overline{Nu}}$ is not very great, however: for $\frac{1}{Pe} \cdot \frac{l}{d_e} > 0.01$ and $\gamma = 1 - 0.5$, it does not exceed 3%, increasing to 14% when $\gamma \simeq 0.1$. Without a special analysis, it is difficult to give preference to one set of data or the other. Since the calculations are not accurate enough in the region of small $\frac{1}{Pe} \cdot \frac{x}{d_e}$, Eqs. (14-18) and (14-20) can be used when $\frac{1}{Pe} \cdot \frac{x}{d_e} > 0.01$ for tubes that are not too short.

The values of $\overline{\overline{Nu}}$ and, in particular, $\overline{Nu}_\infty$ for rectangular and triangular tubes, calculated from the equivalent diameter, deviate significantly from Nu for a round tube. This occurs since the velocity and temperature profiles depend substantially on cross-section geometry. Thus large errors may result when heat transfer for prismatic tubes is determined from the round-tube equations and the equivalent diameter. Near the tube entrance, i.e., in the thermal and hydrodynamic initial segments, the velocity and temperature fields depend little on cross-section geometry, since almost all the velocity and temperature changes are concentrated in the layer near the wall. Thus near the entrances of prismatic tubes, Nu and $\overline{\overline{Nu}}$ computed from d_e will differ little from the corresponding round-tube values. In passing, we note that approximate determination of heat exchange in the hydrodynamic initial segment of a rectangular tube for $x \ll l_{n.g}$ can be based on the bar-flow model (see §12-2, paragraph 2).

TABLE 14-2

Values of $\overline{Nu}_\infty$ and C for Tubes of Elliptical Cross Section as Function of Ratio Between Semimajor and Semiminor Axes

b_1/b_2	1.25	2.0	4.0	8.0	16.0
$\overline{Nu}_\infty$	3.67	3.74	3.79	3.72	3.65
C	0.0138	0.0158	0.0239	0.0388	0.0578

3. Calculations for heat exchange in a tube of *elliptical cross section* have been given in [6] for constant fluid temperature at the entrance and constant wall temperature. Table 14-2 shows values of Nusselt numbers averaged over the perimeter, calculated from the equivalent diameter. They depend on the ratio b_1/b_2 of of ellipse semiaxes, but vary within fairly narrow limits and are close to the values of Nu_∞ for a round tube. The Nusselt number

averaged over the perimeter and over the length can be found from the approximate expression

$$\frac{\overline{\overline{Nu}}}{\overline{Nu}_\infty} \approx 1 + \frac{C}{\frac{1}{Pe}\cdot\frac{x}{d_s}},\tag{14-21}$$

which holds for values $\frac{1}{Pe}\cdot\frac{x}{d_s} > 0,02$. Table 14-2 gives values of C as a function of b_1/b_2.
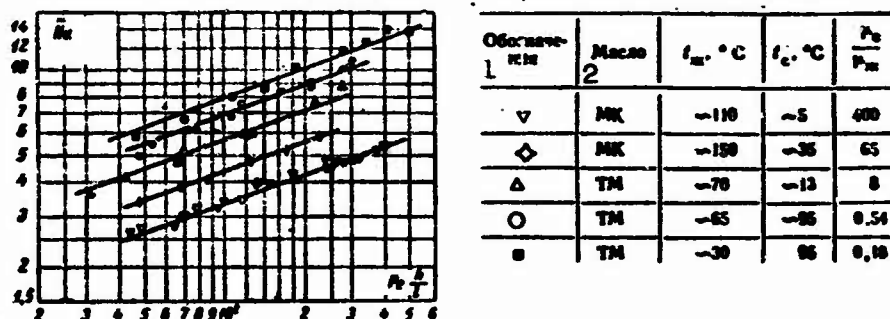

Fig. 14-6. Dependence of $\overline{\overline{Nu}}$ as function of Pe h/l and μ_s/μ_{zh} for motion in rectangular tube. 1) Symbols; 2) oil.

Fig. 14-7. Heat transfer in rectangular tube as a function of μ_s/μ_{zh}.

4. We have so far assumed that the physical properties of the fluid are constant. If heat exchange occurs under sufficiently great temperature differences, we must allow for the variation in physical properties with temperature. So far as we know, there have been no theoretical evaluations of the influence of variable physical properties on heat exchange in prismatic tubes. There is an experimental study by Ye.A. Krasnoshchekov and the author [7] in which the mean heat exchange was measured in a rectangular tube $(h/b = 0,192;\ l/h = 227;\ h = 3,3\ mm)$ with flows of type MK oil and transformer oil. The measurements were carried out in the following ranges: $20 < Re < 2070,\ 1,6\cdot10^{-3} < \frac{1}{Pe}\cdot\frac{l}{h} < 0,03$ and $0,2 < \frac{\mu_c}{\mu_m} < 420$ with both heating and coo of the fluid.

The measurement results are shown in Fig. 14-6; we see that in the thermal initial segment of the rectangular tube, as for round and flat tubes, $\overline{\overline{Nu}} \sim \left(Pe\,\frac{h}{l}\right)^{1/3}$. [3] The effect of variable viscosity

is shown in Fig. 14-7, which shows the same data with $\overline{Nu}/\overline{Nu_0}$ as a function of μ_s/μ_{zh}. Here $\overline{Nu}$ is the experimentally determined Nusselt number, while $\overline{Nu_0}$ is the value computed from Eq. (6-58) for a flat tube on the assumption that the physical properties of the fluid are constant; μ_g is the value of the dynamic-viscosity coefficient at the wall temperature, while μ_{zh} is the value at $t = t_c - \overline{\Delta t_x}$.

The measurement results are quite satisfactorily described by the following equation (see the curve of Fig. 14-7):

$$\overline{\overline{Nu}} = 1.85\left(Pe\,\frac{d_2}{l}\right)^{1/3}\left(\frac{\mu_c}{\mu_m}\right)^{-0.10}, \qquad (14-22)$$

where

$$\overline{\overline{Nu}} = \frac{\overline{\overline{a}}d_0}{\lambda_r} = \frac{\overline{\overline{q}}_c d_2}{\overline{\Delta t}_x \lambda_r}; \quad Pe = \frac{\overline{w}d_0}{a_r};$$

here $\overline{\overline{q_s}}$ is the heat-flux density at the wall, averaged over the perimeter and the length; $\overline{\Delta t_1}$ is the mean logarithmic temperature head. The values of the thermal-conductivity and thermal-diffusivity coefficients λ_g and a_g are taken at a temperature $t_r = t_c - \frac{1}{2}\overline{\Delta t_x}$.

The fact that $\overline{\overline{Nu}}$ depends on $Pe\, d_e/l$ in the same way for a rectangular tube with side ratio $h/b = 0.192$ as for a flat tube (when $\mu_s/\mu_{zh} = 1$) naturally does not give sufficient reason for extending this result to rectangular tubes with other side ratios.

The method of allowing for the variable viscosity as a correction factor $(\mu_s/\mu_{zh})^{-0.10}$ and, in approximation, for the variation in λ and a by referring them to the temperature t_g can evidently be used to determine heat transfer in prismatic tubes varying in geometry (until more complete data is obtained). Naturally, these corrections must be introduced into equations obtained on the assumption that the physical properties remain constant for tubes of the given form. We also note that they are valid only for liquids. thods developed for round tubes (see Chapters 7, 9) can be used in approximation to allow for the influence of all variable physical properties (and not just viscosity) on heat exchange in cylindrical tubes with noncircular cross-sectional shapes.

See §7-6 for hydraulic resistance in prismatic tubes with allowance for the dependence of μ on t.

14-3. HEAT EXCHANGE IN PRISMATIC AND CYLINDRICAL TUBES UNDER MIXED BOUNDARY CONDITIONS

1. In this section, we shall consider heat exchange in prismatic and cylindrical tubes where the heat-flux density at the wall is constant along the length and the wall temperature is constant along the perimeter, i.e., under mixed boundary conditions. These

specific conditions correspond to uniform supply or removal of heat along the length, while the wall is sufficiently thick and a sufficiently good conductor of heat to ensure temperature equalization over the perimeter. In this case, q_s must naturally vary over the perimeter and t_s along the length. We do not know the nature of the variation in q_s and t_s, however. We are only given the heat-flux density $\bar{q}_s$ at the wall, which is averaged over the perimeter, but constant along the length.

We shall only analyze heat exchange with a fully developed (stabilized) temperature field, on the assumption that the physical properties of the fluid are constant, the flow is stabilized, and the heat of friction is negligible. Under such conditions, the temperature and pressure gradients in the axial direction at any point in the flow will be constant:

$$\frac{\partial t}{\partial x} = \frac{d\bar{t}}{dx} = \frac{\bar{q}_s s}{\rho c_p \bar{w} f} = c_1,$$

$$\frac{\partial p}{\partial x} = -\frac{\Delta p}{l} = -\xi \frac{\rho \bar{w}^2}{2} \cdot \frac{1}{d_e} = c_2.$$

where c_1 and c_2 are constants; f, s are the area and perimeter of the tube cross section; Δp is the pressure drop across a tube segment of length l; ξ is the friction resistance coefficient.

Taking these relationships into account, we can write the energy and motion equations in the form

$$\nabla^2 \vartheta = \frac{c_1}{a} w_x, \tag{14-23}$$

$$\nabla^2 w_x = \frac{c_2}{\mu}. \tag{14-24}$$

where $\vartheta = t - t_c$ (we note that t_s = const + $c_1 x$).

The boundary conditions are

$$\vartheta_c = 0, \quad (w_x)_c = 0, \tag{14-25}$$

where the subscript "s" indicates conditions at the wall.

Direct solution of (14-23) involves difficulties which can be removed, however, by combining (14-23) and (14-24):

$$\nabla^2 (\nabla^2 \vartheta) = \frac{c_1}{a} \nabla^2 w_x,$$

or, taking (14-24) into account,

$$\nabla^2 (\nabla^2 \vartheta) = \frac{c_1 c_2}{a \mu}. \tag{14-26}$$

where c_1, c_2, a and μ are independent of the coordinates.

The solution of (14-26) must satisfy the boundary conditions

- 336 -

$$\theta_c = 0 \to (\nabla^2 \theta)_c = 0. \qquad (14\text{-}27)$$

The first condition means that the fluid temperature at the wall equals the wall temperature, while the second follows from (14-23), since the fluid has zero velocity at the wall.

Thus a solution of (14-26) satisfying Conditions (14-27) is at the same time a solution of (14-23) and (14-24); the velocity w_x can be found with the aid of (14-23).

Equation (14-26) is analogous to the familiar Lagrance equation in the theory of small deflections of uniformly loaded thin plates, which has the form

$$\nabla^2(\nabla^2\varepsilon) = \frac{\sigma}{D},$$

where ε is the plate deflection; σ and D are the specific load and the plate stiffness in bending (they are constants).

For plates freely supported on the entire perimeter, the boundary conditions will also resemble Conditions (14-27):

$$\varepsilon_s = 0 \text{ and } (\nabla^2 \varepsilon)_s = 0,$$

where the subscript "s" indicates conditions on the perimeter.

Solutions have been obtained by Timoshenko [8] to the Lagrange equation for plates of various geometries under the indicated bound-conditions, and other boundary conditions. They can also be used for heat-exchange problems described by Eq. (14-26) with boundary conditions (14-27). To obtain a solution to a heat-exchange problem, in the solution for a plate geometrically similar to the tube cross section we need only replace ε by ϑ and σ/D by $c_1 c_2/a\mu$. It should be noted, however, that when the perimeter includes not only straight-line segments, but curve lines as well, direct substitution of variables may lead to an incorrect solution of (14-26). This is associated with the fact that the boundary condition for the plate in this case does not satisfy the condition $(\nabla^2 \theta)_c = 0.$ Thus to satisfy this condition, some transformation of the constants of integration is required.

Table 14-3 gives equations for the temperature distribution in tubes of various cross sections; they are obtained by adaptation of the corresponding elasticity-theory problems [9, 10], or direct solution of the motion and energy equations, using functions of a complex variable (for an elliptical tube [11]). The constant $c_1 c_2/a\mu$ is found from the relationships given at the beginning of paragraph 1 for c_1 and c_2:
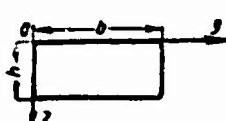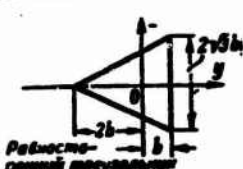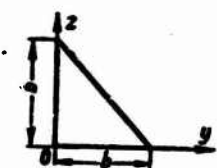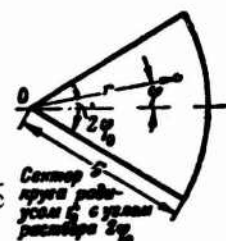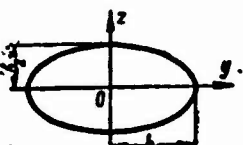
$$\frac{c_1 c_2}{a\mu} = -\frac{2\overline{q_c}}{\lambda d_3^3} t\text{Re},$$

where

$$\text{Re} = \frac{\overline{w} d_3}{\nu}.$$

TABLE 14-3

Equations for Temperature Distribution in Prismatic and Elliptical Tubes with $\bar{q}_s$ = const over the Length and t_s = const over the Perimeter

1 Форма поперечного сечения	2 Уравнения для ϑ
3 *Прямоугольник*	$$\vartheta = \frac{16c_1c_2}{\pi^4 a\mu} \sum_{m=1,3,5\ldots}^{\infty} \sum_{n=1,3,5\ldots}^{\infty} \frac{\sin\frac{m\pi y}{b}\sin\frac{n\pi z}{h}}{mn\left(\frac{m^2}{b^2}+\frac{n^2}{h^2}\right)^2}$$
4 *Равносторонний треугольник*	$$\vartheta = \frac{c_1c_2}{192b a\mu}(y-b)\left[(b+2b)^2-3z^2\right](y^2+z^2-4b^2)$$
5 *Прямоугольный равнобедренный треугольник*	$$\vartheta = \frac{16b^4c_1c_2}{\pi^6 a\mu}\left[\sum_{m=1,3,5\ldots}^{\infty}\sum_{n=2,4,6\ldots}^{\infty}\frac{n\sin\frac{m\pi y}{b}\sin\frac{n\pi z}{b}}{m(n^2-m^2)(m^2+n^2)^2}+\right.$$ $$\left.+\sum_{m=2,4,6\ldots}^{\infty}\sum_{n=1,3,5\ldots}^{\infty}\frac{m\sin\frac{m\pi y}{b}\sin\frac{n\pi z}{b}}{n(m^2-n^2)(m^2+n^2)^2}\right]$$
6 *Сектор круга радиусом r_0 с углом раствора $2\varphi_0$*	$$\vartheta = \frac{r_0^4 c_1 c_2}{a\mu}\sum_{m=1,3,5\ldots}^{\infty}(-1)^{\frac{m+1}{2}}\left\{\frac{4r^4}{m\pi\left[16-\left(\frac{m\pi}{2\varphi_0}\right)^2\right]\left[4-\left(\frac{m\pi}{2\varphi_0}\right)^2\right]r_0^4}+\right.$$ $$+\left(\frac{r}{r_0}\right)^{\frac{m\pi}{2\varphi_0}}\frac{\frac{m\pi}{2\varphi_0}+6}{m\pi\left[16-\left(\frac{m\pi}{2\varphi_0}\right)^2\right]\left[2+\frac{m\pi}{2\varphi_0}\right]\left[1+\frac{m\pi}{2\varphi_0}\right]}-$$ $$\left.-\left(\frac{r}{r_0}\right)^{\frac{m\pi}{2\varphi_0}+2}\frac{1}{m\pi\left[4-\left(\frac{m\pi}{2\varphi_0}\right)^2\right]\left[1+\frac{m\pi}{2\varphi_0}\right]}\right\}\cos\frac{m\pi}{2\varphi_0}\varphi$$
7 *Эллипс с полуосями b_1 и b_2*	$$\vartheta = \frac{c_1c_2(b_2^2 y^2 + b_1^2 z^2 - b_1^2 b_2^2)}{32(b_1^2+b_2^2)a\mu}\left\{(A_1-2A_2)y^2+(A_1+2A_2)z^2+\right.$$ $$\left.+\frac{2b_1^2 b_2^2}{b_1^2+b_2^2}A_1-A_3\right\},$$ где $$A_1=\frac{2}{3}\cdot\frac{b_1^4+b_2^4+10b_1^2 b_2^2}{b_1^4+b_2^4+6b_1^2 b_2^2},\quad A_2=\frac{1}{3}\cdot\frac{b_1^4-b_2^4}{b_1^4+b_2^4+6b_1^2 b_2^2};$$ $$A_3=8\frac{b_1^2 b_2^2}{b_1^2+b_2^2}$$

1) Cross-section shape; 2) equations for ϑ; 3) rectangle; 4) equilateral triangle; 5) right isoceles triangle; 6) sector of circle

with radius r_0, aperture angle of $2\varphi_0$; 7) ellipse with semiaxes b_1 and l_2; 8) where.

Using the equations for the temperature profile (Table 14-3) and velocity profile (see Table 5-2), we can determine the distribution of local heat-flux densities q_s and heat-transfer coefficient α_∞ over the perimeter, and can also find the limiting Nusselt number averaged over the perimeter.

In our case, $\frac{q_c}{\overline{q}_c}=\frac{\alpha_\infty}{\overline{\alpha}_\infty}$. since t_s is constant over the perimeter. This ratio can be expressed in terms of the temperature gradients at the wall

$$\frac{q_c}{\overline{q}_c}=\frac{\alpha_\infty}{\overline{\alpha}_\infty}=\frac{\left(\frac{\partial\theta}{\partial n}\right)_{n=0}}{\frac{1}{s}\int_s\left(\frac{\partial\theta}{\partial n}\right)_{n=0}ds},\qquad(14\text{-}28)$$

where n is the normal to the wall; e is the tube perimeter.

The mean limiting Nusselt number is

$$\ddot{N}u_\infty=\frac{\overline{\alpha}_\infty d_\bullet}{\lambda}=\frac{\overline{q}d_\bullet}{(t_c-\overline{t})\lambda}=-\left(\frac{1}{f}\iint_f\theta W_x\,dydz\right)^{-1}.\qquad(14\text{-}29)$$

where

$$\theta=\frac{\partial\lambda}{q_c d_\bullet}=\frac{(t-t_c)\lambda}{\overline{q}_c d_\bullet};\quad\dot{W}_x=\frac{w_x}{\overline{w}}.$$

Let us look at heat-transfer calculations for certain cross-section shapes.

2. *Rectangular tube.* For simplicity, we shall compute the distributions of q_s and α_∞ for a tube of square cross section. With $= h$, we use the first equation of Table 14-3, obtaining

$$\left(\frac{\partial\theta}{\partial y}\right)_{y=0}=\frac{16c_1c_2}{\pi^6 a\mu}b^3\sum_{m=1,3,5\ldots}^{\infty}\sum_{n=1,3,5\ldots}^{\infty}\frac{\sin\frac{n\pi z}{h}}{n(m^2+n^2)^2},$$

$$-\frac{2}{h}\int_0^{h/2}\left(\frac{\partial\theta}{\partial y}\right)_{y=0}dz=\frac{32c_1c_2}{\pi^6 a\mu}b^3\sum_{m=1,3,5\ldots}^{\infty}\sum_{n=1,3,5\ldots}^{\infty}\frac{1}{n^2(m^2+n^2)^3}.$$

The ratio

$$\frac{q_c}{\overline{q}_c}=\frac{\alpha_\infty}{\overline{\alpha}_\infty}=\frac{\pi}{2}\cdot\frac{\displaystyle\sum_{m=1,3,5\ldots}^{\infty}\sum_{n=1,3,5\ldots}^{\infty}\frac{\sin\frac{n\pi z}{h}}{n(m^2+n^2)^3}}{\displaystyle\sum_{m=1,3,5\ldots}^{\infty}\sum_{n=1,3,5\ldots}^{\infty}\frac{1}{n^2(m^2+n^2)^3}}.\qquad(14\text{-}30)$$
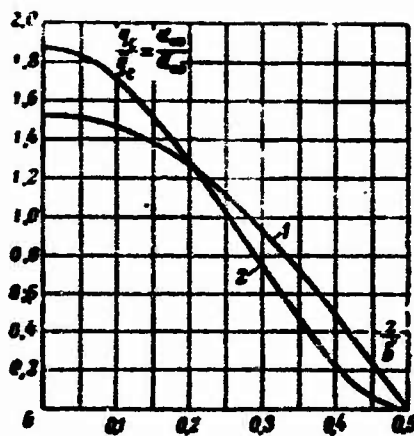
- 339 -

Fig. 14-8. Heat-transfer distribution over perimeter of prismatic tubes. 1) Square; 2) equilateral triangle (here x is the distance from the center of an edge, $2b'$ is the width of an edge).
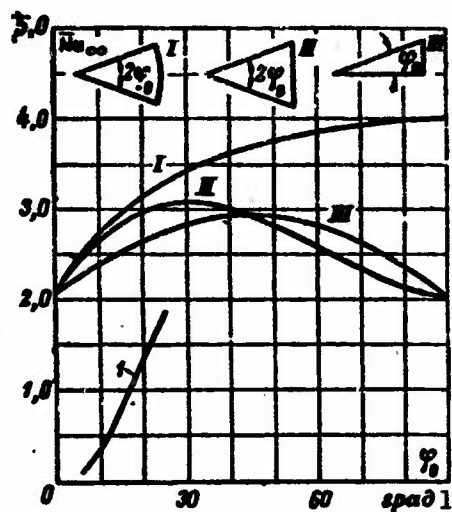

Fig. 14-9. Values of $\overline{Nu}_\infty$ for tubes with cross section in form of sector of circles, isoceles triangle, and right triangle for $\overline{q}_s$ = = const with the length and t_s = const over the perimeter. 1) The same, for sector of circle with q_s = const along perimeter and along length. 1) deg.

The calculations yield the following distribution of $q_s/\overline{q}_s$ over the perimeter of a square tube:

z/h	0	$1/12$	$1/8$	$1/4$	$1/3$	$2/5$	$1/2$
$\dfrac{q_c}{\overline{q}_c}=\dfrac{a_\infty}{\overline{a}_\infty}$	0	0.427	0.809	1.121	1.350	1.481	1.535

This relationship is illustrated in Fig. 14-8.

To find $\overline{Nu}_\infty$ for a rectangular tube, we substitute the expressions for ϑ and W_x from Tables 14-3 and 5-2 into (14-29). Integrating, we obtain

$$\overline{Nu}_{\infty} = \frac{64}{(1+\gamma)^2 \pi^3} \frac{\left[\sum\limits_{m=1,3,5\ldots}^{\infty} \sum\limits_{n=1,3,5\ldots}^{\infty} \frac{1}{m^3 n^3 (m^2 \gamma^2 + n^2)}\right]^2}{\sum\limits_{m=1,3,5\ldots}^{\infty} \sum\limits_{n=1,3,5\ldots}^{\infty} \frac{1}{m^2 n^2 (m^2 \gamma^2 + n^2)^2}}, \qquad (14\text{-}31)$$

where $\gamma = h/b$ is the side ratio for the cross section. The series in the equation converge very rapidly, so that a few terms suffice for a good approximation.

Figure 14-4 (curve 2) shows $\overline{Nu}_{\infty}$ as a function of γ on the basis of Eq. (14-31). It agrees well with the results of numerical computation [5], and with results obtained by a variational method for $\gamma = 1$ [12]. Thus, for example, when $\gamma = 0$, 0.5, and 1, according to Eq. (14-31), $\overline{Nu}_{\infty} = 8.21$, 4.12, and 3.60; according to the data of [5], we have 8.23, 4.11, and 3.63, respectively, while according to [12], we have 3.60 (for $\gamma = 1$).

3. *Triangular tube*. For a tube whose cross section is an isoceles triangle, the heat-transfer distribution over the perimeter is represented by the equation

$$\frac{q_c}{\bar{q}_c} = \frac{\alpha_{\infty}}{\bar{\alpha}_{\infty}} = \frac{15}{8}\left(1 - \frac{1}{3} \cdot \frac{z^2}{b^2}\right)^2 \qquad (14\text{-}32)$$

(see Fig. 14-8), while the limiting Nusselt number averaged over the perimeter is

$$\overline{Nu}_{\infty} = \frac{\bar{\alpha}_{\infty} d_e}{\lambda} = \frac{28}{9} \approx 3.11. \qquad (14\text{-}33)$$
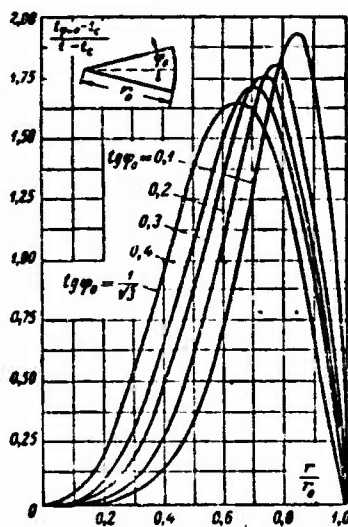

Fig. 14-10. Temperature pro-
files along centerline of tube
with cross section in form of
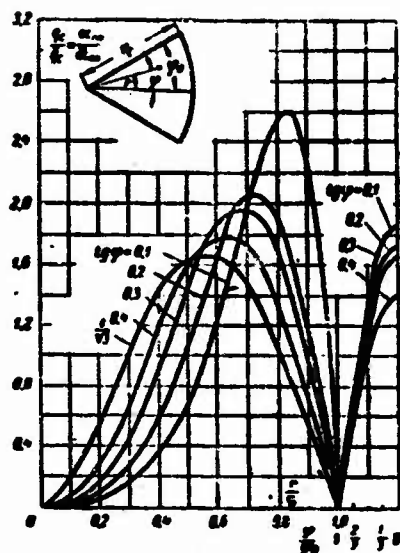sector of circle.

Fig. 14-11. Distribution of
heat transfer along perimeter
of tube with cross section in
form of sector of circle.

Figure 14-9 gives values of $\overline{Nu}_\infty$ as a function of aperture angle
for tubes with cross sections in the form of isoceles and right
triangles [13].

4. For tubes with cross section in the form of a *sector of a
circle*, the computational results for heat exchange are shown in
Figs. 14-9, 14-10, and 14-11 [10]. The second figure shows the
temperature profile along the centerline ($\varphi = 0$) for various aper-
ture angles. As we might expect, as the aperture angle decreases,
the maximum temperature increases, while simultaneously approach-
ing the curved wall. Figure 14-11 shows the distribution of heat
transfer over the perimeter for various aperture angles. At each
wall, q_s and α_∞ pass through a maximum, while vanishing at the corn-
ers. The mean value of $\overline{Nu}_\infty$ over the perimeter depends solely on the
tube shape, i.e., on the aperture angle $2\varphi_0$ in this case. This re-
lationship is shown in Fig. 14-9.

5. For a tube of *elliptical cross section*, the limiting Nus-
selt number averaged over the perimeter is represented by the
equation

$$\overline{Nu}_\infty = \frac{\overline{a}_\infty d_\ni}{\lambda} = \left[\frac{3\pi}{E(k)}\right]^2 \frac{(1+\omega^2)(1+\omega^4+6\omega^2)}{17(1+\omega^4)+98\omega^2} \tag{14-34}$$

where $E(k)$ is a total elliptic integral of the second kind;[4] $k =$
$= (1-\omega^2)^{1/2}$; $\omega = b_2/b_1$ is the ratio of ellipse semiaxes.

For a round tube, $\omega = 1$, $E(0) = \pi/2$ and, consequently, $\overline{Nu}_\infty =$
$= 48/11 \approx 4.36$; this corresponds to the value found previously. The

other limiting case, $\omega = 0$, has no real physical meaning, and does not correspond to flow in a flat tube. In fact, for $\omega=0$, $E(1)=1$ and $\overline{Nu}_\infty = \frac{9}{17}\pi^4 \approx 5.225$. For a flat tube, however, as we have already established, $\overline{Nu}_\infty = 140/17 \approx 8.23$. Thus (14-34) does not hold for a flat tube.
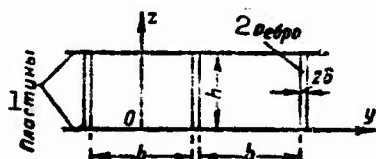

Fig. 14-12. Rectangular tube
formed by two parallel plates
connected by longitudinal ribs.
1) Plates; 2) ribs.

TABLE 14-4

Values of Functions
$F(K, \gamma)$ in Eq. (14-35)

$K=\dfrac{\delta\lambda_p}{h\lambda}$	$\gamma=\dfrac{h}{b}$			
	0,20	0,25	0,50	1,00
0	0,138	0,207	0,587	0,968
1	0,645	0,710	0,892	0,993
2	0,777	0,823	0,938	0,996
4	0,873	0,898	0,966	0,998
10	0,944	0,957	0,986	0,999

6. Also of interest is heat exchange in a *rectangular tube formed by parallel plates connected by longitudinal ribs* (Fig. 14-12). The same conditions considered in this section for the other cases obtain at the inside surface of the plates ($\overline{q}_s$ = const over the length and t_s = const over the perimeter. Heat is transmitted to the ribs by the plates owing to conduction, and is delivered to the flow from the rib surfaces. Thus the rib temperature will be variable.

The variation in rib temperature in the z-axis direction depends on the parameter $K=\delta\lambda_p/h\lambda$, where δ and h are the half-thickness and the width of the ribs; λ_r and λ are the thermal-conductivity coefficients of the rib material and the fluid. When $K \to \infty$, the temperature will be constant over the rib width, and will equal the temperature of the plates. Here the problem reduces to the previous one of heat exchange in a rectangular tube (see paragraph 2) and the limiting Nusselt number $(\overline{Nu}_\infty)_{K\to\infty}$ averaged over the perimeter (including the rib) is found from Eq. (14-31). When K is finite, the temperature will vary more strongly over the rib width the smaller K. In this case, according to the data of [14]

$$\overline{Nu}_\infty = (\overline{Nu}_\infty)_{K\to\infty} F(K, \gamma). \qquad (14-35)$$

The values of the function F are given in Table 14-4, which shows that there may be a very substantial reduction in $\overline{Nu}_\infty$ for small values of K and $\gamma = h/b$.

In addition to those considered here, other solutions are also known for problems of heat exchange in prismatic and cylindrical tubes with mixed boundary conditions. Thus solutions are given

in [15] for problems involving tubes with cross sections in the shape of cardioids and regular hexagons, while in [15a], the "point congruence" method is used to consider problems of flow and heat exchange in tubes having cross sections in the form of regular polygons with between 3 and 20 sides.

Example. Hydrogen flows in a tube whose cross section takes the form of an equilateral triangle with altitude $3b = 6$ mm. The hydrogen flows at a rate $G = 0.280 \cdot 10^{-4}$ kg/s; the entrance temperature $t_0 = 100°C$; the heat-flux density averaged over the perimeter and constant over the length is $\bar{q}_s = 2.34 \cdot 10^4$ W/m^2. We are to determine the heat-transfer coefficient $\bar{\alpha}_\infty$ averaged over the perimeter, and the wall temperature t_s (t_s is assumed to be constant over the perimeter) at a distance $x = 0.4$ m from the entrance. In this same section, we are also to find the local values of α_∞ and q_s at the center of each side.

The tube perimeter is $s = 6\sqrt{3}\,b = 20.8$ mm; $d_\circ = 2b = 4$ mm. The mean mass temperature of the gas at a distance x from the entrance is

$$\bar{t} = t_\circ + \frac{\bar{q}_s s x}{G c_p} = 100 + \frac{2.34 \cdot 10^4 \cdot 0.0208 \cdot 0.4}{0.28 \cdot 10^{-4} \cdot 1.46 \cdot 10^4} = 576°C$$

($c_p = 1.46 \cdot 10^4$ J/kg·deg in the interval from t_0 to $\bar{t}$).

In accordance with (14-33), $\overline{Nu}_\infty = 3.11$. For $\bar{t} = 576°C$, $\lambda = 0.419$ W/m·deg. Consequently,

$$\bar{a}_\infty = 3.11 \frac{\lambda}{d_\circ} = \frac{3.11 \cdot 0.419}{0.004} = 326 \ \frac{W}{m^2 \cdot deg}.$$

The wall temperature at section x is

$$t_c = \bar{t} + \frac{\bar{q}_c}{a_\infty} = 576 + \frac{2.34 \cdot 10^4}{326} = 648°C.$$

The local values of α_∞ and q_s at the center of each side, i.e., for $z = 0$, is found from (14-32):

$$\frac{q_c}{\bar{q}_c} = \frac{a_\infty}{\bar{a}_\infty} = \frac{15}{8},$$

from which we have $q_s = 4.39 \cdot 10^4$ W/m^2 and $\alpha_\infty = 611$ W/m^2·deg.

14-4. HEAT EXCHANGE IN A BANK OF CYLINDERS IN A LONGITUDINAL FLOW UNDER MIXED BOUNDARY CONDITIONS

We consider heat exchange in a system formed by an infinite number of circular cylinders located at the corners of equilateral triangles parallel to one another (Fig. 14-13). The fluid moves between the cylinders in the axial direction. The fluid flow is stabilized. The heat-flux density, constant along the length, is specified at the outside surface of the cylinders (q_s may vary circumferentially). The temperature of the outside surface is constant along the circumference, but may vary along the length.
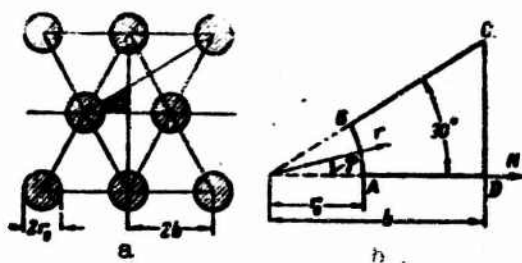
Fig. 14-13. The problem of heat
exchange with longitudinal flow
past a bank of cylinders. a)
Bank cross section; b) cross-
sectional element.

Such boundary conditions correspond, for example, to uniform re-
lease of heat in bars or tubes with high thermal conductivity.
We confine the discussion to heat exchange in the region with
incipient thermal stabilization, which eliminates the need to
consider the influence of entrance conditions.

Since the system is symmetric, we can consider heat exchange
within one cross sectional element, shown in black on Fig. 14-13a,
and represented in larger scale in Fig. 14-13b. The flow in such
a system has been considered in §5-3, where we have also given an
expression for the velocity profile. If we assume the physical
properties to be constant and ignore the heat of friction, we can
represent the temperature field for this case by the energy equa-
tion in the form (14-23). Substituting Expression (5-21) for the
velocity profile into this equation, we obtain

$$\frac{\partial^2 t}{\partial r^2} + \frac{1}{r} \cdot \frac{\partial t}{\partial r} + \frac{1}{r^2} \cdot \frac{\partial^2 t}{\partial \varphi^2} = \frac{2Ab^2}{d_{\ni}^3} \cdot \frac{\overline{q_c}}{\lambda} \left\{ \frac{\sqrt{3}}{\pi} \ln \frac{r}{r_0} - \right.$$
$$\left. - \frac{1}{4} \left[\left(\frac{r}{b} \right)^2 - \left(\frac{r_0}{b} \right)^2 \right] + \sum_{j=1}^{\infty} \frac{\delta_j}{6j} \left(\frac{r}{b} \right)^{6j} \left[1 - \left(\frac{r_0}{r} \right)^{12j} \right] \cos 6j\varphi \right\}. \tag{14-36}$$

where r and φ are the coordinates of the point (Fig. 14-13b), and
r_0 and $2b$ are the cylinder radius and the separation of the cylin-
der centers; d_e is the equivalent diameter of the bank flow sec-
tion; $A = \xi \mathrm{Re}$ is a constant that depends on b/r_0 (see §5-3); $\overline{q}_s$ is
the heat-flux density at the wall, averaged over the perimeter;
the δ_j are constants that depend on b/r_0 (see Table 5-3).

The boundary conditions are written in the form

$$\left. \begin{array}{l} \text{for } r = r_0 \quad t = t_c, \\[4pt] \text{for } \varphi = 0 \text{ and } \varphi = 30° \quad \dfrac{\partial t}{\partial \varphi} = 0, \\[4pt] \text{for } r = \dfrac{b}{\cos \varphi} \quad \dfrac{\partial t}{\partial N} = 0. \end{array} \right\} \tag{14-37}$$

- 345 -

TABLE 14-5

Values of Constants ω_n in Equation for Temperature Distribution in Flow for Longitudinal Flow Past Bank of Cylinders

b/r_0	$a_1 \cdot 10^?$	$a_2 \cdot 10^?$	$a_3 \cdot 10^?$	$a_4 \cdot 10^?$
1.1	0.25961	−0.2065	−1.12	7.0
1.2	0.37039	−0.1323	−1.20	−6.0
1.5	0.71081	0.014556	−0.196	−1.5
2.0	1.2712	9.12031	0.136	0.06
4.0	2.9349	0.38239	0.579	0.3

The last two conditions follow directly from the system symmetry properties.

Equation (14-36) has been solved in [16] under boundary conditions (14-37). As a result, the following expression was obtained for the temperature distribution:

$$
t - t_c = \frac{2w^2}{d_o^2} \cdot \frac{\bar{q}_c}{\lambda} \left\{ \left[\frac{\sqrt{3}}{4\pi}(r^2 + r_0^2) - \frac{1}{16}\cdot\frac{r_0^4}{b^2} - \frac{r_0^2 b_0^2}{2b^2} \right] \ln\frac{r}{r_0} - \frac{1}{64}\cdot\frac{r^4 - r_0^4}{b^2} + \right.
$$

$$
+ \left[-\frac{\sqrt{3}}{4\pi} + \frac{1}{16}\left(\frac{r_0}{b}\right)^2 \right](r^2 - r_0^2) + r^2 \sum_{m=1}^{\infty} \frac{a_m}{6m}\left(\frac{r}{b}\right)^{6m}\left[1 - \left(\frac{r}{b}\right)^{12m}\right]\cos 6m\varphi +
$$

$$
\left. + r^2 \sum_{j=1}^{\infty} b_j \cos 6j\varphi \left[\frac{1}{24j}\left(\frac{r}{b}\right)^{6j}\left(\frac{1}{6j+1} + \frac{(r_0/r)^{12j}}{6j-1}\right) - \frac{(r_0/r)^{6j}}{2(36j^2-1)}\cdot\frac{r_0^{12j}}{r^{12j}} \right] \right\}. \tag{14-38}
$$

where the ω_n are constants depending on b/r_0, whose values are given in Table 14-5.

The mean limiting Nusselt number is

$$
\overline{Nu}_\infty = \frac{\bar{a}_\infty d_o}{\lambda} = \frac{\bar{q}_c d_o}{(t_c - \bar{t})\lambda},
$$

where

$$
t_c - \bar{t} = \frac{1}{f_\Lambda w} \int_0^{\pi/6} d\varphi \int_{r_0}^{\frac{b}{\cos\varphi}} (t_c - t) w_{xr}\, dr;
$$

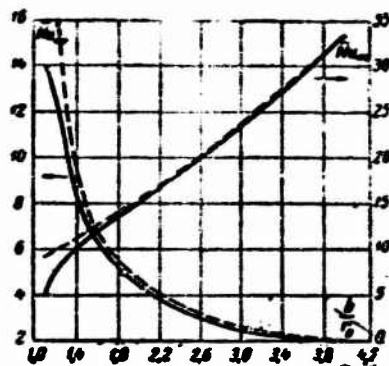here f_Λ is the area of element ABCD (Fig. 14-13b).

Fig. 14-14. Dependences of
$\overline{Nu}_\infty$ and $\overline{Nu}'_\infty$ on b/r_0 for bank
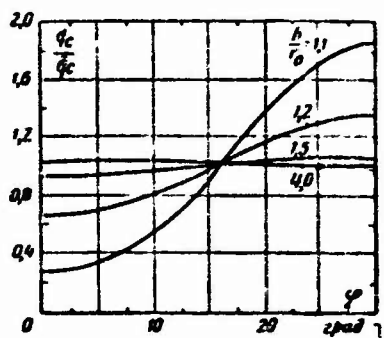of cylinders in longitudinal
flow.

Fig. 14-15. Distribution of
local heat-flux density over
cylinder circumference for
various values of b/r_0. 1) deg.

The analytic expression for $\overline{Nu}_\infty$ as a function of b/r_0 is
extremely cumbersome, and thus is not given here. This relation-
ship is represented graphically in Fig. 14-14 (the solid line
corresponding to the right-hand ordinate scale). It is clear that
despite the utilization of d_e as the characteristic dimension,
$\overline{Nu}_\infty$ varies essentially as a function of b/r_0. If the cylinder
diameter $d = 2r_0$ is used as the characteristic dimension, then
$\overline{Nu}'_\infty = \bar{a}_\infty d/\lambda$ will vary just as intensively, but the nature of the
relationship will differ (solid line in Fig. 14-14, correspond-
ing to left-hand ordinate scale).

The following relationship is convenient for determining
the wall temperature:

$$t_c - t_0 = \frac{\overline{q}_c d_e}{\lambda}\left(4 \frac{1}{Pe} \cdot \frac{x}{d_e} + \overline{Nu}_\infty^{-1}\right),$$

which is easily obtained from the heat-balance equation. Here

- 347 -

t_0 is the fluid entrance temperature; $Pe = \bar{w} d_s / a$.

The variation in local heat-flux density $q_c = -\lambda \left(\frac{\partial t}{\partial r} \right)_{r=r_s}$ along the cylinder circumference is of interest. Computing the derivative by means of (14-38), after certain manipulations we obtain

$$\frac{q_c}{q_s} = 1 - \frac{2Ab^4}{r_s d_s^3} \left\{ \sum_{n=1}^{x} 2\omega_n \left(\frac{r_s}{b} \right)^{6n} \cos 6n\varphi + \sum_{j=1}^{\infty} \frac{\delta_j \left(\frac{r_s}{b} \right)^{6j+6}}{2(6j-1)} \cos 6j\varphi \right\}. \quad (14\text{-}39)$$

This relationship is illustrated in Fig. 14-15. For closely spaced banks, i.e., with $\frac{b}{r_s} < 1.5$, considerable nonuniformity is observed in the circumferential distribution of q_s. Here minimum heat transfer corresponds to $\varphi = 0$, and maximum transfer to $\varphi = 30°$, i.e., to the place near which the flow cross-sectional area is greatest. This q_s distribution is associated with the angular non-uniformity of the velocity profile resulting from the influence of the nearby cylinders. For $\frac{b}{r_s} > 2$, and with somewhat less accuracy even for $\frac{b}{r_s} \geqslant 1.5$, the heat transfer can be assumed to be uniform over the cylinder circumference.

In the latter case, there is reason for supposing that $t - t_s$ is a function of r_0 alone. Then the actual flow section per single cylinder can be replaced by the cross section of a ring of equivalent area with inside radius r_0 and outside radius r_* (see §5-3). This substitution permits us to reduce the problem of heat exchange with longitudinal flow past a bank of cylinders to the problem of heat exchange in an annular tube at whose inside wall $t_{r=r_s} = t_c$, while $\left(\frac{\partial t}{\partial r} \right)_{r=r_*} = 0'$ at the outside wall. The temperature field in such a tube is described by Eq. (14-38) but without the terms containing series and representing the angular temperature variation. The dashed curves of Fig. 14-14 show $\overline{Nu}_{\infty}$ and $\overline{Nu}'_{\infty}$ calculated on this assumption as functions of b/r_0. When $\frac{b}{r_s} \geqslant 1.5$, the error in the Nusselt numbers found by the approximate method does not exceed 5%. The error rises noticeably for smaller b/r_0.

14-5. HEAT EXCHANGE IN PRISMATIC TUBES UNDER BOUNDARY CONDITIONS OF THE SECOND KIND

Heat exchange in prismatic tubes under boundary conditions of the second kind has been studied almost exclusively for fully developed velocity and temperature profiles [10, 12, 17, 18, 19]. The physical properties of the fluid are assumed to be constant, and energy dissipation is ignored. The calculations involve cumbersome equations, and their results are difficult to express in compact analytic form. Thus we shall restrict our discussion to

computational results represent d graphically.

1. Let the heat-flux density q_{sb} be specified at the wide faces of a *rectangular tube*, and let the density q_{sh} be specified at the narrow faces; the values of q_{sb} and q_{sh} are constant along the width and length of the faces, but they are not equal. For stabilized flow and heat exchange, the expression for the temperature distribution in the flow can be represented as

$$\frac{t - t_e}{Q_c\lambda^{-1}} = \frac{4\gamma}{(1+\gamma)^2} \cdot \frac{1}{Pe} \cdot \frac{x}{d_e} + \frac{t - \bar{t}}{Q_c\lambda^{-1}}, \tag{14-40}$$

where $Q_c = 2(q_{cb}b + q_{ch}h)$ is the heat flux at the wall per unit length of tube; $\gamma = h/b$; $Pe = \overline{w}d_e/a$; t_e is the fluid temperature at the entrance. The dimensionless temperature $\frac{t - \bar{t}}{Q_c\lambda^{-1}}$ depends only on the Y and Z coordinates and the parameters γ and $\beta = q_{sh}/q_{sb}$. For a square tube ($\gamma = 1$) and $\beta = 1$, from the data of [12] we have

$$\frac{t - \bar{t}}{Q_c\lambda^{-1}} = \frac{1}{16}(Y^2 + Z^2) - 0.02004\left[(Y^2 - 1)^2 + (Z^2 - 1)^2\right] - \tag{14-41}$$
$$- 0.01661\left[(Y^2 - 1)(Z^2 - 1)\right]^2 + 0.008504,$$

where $Y = \frac{y}{\frac{1}{2}b}$; $Z = \frac{z}{\frac{1}{2}h}$ ($h = b$ in this case).

It follows from (14-40) that the wall temperature of a rectangular tube can be represented as

$$\frac{t_c - t_e}{Q_c\lambda^{-1}} = \frac{4\gamma}{(1+\gamma)^2} \cdot \frac{1}{Pe} \cdot \frac{x}{d_e} + \frac{t_c - \bar{t}}{Q_c\lambda^{-1}}. \tag{14-42}$$

For a square tube with $\beta = 1$, letting $Z = 1$ (or $Y = 1$) in (14-41), we obtain

$$\frac{t_c - \bar{t}}{Q_c\lambda^{-1}} = \frac{1}{16}(Y^2 + 1) - 0.02004(Y^2 - 1)^2 + 0.008504. \tag{14-43}$$

Figures 14-16 and 14-17 show the distribution of the dimensionless wall temperature $\frac{t_c - \bar{t}}{Q_c\lambda^{-1}}$ over the perimeter of rectangular tubes with different side ratios ($\gamma = 0-1$) for uniform heating of all walls ($\beta = 1$) and heating of the wide wall alone ($\beta = 0$). The same data is shown in Fig. 14-18, but for tubes with side ratios $\gamma = 0.05$ and 1, and for values of β from 0 to 1.

Since the heat-flux density is constant at each face, while the heat-transfer conditions are not the same at different points on the perimeter, the wall temperature will vary over the perimeter. The nature of the change in wall temperature depends essentially on the parameters γ and β. For any combination of parameters, however, the maximum wall temperatures (where the fluid is heated) is found at the corners, where fluid velocity is least. As we move away from the corners, the wall temperature drops, and at the center of each side it will have a minimum value corresponding to the nature of
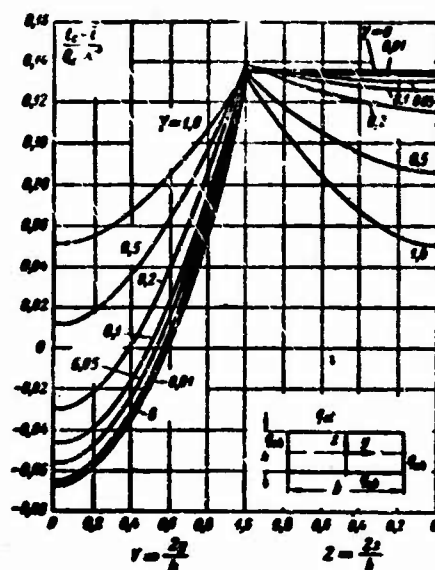
Fig. 14-16. Temperature distrib-
ution over perimeter of rectan-
gular tube with various side
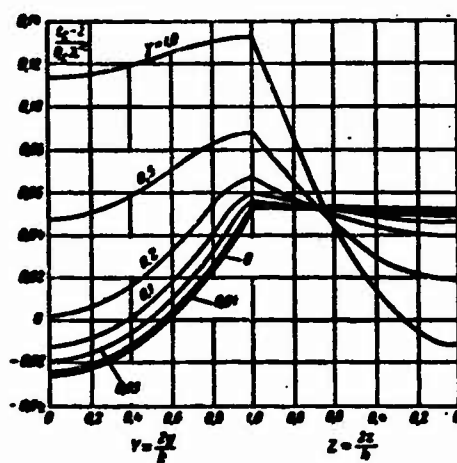ratios, $\beta = 1$.

Fig. 14-17. Temperature dis-
tribution over perimeter of
rectangular tube with various
side ratios, $\beta = 0$.

the velocity profile. The dimensionless wall temperature can take
on negative values at the center areas of the faces. The reason is
that the wall temperature at a given point on the perimeter can be
less than the mean mass temperature of the fluid ($t_s < \bar{t}$) even
though the heat flux is directed from the wall to the fluid. In the
limiting case, when $\gamma \to 0$, the wall temperature distribution over
the perimeter will approach a certain limiting, but nonuniform,
distribution, in contrast to a flat tube (i.e., an infinite slot
with no side walls) which is characterized by a uniform wall-temp-
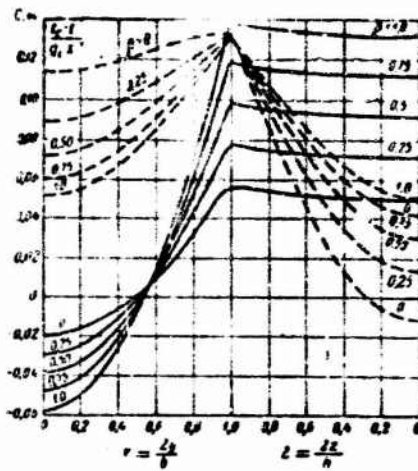erature distribution.

Fig. 14-18. Temperature distribution over perimeter of rectangular tube, $\gamma = 0.05$ (solid lines) and $\gamma = 1$ (dashed lines) for various values of β.
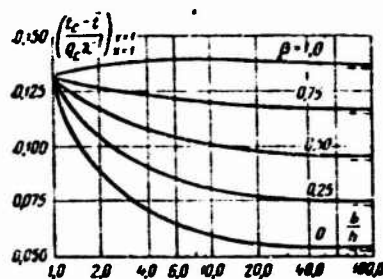

Fig.14-19. Wall temperature at corners of rectangular tube as function of b/h for various values of β.
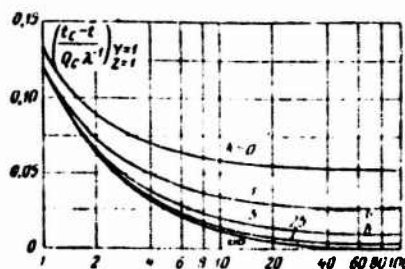

Fig. 14-20. Wall temperature at corners of rectangular tube as function of b/h for various values of K.

Figure 14-19 shows the variation in dimensionless wall temperature at the corners as a function of $b/h = 1/\gamma$ for various values of β. As we can see from the figure, the temperature in the corners may be reduced substantially by increasing b/h while simul-

taneously decreasing β. From this viewpoint, it is advantageous to employ tubes with $b/h > 10$ for $\beta = 0$ (i.e., with no heating of the side walls).

The calculated data shown in Figs. 14-16, 14-17, 14-18 and 14-19 were obtained with no allowance for heat transfer by conduction over the tube wall along the perimeter (the wall is assumed to be infinitely thin). A determination has been made of heat exchange with allowance for wall conduction with heating of wide faces and heat-insulated narrow faces ($\beta = 0$) [19]. In this case, the wall temperature distribution over the perimeter depends essentially on the parameter $K = \frac{2\delta\lambda_c}{h\lambda}$, where λ_c and λ are the thermal-conductivity coefficients for the wall and the fluid, while δ is the wall thickness. When $K = 0$, i.e., for the case considered above, the temperature distribution over the perimeter has its greatest nonuniformity. As K increases, the temperature distribution becomes substantially smoother. Figure 14-20 shows the change in dimensionless wall temperature at corner points (where this temperature has its greatest value) as a function of b/h for $\beta = 0$ and various values of the parameter K. It is clear from the figure that a significant reduction in maximum wall temperature can be attained not only by increasing b/h, but also by increasing K, i.e., by appropriate choice of wall material and thickness. We note that if the medium flowing in the tube is transparent to radiation, then radiant heat exchange between wall elements at different temperatures will also equalize the temperature distribution over the perimeter.

The heat-transfer coefficient averaged over the perimeter of a rectangular tube is

$$\bar{\alpha}_\infty = \frac{Q_c}{2(b+h)(\bar{t}_c - \bar{t})},$$

where $\bar{t}_s$ is the wall temperature averaged over the perimeter:

$$\bar{t}_c - \bar{t} = \frac{1}{s}\int_s (t_c - \bar{t})\,ds,$$

where s is the perimeter of the tube.

The limiting Nusselt number averaged over the perimeter will obviously be

$$\overline{Nu}_\infty = \frac{\bar{\alpha}_\infty d_\bullet}{\lambda} = \frac{Q_c}{(\bar{t}_\bullet - \bar{t})\lambda} \cdot \frac{\gamma}{(1+\gamma)^2}. \qquad (14\text{-}44)$$

Thus for a square tube ($\gamma = 1$) with $\beta = 1$, using (14-43) we find

$$\frac{(\bar{t}_c - \bar{t})}{Q_c \lambda^{-1}} = \int_0^1 \left[\frac{1}{16}(Y^2 - 1) - 0{,}02004\,(Y^2 - 1)^2 + 0{,}008504 \right] dY = 0{,}08117$$

and, consequently,

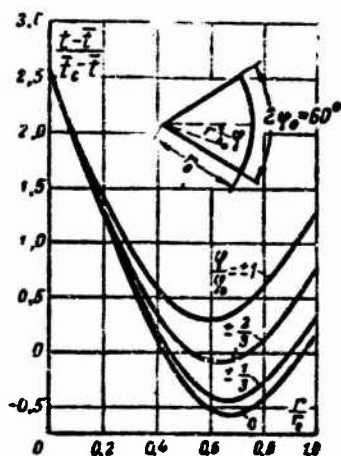$$\overline{Nu}_\infty = \frac{1}{0{,}08117 \cdot 4} = 3{,}08.$$

- 352 -

Fig. 14-21. Tempera-
ture profiles in tube
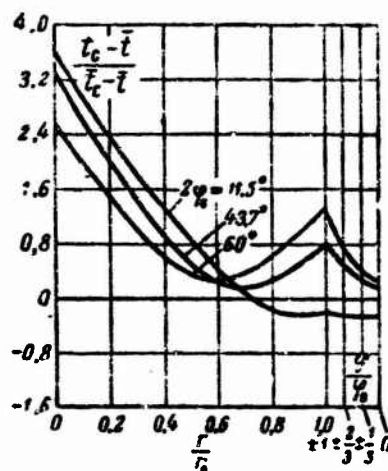with section in form
of sector of circle
(2_0 = 60°), q_s = const.

Fig. 14-22. Variation
in wall temperature
over perimeter of tube
with section in form of
sector of circle, q_s =
const.

Using the curves given in Figs. 14-16, 14-17, and 14-18, we can also compute $\overline{Nu}_\infty$ for other values of γ and β. For example, for $\gamma = 0.1$ and $\beta = 1$, we have $\overline{Nu}_\infty = 2$ As we can see, in rectangular tubes with q_s = const, the number $\overline{Nu}_\infty$ deviates but little from 3 when the side ratio varies from 0.1 to 1. But when t_s = const over the perimeter and q_s = const along the length, $\overline{Nu}_\infty$ varies from 6.8 to 3.6 when γ varies within the same limits. The lower values of $\overline{Nu}_\infty$ for q_s = const are explained by the great nonuniformity in the distribution of wall temperature over the perimeter.

2. Figures 14-21, 14-22, and 14-9 show the results of heat-exchange calculations for tubes with sections in the form of a *sector of a circle* with q_s = const over the perimeter and the length [10]. The first figure shows the temperature distribution over the tube cross section for a sector aperture angle 2_0 = 60°. As we can see, near the vertex of the sector, where the velocities are small, there is a significant temperature increase. The second figure shows the distribution of dimensionless wall temperature $\frac{t_c - \bar{t}}{t_c - \bar{t}}$ over the tube perimeter for various sector aperture angles. The limiting value $\overline{Nu}_\infty$ averaged over the perimeter is shown in Fig. 14-9 as a function of the sector aperture angle (curve 1). It is noteworthy that when the heat-flux density is constant over the perimeter, $\overline{Nu}_\infty$ is far less than when the wall temperature is con-stant over the perimeter.

- 353 -

14-6. HEAT EXCHANGE IN CURVED TUBE.

The heating surfaces of heat-exchange devices are often made of tubes bent to form spirals (coils). Flow characteristics for such tubes have been considered in §5-6. There it was noted that for values of the parameter $Re\sqrt{\frac{d}{D}} > 13.5$ secondary flows appear, that cause the velocity profile to become asymmetric (see Fig. 5-16). If heat exchange takes place in such a tube, the temperature field in the flow will also be asymmetric about the axis for the same reasons. This is quite clear from Fig. 14-23, which shows the temperature profiles in the AB and CD planes (see Fig. 5-16b) in a curved tube; the measurements were made by Mori and Nakayama [20]. The temperature maximum, like the velocity maximum, is shifted away
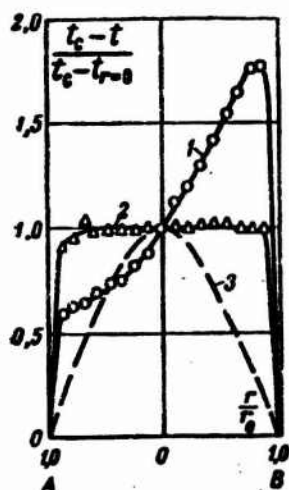

Fig. 14.23. Temperature distribution in curved tube with $D/d = 40$ and $Re = 4000$. 1) In AB plane; 2) in CD plane; 3) the same, straight tube.
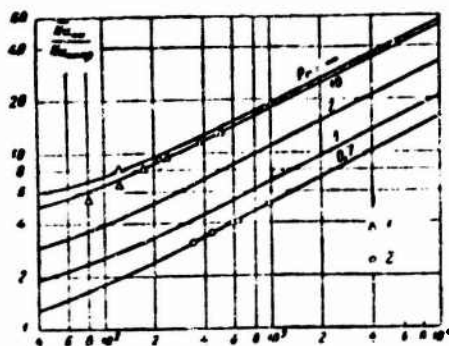

Fig. 14-24. Ratio of Nusselt numbers for curved and straight tubes according to data from theoretical calculations (curves) and experiments. 1) Oil experiments; 2) air experiments.

from the coil center of curvature. It is also noteworthy that the temperature gradients at the wall are large as compared with the temperature gradients in the flow core.

Heat exchange during laminar flow in round tubes bent into a circle has been investigated theoretically by Mori and Nakayama in the paper cited. The calculations were carried out for fully developed flow and heat exchange with constant physical properties of the fluid, and no energy dissipation in the flow. As the boundary conditions, the authors took constant heat-flux density at the wall over the length and constant wall temperature along the circumference (i.e., mixed boundary conditions). The problem was solved on the assumption that the parameter $Re \sqrt{\frac{d}{D}}$ is sufficiently large. Here it is convenient to divide the flow into two regions: the core, within which we can neglect the viscosity forces and the heat transferred by conduction, and the boundary layer (thermal and hydrodynamic). The boundary-layer calculations made use of integral equations. The velocity and temperature profiles in the core and the boundary layer were joined smoothly by the boundary conditions. In second approximation, the following equation was obtained for the limiting Nusselt number averaged over the perimeter:

$$\frac{\overline{Nu}_\infty}{Nu_{comp}} = \frac{0.1979 K^{1/2}}{\chi[1 + F(\chi)K^{-1/2}]}. \tag{14-45}$$

where $\overline{Nu}_\infty = \frac{\bar{q}_c d}{\lambda(t_e - \bar{t})}$; Nu_{comp} is the Nusselt number for a straight tube, equaling 48/11; $K = Re\sqrt{\frac{d}{D}}$; $D = 2R$; $Re = \frac{\overline{w}d}{\nu}$ is the coil radius of curvature; $\chi = \Delta/\delta$ is the ratio of the widths of the thermal and hydrodynamic boundary layers. The function $F(\chi)$, in which $\chi = \chi(Pr)$, has the following form:

for $Pr \geqslant 1 (\chi < 1)$
$$F(\chi) = \frac{37.05}{\chi}\left[\frac{1}{40} - \frac{17}{120}\chi + \left(\frac{1}{10\chi} + \frac{13}{30}\right)\frac{1}{10 Pr}\right].$$

$$\chi = \frac{2}{11}\left(1 + \sqrt{1 + \frac{77}{4}\cdot\frac{1}{Pr^2}}\right);$$

for $Pr < 1 (\chi > 1)$
$$F(\chi) = -\frac{37.05}{\chi}\left[\frac{\chi^2}{12} + \frac{1}{24} - \frac{1}{12\chi} - \left(\frac{4}{3}\chi - \frac{1}{3\chi} + \frac{1}{15\chi^2}\right)\frac{1}{20 Pr}\right].$$

$$\chi = \frac{1}{5}\left(2 + \sqrt{\frac{10}{Pr^2} - 1}\right).$$

Figure 14-24 shows the ratio of Nusselt numbers for curved and straight tubes as a function of K for several values of Pr. For large Pr, the Nu ratio depends basically on the intensity of the secondary flows, which is characterized by K, and very little on Pr. In accordance with the assumption, (14-45) is valid only when K is large enough, apparently when $K \geq 100$.

Experimental data on heat transfer for laminar flow in curved tubes have been given in [20-22]. The measurement results obtained with air [20] and with oil [22] agree well with (14-45), as we can see from Fig. 14-24.

Footnotes

329   [1]If we compute $\overline{Nu}_\infty$ from Eq. (14-12), we obtain $\overline{Nu}_\infty \approx 4$, which is substantially greater than the value found above. Nonetheless, Fig. 14-2 seems quite properly to reflect the distribution of $\dfrac{\alpha_\infty}{\alpha_\omega}$ over the tube perimeter. Naturally, in using Fig. 14-2 to determine α_∞, we should find $\bar{\alpha}_\infty$ from Relationship (14-14).

330   [2]The departure of certain experimental points from the calculated curve may possibly be explained by the fact that most of the experiments were carried out with models of rotating regenerators, i.e., under conditions differing somewhat from those of the calculation.

334   [3]In the experiments reported in [7], the hydrodynamic initial segment formed only a small part of the thermal initial segment, which encompassed the entire tube. Thus the hydrodynamic initial segment had almost no influence on $\overline{Nu}$.

342   [4]The function $E(k)$ has been tabulated; see, for example, Nake and Emde, Table of Functions, Gostekhizdat, 1949.

Transliterated Symbols

325   c = s = stenka = wall

325   э = e = ekvivalentnyy = equivalent

32?   н.г = n.g = gidrodinamicheskiy nachal'nyy = hydrodynamic initial

334   ж = zh = zhidkost' = fluid, liquid

335   л = l = logarifmicheskiy = logarithmic

335   г = g = granichnyy = limiting

343   p = r = rebro = rib

35?   пp = pr = pryamoy = straight

Chapter 15

HEAT EXCHANGE IN TUBES WHEN THE FLOW CONTAINS INTERNAL HEAT SOURCES AND THERE IS ENERGY DISSIPATION

15-1. HEAT EXCHANGE WITH DEVELOPED TEMPERATURE FIELD IN ROUND TUBE WHEN THERE IS ENERGY DISSIPATION IN THE FLOW

Internal heat sources may appear in a flow owing to nuclear or chemical reactions, liberation of Joule heat when electric current is passed through a conducting medium, and for other reasons. In general, the power of internal sources will be a specified function of the coordinates and the time.

The heat of friction liberated in the flow by dissipation of mechanical energy can also be treated as resulting from the action of internal heat sources. In contrast to other internal sources, the distribution of the heat of friction in the flow is determined by the laws governing the variation in the viscosity coefficient and the velocity over the tube cross section and length. In the general case, therefore(with variable physical properties of the fluid), the distribution of the heat of friction in the flow may not be specified in advance. If the physical properties are constant, then the velocity distribution may be calculated in advance. Then when the temperature field is calculated, the distribution of the heat of friction in the flow will be specified, and the calculations can be carried out just as when other internal heat sources are present.

In this section, we shall consider heating of a fluid in a round tube owing to the heat of friction, on the assumption that the wall temperature is maintained constant. If the fluid temperature at the entrance equals the wall temperature, over a certain segment, the fluid will gradually be heated by internal friction. This process continues until the amount of heat removed through the wall becomes equal to the amount of heat liberated in the flow. Beginning with the cross section at which this equilibrium is established, the fluid temperature will cease to change with the length, i.e., temperature-field stabilization will set in (provided, naturally, the velocity field has already been stabilized before this section). We shall consider just such a thermally and hydrodynamically stabilized flow. If, moreover, the flow is steady and axisymmetric, then

$$\frac{\partial w_x}{\partial \tau} = \frac{\partial l}{\partial \tau} = 0, \quad \frac{\partial w_x}{\partial x} = \frac{\partial w_x}{\partial \varphi} = 0, \quad w_r = w_\varphi = 0 \text{ and } \frac{\partial l}{\partial x} = \frac{\partial l}{\partial \varphi} = 0.$$

Allowing for the above, we write the energy and motion equations in the form

$$\frac{d}{dr}\left(\lambda\frac{dt}{dr}\right)+\frac{1}{r}\left(\lambda\frac{dt}{dr}\right)+\mu\left(\frac{dw_x}{dr}\right)^2=0,\qquad (15\text{-}1)$$

$$\frac{d}{dr}\left(\mu\frac{dw_x}{dr}\right)+\frac{1}{r}\left(\mu\frac{dw_x}{dr}\right)-\frac{dp}{dx}=0,\qquad (15\text{-}2)$$

where $\frac{dp}{dx}=-\frac{\Delta p}{l}=$ const; Δp is the pressure drop across the tube segment of length l.

The boundary conditions will be

$$\left.\begin{array}{l}\left(\dfrac{dt}{dr}\right)_{r=0}=0,\ t(r_0)=t_c;\\[2mm]\left(\dfrac{dw_x}{dr}\right)_{r=0}=0,\ w_x(r_0)=0,\end{array}\right\}\qquad (15\text{-}3)$$

where r_0 is the tube radius; t_s is the wall temperature.

Thus t and w_x depend solely on r.

If we assume that the viscosity coefficient is independent of the temperature, there is a known solution for w_x:

$$w_x=2\bar{w}\left(1-\frac{r^2}{r_0^2}\right).$$

Substituting this expression into (15-1), assuming the thermal-conductivity coefficient to be constant, and integrating with allowance for the boundary conditions, we obtain

$$t-t_c=\frac{\mu\bar{w}^2}{\lambda}\left(1-\frac{r^4}{r_0^4}\right).\qquad (15\text{-}4)$$

Thus for the given assumptions, the temperature distribution established in the flow follows a parabola of degree four (Fig. 15-1). Here the temperature on the tube axis will exceed the wall temperature by the amount $\mu\bar{w}^2/\lambda$. The heat-flux density at the wall is

$$q_0=\lambda\left(\frac{\partial t}{\partial r}\right)_{r=r_0}=-4\frac{\mu\bar{w}^2}{r_0}.\qquad (15\text{-}5)$$

the mean mass temperature is

$$\bar{t}-t_c=\frac{5}{6}\cdot\frac{\mu\bar{w}^2}{\lambda}$$

and the limiting Nusselt number is

$$\mathrm{Nu}_\infty=-\frac{q_c 2r_0}{(t_c-\bar{t})\lambda}=\frac{48}{5}=9,6.\qquad (15\text{-}6)$$

It is interesting that $t(0)-t_s$ and $\bar{t}-t_s$ are independent of the tube diameter.

To obtain some idea of the possible increase in temperature on the axis above the wall temperature, we look at the following ex-
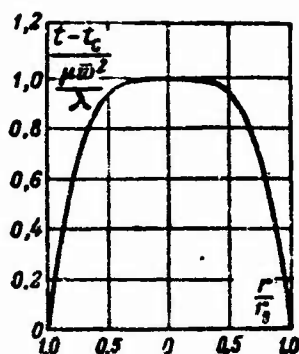
- 358 -

Fig. 15-1. Temperature field
appearing in fluid flow in
round tube owing to dissipa-
tion of kinetic energy.

ample. Let a viscous oil move in a tube with velocity $\bar{w}$ = 1.6 m/s;
the oil has the following physical properties: μ = 1.00 N·s/m² and
λ = 0.132 W/m·deg. We find $t(0) - t_s$ = 19.4°C. Thus for viscous
fluids, even at moderate velocities, a considerable temperature
increase results. But it is precisely for such fluids that the
viscosity coefficient varies sharply with temperature. Thus the
previous assumption of constant viscosity may introduce signifi-
cant errors into the calculations. Thus it is of interest to con-
sider the problem with allowance for the way in which the viscosity
coefficient depends on temperature, with the thermal-conductivity
coefficient assumed to be constant as before. This problem has been
investigated by Hausenblas [1] and Re--trer [2].

Integrating (15-2) with respect to r between 0 and r, we ob-
tain

$$\frac{dw_s}{dr} = -\frac{\Delta p}{2l} \cdot \frac{r}{\mu(t)}.$$

(15-7)

Substituting this expression into (15-1), for λ = const we find

$$\frac{d^2t}{dr^2} + \frac{1}{r} \cdot \frac{dt}{dr} + \frac{1}{4\lambda} \left(\frac{\Delta p}{l}\right)^2 \frac{r^2}{\mu(t)} = 0.$$

(15-8)

We represent the relationship between the viscosity coef-
ficient and the temperature in the form

$$\frac{1}{\mu} = k_0 + k_1 t.$$

(15-9)

where k_0 and k_1 are constants.

In place of the dependent variable t we introduce the variable
$\vartheta = t + \frac{k_0}{k_1}$. When ϑ = 0, the function $\mu = \frac{1}{k_1 \vartheta}$ has a discontinuity at ϑ = 0,
while it becomes negative when ϑ < 0. Since a negative value of vis-
cosity has no physical meaning, the temperature dependence used

- 359 -

here for the viscosity, like the temperature distribution, which can be found by solving Eq. (15-8), can only be used for $\vartheta > 0$.

Substituting the value of $1/\eta$ from (15-9) into (15-8), and going over to the variable ϑ, we obtain

$$\frac{d^2\vartheta}{dr^2}+\frac{1}{r}\cdot\frac{d\vartheta}{dr}+Nr^4\vartheta=0,\qquad(15\text{-}10)$$

where

$$N=\frac{k_1}{4\lambda}\left(\frac{\Delta p}{l}\right)^2.$$

TABLE 15-1

Values of the Functions $J_0(x)$, $F_1(x)$ and $F_2(x)$

x	$J_0(x)$	$F_1(x)$	$F_2(x)$
0,0	1.0000	0.50000	0,25000
0,1	0,9975	0,49958	0,24968
0,2	0,9900	0,49334	0,24876
0,3	0,9776	0,49626	0,24720
0,4	0,9604	0,49337	0,24503
0,5	0,9385	0,48968	0,24227
0,6	0,9120	0,48520	0,23892
0,7	0,8812	0,47995	0,23499
0,8	0,8463	0,47397	0,23053
0,9	0,8075	0,46726	0,22553
1,0	0,7652	0,45987	0,22003
1,1	0,7196	0,45182	0,21405
1,2	0,6711	0,44315	0,20762
1,3	0,6201	0,43390	0,20078
1,4	0,5669	0,42411	0,19355
1,5	0,5118	0,41382	0,18598
1,6	0,4554	0,40307	0,17809
1,7	0,3980	0,39191	0,16993
1,8	0,3400	0,38039	0,16153
1,9	0,2818	0,38855	0,15294
2,0	0,2239	0,35644	0,14418
2,1	0,1666	0,34412	0,13531
2,2	0,1104	0,33162	0,12636
2,3	0,0555	0,31900	0,11736
2,4	0,0025	0,30631	0,10837
2,5	−0,0484	0,29360	0,09942

When allowance is made for the boundary condition $\vartheta'(0)=0$ on the axis, differential equation (15-10) has the solution

$$\vartheta=C_1 J_0\left(\frac{1}{2}\sqrt{N}\,r^2\right).$$

where $J_0(x)$ is a zero-order Bessel function of the first kind.

Determining the constant C_1 from the boundary condition at the wall, $\vartheta(r_0)=$ $=\vartheta_c=t_c+\frac{k_0}{k_1}$, we obtain an expression for the temperature distribution:

$$\vartheta=\frac{\vartheta_c J_0(H_1 R^2)}{J_0(H_1)},\qquad(15\text{-}11)$$

where

$$H_1=\frac{1}{2}\sqrt{N}\,r_0^2=\frac{1}{16}\sqrt{\frac{k_1}{\lambda}\cdot\frac{\Delta p}{l}}\,d^2;\ R=\frac{r}{r_0};$$

$$J_0(x)=\sum_{v=0}^{\infty}\left(\frac{1}{v!}\right)^2\left(\frac{ix}{2}\right)^{2v}.$$

Table 15-1 gives values of the function $J_0(x)$ within the region of interest to us, i.e., up to its first root ($x \approx 2.4$).

The temperature has its maximum on the tube axis, equaling

$$\vartheta(0)=\frac{\vartheta_c}{J_0(H_1)}.\qquad(15\text{-}12)$$

since $J_0(0)=1$.

Figure 15-2 shows profiles for the dimensionless temperature

$$\frac{\vartheta-\vartheta_c}{\vartheta_c}=\frac{t}{t_c+\frac{k_0}{k_1}}\cdot\frac{J_0(H_1 R^2)}{J_0(H_1)}\qquad(15\text{-}13)$$

for various values of the parameter H_1. As H_1 increases, the tempera-

ture difference between the flow and the wall increases. The case $H_1 = 0$ corresponds to isothermal flow.[1]

To find the velocity distribution, we substitute the value $1/\mu = k_1 \vartheta$, into (15-7), where ϑ is determined from Eq. (15-11); we integrate the resulting expression between r and r_0. We then obtain

$$w_x = \frac{r_0^2}{2\mu_0} \frac{\Delta p}{l} \int_R^1 R J_0 (H_1 R)\, dR,$$

where μ_0 is the value of the viscosity coefficient on the tube axis:

$$\mu_0 = \frac{1}{k_1 \vartheta (0)} = \frac{J_0 (H_1)}{k_1 \vartheta_c}.$$

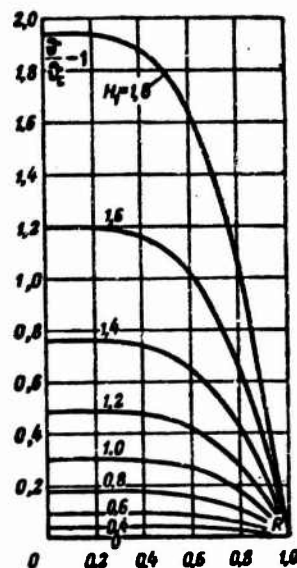Fig. 15-2. Temperature distribution in round tube for various values of H_1.
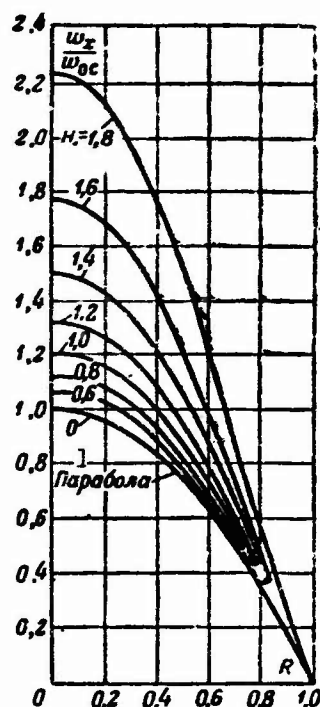

Fig. 15-3. Velocity profiles in round tube for various values of H_1. 1) Parabola.

Integrating, we find

$$w_x = \frac{r_0^2}{2\mu_0} \cdot \frac{\Delta p}{l} [F_1 (H_1) - R^2 F_1 (H_1 R)]. \tag{15-14}$$

where

$$F_1 (x) = \sum_{v=0}^{\infty} \left(\frac{1}{v!} \right)^2 \frac{1}{4v+2} \left(\frac{ix}{2} \right)^{2v}.$$

The mean fluid velocity over the cross section is

$$\bar{w} = 2 \int_0^1 w_x R\, dR = \frac{r_0^2}{2\mu_s} \frac{\Delta f}{l} F_3(H_1),$$ (15-15)

where

$$F_3(x) = F_1(x) - F_2(x);$$

$$F_3(x) = \sum_{\nu=0}^{\infty} \left(\frac{1}{\nu!}\right)^2 \frac{1}{(4\nu+2)(2\nu+2)} \left(\frac{ix}{2}\right)^{2\nu}.$$

Table 15-1 gives values of the functions $F_1(x)$ and $F_2(x)$.

As a scale factor for w_x, we select the velocity on the tube axis for isothermal flow at a temperature equaling the wall temperature; the scale factor for $\bar{w}$ is the value of the mean velocity under the same conditions. Letting $(w_x)_{r=0, l=l_c} = w_{oc}$ and $\bar{w}_{l=l_c} = \bar{w}_c$, for the scale factors, we obtain

$$w_{oc} = 2\bar{w}_c = \frac{1}{4} \frac{r_0^2}{\mu_c} \cdot \frac{\Delta p}{l},$$

where μ_s is the viscosity coefficient at the temperature of the fluid at the wall.
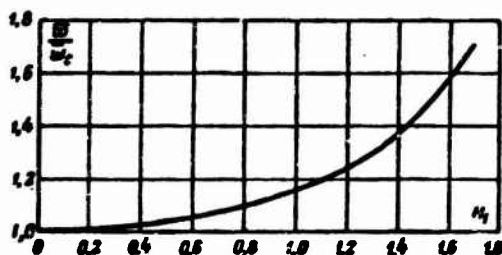
Fig. 15-4. Ratio $\bar{w}/\bar{w}_s$ as function of H_1 for round tube.

Using these scale factors, we obtain the following expressions for the dimensionless velocity and dimensionless mean velocity:

$$\frac{w_x}{w_{oc}} = \frac{2}{J_0(H_1)}[F_1(H_1) - R^2 F_1(H_1 R)],$$ (15-16)

$$\frac{\bar{w}}{w_c} = 4 \frac{F_3(H_1)}{J_0(H_1)}.$$ (15-17)

When $H_1 = 0$, which corresponds to isothermal flow, the velocity distribution (15-16) becomes parabolic, and the ratio $\bar{w}/\bar{w}_s = 1$.

The velocity profiles for several values of H_1 are shown in Fig. 15-3. They differ substantially from the parabolic profile, owing to the viscosity-field nonuniformity produced by the tempera-

ture-dependence of the viscosity. For large H_1, the velocity profiles have a point of inflection. The velocity gradients at the wall are the same for different H_1, since the fluid viscosity at the wall has the same value for all profiles.

As Fig. 15-3 shows, for the same value of $\Delta p/l$, the mean fluid velocity (or the volume flowrate) rises as H_1 increases. Figure 15-4 illustrates the relationship between $\bar{w}/\bar{w}_s$ and H_1. Thus when $H_1 = 6$, the mean fluid velocity is roughly 1.6 times the value for isothermal flow with a flow temperature equaling the wall temperature.

15-2. HEAT EXCHANGE WITH DEVELOPED TEMPERATURE FIELD IN FLAT TUBE WHEN THERE IS ENERGY DISSIPATION IN THE FLOW

The problem of fluid heating in a flat tube owing to the heat of friction is considered under the same conditions as above, with the velocity and temperature assumed to remain constant over the length. Here the energy and motion equation will have the form

$$\frac{d}{dy}\left(\lambda \frac{dt}{dy}\right)+\mu\left(\frac{dw_x}{dy}\right)^2 = 0. \tag{15-18}$$

$$\frac{d}{dy}\left(\mu \frac{dw_x}{dy}\right)-\frac{\partial p}{\partial x} = 0. \tag{15-19}$$

We first solve this problem on the assumption that μ and λ do not depend on the temperature. Such a solution has been obtained by Schlichting [4] for the case in which the temperatures of both walls are constant over the surface, but not equal, i.e.,

$$t=t_{c1} \text{ for } y=-r_0 \text{ and } t=t_{c2} \text{ for } y=+r_0, \tag{15-20}$$
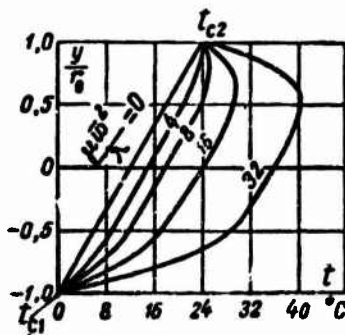
where $2r_0 = h$ is the width of the flat tube.

Fig. 15-5. Temperature field in flat tube resulting from energy dissipation ($t_{s1} = 0$ and $t_{s2} = 24°C$).

A solution of (15-19) is known for $\mu = $ const. Here the velocity profile is described by Eq. (5-11). When $\lambda = $ const, we can use (5-11)

to rewrite (5-18) as

$$\frac{d^2 t}{dy^2} = -9 \frac{\mu \bar{w}^2}{\lambda r_0^4} y^2.$$

(15-21)

Solving (15-21) with allowance for (15-20), we find the temperature distribution:

$$t = \frac{1}{2}(t_{c_1} + t_{c_2}) - \frac{1}{2}(t_{c_1} - t_{c_2})\frac{y}{r_0} + \frac{3}{4} \cdot \frac{\mu \bar{w}^2}{\lambda}\left(1 - \frac{y^4}{r_0^4}\right).$$

(15-22)

This relationship is illustrated in Fig. 15-5. When there is no dissipation ($\mu \bar{w}^2 = 0$), the temperature varies linearly, and the velocity field has no influence on the temperature field. On this linear distribution there is superposed the temperature increase caused by the heat of friction, which is allowed for by the last term of (15-22).

The heat-flow densities at the lower and upper walls equal, respectively:

$$q_{c_2} = -\lambda\left(\frac{dt}{dy}\right)_{y=-r_0} = \frac{\lambda}{2r_0}(t_{c_1} - t_{c_2}) - 3\frac{\mu \bar{w}^2}{r_0}.$$

(15-23)

$$q_{c_1} = \lambda\left(\frac{dt}{dy}\right)_{y=r_0} = \frac{\lambda}{2r_0}(t_{c_2} - t_{c_1}) - 3\frac{\mu \bar{w}^2}{r_0}.$$

(15-24)

To be definite, let us assume that $t_{c2} > t_{c1}$. It then follows from (15-24) that the heat flow at the hotter wall will vanish for values of the parameter $\frac{\mu \bar{w}^2}{\lambda} = \frac{1}{6}(t_{c2} - t_{c1})$; for greater values of this parameter, $q_{s2} < 0$, i.e., the heat flow is directed from the fluid to the wall; for lower values, it is directed from the wall to the fluid.

If both walls are at the same temperature $(t_{c1} = t_{c2} = t_c)$, then according to (15-22), the temperature distribution

$$t - t_c = \frac{3}{4} \cdot \frac{\mu \bar{w}^2}{\lambda}\left(1 - \frac{y^4}{r_0^4}\right).$$

(15-25)

will be established in the flow.

If one of the walls, the lower wall for example, is heat-insulateo, while the temperature t_{s2} of the second wall is maintained constant, then solving (15-21) under the boundary conditions $t(r_0) = t_{c2}$ and $t'(-r_0) = 0$, we obtain

$$t - t_{c2} = \frac{3}{4} \cdot \frac{\mu \bar{w}^2}{\lambda}\left(5 - 4\frac{y}{r_0} - \frac{y^4}{r_0^4}\right).$$

(15-26)

The temperature of the insulated wall (the so-called adiabatic wall temperature) will equal

$$t_{a.c} = t_{c2} + 6\frac{\mu \bar{w}^2}{\lambda}.$$

(15-27)

Let us consider the same problem, but with allowance for the temperature-dependence of the viscosity, using (15-9), on the as-

sumptior that both walls are at the same temperature t_s. The solution obtained for this problem in [1, 2] reduces to integration of (15-18), and (15-19) (with λ = const) with allowance for the temperature dependence (15-9) of the viscosity under the following boundary conditions

$$t(r_0) = t_c, \quad t'(0) = 0;$$
$$w_x(r_0) = 0, \quad w'_x(0) = 0.$$
$$\left. \right\} \qquad (15\text{-}28)$$

TABLE 15-2

Values of the Functions
$\Lambda_{-\frac{1}{4}}(x), \varphi_1(x)$

x	$\Lambda_{-\frac{1}{4}}(x)$	$\varphi_1(x)$	$\varphi_0(x)$
0.0	1.0000	0.50000	0.33333
0.1	0.997	0.49994	0.33285
0.2	0.987	0.49778	0.33143
0.3	0.970	0.49502	0.32907
0.4	0.947	0.49117	0.32577
0.5	0.918	0.48626	0.32156
0.6	0.883	0.48031	0.31647
0.7	0.842	0.47334	0.31051
0.8	0.796	0.46541	0.30373
0.9	0.745	0.45654	0.29616
1.0	0.690	0.44677	0.28783
1.1	0.630	0.43617	0.27880
1.2	0.567	0.42479	0.26911
1.3	0.501	0.41267	0.25881
1.4	0.433	0.39988	0.24796
1.5	0.362	0.38648	0.23661
1.6	0.291	0.37255	0.22484
1.7	0.219	0.35813	0.21267
1.8	0.147	0.34331	0.20020
1.9	0.075	0.32816	0.18748
2.0	0.004	0.31274	0.17457
2.1	−0.065	0.29713	0.16154
2.2	−0.132	0.28139	0.14844

Omitting calculations resembling those carried out in the preceding section, we write the final equation for the temperature distribution in a flat tube:

$$\vartheta = \vartheta_c \frac{\Lambda_{-\frac{1}{4}}(H_2 Y^2)}{\Lambda_{-\frac{1}{4}}(H_2)}, \qquad (15\text{-}29)$$

where $\vartheta = t + \dfrac{k_0}{k_1}$; $\vartheta_c = t_c + \dfrac{k_0}{k_1}$; k_0 и k_1 are the constants in (15-9); $H_2 = \dfrac{1}{8} \times \sqrt{\dfrac{k_1}{\lambda} \cdot \dfrac{\Delta p}{l} h^2}$; $Y = \dfrac{y}{r_0}$; $h = 2 r_0$; $\Lambda_{-\frac{1}{4}}(x)$ is the series occurring in the expression for the Bessel function of the first kind, $J_{-\frac{1}{4}}(x)$:

$$\Lambda_{-\frac{1}{4}}(x) = \sum_{\nu=0}^{\infty} \frac{1}{\nu!} \frac{\left(-\frac{1}{4}\right)!}{\left(-\frac{1}{4}+\nu\right)!} \left(\frac{ix}{2}\right)^{2\nu} = 1 - \frac{x^2}{3} + \frac{x^4}{42} - \ldots$$

Like the corresponding equation for a round tube, Eq. (15-29) is valid only for $\vartheta > 0$. Accordingly, the values of $\Lambda_{-\frac{1}{4}}(x)$ are given in Table 15-2 only up to the first root ($x \approx 2$).

The function $\Lambda_{-\frac{1}{4}}(x)$ differs little from the function $J_0(x)$ in (15-13), so that the dimensionless-temperature profiles are roughly the same in nature for flat and round tubes. For exactly the same values of k_1, λ, $\Delta p/l$ and $h = d$, the maximum temperature rise at the center of the flat tube will be greater than on the axis of the round tube. The reason is that heat is removed from the flow in two directions for the flat tube, while it is removed along all radial directions for the round tube.

The velocity distribution over the cross section of the flat tube is described by the equation

$$\frac{w_x}{w_{xc}} = \frac{2}{\Lambda_{-\frac{1}{4}}(H_2)} [\varphi_1(H_2) - Y^2 \varphi_1(H_2 Y)]. \qquad (15\text{-}30)$$

where

$$w_{xc} = \frac{3}{2} \bar{w}_c = \frac{1}{8} \cdot \frac{h^2}{\mu_0} \cdot \frac{\Delta p}{l};$$

here w_{0s} and $\bar{w}_s$ are the velocity on the tube axis and the velocity averaged over the cross section for isothermal flow at a temperature equaling the wall temperature and the same values of h and $\Delta p / l$ as for nonisothermal flow;

$$\varphi_1(x) = \sum_{\nu=0}^{\infty} \frac{1}{\nu!} \cdot \frac{\left(-\frac{1}{4}\right)!}{\left(-\frac{1}{4}+\nu\right)!} \cdot \frac{1}{4\nu+2}\left(\frac{ix}{2}\right)^{2\nu}$$

The fluid velocity averaged over a cross section is

$$\frac{\bar{w}}{\bar{w}_c} = 3 \frac{\varphi_2(H_2)}{\Lambda_{-\frac{1}{4}}(H_2)^2} \qquad (15\text{-}31)$$

where

$$\varphi_2(x) = \varphi_1(x) - \varphi_3(x)$$

and

$$\varphi_3(x) = \sum_{\nu=0}^{\infty} \frac{1}{\nu!} \cdot \frac{\left(-\frac{1}{4}\right)!}{\left(-\frac{1}{4}+\nu\right)!} \cdot \frac{1}{(4\nu+2)(4\nu+3)}\left(\frac{ix}{2}\right)^{2\nu}.$$

The values of the functions φ_1 and φ_2 are given in Table 15-2. The deviation of the velocity profile from the isothermal profile, caused by the temperature-dependence of the viscosity, is greater in the flat tube than in the round. The reason for this is clear in the light of the previous discussion.

The calculations discussed for flow in flat and round tubes with allowance for viscosity variation are based on linear interpolation for the relationship between $1/\mu$ and t. For the relationships $\mu = f(t)$ ordinarily encountered, such interpolation gives satisfactorily accurate results for values of the parameters H_1 and

H_2 less than or equal to 1.7. When the dependence of $1/\mu$ on t is sharply nonlinear, the calculations can make use of quadratic interpolation or a graphical method valid for any relationship between $1/\mu$ and t.

15-3. HEAT EXCHANGE IN A ROUND TUBE WITH HEAT SOURCES IN THE FLOW UNDER BOUNDARY CONDITIONS OF THE FIRST KIND

1. In this section, we shall consider heat exchange in a round tube with heat sources in the flow, including the thermal initial section. The fluid physical properties are assumed to be constant, the flow to be stabilized, and the heat conduction along the axis to be negligible. The fluid temperature at the entrance and the wall temperature are taken to be constant and equal, respectively, to t_0 and t_s.

The volume density of the internal heat sources is specified as a certain function of the radius on the assumption that it does not vary with the length. Thus

$$q_v = \bar{q}_\tau j(R),$$

where

$$\bar{q}_v = 2 \int_0^1 q_\tau R \, dR; \quad R = \frac{r}{r_*}.$$

The quantity q_v may include not only the heat released owing to action of the internal heat sources proper, but also owing to the heat of friction.

This problem has been considered by Topper [5] for a Newtonian fluid with q_v = const, and by Toor [6] for non-Newtonian fluids. We shall only give the solution of this problem for a Newtonian fluid with $q_v = q_v(r)$.

The energy equation for this problem has the form

$$w_x \frac{\partial t}{\partial x} = a \frac{1}{r} \cdot \frac{\partial}{\partial r} \left(r \frac{\partial t}{\partial r} \right) + \frac{\bar{q}_v}{\rho c_p} f \left(\frac{r}{r_*} \right).$$

Substituting the value $w_x = 2\bar{w}(1 - R^2)$ into this equation, and introducing the dimensionless variables

$$\theta = \frac{t - t_*}{\frac{q_v r_0^2}{\lambda}}, \quad \dot{R} = \frac{r}{r_*} \text{ and } X = 2 \frac{1}{\text{Pe}} \cdot \frac{x}{d}.$$

where $\text{Pe} = \frac{\bar{w} d}{a}$, we obtain

$$(1 - R^2) \frac{\partial \theta}{\partial X} = \frac{1}{R} \cdot \frac{\partial}{\partial R} \left(R \frac{\partial \theta}{\partial R} \right) + f(R). \tag{15-32}$$

The boundary conditions have the form

$$\theta(0, R) = \theta_* = \frac{(t_* - t_c)\lambda}{\bar{q}_v r_0^2}; \tag{15-33a}$$

$$\theta(X, 1) = 0; \quad \left(\frac{\partial \theta}{\partial R} \right)_{R=0} = 0. \tag{15-33b}$$

For large X, i.e., within the region with incipient thermal stabilization, the temperature (which we represent by θ_* in this case) will be independent of X, and (15-32) will be simplified:

$$\frac{1}{R} \cdot \frac{d}{dR} \left(R \frac{d\theta_*}{dR} \right) + f(R) = 0. \tag{15-34}$$

Integrating (15-34) with allowance for (15-33b), we find

$$\theta_* = \int_0^1 \frac{1}{R} \left[\int_0^R f(R) R \, dR \right] dR. \tag{15-35}$$

We represent the solution of (15-32) in the form

$$\theta(X, R) = \theta_{\bullet}(R) + \theta_1(X, R). \tag{15-36}$$

After substituting this expression into (15-32), we obtain an equation for θ_1 that does not contain the dissipation term:

$$(1 - R^2)\frac{\partial \theta_1}{\partial X} = \frac{1}{R} \cdot \frac{\partial}{\partial R}\left(R\frac{\partial \theta_1}{\partial R}\right). \tag{15-37}$$

The boundary conditions for θ_1 are written in the form

$$\theta_1(0, R) = \theta_{\bullet} - \theta_{\bullet}; \quad \theta_1(X, 1) = 0; \quad \left(\frac{\partial \theta_1}{\partial R}\right)_{R=0} = 0. \tag{15-38}$$

We thus arrive at the Graetz problem for the function θ_1 (see §6-1), with the sole difference that when $X = 0$, in place of the condition $\theta_1(0, R) = 1$ (in the Graetz problem), we have the condition $\theta_1(0, R) = \theta_{\bullet} - \theta_{\bullet}$.

As was shown in §6-1, the solution of Problem (15-37) and (15-38) has the form

$$\theta_1 = \sum_{n=0}^{\infty} A'_n \psi_n(R) e^{-\epsilon_n^2 X} \tag{15-39}$$

where ϵ_n and $\psi_n(R)$ are the eigenvalues and eigenfunctions for the Graetz problem; their values have been given in Tables 6-1 and 6-2;

$$A'_n = \frac{\int_0^1 (\theta_{\bullet} - \theta_{\bullet}) \psi_n(R) R(1 - R^2)\, dR}{\int_0^1 \psi_n^2(R) R(1 - R^2)\, dR}.$$

Substituting θ_1 from (15-39) into (15-36), we obtain the general solution of the problem:

$$\theta = \theta_{\bullet}(R) + \sum_{n=0}^{\infty} (\theta_{\bullet} A_n - A^*_n) \psi_n(R) \exp\left(-2\epsilon_n^2 \frac{1}{Pe} \cdot \frac{x}{r}\right). \tag{15-40}$$

where

$$\left. \begin{aligned} A_n &= \frac{\int_0^1 \psi_n(R) R(1 - R^2)\, dR}{\int_0^1 \psi_n^2(R) R(1 - R^2)\, dR}; \\[2em] A^*_n &= \frac{\int_0^1 \theta_{\bullet}(R) \psi_n(R) R(1 - R^2)\, dR}{\int_0^1 \psi_n^2(R) R(1 - R^2)\, dR}. \end{aligned} \right\} \tag{15-41}$$

The constants A_n coincide with the corresponding constants in the Graetz problem; their values have been given in Table 6-2. The

- 368 -

constants A^{*}_{n} can be computed with the aid of (15-41), since $f(R)$ is given and, consequently, $\theta_{*}(R)$ is easily determined, while the $\psi_{n}(R)$ are known.

If we divide it by θ_0, we can represent (15-40) as

$$\frac{t-t_c}{t_0-t_c}=\frac{1}{\theta_0}\left[\theta_*(R)-\sum_{n=0}^{\infty}A^{*}_{n}\psi_{n}(R)\exp\left(-2\varkappa^2_n\frac{1}{Pe}\cdot\frac{x}{d}\right)\right]+$$
$$+\sum_{n=0}^{\infty}A_{n}\psi_{n}(R)\exp\left(-2\varkappa^2_n\frac{1}{Pe}\cdot\frac{x}{d}\right).$$

(15-42)

The expression in brackets on the right side of (15-42) rises as X increases from a value of zero at $X = 0$ to the maximum value of θ_* at $X \to \infty$, while the last term on the right side decreases from unity when $X = 0$ to zero when $X \to \infty$.

If there is no internal heat release, then (15-42) reduces to the expression

$$\frac{t'-t_c}{t_0-t_c}=\sum_{n=0}^{\infty}A_{n}\psi_{n}(R)\exp\left(-2\varkappa^2_n\frac{1}{Pe}\frac{x}{d}\right).$$

which is a solution of the Graetz problem.

If the fluid temperature at the entrance equals the wall temperature ($t_0 = t_s$), we then obtain the following type of solution from (15-40):

$$\frac{t''-t_c}{\frac{q_v r_0^2}{\lambda}}=\theta_*(R)-\sum_{n=0}^{\infty}A^{*}_{n}\psi_{n}(R)\exp\left(-2\varkappa^2_n\frac{1}{Pe}\frac{x}{d}\right).$$

(15-43)

From this and (15-42), we find that

$$\frac{t-t_c}{t_0-t_c}=\frac{t''-t_c}{t_0-t_c}+\frac{t'-t_c}{t_0-t_c}.$$

(15-44)

In other words, in the general case the reduced temperature at any point will equal the sum of two reduced temperatures; one of them corresponds to flow with internal heat sources and the fluid entrance temperature equaling the wall temperature; the other corresponds to flow without internal heat sources. Since the temperature field has been found, it is not difficult to determine the mean mass temperature of the fluid in a given cross section and the local Nusselt number.

$$\bar{\theta}=\frac{\bar{t}-t_c}{\frac{q_v r_0^2}{\lambda}}=4\int_{0}^{1}\theta(1-R^2)\,R\,dR.$$

Substituting the value of θ from (15-40) into this expression and dividing it by θ_0, we find

$$\frac{\bar{\theta}}{\theta_0} = 4\frac{1}{\theta_0}\int_0^1 \theta_s(R)(1-R^2)R\,dR +$$

$$+ 4\sum_{n=0}^{\infty}\left(A_n - \frac{A^*_n}{\theta_0}\right)\exp\left(-2\varepsilon_n^2\frac{1}{Pe}\frac{x}{d}\right)\int_0^1 \psi_n(R)(1-R^2)R\,dR.$$

Transforming the second term on the right side with the aid of Relationship (6-17), we finally obtain

$$\frac{\bar{\theta}}{\theta_0} = \frac{\bar{t}-t_0}{t_0-t_c} = 4\frac{1}{\theta_0}\int_0^1 \theta_s(R)(1-R^2)R\,dR +$$

$$+ 8\sum_{n=0}^{\infty}\frac{1}{\varepsilon_n^2}\left(B_n - \frac{B^*_n}{\theta_0}\right)\exp\left(-2\varepsilon_n^2\frac{1}{Pe}\frac{x}{d}\right). \qquad (15\text{-}45)$$

where

$$B_n = -\frac{1}{2}A_n\left(\frac{d\psi_n}{dR}\right)_{R=1};$$

$$B^*_n = -\frac{1}{2}A^*_n\left(\frac{d\psi_n}{dR}\right)_{R=1}.$$

We see that B_n coincides with the corresponding constant in the Graetz problem.

It follows from (15-45) that $\frac{\bar{t}-t_s}{t_0-t_c}$ can also be represented as the sum of the two reduced temperatures mentioned previously.

Referring the local heat-transfer coefficient to the temperature difference $t_s - \bar{t}$, we obtain the following expression for Nu:

$$Nu = -\frac{2}{\bar{\theta}}\left(\frac{\partial\theta}{\partial R}\right)_{R=1}.$$

Substituting in the value of θ from (15-40) and $\bar{\theta}$ from (15-45), after simple manipulations we obtain

$$Nu = \frac{\sum_{n=0}^{\infty}\left(B_n - \frac{B^*_n}{\theta_0}\right)\exp\left(-2\varepsilon_n^2\frac{1}{Pe}\frac{x}{d}\right) - \frac{1}{2\theta_0}\left(\frac{d\theta_s}{dR}\right)_{R=1}}{2\sum_{n=0}^{\infty}\frac{1}{\varepsilon_n^2}\left(B_n - \frac{B^*_n}{\theta_0}\right)\exp\left(-2\varepsilon_n^2\frac{1}{Pe}\frac{x}{d}\right) + \frac{1}{\theta_0}\int_0^1 \theta_s(1-R^2)R\,dR}. \qquad (15\text{-}46)$$

TABLE 15-3

Values of Constants A^*_n and B^*_n in Problem of Heat Exchange in Round Tube With Heat Sources in Flow, $q_v =$ = const and t_s = const

n	0	1	2
A^*_n	0,292	0,051	0,019
B^*_n	0,148	—0,0340	0,0173

When $\frac{1}{Pe}\cdot\frac{x}{d} \to \infty$, the first terms in the numerator and denominator of (15-46) become small as compared with the second terms, and Nu approaches the constant value

$$Nu_\infty = -\frac{1}{2}\cdot\frac{\left(\frac{d\theta_s}{dR}\right)_{R=1}}{\int_0^1 \theta_s(1-R^2)R\,dR}. \qquad (15\text{-}47)$$

- 370 -

2. Equations (15-40)-(15-47) were derived on the assumption that the density of the internal heat sources varied radially, but is constant along the length. Let us use these equations to analyze the case in which the internal sources are uniformly distributed. Here $q_v = \bar{q}_v = $ const and $f(R) = 1$. From (15-35) we obtain

$$\theta_v = \tfrac{1}{4}(1 - R^2),$$

$$\int_0^1 \theta_v (1 - R^2) R\,dR = \tfrac{1}{4}\int_0^1 (1 - R^2)^2 R\,dR = \tfrac{1}{24}$$

and

$$\left(\frac{d\theta_v}{dR}\right)_{R=1} = -\tfrac{1}{2}.$$

Substituting these values into (15-42), (15-45), and (15-46), we obtain

$$\frac{t - t_c}{t_0 - t_c} = \sum_{n=0}^{\infty}\left(A_n - A^*_n \frac{1}{\theta_0}\right)\psi_n(R)\exp\left(-2\varepsilon_n^2 \frac{1}{Pe}\frac{x}{d}\right) + \frac{1}{4\theta_0}(1 - R^2); \quad (15\text{-}48)$$

$$\frac{\bar{t} - t_c}{t_0 - t_c} = 8\sum_{n=0}^{\infty}\frac{1}{\varepsilon_n^2}\left(B_n - B^*_n \frac{1}{\theta_0}\right)\exp\left(-2\varepsilon_n^2\frac{1}{Pe}\frac{x}{d}\right) + \frac{1}{6\theta_0}; \quad (15\text{-}49)$$

$$Nu = \frac{\displaystyle\sum_{n=0}^{\infty}\left(B_n - B^*_n\frac{1}{\theta_0}\right)\exp\left(-2\varepsilon_n^2\frac{1}{Pe}\frac{x}{d}\right) + \frac{1}{4\theta_0}}{\displaystyle 2\sum_{n=0}^{\infty}\frac{1}{\varepsilon_n^2}\left(B_n - B^*_n\frac{1}{\theta_0}\right)\exp\left(-2\varepsilon_n^2\frac{1}{Pe}\frac{x}{d}\right) + \frac{1}{24\theta_0}}. \quad (15\text{-}50)$$

The parameter

$$\frac{1}{\theta_0} = \frac{q_v r_0^2}{\lambda(t_0 - t_c)}.$$

The eigenfunctions $\psi_n(R)$ and constants ε_n, A_n, and B_n are given in Tables 6-1 and 6-2. The constants A^*_n and B^*_n are given in Table 15-3.

We find from (15-50) that when $q_v = $ const,

$$Nu_\infty = 6. \quad (15\text{-}51)$$

Figures 15-6 and 15-7 show the results of the temperature-field computations, while Figs. 15-8 and 15-9 give the mean mass temperature of the fluid and Nu when $q_v = $ const. The curves for $\theta_0^{-1} = 0$ correspond to the case in which there are no heat sources in the fluid flow. The curves for $\theta_0^{-1} > 0$ correspond to cooling of the fluid with internal release of heat $(t_0 > t_c \text{ and } q_v > 0)$ or heating of the fluid with internal absorption of heat $(t_0 < t_c \text{ and } q_v < 0)$. The curves for $\theta_0^{-1} < 0$ correspond to cooling of the fluid with internal absorption of heat $(t_0 > t_c, q_v < 0)$ or heating of the fluid with internal release of heat $(t_0 < t_c, q_v > 0)$.
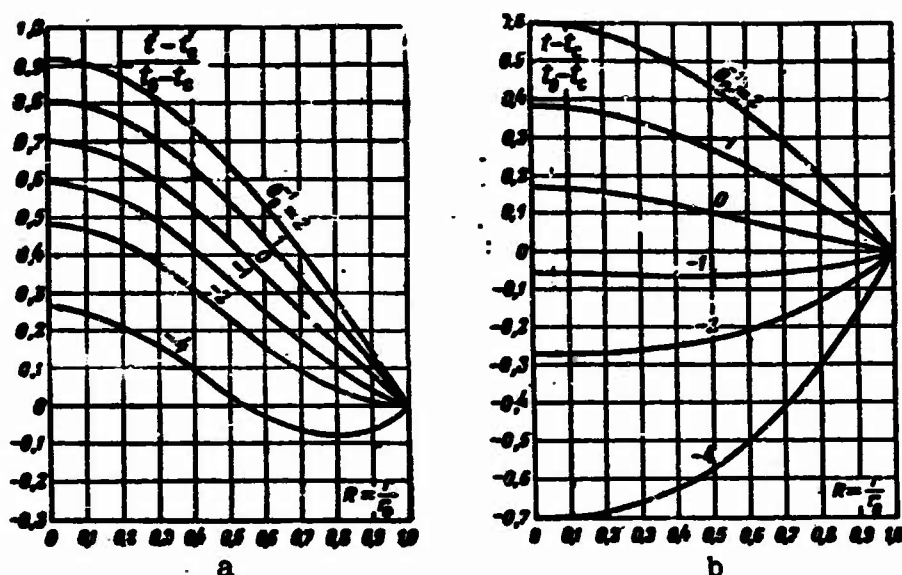
Fig. 15-6. Temperature profiles in tube sections corresponding to values a) $(1/Pe)(x/d) = 0.05$; b) $(1/Pe)(x/d) = 0.15$.

For values $\theta_0^{-1} > 0$, as this parameter increases, the heat-flux density at the wall will rise more rapidly than the mean mass temperature of the fluid; this leads to an increase in Nu (Fig. 15-9). In the region of θ_0^{-1} values from 0 to 5, Nu first decreases as $\frac{1}{Pe}\frac{x}{d}$ increases, and then begins to rise, approaching a limit. For values $\theta_0^{-1} > 5$, Nu decreases along the length.

If $\theta_0^{-1} < 0$, then at a certain value $\theta_0^{-1} = (\theta_0^{-1})_1$, the heat-flux density at the wall will pass through zero, reversing its sign (see Fig. 15-6). The reduced length X_1 corresponds to this value of θ_0^{-1}. Thus between the entrance and section X_1, heat is delivered from the fluid to the wall, while beyond this section it is delivered to the fluid from the wall. In the section at X, $\left(\frac{\partial t}{\partial r}\right)_{r=r_0} = 0$, while $\bar{t} - t_s \neq 0$; as a consequence, Nu vanishes at this section (in Fig. 15-9, see the curves for θ_0^{-1} equaling -1 and -2). For a reduced length $X = X_2$, the mean mass temperature of the fluid $\frac{\bar{t}-t_0}{t_s-t_0} = 0$ (see Fig. 15-8), and the temperature gradient at the wall $(\partial t/\partial r)_{r=r_0} \neq 0$ (we note that $X_2 > X_1$ and that it depends on θ_0^{-1}). In this section, consequently, Nu will approach $\pm\infty$. Thus when $X = X_2$, Nu(X) will have a discontinuity: both branches of the curve will go to infinity for $\theta_0^{-1} = -1$ and -2.
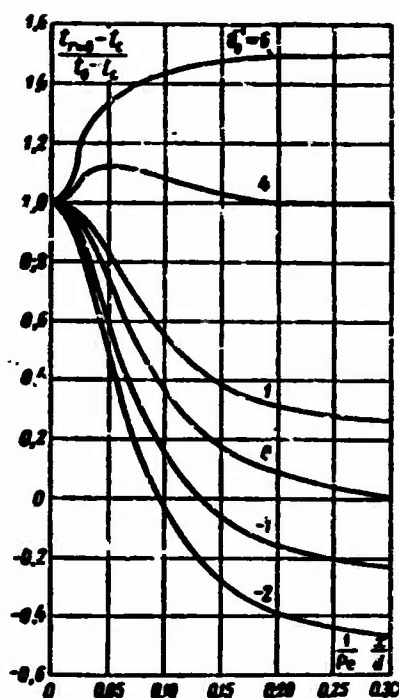
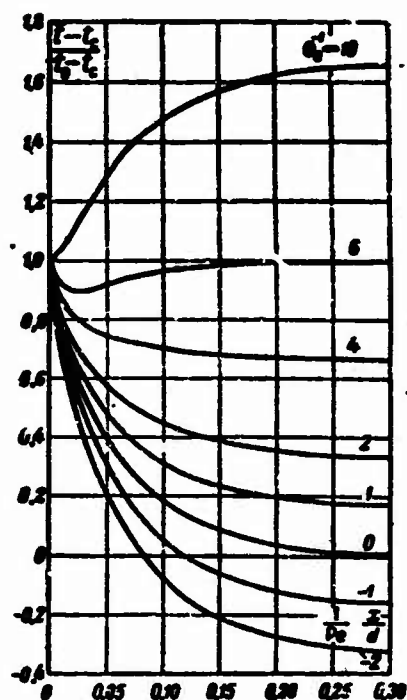Fig. 15-7. Variation in temperature on axis with tube length for various values of θ_0^{-1}.

Fig. 15-8. Variation in mean mass temperature of fluid along length for various values of θ_0^{-1}.

3. If heat is released in the flow solely by energy dissipation, then

$$q_v = \mu \left(\frac{d\bar{w}_x}{dr}\right)^2 = 16 \frac{\mu \bar{w}^2}{r_0^2} R^2;$$

$$\bar{q}_v = 2\int_0^1 q_v R\, dR = 8 \frac{\mu \bar{w}^2}{r_0^2};$$

$$\frac{q_v}{\bar{q}_v} = f(R) = 2R^2;$$

$$\theta_* = \frac{1}{8}(1 - R^4);$$

$$\int_0^1 \theta_* (1 - R^2) R\, dR = \frac{5}{8\cdot 24}; \quad \left(\frac{d\theta_*}{dR}\right)_{R=1} = -\frac{1}{2};$$

$$\frac{1}{\theta_0} = \frac{\bar{q}_v r_0^2}{\lambda (t_0 - t_c)} = 8 \frac{\mu \bar{w}^2}{\lambda (t_0 - t_c)}.$$

Substituting the values found into Eqs. (15-42), (15-45), and (15-46), we obtain

$$\frac{t - t_0}{t_0 - t_c} = D(1 - R^4) + \sum_{n=0}^{\infty}(A_n - 8DA^*_n)\,\psi_n(R)\exp\left(-2\varepsilon_n^2 \frac{1}{Pe}\frac{x}{d}\right); \qquad (15\text{-}52)$$

- 373 -

$$\frac{\bar{t}-t_c}{t_o-t_c}=\frac{5}{6}D+8\sum_{n=0}^{\infty}\frac{1}{\epsilon_n^2}(B_n-8DB^*{}_n)\exp\left(-2\epsilon_n^2\frac{1}{Pe}\frac{x}{d}\right).\qquad(15\text{-}53)$$

$$Nu=\frac{2D+\sum_{n=0}^{\infty}(B_n-8DB^*{}_n)\exp\left(-2\epsilon_n^2\frac{1}{Pe}\frac{x}{d}\right)}{\frac{5}{24}D+2\sum_{n=0}^{\infty}\frac{1}{\epsilon_n^2}(B_n-8DB^*{}_n)\exp\left(-2\epsilon_n^2\frac{1}{Pe}\frac{x}{d}\right)}.\qquad(15\text{-}54)$$

where

$$\begin{aligned}&[Л.7]\ 8A^*{}_o=\\&=1{,}354;\ 8A^*{}_1=-0{,}503;\ 8B^*{}_o=\\&=0{,}0939\ \epsilon_o^2;\ 8B^*{}_1=0{,}00757\epsilon_1^2.\end{aligned}$$
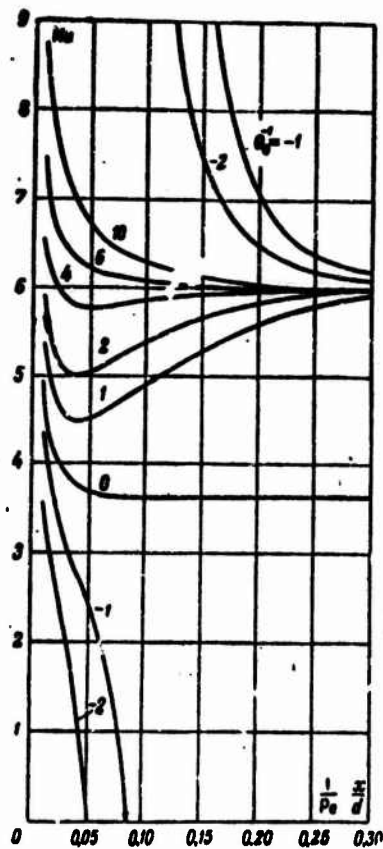

Fig. 15-9. Dependence of Nu on $\frac{1}{Pe}\cdot\frac{x}{d}$ for various θ_0^{-1}.

According to published data [7], $D=\frac{1}{8\theta_o}=\frac{\mu\bar{w}^2}{\lambda(t_o-t_c)}$.

Qualitatively, the curves for Nu with allowance for energy dissipation are the same in nature as those of Fig. 15-9. As we can see from (15-54), however, $Nu_\infty = \frac{48}{5} = 9.6$, which corresponds to the value found previously (see §15-1). Naturally, energy dissipation has a substantial influence on heat exchange only when the parameter D is sufficiently large.

4. Applying the method used here, it is also not difficult to generalize the heat release in the flow for the problem of heat exchange in a flat tube under boundary conditions of the first kind, or the problems of heat exchange in round and flat tubes under boundary conditions of the third kind, to the case in which the temperature of the surrounding medium is specified rather than the wall temperature.

15-4. HEAT EXCHANGE WITH DEVELOPED TEMPERATURE FIELD IN ROUND TUBE WITH HEAT SOURCES IN FLOW UNDER BOUNDARY CONDITIONS OF THE SECOND KIND

We shall investigate heat exchange in a round tube with heat sources in the flow and constant heat-flux density at the wall. Let the volume density of the internal heat sources vary radially, but be constant along the length, i.e.,

$$q_v = \bar{q}_v f(R),$$

where

$$\bar{q}_v = 2 \int_0^1 q_v R\, dR = \text{const and } R = \frac{r}{r_0}.$$

Assuming the physical properties of the fluid to be constant, we consider the flow region far from the tube entrance, where the velocity and temperature profiles are stabilized. Heat exchange under these conditions has been studied elsewhere [8, 9, 10].

The problem reduces to solution of the energy equation

$$w_x \frac{\partial t}{\partial x} = \frac{a}{r} \frac{\partial}{\partial r}\left(r \frac{\partial t}{\partial r}\right) + \frac{\bar{q}_v}{\rho c_p} f\left(\frac{r}{r_0}\right)$$

under the boundary conditions

$$\left(\frac{\partial t}{\partial r}\right)_{r=0} = 0 \text{ and } \left(\frac{\partial t}{\partial r}\right)_{r=r_0} = \frac{q_c}{\lambda}. \tag{15-55}$$

Since q_s and $\bar{q}_v$ are constant over the length, while the heat-exchange process is stabilized, then

$$\frac{\partial t}{\partial x} = \frac{dt_c}{dx} = \frac{d\bar{t}}{dx} = \frac{\bar{q}_v r_0 + 2q_c}{\rho c_p \bar{w} r_0} = \text{const}, \tag{15-56}$$

i.e., the temperature at any point in the flow varies linearly with the length.

Substituting the value of $\partial t/\partial x$ from (15-56) into the initial equation, after certain manipulations we obtain

$$\frac{\partial}{\partial R}\left(R\frac{\partial t}{\partial R}\right)=\frac{\bar{q}_c r_0^2}{\lambda}[W_x-f(R)]R+\frac{2q_r r_0}{\lambda}W_x R,\qquad(15\text{-}57)$$

where

$$W_x=\frac{w_x}{\overline{w}}.$$

Integrating this expression twice with respect to R, we find the radial temperature distribution:

$$t_c-t=\frac{\bar{q}_c r_0^2}{\lambda}\int_R^1\left\{\frac{1}{R}\int_0^R[W_x-f(R)]R\,dR\right\}dR+\frac{2q_r r_0}{\lambda}\int_R^1\left[\frac{1}{R}\int_0^R W_x R\,dR\right]dR.\quad(15\text{-}58)$$

The difference between the wall temperature and the mean mass temperature of the fluid is

$$t_c-\bar{t}=2\int_0^1(t_c-t)W_x R\,dR.$$

Integrating this relationship by parts and substituting in the value of $(t_s - t)$ from (15-58), we obtain

$$t_c-\bar{t}=\frac{2\bar{q}_c r_0^2}{\lambda}\int_0^1\frac{1}{R}\left(\int_0^R W_x R\,dR\right)\left\{\int_0^R[W_x-f(R)]R\,dR\right\}dR+$$

$$+\frac{4q_r r_0}{\lambda}\int_0^1\frac{1}{R}\left(\int_0^R W_x R\,dR\right)^2 dR.\qquad(15\text{-}59)$$

If the heat-transfer coefficient is referred, as usual, to the temperature difference $t_s - \bar{t}$ and we correspondingly define the limiting Nusselt number as

$$\mathrm{Nu}_\infty=\frac{a_\infty d}{\lambda}=\frac{q_c\cdot 2r_0}{(t_c-\bar{t})\lambda},$$

we then find from (15-59)

$$\frac{1}{\mathrm{Nu}_\infty}=2Z\int_0^1\frac{1}{R}\left(\int_0^R W_x R\,dR\right)\left\{\int_0^R[W_x-f(R)]R\,dR\right\}dR+$$

$$+2\int_0^1\frac{1}{R}\left(\int_0^R W_x R\,dR\right)^2 dR,\qquad(15\text{-}60)$$

where $Z=\frac{q_r r_0}{2q_c}$ is the relative density of internal heat sources.

Equations (15-58), (15-59) and (15-60) hold for any axisymmetric velocity profile that does not vary along the length. It is clear from these equations that the heat sources have a greater influence on the temperature profile and the heat transfer the greater the absolute value of the parameter Z and the difference $W_x(R)-f(R)$. The heat sources do not affect the radial temperature distribution, and consequently, do not affect heat transfer in two cases: when $Z=0$ or $W_x(R)=f(R)$. The latter condition means that W_x and $q_r/\bar{q}_r$ are identically distributed over a cross section. Here the tempera-

- 376 -

ture variation caused by the action of the sources will be identical at each point in the flow. Thus the temperature profile and the heat-transfer coefficient will not vary. Accordingly, when $Z = 0$ or $f(R) = W_x$, Eqs. (15-58) and (15-60) go over to the familiar relationships for heat exchange without heat sources:

$$t_c - t = \frac{2q_r r_0}{\lambda} \int_R^1 \left[\frac{1}{R} \int_0^R W_x R \, dR \right] dR \tag{15-58a}$$

and

$$\frac{1}{Nu_\infty} = 2 \int_0^1 \frac{1}{R} \left(\int_0^R W_x R \, dR \right)^2 dR. \tag{15-60a}$$

Equations (15-58) and (15-60) make it possible to determine the temperature distribution and Nu_∞ for a flow with a parabolic velocity profile, whatever the law governing the radial variation of q_v. For a uniform distribution of internal heat sources, letting $q_v = \bar{q}_v$ or $f(R) = 1$ and $W_x = 2(1 - R^2)$, we obtain

$$\frac{t_c - t}{\frac{q_c r_0}{4\lambda}} = Z(1 - R^2)^2 + (1 - R^2)(3 - R^2) \tag{15-61}$$

or

$$\frac{t_c - t}{\frac{q_v r_0^2}{8\lambda}} = (1 - R^2) + \frac{1}{Z}(1 - R^2)(3 - R^2); \tag{15-61a}$$

$$Nu_\infty = \frac{q_r \cdot 2r_0}{(t_c - \bar{t})\lambda} = \frac{48}{3Z + 11}. \tag{15-62}$$

The temperature profiles calculated from (15-61) and (15-61a) for various values of the parameter Z are shown in Fig. 15-10a (for constant q_s) and Fig. 15-10b (for constant q_v). When $Z = 1$, the amount of heat supplied to (or removed from) the flow through the wall will equal the amount of heat liberated (or absorbed) by the sources. When $Z = -1$, these quantities of heat will be equal in absolute magnitude, but opposite in sign. In the latter case, as we can see from (15-56), the temperature at any point in the flow will not vary with the length, but the radial temperature distribution will become similar to the velocity distribution:

$$\frac{t_c - t}{\frac{q_r r_0}{4\lambda}} = -\frac{t_c - t}{\frac{q_v r_0^2}{8\lambda}} = 2(1 - R^2).$$

When $Z < -2$, there will be a second extremum point on the temperature profile (not coinciding with the tube axis), with coordinate

$$R_0 = \sqrt{\frac{Z + 2}{Z + 1}}. \tag{15-63}$$

When Z changes from −2 to −∞, this point moves from the tube axis to the wall.
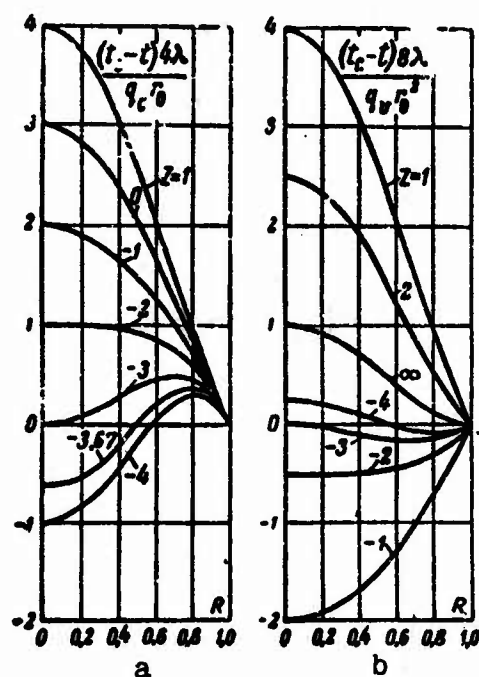
Fig. 15-10. Temperature pro-
files for uniform heat release
in flow. a) q_s = const; b) q_v =
= const.
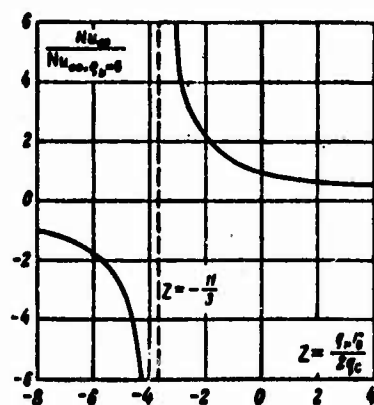
Fig. 15-11. Dependence of
$$\frac{Nu_\infty}{Nu_{\infty,\,q_v=0}} \quad \text{on } Z.$$

As we can see from (15-62), depending on Z, Nu_∞ can vary be-
tween $-\infty$ and $+\infty$ (Fig. 15-11). When $Z = -\frac{11}{3} \approx -3.67$, the temperature
difference $t_s - \bar{t}$ vanishes. Since $q_s \neq 0$ in this case, $Nu_\infty = \pm\infty$.
When $z < -11/3$, the heat-flux density q_s and the difference $t_s - \bar{t}$
will be opposite in sign, corresponding to a finite negative value
of Nu_∞.

Thus if the heat-transfer coefficient refers to the temperature difference $t_s - \bar{t}$ [i.e., $\alpha = q_s/(t_s - \bar{t})$], then when there are heat sources in the flow, the sign of the temperature head will not determine the sign of the heat flow (for example, when $t_s - \bar{t} > 0$, α and q_s may be either greater or smaller than zero); moreover, in some cases when $t_s - \bar{t} = 0$, $q_s \neq 0$. Thus it does not make intuitive sense to refer α to $(t_s - \bar{t})$, and it is inconvenient in practice. We can so define the heat-transfer coefficient, however, that this drawback is eliminated.

As we can see from (15-59), the temperature head $t_s - \bar{t}$, which we represent by Δt_s, is determined by the sum of two integrals. The first of them is the temperature head when $q = 0$ or, in other words, when the tube wall is adiabatic. We represent it by $\Delta t_{a.s}$. Thus (15-59) can be written as

$$\Delta t_c - \Delta t_{a.c} = \frac{4q_c r_0}{\lambda} \int_0^1 \frac{1}{R} \left(\int_0^R W_x R \, dR \right)^2 dR. \tag{15-64}$$

The quantity $\Delta t_c = t_c - \bar{t}$ can be treated as the wall temperature, measured from $\bar{t}$, and $\Delta t_{a.c} = t_{a.c} - \bar{t}_{q_{c=0}}$ as the adiabatic wall temperature, measured from $\bar{t}_{q_{c=0}}$.

Defining the heat-transfer coefficient and the Nusselt number as

$$\alpha^*_\infty = \frac{q_c}{\Delta t_c - \Delta t_{a.c}} \quad \text{and} \quad Nu^*_\infty = \frac{q_c \cdot 2r_0}{(\Delta t_c - \Delta t_{a.c})\lambda},$$

we obtain from (15-64)

$$\frac{1}{Nu^*_\infty} = 2 \int_0^1 \frac{1}{R} \left(\int_0^R W_x R \, dR \right)^2 dR. \tag{15-65}$$

This expression coincides with (15-60a). Consequently, if the heat-transfer coefficient is referred to the difference between the wall temperature and the adiabatic wall temperature, the expression for Nu^*_∞ will have the same form when there are internal heat sources in the flow as when there is heat exchange with no heat sources. Thus for a parabolic velocity profile, we obtain from (15-65)

$$Nu^*_\infty = \frac{48}{11} \approx 4.36,$$

which corresponds to the value found previously with no internal heat sources in the flow.

For the adiabatic wall temperature we have the expression

$$\Delta t_{a.c} = \frac{2\bar{q}_v r_0^2}{\lambda} \int_0^1 \frac{1}{R} \left(\int_0^R W_x R\,dR \right) \left\{ \int_0^R [W_x - f(R)] R\,dR \right\} dR. \qquad (15\text{-}66)$$

With a parabolic velocity profile and uniform distribution of heat sources, we have

$$\Delta t_{a.c} = \frac{q_v r_0^2}{16\lambda}$$

or

$$\theta_{a.c} = \frac{t_{a.c} - \bar{t}_{q_v=0}}{\frac{q_v r_0^2}{\lambda}} = \frac{1}{16}. \qquad (15\text{-}67)$$

If there are no heat sources or $\bar{W}_x(R) = f(R)$, то $\Delta t_{a.c} = 0$ и $a^* = a$.

The heat liberated in the flow by energy dissipation can be treated as the action of internal heat sources, distributed as

$$q_v = \mu \left(\frac{dw_x}{dr} \right)^2 = \frac{16\mu \bar{w}^2}{r_0^2} R^2$$

or

$$\frac{q_v}{\bar{q}_v} = f(R) = 2R^2.$$

If there are no other heat sources, we can use (15-66) to obtain

$$\Delta t_{a.c} = \frac{\bar{q}_v r_0^2}{8\lambda} = \frac{\mu \bar{w}^2}{\lambda}.$$

Thus with the heat sources distributed in accordance with the law $q_v/\bar{q}_v = 2R^2$, the adiabatic wall temperature is 2 times that for a uniform distribution.

Example. Mercury flows in a round tube of diameter $d = 12$ at a rate $\bar{w} = 0.0143$ m/s. The temperature of the mercury at the entrance is $t_0 = 20°C$. An electric current is passed through the mercury. The volume density of heat release is $q_v = 25 \cdot 10^6$ W/m³; it is distributed uniformly over the cross section and along the length. We are to determine the tube wall temperature at a distance $x = 300$ mm from the entrance for two cases: a) with no heat flux at the wall ($q_s = 0$); b) with a heat flux $q_s = -30 \cdot 10^2$ W/m² at the wall (the heat flow is directed from the fluid to the wall) on the assumption that the velocity and temperature profiles are stabilized. As we can see without difficulty, the flow will be laminar under these conditions.

In the first case, the wall temperature equals the adiabatic wall temperature $t_{a.s}$,

$$t_{\text{s.c}} - \bar{t}_{q_c=0} = \frac{q_v r_0^2}{16\lambda} = \frac{25 \cdot 10^6 (6 \cdot 10^{-3})^2}{16 \cdot 9.7} \approx 5.8^\circ C;$$

and

$$\bar{t}_{q_c=0} = t_0 + \frac{q_v x}{\rho c_p w} = 20 + \frac{25 \cdot 10^6 \cdot 0.3}{13\,230 \cdot 0.1374 \cdot 10^3 \cdot 0.0143} = 309^\circ C$$

$$t_{\text{s.c}} = 309 + 5.8 \approx 315^\circ C.$$

Here we take $\lambda = 9.7$ W/m·deg; $\rho = 13{,}230$ kg/m³, and $c_p = 0.1374$ kJ/kg·deg (for $t \approx 150^\circ C$).

In the second case, the wall temperature is found from the relationships

$$Nu^*_\infty = \frac{q_c d}{(\Delta t_c - \Delta t_{\text{s.c}})\lambda} = 4.36.$$

From this we have

$$\Delta t_c = t_0 - \bar{t} = \frac{q_c d}{4.36\lambda} + \Delta t_{\text{s.c}} = -\frac{30 \cdot 10^3 \cdot 12 \cdot 10^{-3}}{4.36 \cdot 9.7} + 5.8 \approx -2.7^\circ C;$$

$$\bar{t} = t_0 + \frac{(q_v r_0 + 2q_c) x}{\rho c_p w r_0} = 20 + \frac{(25 \cdot 10^3 \cdot 6 \cdot 10^{-3} - 2 \cdot 30 \cdot 10^3) 0.3}{13\,230 \cdot 0.1374 \cdot 10^3 \cdot 0.0143 \cdot 6 \cdot 10^{-3}} = 193^\circ C$$

and, consequently,

$$t_c = 193 - 2.7 \approx 190^\circ C.$$

15-5. HEAT EXCHANGE IN ROUND TUBE WITH HEAT SOURCES IN FLOW UNDER BOUNDARY CONDITIONS OF THE SECOND KIND

We consider the same problem as in the preceding paragraph, but allowing for the thermal initial segment alone. The fluid entrance temperature is taken to be constant over the cross section and equal to t_0. The density of internal heat sources is assumed to be a function of x and r, while the heat-flux density at the wall is a function of x. The problem has been solved by Sparrow and Siegel [11].

Assuming the fluid properties to be constant and the flow to be stabilized, and neglecting heat conduction along the axis, we write the energy equation as

$$w_x \frac{\partial \vartheta}{\partial x} = a \frac{1}{r} \frac{\partial}{\partial r}\left(r \frac{\partial \vartheta}{\partial r}\right) + \frac{q_v}{\rho c_p},$$

where

$$\vartheta = t - t_0.$$

The boundary conditions have the form

$$\left(\frac{\partial \vartheta}{\partial r}\right)_{r=0} = 0, \quad \left(\frac{\partial \vartheta}{\partial r}\right)_{r=r_0} = \frac{q_c}{\lambda}, \quad \vartheta(0, r) = 0.$$

Since the equation and the boundary conditions are linear in the temperature, the solution of this problem can be represented as the sum of the solutions for two simpler problems:

$$\vartheta = \vartheta_1 + i\vartheta_2, \tag{15-68}$$

where ϑ_1 is the solution for heat exchange through the wall in the absence of internal heat sources in the flow ($q_v = 0$); ϑ_2 is the solution for the heat-insulated wall ($\dot{q}_s = 0$) with heat sources in the fluid flow.

We have the following equations and boundary conditions for ϑ_1 and ϑ_2:

$$\left. \begin{array}{c} w_x \dfrac{\partial \vartheta_1}{\partial x} = a \dfrac{1}{r} \dfrac{\partial}{\partial r}\left(r \dfrac{\partial \vartheta_1}{\partial r}\right); \\[2mm] \left(\dfrac{\partial \vartheta_1}{\partial r}\right)_{r=0} = 0; \ \left(\dfrac{\partial \vartheta_1}{\partial r}\right)_{r=r_0} = \dfrac{q_c}{\lambda}; \ \vartheta_1(0, r) = 0; \end{array} \right\} \tag{15-69}$$

$$\left. \begin{array}{c} w_x \dfrac{\partial \vartheta_2}{\partial x} = a \dfrac{1}{dr} \dfrac{\partial}{\partial r}\left(r \dfrac{\partial \vartheta_2}{\partial r}\right) + \dfrac{q_v}{\rho c_v}; \\[2mm] \left(\dfrac{\partial \vartheta_2}{\partial r}\right)_{r=0} = 0; \ \left(\dfrac{\partial \vartheta_2}{\partial r}\right)_{r=r_0} = 0; \ \vartheta_2(0, r) = 0. \end{array} \right\} \tag{15-70}$$

1. A solution of the first problem has been given in §8-1 for constant density of the heat flux at the wall (q_s = const). This solution has the form

$$\vartheta_1 = \frac{q_c d}{\lambda}\left[\frac{4}{Pe}\frac{x}{d} + \frac{1}{2}R^2 - \frac{1}{8}R^4 - \frac{7}{48} + \right.$$
$$\left. + \sum_{i=1}^{\infty} A_i \psi_i(R) \exp\left(-2\varepsilon_i^2 \frac{1}{Pe}\frac{x}{d}\right)\right]. \tag{15-71}$$

Letting $R = 1$, we find the expression for the wall temperature:

$$\vartheta_{1c} = \frac{q_c d}{\lambda}\left[\frac{4}{Pe}\frac{x}{d} + \frac{11}{48} + \sum_{i=1}^{\infty} A_i \psi_i(1) \exp\left(-2\varepsilon_i^2 \frac{1}{Pe}\frac{x}{d}\right)\right]. \tag{15-72}$$

The values of the constants in (15-71) and (15-72) are given in Table 8-1.

Equation (15-72) can be generalized to the case in which q_s varies arbitrarily along the tube length (see §8-4). If

$$q_c = \bar{q}_c \varphi(\tilde{x}),$$

then

$$\vartheta_{1c} = \frac{\bar{q}_c d}{\lambda}\frac{1}{Pe}\frac{l}{d}\int_0^{\tilde{x}}\left\{4 + \sum_{i=1}^{\infty} N_i \exp\left[-2\varepsilon_i^2\frac{1}{Pe}\frac{l}{d}\ (\tilde{x} - \tilde{\xi})\right]\right\} \varphi(\tilde{\xi})\, d\tilde{\xi}, \tag{15-73}$$

here $\bar{q}_s$ is the heat-flux density at the wall averaged over the tube length l; $\tilde{x} = x/l$; $N_i = -2\varepsilon_i^2 A_i \psi_i(1)$.

2. The solution of the second problem (determination of ϑ_2) is first considered for the case in which the density of the internal heat sources is constant along the length and variable along the radius:

$$q_v = \bar{q}_v f(R), \text{ where } \bar{q}_v = \text{const.}$$

We introduce the function

$$\vartheta^*_2 = \vartheta_2 - \vartheta_{2т.с}, \tag{15-74}$$

where $\vartheta_{2t.s}$ is the solution to this problem for the thermal-stabilization region.

A solution for the region of thermal stabilization in more general form (with allowance for the heat flux at the wall) has been obtained in an earlier section. We need only represent it in a form convenient for the present case. Letting $q_s = 0$ in (15-58) and (15-59), subtracting the first equation from the second, and combining the results with the expression that follows from the heat balance,

$$\bar{\delta}_2 = \frac{\bar{q}_v r_0^2}{\lambda} \frac{4}{Pe} \frac{x}{d}, \tag{15-75}$$

we find

$$\vartheta_{2т.с} = \frac{\bar{q}_v r_0^2}{\lambda} \left\{ \frac{4}{Pe} \frac{x}{d} - \int_R^1 \left[\frac{1}{R} \int_0^R (W_x - f(R)) R \, dR \right] dR + \right.$$

$$\left. + 2 \int_0^1 \frac{1}{R} \left(\int_0^R W_x R \, dR \right) \left[\int_0^R (W_x - f(R)) R \, dR \right] dR \right\}. \tag{15-76}$$

Substituting $W_x = 2(1 - R^2)$ into this expression, we finally obtain

$$\vartheta_{2т.с} = \frac{\bar{q}_v r_0^2}{\lambda} \left[\frac{4}{Pe} \frac{x}{d} + \frac{1}{2} \left(R^2 - \frac{1}{4} R^4 \right) + H(R) + K \right], \tag{15-77}$$

where

$$H(R) = - \int_0^R \left[\frac{1}{R} \int_0^R f(R) R \, dR \right] dR;$$

$$K = -4 \left[\int_0^1 H(R)(R - R^3) \, dR + \frac{7}{193} \right].$$

For the special case of uniform heat release in the flow, $f(R) = 1$, and (15-77) takes the form

$$\vartheta_{2т.с} = \frac{q_v r_0^2}{\lambda} \left[\frac{4}{Pe} \cdot \frac{x}{d} + \frac{1}{4} \left(R^2 - \frac{1}{2} R^4 - \frac{1}{4} \right) \right]. \tag{15-78}$$

To determine the unknown function ϑ^*_2, in (15-70) we replace ϑ_2 by the sum $\vartheta^*_2 + \vartheta_{2t.s}$ in accordance with (15-74). Since (15-70)

- 383 -

is valid for both ϑ_2 and $\vartheta_{2t.s}$, we obtain

$$w_x \frac{\partial \vartheta^*_2}{\partial x} = a \frac{1}{r} \frac{\partial}{\partial r} \left(r \frac{\partial \vartheta^*_2}{\partial r} \right); \qquad (15\text{-}79)$$

$$\left(\frac{\partial \vartheta^*_2}{\partial r} \right)_{r=0} = 0, \quad \left(\frac{\partial \vartheta^*_2}{\partial r} \right)_{r=r_0} = 0,$$

$$\vartheta^*_2(0, r) = - \vartheta_{2t.s}(0, r) = - \frac{\tilde{q}_v r_0^2}{\lambda} \left[\frac{1}{2} \left(R^2 - \frac{1}{4} R^4 \right) + H(R) + K \right]. \qquad (15\text{-}80)$$

Thus the term that allows for the effect of the internal heat sources does not appear in (15-79).

We note that from the mathematical viewpoint, the problem of finding $\bar{\vartheta}^*_2$ or $w_x = 2\bar{w}(1-R^2)$ is analogous to the problem considered in §8-1 [Eqs. (8-8) and (8-9)]; the sole difference lies in the boundary conditions at the entrance section. On the basis of Solution (8-10) for this problem, we can at once write a solution for ϑ^*_2:

$$\vartheta^*_2 = \frac{q_v r_0^2}{\lambda} \sum_{i=1}^{\infty} E_i \psi_i(R) \exp \left(-2\varepsilon_i^2 \frac{1}{Pe} \cdot \frac{x}{d} \right), \qquad (15\text{-}81)$$

where ε_i and $\psi_i(R)$ are the same eigenvalues and eigenfunctions as in (8-10) (see Table 8-1). The coefficients E_i are found with the aid of the last boundary condition of (15-80). This condition yields

$$\sum_{i=1}^{\infty} E_i \psi_i(R) = - \left[\frac{1}{2} \left(R^2 - \frac{1}{4} R^4 \right) + H(R) + K \right],$$

and we can use this and the orthogonality property of the eigenfunctions to obtain

$$E_i = - \frac{\int_0^1 \left[H(R) + \frac{1}{2} R^2 - \frac{1}{8} R^4 \right] \psi_i(R)(1 - R^2) R \, dR}{\int_0^1 \psi_i^2(R)(1 - R^2) R \, dR}. \qquad (15\text{-}82)$$

Thus in (15-81), only the coefficients E_i depend on the way in which the internal heat sources are distributed over the tube radius, i.e., on the form of $f(R)$.

With uniform heat release, corresponding to $f(R) = 1$, the expression for E_i (we let it be represented by E'_i) takes the form

$$E'_i = - \frac{\frac{1}{4} \int_0^1 \left(R^2 - \frac{1}{2} R^4 \right) \psi_i(R)(1 - R^2) R \, dR}{\int_0^1 \psi_i^2(R)(1 - R^2) R \, dR}. \qquad (15\text{-}83)$$

The coefficients E'_i, computed from (15-83) have the following numerical values:

i	1	2	3	4	5	6	7
E'_i	0.0799573	−0.0254050	0.0124496	−0.00738848	0.00489305	−0.0034795	0.0026019

There now is no difficulty in writing a general solution for the second problem, i.e., an expression for ϑ_2. In accordance with (15-74), we add Expression (15-81) to (15-77) or (15-78), obtaining:

for $q_v = \bar{q}_v f(R)$

$$\vartheta_2 = \frac{\bar{q}_v r_0^2}{\lambda}\left[\frac{4}{Pe}\frac{x}{d}+\frac{1}{2}\left(R^2-\frac{1}{4}R^4\right)+H(R)+K+\right.$$
$$\left.+\sum_{i=1}^{\infty}E_i\phi_i(R)\exp\left(-2\varepsilon_i^2\frac{1}{Pe}\frac{x}{d}\right)\right]; \qquad (15\text{-}84)$$

for $q_v = $ const

$$\vartheta_2 = \frac{q_v r_0^2}{\lambda}\left[\frac{4}{Pe}\frac{x}{d}+\frac{1}{4}\left(R^2-\frac{1}{2}R^4-\frac{1}{4}\right)+\right.$$
$$\left.+\sum_{i=1}^{\infty}E'_i\phi_i(R)\exp\left(-2\varepsilon_i^2\frac{1}{Pe}\frac{x}{d}\right)\right]. \qquad (15\text{-}85)$$

In the first case, the value of ϑ_2 at the wall will be

$$\vartheta_{2c} = \frac{\bar{q}_v r_0^2}{\lambda}\left[\frac{4}{Pe}\frac{x}{d}+\frac{3}{8}+H(1)+K+\right.$$
$$\left.+\sum_{i=1}^{\infty}E_i\phi_i(1)\exp\left(-2\varepsilon_i^2\frac{1}{Pe}\frac{x}{d}\right)\right]; \qquad (15\text{-}86)$$

in the second case, we have

$$\vartheta_{2c} = \frac{q_v r_0^2}{\lambda}\left[\frac{4}{Pe}\frac{x}{d}+\frac{1}{16}+\sum_{i=1}^{\infty}E'_i\phi_i(1)\exp\left(-2\varepsilon_i^2\frac{1}{Pe}\frac{x}{d}\right)\right]. \qquad (15\text{-}87)$$

We note that ϑ_{2s} is nothing but the adiabatic wall temperature, measured from the fluid temperature at the entrance.

Equation (15-87) can be represented as

$$\frac{\vartheta_{2c}-\bar{\vartheta}_2}{(\vartheta_{2c}-\bar{\vartheta}_2)_{T.c}}=1+16\sum_{i=1}^{\infty}E'_i\phi_i(1)\exp\left(-2\varepsilon_i^2\frac{1}{Pe}\frac{x}{d}\right), \qquad (15\text{-}88)$$

where $\bar{\vartheta}_2$ is determined from (15-75), and

$$(\vartheta_{2c}-\vartheta_2)_{T.c}=\frac{q_v r_0^2}{\lambda}\frac{1}{16}.$$

Figure 15-12 shows the results of calculations using (15-88). For $\frac{1}{Pe}\cdot\frac{x}{d}\approx 0.05$, the value of $\vartheta_{2s}-\bar{\vartheta}_2$ differs by no more than 5% from

the value $(\vartheta_{2s} - \bar{\vartheta}_2)_{t.s}$ for the thermal-stabilization region. In passing, we note that the results of wall-temperature measurements with uniform heat release [12] are in good agreement with Eq. (15-88).

Let us now generalize the solutions obtained for ϑ_{2s} to the case in which the internal sources are distributed arbitrarily over the length of the tube.
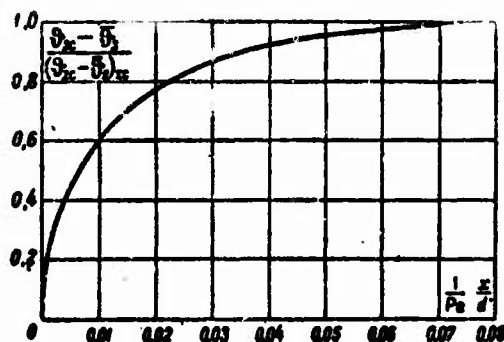

Fig. 15-12. $\dfrac{\vartheta_{2s} - \bar{\vartheta}_2}{(\vartheta_{2s} - \bar{\vartheta}_2)_{t.s}}$ as function of $\dfrac{1}{Pe} \cdot \dfrac{x}{d}$.

First of all, let us consider the case in which the internal heat liberation is uniform over the section, but varies in length, i.e., $q_v = q_v(x)$.

If there are no internal sources on the tube segment from $x = 0$ to $x = \xi$, and if when $x \geq \xi$, uniformly distributed sources with power Δq_v act, then in accordance with (15-87) we have the following expression for the wall temperature:

$$\vartheta_{2c} = \frac{r_0^2}{\lambda} \Delta q_v \left[\frac{4}{Pe} \frac{x - \xi}{d} + \frac{1}{16} + \sum_{i=1}^{\infty} E'_i \psi_i (1) \exp\left(-2\varepsilon_i^2 \frac{1}{Pe} \frac{x - \xi}{d} \right) \right] \text{ for } x \geq \xi).$$

If, however, q_v varies continuously over the length then, going from Δq_v to the differential dq_v and integrating the right side of this expression with respect to x (integration is carried out by parts), we obtain an equation for the wall temperature when q_v varies arbitrarily with the length:

$$\vartheta_{2c} = \frac{\bar{q}_v r_0^2}{\lambda} \cdot \frac{1}{Pe} \cdot \frac{l}{d} \int_0^{\tilde{x}} \Big\{ 4 + \tag{15-89}$$
$$+ \sum_{i=0}^{\infty} M'_i \exp\left[-2\varepsilon_i^2 \frac{1}{Pe} \frac{l}{d} (\tilde{x} - \tilde{\xi}) \right] \Big\} \Psi(\tilde{\xi}) d\tilde{\xi},$$

where $\bar{q}_v$ is the density of the internal heat sources, averaged over

the tube length l; $\tilde{x}=x/l$ is the dimensionless coordinate; $M'_i=-2\varkappa_i^2\,E'_i\psi_i(1)$ is a constant; $q_v/\bar{q}_v=\Phi(\tilde{x})$ is the specified distribution function for q_v over the tube length.

Finally, let the internal heat release vary both radially and along the tube length under the condition, however, that the density of the internal sources can be represented as the product of two functions, one giving the length distribution and the other the radial distribution, i.e.,

$$q_v=q_{v0}\Phi(\tilde{x})f(R),$$

where q_{v0} is the density of the internal heat sources at any fixed point on the tube axis (for example, at $\tilde{x} = 1/2$).

In this case, we obtain the following equation for the wall temperature:

$$\vartheta_{sc}=\frac{q_{v0}r_0^2}{\lambda}\frac{1}{Pe}\frac{l}{d}\left[2\int_0^1 f(R)\,R\,dR\right]\int_0^{\tilde{x}}\left\{4+\right.$$

$$\left.+\sum_{i=1}^{\infty}M_i\exp\left[-2\varkappa_i^2\frac{1}{Pe}\frac{l}{d}\,(\tilde{x}-\tilde{\xi})\right]\right\}\Phi(\tilde{\xi})\,d\tilde{\xi}, \qquad (15\text{-}90)$$

where

$$M_i=-2\varkappa_i^2 E_i\psi_i(1).$$

3. In paragraph 1, equations were given for the wall temperature $_{1s}$ in the absence of internal heat release; in paragraph 2, equations were given for the wall temperature $_{2s}$ when there is no heat flux at the wall (i.e., for an adiabatic wall temperature). To determine the wall temperature $_s$ when there are heat sources and there is heat flowing through the wall, we use a relationship following from (15-68):

$$\vartheta_c=\vartheta_{1c}+\vartheta_{2c}. \qquad (15\text{-}91)$$

If q_s = const and $q_v = q_v(r)$, to determine $_s$ we add Eqs. (15-72) and (15-86); if, however, $q_s = q_s(x)$ and $q_v = q_v(x)$, we add (15-73) and (15-89). In the most general case [when $q_s = q_s(x)$ and $q_v = q_v(x, r)$], to determine $_s$ we must add (15-73) and (15-90).

The mean mass temperatures of the fluid $^-$, $^-_1$, and $^-_2$ are connected by the relationship

$$\bar{\vartheta}=\bar{\vartheta}_1+\bar{\vartheta}_2.$$

Subtracting this relationship from (15-91), we obtain

$$(\vartheta_c-\bar{\vartheta})-(\vartheta_{2c}-\bar{\vartheta}_2)=\vartheta_{1c}-\bar{\vartheta}_1.$$

Using the definitions of the preceding section, $\vartheta_c-\bar{\vartheta}=\Delta t_c$ and

$\vartheta_{sc} - \bar{\vartheta}_s = \Delta t_{a.c.}$ we introduce the Nusselt number with and without internal heat sources in the flow:

$$Nu^{\bullet} = \frac{a^{\bullet}d}{\lambda} = \frac{q_c d}{\lambda(\Delta t_c - \Delta t_{a.c})}, \\ Nu = \frac{ad}{\lambda} = \frac{q_c d}{\lambda(\vartheta_{sc} - \bar{\vartheta}_s)}. \quad\Bigg\} \qquad (15\text{-}92)$$

Since $\Delta t_c - \Delta t_{a.c} = \vartheta_{sc} - \bar{\vartheta}_s$, then $Nu^{\bullet} = Nu$.

Thus the following statement, formulated in the preceding section, is valid not only for the region of stabilized heat exchange with q_s = const and $q_v(r)$, but also for the thermal initial segment with $q_s(x)$ and $q_v(x, r)$: if the heat-transfer coefficient refers to the difference between the wall temperature and the adiabatic wall temperature, then the expression for Nu when there are internal heat sources in the flow will have the same form as when there is heat exchange without heat sources.

15-6. HEAT EXCHANGE WITH DEVELOPED TEMPERATURE FIELD IN ANNULAR AND FLAT TUBES WITH HEAT SOURCES IN THE FLOW UNDER BOUNDARY CONDITIONS OF THE SECOND KIND

We first consider heat exchange in an annular tube and then, as a special case, in a flat tube. The analysis is carried out for fully developed velocity and temperature profiles. We assume that the power of internal heat sources is variable over the radius, but constant over the length:

$$q_v = \bar{q}_v f(R),$$

where

$$\bar{q}_v = \frac{2}{1 - R^2} \int_{R_1}^{1} q_v R \, dR,$$

$$R = r/r_2, \quad R_1 = r_1/r_2;$$

here r is the running radius, r_1 and r_2 are the inside and outside radii of the annular tube. The heat-flux densities q_{s1} and q_{s2} at the inside and outside walls will be constant with the length, but will not be identical.

This problem is a generalization of special problems considered earlier (see §§13-2 and 15-4). It can easily be solved by the same method. Thus, omitting the quite obvious calculations, we only give the final results.

The temperature at an arbitrary point in the flow, measured from the temperature of the inside wall, is determined by the equation

$$t - t_{c_1} = C \int_{R_1}^{R} \frac{1}{R} \left(\int_{R_1}^{R} W_x R \, dR \right) dR - \frac{q_{c_1} r_1}{\lambda} \ln \frac{R}{R_1} +$$

$$+ \frac{\bar{q}_v r_2^2}{\lambda} \int_{R_1}^{R} \left\{ \frac{1}{R} \int_{R_1}^{R} [W_x - f(R)] R \, dR \right\} dR, \tag{15-93}$$

where

$$C = \frac{2(q_{c_1} r_1 + q_{c_2} r_2) r_2^2}{\lambda (r_2^2 - r_1^2)}.$$
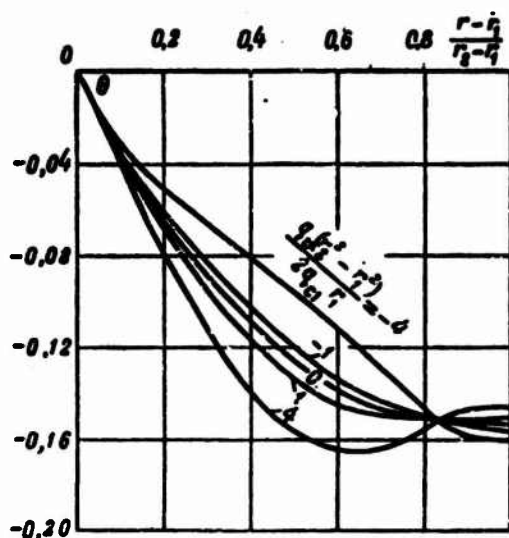
Fig. 15-13. Temperature profiles in annular tube with heat sources in flow, $R_1 = 0.75$ and $q_s = 0$.

Equation (15-93) holds for any axisymmetric velocity profile. For laminar stabilized flow and uniform heat release ($q_v = \bar{q}_v =$ = const), we substitute the value of W_x from (13-5) into (15-93) and let $f(R) = 1$, obtaining

$$t - t_{c_1} = CE(R) - \frac{q_{c_1} r_1}{\lambda} \ln \frac{R}{R_1} + \frac{q_v r_2^2}{\lambda} \left[E(R) - \frac{1}{4} (R^2 - R_1^2) + \frac{1}{2} R_1^2 \ln \frac{R}{R_1} \right]. \tag{15-93}$$

where

$$E(R) = \frac{(1+Z)(R^2 - R_1^2) - \frac{1}{4}(R^4 - R_1^4) - Z(R^2 \ln R - R_1^2 \ln R_1) - (Z + R_1^2) R_1^2 \ln \frac{R}{R_1}}{2(1 + R_1^2 + Z)},$$

$$Z = \frac{1 - R_1^2}{\ln R_1}.$$

As an example, Fig. 15-13 shows temperature profiles in an annular tube, calculated from (15-94) with $R_1 = 0.75$ and $q_{s2} = 0$.

The axis of ordinates shows $\theta = \frac{(t - t_{s1})\lambda}{q_{c1}r_1}$. The parameter is the ratio of the amounts of heat liberated by the sources and transferred through the wall. It is interesting that there is a point in the flow whose temperature, measured with respect to t_{s1}, does not depend on the power of the internal sources. The coordinate of this point is found from the condition requiring that the expression in brackets on the right side of (15-94) equal zero.

For the temperatures of the inside and outside walls we have the equations

$$t_{s1} - \bar{t} = \frac{2}{1-R_1^2} \int\limits_{R_1}^{1} \frac{1}{R} \left(\int\limits_{R}^{1} W_x R\, dR \right) \left\{ C \int\limits_{R}^{1} W_x R\, dR - \frac{q_{c1}r_1}{\lambda} + \right.$$

$$\left. + \frac{\bar{q}_v r_2^2}{\lambda} \int\limits_{R}^{1} [W_x - f(R)] R\, dR \right\} dR; \qquad (15\text{-}95)$$

$$t_{s2} - \bar{t} = \frac{2}{1-R_1^2} \int\limits_{R_1}^{1} \frac{1}{R} \left(\int\limits_{R_1}^{R} W_x R\, dR \right) \left\{ C \int\limits_{R_1}^{R} W_x R\, dR - \frac{q_{c1}r_1}{\lambda} + \right.$$

$$\left. + \frac{\bar{q}_v r_2^2}{\lambda} \int\limits_{R_1}^{R} [W_x - f(R)] R\, dR \right\} dR. \qquad (15\text{-}96)$$

In (15-95) and (15-96), q_{s1} and q_{s2} are positive, in accordance with Definition (2-1), if the heat flows from the wall to the fluid.

The mean mass temperature of the fluid is

$$\bar{t} = t_* + 4 \frac{1}{\text{Pe}} \frac{x}{d_*} (1 - R_1^2) \left(C + \frac{\bar{q}_v r_2^2}{\lambda} \right).$$

where

$$\text{Pe} = \frac{\bar{w} d_*}{a}, \quad d_* = 2(r_* - r_1).$$

If we let $q_{s1} = q_{s2} = 0$ in (15-95) and (15-96), i.e., if we assume that both walls are heat-insulated, we obtain the corresponding expressions for the adiabatic wall temperatures:

$$\theta_{a.c_1} = \frac{t_{a.c_1} - \bar{t}_{q_c=0}}{\frac{\bar{q}_v d_*^2}{\lambda}} = \frac{1}{2(1-R_1^2)(1-R_1)^3} \times$$

$$\times \int\limits_{R_1}^{1} \frac{1}{R} \left\{ \int\limits_{R}^{1} W_x R\, dR \int\limits_{R}^{1} [W_x - f(R)] R\, dR \right\} dR; \qquad (15\text{-}97)$$

$$\theta_{a.c_2} = \frac{t_{a.c_2} - \bar{t}_{q_e=0}}{\frac{\bar{q}_\nu d_0^2}{\lambda}} = \frac{1}{2(1-R_1^2)(1-R_1)^2} \times$$

(15-98)

$$\times \int_{R_0}^{1} \frac{1}{R} \left\{ \int_{R_0}^{R} W_x R \, dR \int_{R_1}^{R} [W_x - f(R)] R \, dR \right\} dR.$$

Substituting the value of W_x from (13-5) into these equations, and letting $f(R) = 1$, we obtain $\theta_{a.s1}$ and $\theta_{a.s2}$ for stabilized flow with uniform heat release:

$$\theta_{a.c_1} = \frac{C_1 + \frac{C_2}{\ln R_1} + \frac{C_3}{(\ln R_1)^2} + R_1^2 \ln R_1}{8(1-R_1^2)(1-R_1)^2 A^2},$$

(15-99)

where

$$C_1 = -\frac{1}{8} + \frac{17}{12} R_1^2 - \frac{3}{4} R_1^4 - \frac{15}{12} R_1^6 - \frac{1}{8} R_1^8 ;$$

$$C_2 = -\frac{29}{72} + \frac{55}{36} R_1^2 - \frac{3}{2} R_1^4 + \frac{1}{36} R_1^6 + \frac{25}{72} R_1^8 ;$$

$$C_3 = -\frac{1}{4} + R_1^2 - \frac{3}{2} R_1^4 + R_1^6 - \frac{1}{4} R_1^8 .$$
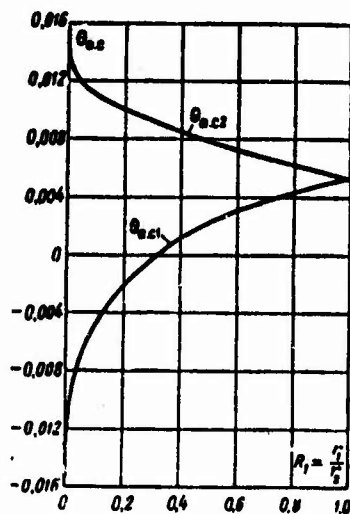
$$A = 1 + R_1^2 + Z.$$

Fig. 15-14. Adiabatic wall temperatures for annular tube.

An expression for $\theta_{a.s2}$ can be obtained from (15-99) if we replace R_1 by its reciprocal.

Figure 15-14 shows $\theta_{a.s1}$ and $\theta_{a.s2}$ as functions of R_1.

- 391 -

We can obtain equations for round and flat tubes as special cases of (15-93), (15-95) and (15-96) for an annular tube. For a flat tube, $R = R_1 = 1$, $1 - R_1 = \frac{r_2 - r_1}{r_2} = \frac{h}{r_2}$, where h is the width of the tube. Introducing the new coordinate $Y = y/h$, where y is the distance from wall 1 to the point considered, we obtain

$$t - t_{c_1} = \frac{(q_{c_1} + q_{c_2})h}{\lambda} \int_0^Y \left(\int_0^Y W_x \, dY \right) dY + \frac{\bar{q}_v h^2}{\lambda} \int_0^Y \left\{ \int_0^Y [W_x - f(Y)] \, dY \right\} dY; \quad (15\text{-}100)$$

$$t_{c_1} - \bar{t} = \int_0^1 \left(\int_Y^1 W_x \, dY \right) \left\{ \frac{(q_{c_1} + q_{c_2})h}{\lambda} \int_Y^1 W_x \, dY - \right.$$

$$\left. - \frac{q_{c_2} h}{\lambda} + \frac{\bar{q}_v h^2}{\lambda} \int_Y^1 [W_x - f(Y)] \, dY \right\} dY; \quad (15\text{-}101)$$

$$t_{c_2} - \bar{t} = \int_0^1 \left(\int_0^Y W_x \, dY \right) \left\{ \frac{(q_{c_1} + q_{c_2})h}{\lambda} \int_0^Y W_x \, dY - \right.$$

$$\left. - \frac{q_{c_1} h}{\lambda} + \frac{\bar{q}_v h^2}{\lambda} \int_0^Y [W_x - f(Y)] \, dY \right\} dY. \quad (15\text{-}102)$$

Substituting the value of W_x for a flat tube into these equations, together with $f(Y)$, we can obtain specific relationships for the fluid temperature and the temperature of the walls for a flow in a flat tube. No difficulties are involved in finding expressions for $\theta_{a.s1}$ and $\theta_{a.s2}$ from (15-101) and (15-102). It is also easy to show that the values of Nu at walls 1 and 2, referred to the corresponding temperature differences $\Delta t_s - \Delta t_{a.s}$, are determined by the same expressions as for heat exchange when there are no internal heat sources in the flow (see §13-2).

15-7. HEAT EXCHANGE IN PRISMATIC AND CYLINDRICAL TUBES WITH HEAT SOURCE IN FLOW

Certain problems involving heat exchange in prismatic and cylindrical tubes under mixed boundary conditions (see §14-3) can also be solved when there are internal heat sources in the flow. Thus, for example, Tao [13] has found solutions for tubes having cross sections in the form of an equilateral triangle and an ellipse. The solutions were obtained for fully developed velocity and temperature profiles with $\bar{q}$ = const over the length and t_s = const over the perimeter (here $\bar{q}_s$ is the heat-flux density at the wall, averaged over the perimeter). We shall give expressions for the limiting Nusselt numbers, averaged over the perimeter, for a uniformly distributed power of the internal heat sources.

For a tube with equilateral-triangle cross section,

$$\overline{Nu}_\infty = \frac{28}{9} \cdot \frac{2 + \frac{q_v d_o'}{q_c}}{2 + \frac{5}{6} \cdot \frac{q_v d_o}{q_c}}.$$ (15-103)

For a tube with elliptical cross section,

$$\overline{Nu}_\infty = \left[\frac{3\pi}{E(k)}\right]^2 \frac{2(1 + \omega^2)\left(2 + \frac{q_v d_o}{q_c}\right)}{\frac{17(1 + \omega^4) + 98\omega^2}{(1 + \omega^4 + 6\omega^2)}\left(4 + \frac{q_v d_o}{q_c}\right) + 12\frac{q_v d_o}{q_c}}.$$ (15-104)

Here $\overline{Nu}_\infty = \frac{\overline{q_c} d_o}{(t_o - \overline{t})\lambda}$; $E(k)$ is a total elliptic integral of the second kind; $k = (1 - \omega^2)^{1/2}$; $\omega = b_o/b$, is the ratio of the ellipse semiminor axis to the semimajor axis.

When there are no internal heat sources ($q_v = 0$), Eqs. (15-103) and (15-104) reduce to the expressions (14-33) and (14-34) obtained previously.

Manu-script Page No.	Footnotes
361	[1]It is clear from (15-12) that at values of $\Delta p/l$ for which H_1 approaches the first root of the function $J_0(x)$, (0) can be arbitrarily large, while no solution exists when H_1 equals the first root. As has been shown in [3], however, for each fluid there is a pressure gradient $(\Delta p/l)_o$ for which steady flow is possible if $\Delta p/l < (\Delta p/l)_o$, while steady flow is impossible for $\Delta p/l > (\Delta p/l)_o$.

Manu-script Page No.	Transliterated Symbols
357	c = s = stenka = wall
365	a.c = a.s = adiabaticheskaya stenka = adiabatic wall
377	э = e = ekstremal'nyy = extremum
383	т = t.s = teplovaya stabilizatsiya = thermal stabilization
390	э = e = ekvivalentnyy = equivalent

Chapter 16

FLOW AND HEAT EXCHANGE IN TUBES UNDER COMBINED ACTION OF FORCED AND FREE CONVECTION

16-1. VISCOUS-GRAVITATIONAL FLOW

In studying flow and heat exchange in tubes, we have so far neglected the volume forces acting in the fluid flow. These forces are produced by corresponding external fields, in particular the gravitational field. For confined flow in tubes, the effect of the gravitational force appears, as we have noted, only when the pressure is distributed nonuniformly in the fluid flow. Here lift forces appear in the flow that cause less dense fluid particles to move upward and denser particles to move downward.

If the sole moving force is lift, the fluid motion that appears is called gravitational free convection.[1] In this case, we shall study the more general flow and heat-exchange case where a nonuniform pressure distribution causes free convection in a fluid flowing as a result of an externally applied pressure drop. The fluid motion observed in this case results from the interaction of the forced and free convection.
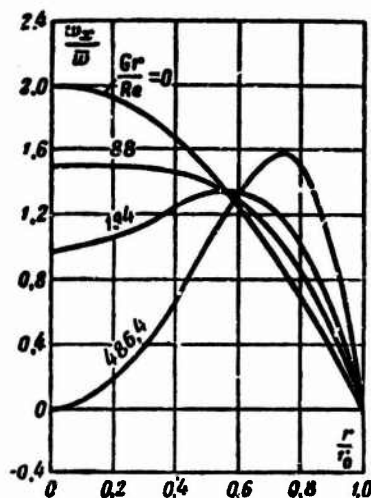

Fig. 16-1. Velocity profiles in vertical tube for heating of fluid moving upward.
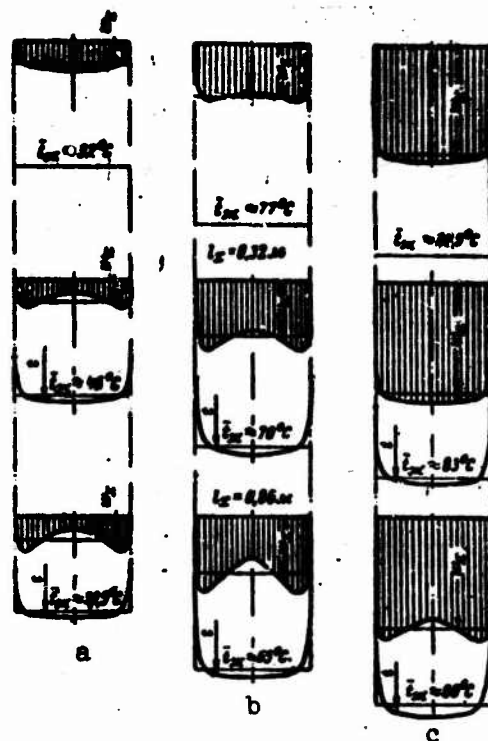
Fig. 16-2. Velocity and tempera-
ture distributions for three
cross sections of a tube on basis
of Watzinger-Jonson experiments.

a — Re—1 500, Δt—14.1° C; b — Re—6 340, Δt—12.8° C;
c — Re—14 200, Δt—8.8° C.

If the lift, viscosity, and inertial forces acting in the
flow are commensurate, the flow is said to be viscous-inertial-
gravitational. In this case, the influence of free convection on
flow and heat exchange appears as the dependence of the velocity
and temperature fields, as well as the heat transfer and resis-
tance, on the Grashof number (Gr) and on the system orientation
in the gravitational field. The latter can be specified, for ex-
ample, by the angle ψ between the vector representing the velo-
city at the tube entrance and the direction of the gravitational-
force vector. For laminar flow, the inertial forces often prove
small as compared with the lift and viscosity forces. Such flow
is said to be viscous-gravitational. Here the influence of free
convection on flow and heat exchange is determined by the product
Gr Pr (which is called the Rayleigh number Ra) and by the angle
ψ or by the number Gr/Re and the angle ψ.

In theoretical investigations, we proceed on the assumption
that any flow satisfying the continuity, motion, and energy equa-
tions will be stable. This is not always so, however. In other
words, not every motion predicted by the theory will actually
exist. We often encounter this situation in studying flows result-

- 395 -

ing from the interaction of force and free convection. To obtain
a qualitative notion of such flows and to analyze their stability,
we shall consider the three most characteristic cases of interac-
tion between forced and free convection.[2]

The first case involves upward flow in a vertical tube when
the fluid is heated and downward flow when it is cooled. When the
fluid is heated, the density near the wall is less than the density
in the flow core. Thus under the action of the lift forces, the
fluid particles near the wall have the velocity of free motion,
directed upward, while the particles in the flow core are directed
downard. If in this case, the velocity of forced flow (produced by
the externally applied pressure drop) is directed upward, the in-
teraction of free and forced convection will cause the velocity
near the wall to increase, while the velocity in the flow core will
decrease as compared with the velocity values at the same point for
isothermal flow. Exactly the same result is observed for cooling
of a fluid moving downward, since here the free- and forced-flow
velocities near the wall will coincide in direction (they will be
directed downward), while in the flow core they will be opposite
in direction.

This is well illustrated by Fig. 16-1, which shows calculated
velocity profiles for various values of Gr/Re for heating of a
fluid moving upward in a vertical tube.[3] The velocity profile is
parabolic for Gr/Re = 0 (isothermal flow). As Gr/Re increases, the
velocity will decrease in the flow core and increase near the wall.
Thus the velocity profile will first become fuller, and then a
minimum will appear on the tube axis with a velocity maximum be-
tween the axis and the wall. As Gr/Re increases, the maximum will
move toward the tube wall. For Gr/Re = 486.4, the velocity on the
axis becomes zero. With a further increase in Gr/Re, a flow should
appear near the axis that is opposite in direction to the flow
near the wall. These fluid flow characteristics have been confirmed
by direct measurements [2], carried out in the initial segment of
a vertical tube with cooling of a fluid moving downward. These
measurements showed that the velocity on the axis has a minimum,
that the velocity increases as we approach the wall, only decreas-
ing at the wall itself (Fig. 16-2). It is interesting to note that
this effect was observed for both small and relatively large Rey-
nolds numbers (up to 14,000).

When we consider the velocity profiles of Fig. 16-1, we na-
turally wonder to what degree the motion is stable. Actually, when
Gr/Re > 100, a point of inflection appears on the velocity profile.[4]
Here, as we know, the flow becomes less stable. On the other hand,
as Gr/Re increases, there is a substantial rise in the fullness of
the velocity profile at the wall, which undoubtedly increases flow
stability in the layer near the wall. Particularly unfavorable
conditions from the stability viewpoint occur at Gr/Re near 500
and above, where the velocity near the axis goes to zero and then
changes sign. Here vortices may appear in the flow core, so that
the stream nature of the flow will be disturbed.

Unfortunately, there are very few experimental data that
would make it possible to determine the stability limits for such

2,3,4/440
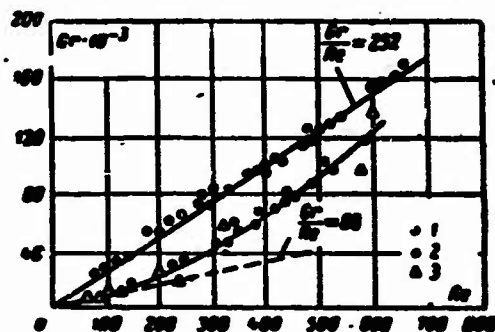
Fig. 16-3. Stability disruption boundaries
for motion of heating liquid through a ver-
tical tube. 1) Flow from top to bottom,
$l/d = 114.3$; 2) flow from bottom to top,
$l/d = 114.3$; 3) the same after other data
for $l/d = 111.9$ and 113.6.
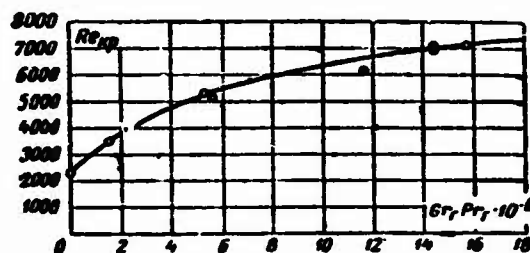
Fig. 16-4. Critical Reynolds
number as a function of $Gr_g Pr_g$
when the forced and free con-
vections have the same direc-
tion (at the wall).

flows. Observations carried out with ink fed to the center of the
flow [3] have disclosed a stability loss at specific values of
Gr, which increase as Re increases. The stability was assumed to
be disturbed when the stream of ink became winding. Here a reduc-
tion in Re with Gr held constant increased the amplitude of the
curvatures, and finally caused the ink to become blurred. Figure
16-3 shows the value of Gr at which stability was disturbed as
a function of Re (lower curve). The flow was stable in the region
below this curve; in the region lying above, it was unstable in
the sense indicated above. It is clear from Fig. 16-3 that th⌐
value of Gr/Re at which stability is lost does not remain constant,
but rises from 88 (corresponding to a flat profile in the core) to
~200 as Re varies between 100 and 600.[5]

The lower curve of Fig. 16-3 characterizes loss of stability
in the flow core alone; this disturbance apparently does not extend

[5]/440

to the wall region, where the flow remains stable in virtue of the fullness of the velocity profile at the wall. Thus the flow as a whole is as yet not turbulent. In other words, the curve of Fig. 16-3 cannot be treated as the boundary with turbulent flow. These considerations have been confirmed, in particular, by experimental data on critical Reynolds numbers obtained by the author together with L.D. Nolde by measurement of heat transfer in a vertical tube with the free and forced convections having the same direction (at the wall.[6] Figure 16-4 shows Re_{kr} as a function of $Gr_g Pr_g$ on the basis of these data.[7] It is clear from the graph that as $Gr_g Pr_g$ increases, so does the critical Reynolds number. Thus, for example, when $Gr_g Pr_g$ varies from zero (isothermal flow) to $15 \cdot 10^6$, Re_{kr} increases from 2300 to 7000, i.e., by more than 3 times. This shift in the transition between laminar (viscous-gravitational) flow and turbulent flow can be explained only if we assume that as $Gr_g Pr_g$ increases, the velocity profile near the wall becomes more and more convex, and the flow more and more stable. A similar phenomenon is observed, for example, with flows in constricting channels (nozzles).
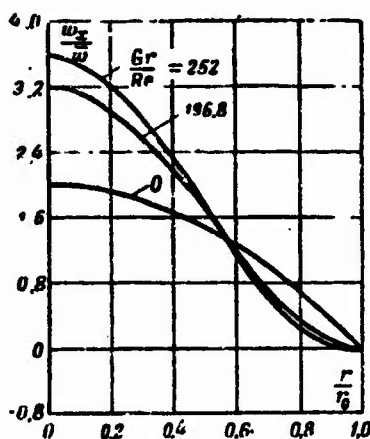
Fig. 16-5. Velocity profiles
in vertical tube for heating
of fluid moving downward.

The transition to turbulent flow is sometimes associated with the appearance near the axis of a flow opposite in direction to the flow at the wall; for $q_s = $ const, this has been observed with Gr/Re > 487. The data given above for critical Re values do not support this assumption; it is possible, however, that there is some definite influence on Re_{kr}.

Thus we can suppose that when the forced and free convection are in the same direction (at the wall), the flow near the wall will become more stable under external disturbances, including those coming from the flow core. This promotes the maintenance of laminar flow for Re values substantially greater than for iso-

6,7/441

thermal flow.

   The second case involves upward flow in a vertical tube with
the fluid heated and downward flow with the fluid cooled. With
both heating of a downward-moving fluid and cooling of an upward-
moving fluid, the velocities of the free and forced flows at the
wall will be opposite in direction, while they will have the same
direction in the flow core. Thus as a result of interaction of
free and forced convection, the velocity will decrease near the
wall while it will increase in the flow core as compared with the
isothermal-flow value. As Gr/Re increases, the velocity profile
will then vary as shown in Fig. 16-5.[8] As we can see, As Gr/Re
increases, the velocity profile becomes less and less full; even
at small values of Gr/Re, a point of inflection appears on the pro-
file, the velocity gradient at the wall decreases, becoming zero
at Gr/Re $\approx$ 200. A further increase in Gr/Re causes a flow to ap-
pear at the wall that is opposite in direction to the core flow.

   The flow will have very little stability with such a velo-
city profile. It is very probable that stability is disturbed at
the instant the flow at the wall begins to travel in the direction
opposite to that of the flow in the core (i.e., at Gr/Re > 200);
here vortices form at the wall and, consequently, laminar flow is
disturbed. Observations carried out by feeding ink to the center
of a flow [3] have actually shown that the stability loss[9] occurs
at Gr/Re $\approx$ 252 (this corresponds to the top curve of Fig. 16-3).
It is still difficult to say whether this value of Gr/Re only de-
termines the limit for stability disturbance, or whether it also
represents the boundary for transition to turbulent flow. We can
only state that when the free and forced convection are opposite
in direction (at the wall), the flow is less stable and, conse-
quently, the critical Reynolds numbers must be significantly less
than for isothermal flow (see, for example §16-3). Special research
is required to determine the critical values of Re under these
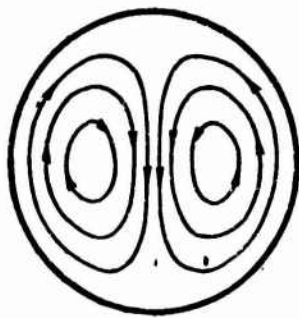conditions.

Fig. 16-6. Schematic represen-
tation of streamline projec-
tions on vertical plane for
flow of heated fluid in hori-
zontal tube.

   The third case involves flow in a horizontal tube with heating
or cooling of the fluid. Here free convection causes the fluid
particles to move in the plane perpendicular to the tube axis,

while forced convection causes these particles to move simultaneously along the tube axis. For heating, owing to the difference in densities, ascending fluid currents will appear at the wall, and descending currents at the center of the tube (Fig. 16-6). The motions will be reversed when the fluid is cooled. The motion appearing in a fluid in a horizontal tube owing to interaction of forced and free convection can be represented schematically as if the fluid were traveling along two helical lines, one of them directed clockwise, and the other counterclockwise. There have been almost no studies of stability for such a flow. We can at best make indirect estimates of stability on the basis of certain heat-transfer measurements (see §16-3).

16-2. HEAT EXCHANGE IN FLAT AND ROUND VERTICAL TUBES UNDER BOUNDARY CONDITIONS OF THE FIRST KIND. APPROXIMATE THEORETICAL ANALYSIS

Significant difficulties are involved in the problem of heat exchange in tubes when forced and free convection interact under boundary conditions of the first kind. No satisfactory solution has as yet been obtained. Martinelli and Boelter have attempted an approximate treatment of heat exchange in a vertical tube when the forced and free convection coincide at the wall. They use the Leveque solution for a round or flat tube (see §6-3):

$$\frac{t - t_c}{t_0 - t_c} = \frac{1}{0.893} \int_0^{\eta} e^{-\eta^3} d\eta, \qquad (6\text{-}52)$$

$$\bar{a} = \frac{\bar{q}_c}{t_c - t_0} = \frac{3}{2} \cdot \frac{\lambda}{0.893} \left(\frac{A}{9al}\right)^{1/3}, \qquad (6\text{-}54)$$

where

$$\eta = \left(\frac{A}{9ax}\right)^{1/3} y; \quad A = \left(\frac{dw_x}{dy}\right)_{y=0}.$$

This solution was constructed on the assumption that the velocity varies linearly within the thermal boundary layer, i.e., $w_x =$
$= Ay$, where A is the velocity gradient, which does not depend on x. Here A is defined as the derivative with respect to y of the actual velocity distribution (a Poiseuille distribution in the Leveque solution), taken at the wall.

Thus Eqs. (6-52) and (6-54) can be applied to flow with any symmetric velocity profile that remains constant over the length. The only difference in the velocity profiles appears in the value of A. Thus for flow with a parabolic velocity profile, $A = 6\,\bar{w}/h$ for a flat tube and $A = 8\,\bar{w}/h$ for a round tube.

Where free convection is superposed on forced flow, the velocity gradient at the wall will depend on the parameters determining both the forced and the free flow. Here A is not known in advance, but it can be found from the equation of motion. We use the equation of motion in simplified form, dropping the inertial terms, but allowing for the lift force. Assuming the physical properties of the fluid (other than density) to be constant, and representing the density as a linear function of the temperature, we have

$$\frac{\partial^2 w_x}{\partial y^2} + \frac{g\beta(t - t_0)}{\nu} + \frac{1}{\mu} \cdot \frac{dp}{dx} = 0. \tag{16-1}$$

where β is the coefficient of volume expansion and t_0 is the flow temperature far from the wall; it can be taken equal to the temperature at the entrance, since within the thermal initial segment, the temperature varies little in the flow core.

Substituting the value of $(t - t_0)$ from (6-52) into (16-1), and inte rating, we can find $(\partial w_x / \partial y)_{y=0}$. To perform the integration analytically, we approximate (6-52) by an equation of the form

$$\frac{t_c - t}{t_c - t_0} = 1 + b_1 e^{-\eta} + b_2 e^{-2\eta} + b_3 e^{-3\eta}. \tag{16-2}$$

which satisfies the boundary conditions, and agrees well with (6-52) when the constants are appropriately chosen.

Substituting $t - t_0$ from (16-2) into (16-1), we find

$$\frac{\partial^2 w_x}{\partial y^2} = \frac{g\beta(t_c - t_0)}{\nu}(b_1 e^{-\eta} + b_2 e^{-2\eta} + b_3 e^{-3\eta}) - D.$$

where

$$D = \frac{1}{\mu} \cdot \frac{dp}{dx} \approx \text{const.}$$

The boundary conditions have the form

for $x = 0$

$$t = t_0, \quad w_x = 6\bar{w}\left(\frac{y}{h} - \frac{y^2}{h^2}\right) \quad \text{or} \quad w_x = 8\bar{w}\left(\frac{y}{d} - \frac{y^2}{d^2}\right);$$

for $y = 0$ $t = t_c$, $w_x = 0$ and $\frac{\partial w_x}{\partial y} = A$.

Integrating and using the boundary conditions, we obtain an expression for the dimensionless velocity gradient at the wall. For a flat tube,

$$\varphi = \frac{Ah^2}{\nu} = 6\,\text{Re} + 0.43\,\text{Gr}\left(\frac{9x}{\text{Pr}\,\varphi h}\right)^{1/3}.$$

where

$$\text{Re} = \frac{\bar{w}h}{\nu}; \quad \text{Gr} = \frac{g\beta(t_c - t_0)h^3}{\nu^2}.$$

Unfortunately, this expression contains φ in implicit form. Thus in [5], it was replaced by the approximate relationship

$$\varphi = 6\,\text{Re} + 0.92\frac{\text{Gr}^{1/4}}{\text{Pr}^{1/4}}\left(\frac{x}{h}\right)^{1/4}.$$

As we see, the initial notion that φ (or A) is constant turns out to be unjustified. However, φ varies relatively little with the length ($\varphi \sim x^{\frac{1}{4}}$). Thus without introducing great error, we can use

its mean value over the segment of length l,

$$\bar{\varphi} = \frac{\overline{A}h^2}{v} = 6\,\mathrm{Re} + 0.736\frac{\mathrm{Gr}^{3/4}}{\mathrm{Pr}^{1/4}}\left(\frac{l}{h}\right)^{1/4}. \qquad (16\text{-}3)$$

Substituting the value of $\overline{A}$ from (16-3) into (6-54), we obtain an expression for the Nusselt number for flow in a flat tube:

$$\overline{\mathrm{Nu}} = 1.467\sqrt[3]{\mathrm{Pe}\frac{h}{l} + 0.123\left(\mathrm{Gr\,Pr}\frac{h}{l}\right)^{3/4}}. \qquad (16\text{-}4)$$

where

$$\overline{\mathrm{Nu}} = \frac{\overline{a}h}{\lambda}; \quad \mathrm{Pe} = \frac{\overline{w}h}{a}.$$

For flow in a round tube, a similar analysis leads to the expression

$$\overline{\mathrm{Nu}} = 1.615\sqrt[3]{\mathrm{Pe}\frac{d}{l} + 0.092\left(\mathrm{Gr\,Pr}\frac{d}{l}\right)^{3/4}}. \qquad (16\text{-}5)$$

where

$$\overline{\mathrm{Nu}} = \frac{\overline{a}d}{\lambda}; \quad \mathrm{Pe} = \frac{\overline{w}d}{a}; \quad \mathrm{Gr} = \frac{g\beta\,(t_c - t_0)\,d^3}{v^2}.$$

The heat-transfer coefficient in (16-4) and (16-5) pertains to the initial temperature head $t_s - t_0$.

Figure 16-7 shows Relationship (16-5) for a round tube. When $\mathrm{Gr\,Pr}\frac{d}{l} \to 0$. $\overline{\mathrm{Nu}}$ approaches a value corresponding to the Leveque equation (6-56).

Equations (16-4) and (16-5) will evidently be approximately correct only for short segments of flat and round tubes near the beginning of the heated segment.

For motion in long tubes, we must allow for the variation in fluid temperature with length, since in this case the temperature head will vary along the length and, consequently, so will the contribution made to heat exchange by free convection. To allow for this, Martinelli and Boelaer applied an analysis resembling the one considered here to elementary segments of a tube, and then averaged over the length. Naturally, such an approach is applicable only as a first rough approximation, primarily since the analysis is based on the Leveque solution, which is valid only for the thermal initial segment. As a result of computations by this method, the following approximate equation has been obtained for heat transfer in round vertical tubes when the forced and free convections coincide at the wall:

$$\overline{\mathrm{Nu}}_{\text{ж}} = 1.615F_1\sqrt[3]{\mathrm{Pe}_{\text{ж}}\frac{d}{l} + 0.092F_3\left(\mathrm{Gr\,Pr}\frac{d}{l}\right)_c^n}. \qquad (16\text{-}6)$$
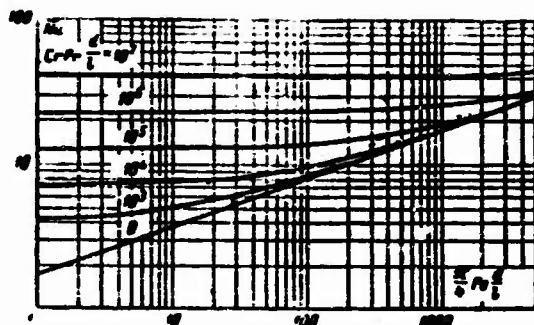
Fig.16-7. Heat transfer in round vertical tube near the entrance when the forced and free convections coincide at the wall.

In this equation, the theoretical value of the exponent is $n = 3/4$; the heat-transfer coefficient $\bar{\alpha}$ refers to the arithmetic mean temperature head $\Delta \bar{t}_a$, while Gr contains the initial temperature head $t_s - t_0$; F_1 and F_2 are functions of the parameter

$$z = \frac{\delta t}{\Delta t_a} = \frac{4 \overline{Nu_m}}{Pe_m \frac{d}{l}},$$

where δt is the difference between the fluid temperatures at the tube entrance and exit. The function $F_1(z)$ appears in connection with the fact that in (16-6), $\bar{\alpha}$ refers to the mean arithmetic temperature head:

$$F_1(z) = \frac{\Delta \bar{t}_s}{\Delta \bar{t}_a} = \frac{z}{\ln \frac{2+z}{2-z}}.$$

.If the mean logarithmic temperature head $(\Delta \bar{t}_l)$ is used in the determination of $\bar{\alpha}$, then F_1 vanishes from (16-6). The function $F_2(z)$ allows for the variation with length of the term in (16-6) that takes into account the influence of free convection. The values of F_1 and F_2 are given in Table 16-1.

It is recommended that a value $n = 0.84$ be taken so that Eq. (16-6) will correspond better to the experimental data of [5, 6]. For the same reason, the physical properties of the fluid in the expressions for $\overline{Nu}_{zh}$ and Pe_{zh} are selected for the arithmetic mean temperature of the fluid, and for the wall temperature in the expression for $(GrPr)_s$.

In Fig. 16-8, when $n = 0.84$ Eq. (16-6) corresponds with the experimental data for heat transfer in vertical tubes when upward-flowing water and oil are heated. The theoretical curves are higher the greater $(GrPr \, d/l)_s$. For sufficiently small $Pe_{zh} \, d/l$, $\overline{Nu}_{zh}$

approaches its asymptotic value, determined by the equation

$$\overline{Nu}_{\text{ж}} = \frac{1}{2} \, Pe_{\text{ж}} \frac{d}{l},$$

(16-7)

TABLE 16-1

Values of Functions F_1 and F_2 in Eq. (16-6)

z	$F_1(z)$	$F_2(z)$
0	1.000	1.000
0.1	0.997	0.952
0.2	0.995	0.910
0.3	0.990	0.869
0.4	0.965	0.828
0.5	0.978	0.787
1.0	0.912	0.588
1.5	0.770	0.403
1.7	0.675	0.320
1.8	0.610	0.272
1.90	0.573	0.212
1.95	0.445	0.164
1.99	0.332	0.095
2.00	0.000	0.000

This equation corresponds to flow in a tube having reduced length such that the fluid temperature at the exit becomes equal to the wall temperature. It can easily be obtained from the heat-balance equation. The experimental data of Fig. 16-8, given by Watzinger and Jonson [2] and American authors [6], agree with Eq. (16-6) to within +25%. Other experimental data (see Table 16-2) show still greater deviation. Thus Eq. (16-6) is quite approximate.[11]

Pigford [7a] and Rosen and Hanratty [7b] have also considered motion and heat exchange in a round vertical tube when the forced and free convections coincide in direction and the wall temperature is constant. These authors take into account the dependences of both the density and the viscosity on temperature (both ρ and $1/\mu$ are assumed to be linear functions of the temperature). The calculations of the first study differ but slightly from those considered earlier. In the second study, the calculations were based on boundary-layer theory.

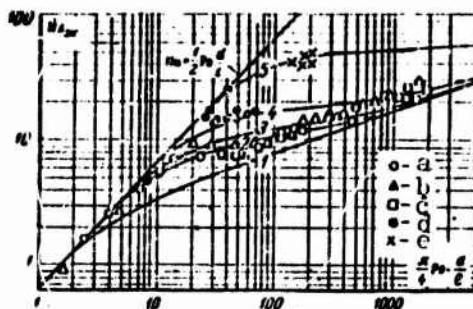Fig. 16-8. Heat transfer in round vertical tube when forced and reconvections coincide at wall. Curves) Calculations using Eq. (16-6). 1, 2, 3, 4, 5) $(GrPr \, d/l)_s = 0$, 10^4, $2 \cdot 10^4$, 10^5, $4.5 \cdot 10^6$; a, b, c) experiments with oil at $(GrPr \, d/l)_s = 1.05 \cdot 10^4$, $2.13 \cdot 10^4$, and $3.1 \cdot 10^4$; ', e) experiments with water at $(GrPr \, d/l)_s = 1.05 \cdot 10^5$, $4.5 \cdot 10^6$

16-3. HEAT EXCHANGE AND RESISTANCE IN ROUND TUBES UNDER BOUNDARY CONDITIONS OF THE FIRST KIND. EXPERIMENTAL DATA

The experimental data on heat exchange when both forced and free convection act can be divided into three groups in accordance with the three basic flow cases:

a) upward flow in vertical tubes with heating and downward flow with cooling;

b) flow in horizontal tubes with heating and cooling;

c) downward flow in vertical tubes with heating and upward flow with cooling.

TABLE 16-2

Characteristics of Experimental Heat-Transfer Data for Round Tubes with Viscous-Gravitational Flow of Fluid, t_s ≈ const

1 Автор	2 Тепоно-ситель	3 Условия взаимодействия вынужденной и свободной конвекции	d, мм	$\frac{l}{d}$	Pr_s	$(GrPr)_s \cdot 10^{-6}$
4 Ватцингер и Джонсон [Л. 2]	5 Вода	6 Течение в вертикальной трубе сверху вниз при охлаждении	50,2	20	2—5	300—3 820
7 Петухов [Л. 8] 9 Петухов и Нольде [Л. 4]	5 Вода 5 Вода	8 То же 10 Течение в вертикальных трубах снизу вверх и сверху вниз при нагревании и охлаждении. Течение в горизонтальной трубе при нагревании и охлаждении	16 16	131,3 131,3	4—6 2—8,5	8—70 8—160
11 Аладьев, Михеев и Федынский [Л. 9]	5 Вода	8 То же	10,2	59	3—7	6—90
12 Мартинелли, Саусвелл и др. [Л. 6]	Вода, минеральные масла	14 Течение в вертикальных трубах снизу вверх при нагревании	12,6 12,6	126 126—602	2,3 86—130	58 13—28
15 Керн и Отмер [Л. 10]	16 Минеральные масла	17 Течение в горизонтальной трубе при нагревании	15,8 30,6 62,7	123 100 48	20—300	85—38 000

In addition to those indicated, there are also studies by Kirchbaum [11] and Wetjen [12]. Their results cannot be used here, however, since there are no tables of experimental data.

1) Author; 2) heat-transport medium; 3) conditions for interaction of forced and free convection; 4) Watzinger and Jonson [2]; 5) water; 6) downward flow in vertical tube with cooling; 7) Petukhov [8]; 8) the same; 9) Petukhov and Nol'de [4]; 10) downward and upward flow in vertical tubes with heating and cooling. Flow in horizontal tube with heating and cooling; 11) Alad'yev, Mikheyev, and Fedynskiy [9]; 12) Martinelli, Southwell, et al. [6]; 13) water, mineral oils; 14) upward flow in vertical tubes with heating; 15) Kern and Othmer [10]; 16) mineral oils; 17) flow in horizontal tube with heating.

In this section, we analyze experimental data on mean heat transfer[12] obtained with constant wall temperature. Table 16-2 summarizes these data.

1. *Flow in vertical tubes when forced and free convections coincide at the wall*. This case has been more completely investi-

[12]/441

gated than the others. Figure 16-9 shows the results of heat-transfer measurements carried out by us in conjunction with L.D. Nol'de [4]. In determining $\overline{Nu}_g$, Pe_g d/l, and $(GrPr)_g$ we used the arithmetic mean temperature difference, while the physical parameters were taken for a temperature $t_g = (t_s + t_{zh})/2$, where t_{zh} is the arithmetic mean fluid temperature over the length. The dashed lines of Fig. 16-9 show asymptotes corresponding to Eq. (16-7); here we should replace ρ_{zh} and c_{pzh} by ρ_g and c_{pg}. For points lying on these lines, the fluid temperature at the tube exit equals the wall temperature. On both the upper and lower graphs we can isolate a region of laminar (viscous-gravitational) flow ($Re < Re_{kr}$), and transition and turbulent regions. In the first region, which has the greatest interest for us in this case, $\overline{Nu}_g$ increases with Pe_g d/l and $(GrPr)_g$. In the second region, $\overline{Nu}_g$ increases rapidly with Pe_g d/l. In the third region, as usual, $\overline{Nu}_g \sim Pe_g^{0.8}$, and is nearly independent of $(GrPr)_g$.[13] Comparing the upper and lower graphs, we can conclude that under the same conditions of forced- and free-convection interaction, the dependence of $\overline{Nu}_g$ on Pe_g d/l and on $(GrPr)_g$ remains the same for heating and cooling of the fluid. The only difference is that the absolute value of heat transfer is greater for heating than for cooling. This is caused by the variation in the viscosity and thermal-conductivity coefficients with temperature.
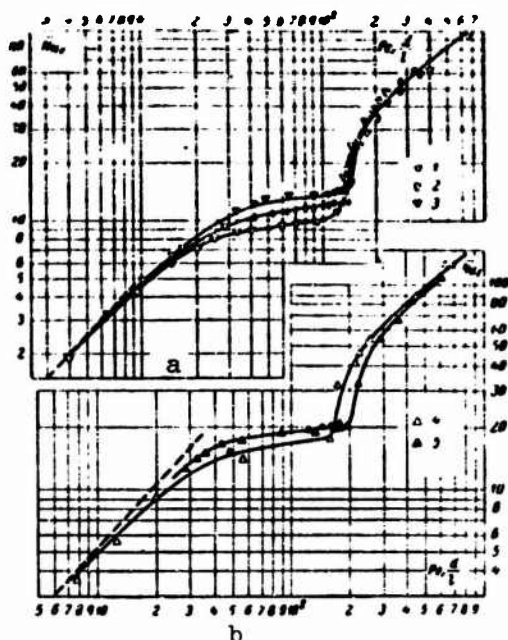

Fig. 16-9. Values of $\overline{Nu}_g$ in round vertical tube when forced and free convections coincide. a) Downward flow with cooling; b) upward flow with heating; 1, 2, 3) $(GrPr)_g \cdot 10^{-6} = 0.8-2.5$, $3-6$, $8.5-14.5$; 4, 5) $(GrPr)_g \cdot 10^{-6} = 6-11$, $12-16$.

Figure 16-10 shows the same experimental data as Fig. 16-9, but as a function of Re_{zh}. Here we see very clearly that the critical Reynolds number rises as GrPr increases. The relationship between Re_{kr} and GrPr, constructed from these data, has been given in §16-1 (see Fig. 16-4). The factors responsible for protraction of laminar flow with increasing GrPr are also explained there. The abrupt transition observed in this case through the critical Reynolds number is natural, since the appearance of turbulent mixing in the protracted laminar flow should produce a rapid rise in heat transfer.

When the forced and free convections coincide at the wall, the experimental data on heat exchange in vertical tubes can be generalized by means of an equation of the form[14]

$$\overline{Nu}_c = C\left(Pe_r \frac{d}{l}\right)^m \left(Gr\,Pr\,\frac{d}{l}\right)_r^r. \tag{16-8}$$

where

$$\overline{Nu}_c = \frac{\bar{a}d}{\lambda_c}; \quad \bar{a} = \frac{\bar{q}_c}{t_c - t_0}; \quad Pe_r = \frac{\bar{w}d}{a_r};$$

$$\left(Gr\,Pr\,\frac{d}{l}\right)_r = \frac{g\beta_r(t_c - t_m)\,d^4}{v_r a_r l};$$

$$t_m = \frac{1}{2}(t_0 + \bar{t}_l);$$

here t_0 and $\bar{t}_l$ are the mean mass temperatures of the fluid at the tube entrance and exit; $\bar{q}_s$ is the mean heat-flux density over the tube surface; C, m, n are constants.
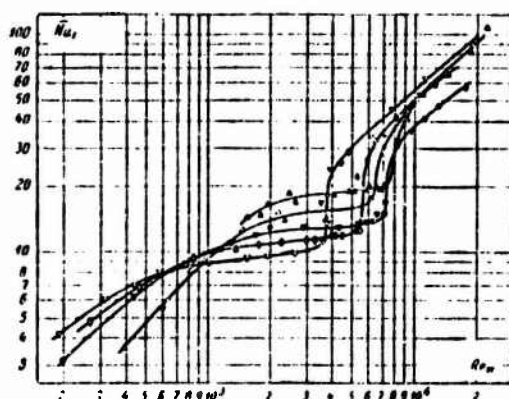
Fig. 16-10. Dependence of $\overline{Nu}_g$ as a function of Re_{zh} in a round vertical tube when the free and forced convections coincide. The symbols are the same as in Fig. 16-9.

Thus in (16-8), $\bar{a}$ refers to the initial temperature difference, while in the expression for Gr, we use the arithmetic mean temperature head. The physical parameters in $\overline{Nu}_s$ are chosen for temperature t_s, while in Pe_r and $\left(Gr\,Pr\frac{d}{l}\right)_r$ they are chosen at t_g; thus approximate al-

lowance can be made for the way in which their temperature dependence affects heat exchange.

In Fig. 16-11, the experimental data are presented in coordinates convenient for following the transition from viscous flow to viscous-gravitational flow.[13] For values $\left(Gr\,Pr\,\frac{d}{l}\right) < 10^4$, the exponent $n \approx 0$. Here $\overline{Nu}_c \left(Pe_r\,\frac{d}{l}\right)^{-1/3} \approx const$, i.e., we have viscous flow. When this numerical complex is large, the flow becomes viscous-gravitational. Here $n \approx 0.18$. In Fig. 16-12, the experimental data are represented as the relationship between $\overline{Nu}_c \left(Pe_r\,\frac{d}{l}\right)^{-1}$ and the numerical complex

$$Y = \left(Pe_r\,\frac{d}{l}\right)\left(Gr\,Pr\,\frac{d}{l}\right)^{\frac{n}{m-1}}.$$ This graph clearly shows the transition to to the asymptotic value of $\overline{Nu}_s$. In approximation, we can replace the transition region $(1 < Y < 2)$ by the point $Y = 1.5$.

The equation

$$\overline{Nu}_c = \frac{1}{4}\,Pe_r\,\frac{d}{l}$$

is defined for $Y < 1,5$ $n = 0$, $m = 1$ and the asymptotic value of $\overline{Nu}_s$.

When $Y > 1.5$, $n \approx 0.18$ and $m = 0.3$. Thus when the forced and free convections coincide at the wall, heat transfer is described by the equation

$$\overline{Nu}_c = 0.35\left(Pe_r\,\frac{d}{l}\right)^{0.3}\left(Gr\,Pr\,\frac{d}{l}\right)_r^{0.18}. \tag{16-9}$$

This equation is valid for values $20 < \frac{l}{d} < 130$, $Pe_r\,\frac{d}{l} < 1\,100$, $8 \cdot 10^3 \leq Gr_r Pr_r < 4 \cdot 10^6$ and $Re_m < Re_{kp}$; here Re_{kr} depends on $Gr_g Pr_g$ (see Fig. 16-4).

In (16-9), in order to go over to $\bar{\alpha}$ (or $\overline{Nu}_s$) referred to the arithmetic mean temperature head, we need only multiply the right side of the equation by $\dfrac{2}{1 + \frac{\Delta t_x}{\Delta t_u}}$, where $\Delta t_u = t_c - t_o$; $\Delta t_x = t_c - \bar{t}_l$.

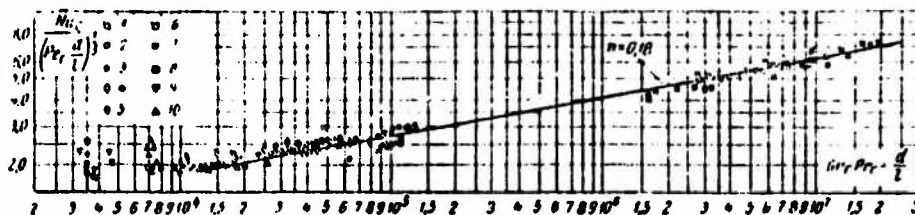Fig. 16-11. Dependence of $\overline{Nu}_s$ on $(Gr Pr\,d/l)_g$ in round vertical tube when free and forced convections coincide at wall. Symbols for experimental data:

a Обозначение	b Теплоноситель, направление теплового потока	$\frac{l}{d}$	$Gr_r Pr_r \cdot 10^{-4}$	c Источник
1	Вода, охлаждение d	131.3	8—64	[Л. 8]
2	То же C	131.3	8—144	[Л. 4]
3	Вода, нагрев f	131.3	70—109	[Л. 4]
4	Вода, охлаждение d	97	9—37	[Л. 9]
5	Вода, нагрев f	90	21—47	[Л. 9]
6	Вода, охлаждение d	70	329—3 650	[Л. 2]
7	Вода, нагрев f	125	56	[Л. 6]
8	Минеральное масло, нагрев g	126	13	[Л. 6]
9	То же e	672	19—28	[Л. 6]
10		297	21	[Л. 6]

a) Symbol; b) heat-transport medium, direction of heat flow; c) source; d) water, cooling; e) the same; f) water, heating; g) mineral-oil, heating.
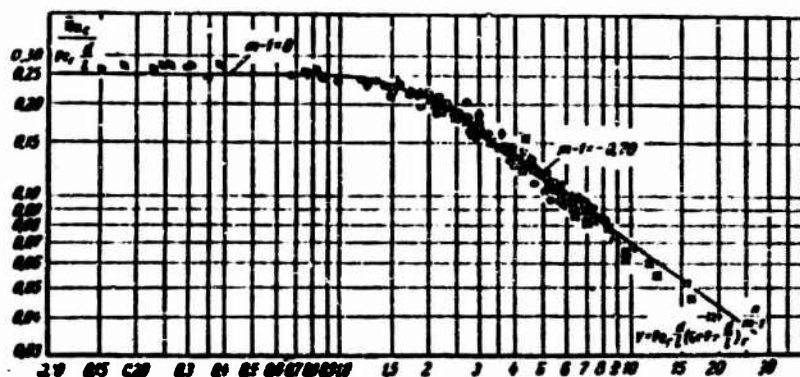
Fig. 16-12. Generalization of experimental data on heat exchange in vertical tubes when forced and free convections coincide at wall. Same symbols as in Fig. 16-11.

2. *Flow in horizontal tubes*. A few experimental data on heat exchange in horizontal tubes have been published in [4, 9, 10].[16] Figure 16-13 gives results for heat-transfer measurements for a water flow on the basis of data from [4] (the coordinates are the same as in Fig. 16-9). Here the region of viscous-gravitational flow ($Re_{zh} < Re_{kr} \approx 2300$) corresponds to values $Pe_g \, d/l \le 90$ and thus is relatively narrow. The reason is that the experiments were carried out with water, i.e., for small values of Pr_g. With viscous fluids, for which Pr is much greater, this region may extend to far larger values of $Pe_g \, d/l$. When $Pe_g \, d/l$ is small, as we can see from the graph, $\overline{Nu}_g$ is close to the asymptotic value, while when $Pe_g \, d/l$ ranges from 30 to 90, the value varies approximately in proportion to $\left(Pe_r\frac{d}{l}\right)^{0.4}$, and also depends on $Gr_g Pr_g$. This relationship between $\overline{Nu}_g$ and $Pe_g \, d/l$ is evidently not universal. Thus experiments with viscous fluids [10], covering a wider region of $Pe_g \, d/l$, and a region further from the asymptote, have shown that $\overline{Nu}_g$ is roughly proportional to $\left(Pe_r\frac{d}{l}\right)^{1/3}$.

16/441
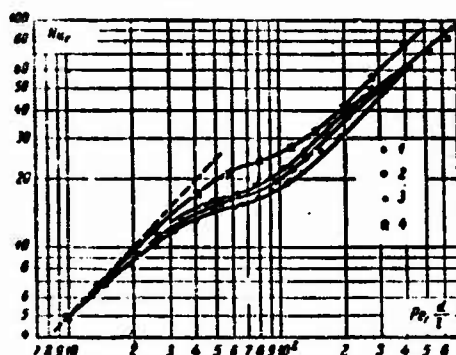
Fig. 16-13. Values of $\overline{Nu}_g$ in horizontal tube with heating and cooling of water. 1, 2, 3) Cooling of fluid with $(GrPr)_g = 0.8-2) \cdot 10^6$, $(2.5-4.5) \cdot 10^6$, $(5-9) \cdot 10^6$; 4) heating with $(GrPr)_g = (11-13) \cdot 10^6$.
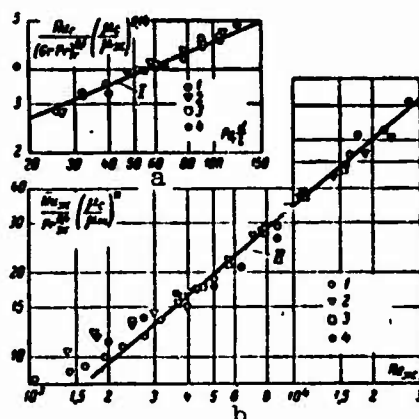
Fig. 16-14. Generalized experimental data for heat exchange in horizontal tube. a) Viscous-gravitational flow ($Re_{zh} < 3000-3500$); b) turbulent flow; I) Eq. (16-10); II) Eq. (16-11); 1, 2, 3) Cooling of fluid at $(GrPr)_g = (1-2.3) \cdot 10^6$, $(2.7-4.9) \cdot 10^6$, $(5.5-8.3) \cdot 10^6$; 4) heating of fluid at $(GrPr)_g = (7.3-13) \cdot 10^6$.

Since the transverse circulation is superposed on the fluid motion near the axis (see §16-1), heat transfer is greater for viscous-gravitational flow in horizontal tubes than in vertical tubes when the forced and free convections coincide at the wall. For this reason, upon transition through the critical Reynolds number, the heat transfer does not rise abruptly, as in the preceding case, but gradually. Since when $Re < Re_{kr}$, there will be a certain amount of mixing owing to free convection, the additional turbulent mixing appearing when $Re \geq Re_{kr}$ will only result in a gradual rise in heat transfer.

We still do not have sufficient experimental data to obtain sufficiently general relationships for heat transfer in horizontal tubes. Nonetheless, the available data can be used to obtain some

useful expressions. Thus, for example, the experimental data of Fig. 16-13 and the corresponding regions of viscous-gravitational flow can be generalized with the aid of the equation

$$\overline{Nu}_r = 0.8 \left(Pe\,\frac{d}{l}\right)_r^{0.4} (Gr\,Pr)_r^{0.1} \left(\frac{\mu_c}{\mu_{\text{ж}}}\right)^{-0.14}. \tag{16-10}$$

Here the heat-transfer coefficient refers to the arithmetic mean temperature head, and all physical properties other than the viscosity were selected for a temperature $t_r = \frac{1}{2}(t_c + t_{\text{ж}})$. The values of the viscosity coefficients μ_s and μ_{zh} correspond to temperatures t_c and $t_{\text{ж}} = \frac{t_c + \bar{t}_l}{2}$. The equation is valid for values $Re_{\text{ж}} < 3000-3500$; $\left(Pe_r\,\frac{d}{l}\right)_{\text{ас}} < Pe_r\,\frac{d}{l} < 120;\ 10^4 < (Gr\,Pr)_r \leqslant 13 \cdot 10^4$ and $2 \leqslant Pr_r \leqslant 10$. Here $\left(Pe_r\,\frac{d}{l}\right)_{\text{ас}}$ is the asymptotic value of $Pe_g\,d/l$. Equation (16-10) is compared with the experimental data in Fig. 16-4a.
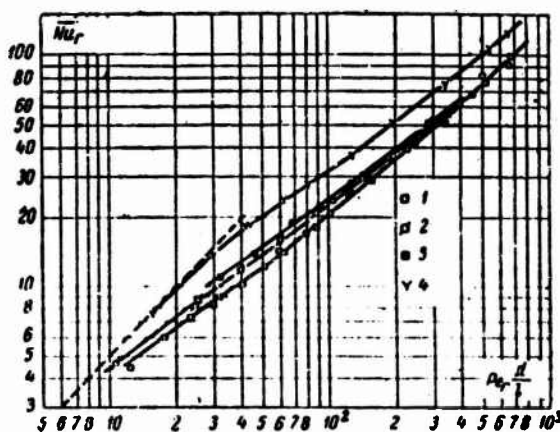
Fig. 16-15. Values of $\overline{Nu}_g$ in round vertical tube with forced and free convections opposite in direction at the wall. 1, 2, 3) Cooling with $(GrPr)_g = (1.5-2.5) \cdot 10^6$, $(3-4.5) \cdot 10^6$, and $(5-8) \cdot 10^6$; 4) heating with $(GrPr)_g = (7.5-11.5) \cdot 10^6$.

For values $Re_{zh} > 3000-3500$, the experimental data given in Fig. 16-13 correspond to a relationship characteristic of turbulent flow:

$$Nu_{\text{ж}} = 0.022\,Re_{\text{ж}}^{0.8} Pr_{\text{ж}}^{0.4} \left(\frac{\mu_c}{\mu_{\text{ж}}}\right)^{-n}, \tag{16-11}$$

where $n = 0.11$ for heating of the fluid and $n = 0.25$ for cooling. This is obvious from Fig. 16-14b, which shows a treatment of these experimental data in accordance with Eq. (16-11). In this case, therefore, i.e., for $Re_{zh} > 3000$ and $(GrPr)_g < 13 \cdot 10^6$, the heat transfer is nearly independent of $(GrPr)_g$ (more accurately, of

Gr_g).

Eubank and Proctor, using experimental data from [10] and certain other data on heat exchange in horizontal tubes with viscous-gravitational flow of mineral oils, have proposed an empirical equation resembling (16-5):

$$\overline{Nu}_{zh} = 1.615 \left(\frac{\mu_c}{\mu_{zh}}\right)^{-0.14} \sqrt[3]{Pe_{zh}\frac{d}{l} + 0.051\left(Gr\,Pr\frac{d}{l}\right)^{3/4}_{zh}}, \qquad (16\text{-}12)$$

in which $\overline{Nu}_{zh}$ and Gr_{zh} are computed from the mean arithmetic temperature head, while the physical properties are chosen at $t_{zh} = \frac{t_0 + \overline{t}_l}{2}$.

The maximum deviation of the experimental data from Eq. (16-12) is 30%. The equation encompasses the region of values of $(GrPr)_g$ between $3.5 \cdot 10^5$ and $8.6 \cdot 10^8$, for Pr_{zh} from 140 to 15,200; it holds for values of Pe_{zh} d/l lying to the right of the asymptote.
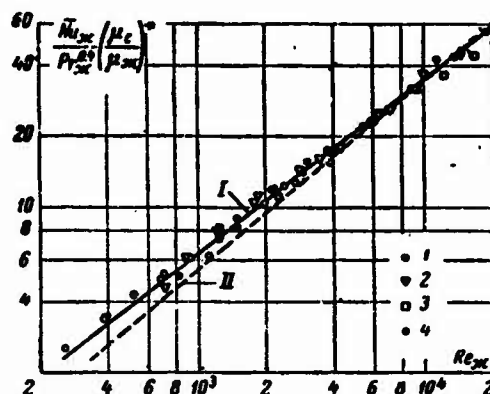
Fig. 16-16. Generalization of experimental data on heat exchange in vertical tube with forced and free convections having opposite directions at wall. 1, 2, 3) Cooling of fluid for values $(GrPr)_g$ = $= (1\text{-}2.2) \cdot 10^6$, $(2.5\text{-}5) \cdot 10^6$, $(5.2\text{-}9) \cdot 10^6$; 4) heating of fluid at $(GrPr)_g = (6\text{-}12) \cdot 10^6$; I) Eq. (16-13); II) Eq. (16-11).

3. *Flow in vertical tubes with forced and free convections having opposite directions at the wall.* Figure 16-15 shows experimental data on heat transfer for water moving upward in a vertical tube with cooling and downward with heating; the data were obtained in [4].[18]

The slopes of the curves are nearly constant and identical, corresponding to an exponent of 0.8 for Pe (or Re); no critical region associated with a change in the form of motion was detected. It is still more noteworthy that Re_{zh} varies between 250 and $2 \cdot 10^4$, Gr_c between 10 and $5 \cdot 10^6$, and $(GrPr)_g$ between $1.5 \cdot 10^6$ and $12 \cdot 10^6$. Processing of these same data in the coordinates usually employed for turbulent flow (Fig. 16-16) shows that they are satisfactorily described by the equation

$$\overline{Nu}_{m} = 0.037\, Re_{m}^{0.75}Pr_{m}^{0.4}\left(\frac{\mu_c}{\mu_m}\right)^{-n}.\qquad (16\text{-}13)$$

wh•re $n = 0.11$ for heating and 0.25 for cooling of the fluid. As in (16-11), the heat-transfer coefficient in (16-13) refers to the arithmetic mean temperature head.

Equation (16-13), shown by the solid line in Fig. 16-16, does not contain Gr, and has the structure characteristic of turbulent flow. It also yields quantitative results close to those of Eq. (16-11), for heat transfer in turbulent flow (dashed line of Fig. 16-16). This is not difficult to understand in the light of what we have said in §16-1 about the characteristics of fluid flow when the forced and free convections have opposite direction at the wall. Here, the free convection produces such intense mixing in the flow that even at $Re_{zh} > 250$, the flow is governed by the laws of turbulent motion. The fact that according to (16-13), Nu is independent of Gr is evidently associated with the narrow range of variation in the latter. When Gr is sufficiently small, the dependence of Nu on Pe d/l should approach the relationship characteristic of viscous flow. On the other hand, when Gr varies within broader limits, the heat transfer in the turbulent region will probably also depend on Gr. We still do not have data available with which to set up a more complete and exact picture of these complex processes.

4. Figure 16-17 compares the relationships for heat transfer when the directions of the forced and free convections at the wall coincide (curve 1), are mutually perpendicular (curve 2), and are opposed (curve 3). All curves correspond to the fluid-cooling case, and to roughly the same value of GrPr. As we can see from the graph, there is a substantial difference in the nature of the relationships and the absolute heat-transfer values.
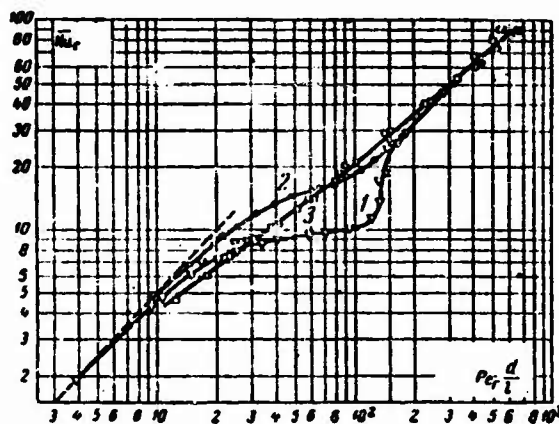
Fig. 16-17. Heat transfer under various conditions of forced- and free-convection interaction. 1) Downward flow in vertical tube with cooling; $(GrPr)_g = (0.8\text{-}2.5)\cdot 10^6$; 2) flow in horizontal tube with cooling; $(GrPr)_g = (0.8\text{-}2)\cdot 10^6$; 3) upward flow in vertical tube with cooling, $(GrPr)_g = (1.3\text{-}2.5)\cdot 10^6$.
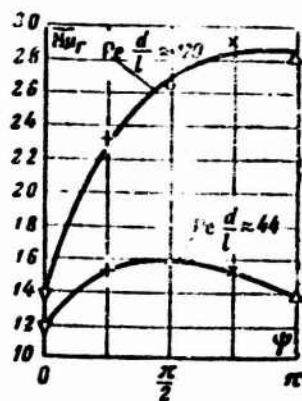
Fig. 16-18. Heat transfer as function of tube inclination angle ψ, $(GrPr)_g \approx 8 \cdot 10^6$.
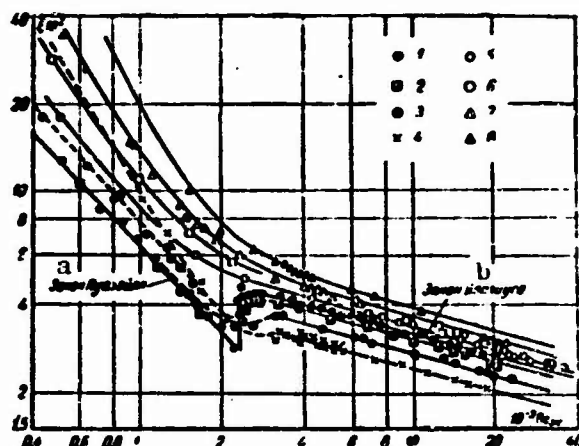
Fig. 16-19. Resistance coefficient for nonisothermal flow of water in horizontal tube, experiments of M.A. Mikheyev. 1) Isothermal motion ($\Delta t = 0$); 2, 3, 4) heating at $\Delta t = 4$-$10°C$, 15-$25°C$, 25-$40°C$, respectively; 5, 6, 7, 8) cooling at $\Delta t = 5$-$13°C$, 13-$17°C$, 18-$30°C$, 30-$35°C$. a) Poiseuille law; b) Blasius law.

Figure 16-18 shows the results of certain heat-transfer measurements for various angles of tube inclination (the angle ψ is assumed to equal zero when the forced and free convections coincide). As we can see, there is a very significant relationship between $\overline{Nu}_g$ and ψ, and it is not the same for different values of $Pe_g\, d/l$.

5. There are very few experimental data on hydraulic resistance when forced and free convection act simultaneously. Figure 16-19 shows experimental data of M.A. Mikheyev, and Fig. 16-20 the data of the author and L.D. Nol'de,[19] obtained for water flowing in horizontal tubes with approximately constant wall temperature. If GrPr (or Δt) are not too small, the resistance coefficient decreases monotonically during the transition from laminar to turbulent flow, and no jumps are observed. This, na-

- 414 -

turally is associated with the presence of transverse circulation, which mixes the flow (see §16-1, as well as §16-3, paragraph 2). The difference in the resistance-coefficient values as compared with an isothermal flow is caused not only by the influence of free convection, but also by the temperature dependence of the viscosity. In the laminar region, free convection evidently exerts the dominant influence. Thus ξ is greater here for both heating and cooling of the fluid than for isothermal flow.[20]. In the turbulent region, the temperature dependence of the viscosity has the principal influence, so that the resistance coefficient is greater for cooling of the fluid and less for heating than in isothermal flow.
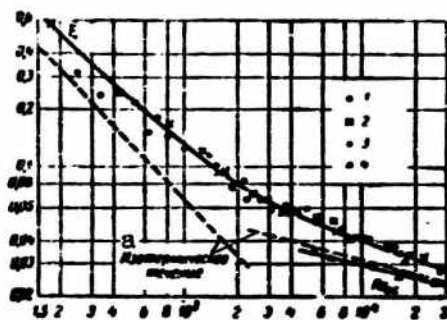
Fig. 16-20. Resistance coefficient for flow in horizontal tube. 1, 2, 3) Fluid cooling for values $(GrPr)_{zh} = (2-4)\cdot10^6$, $(5-9)\cdot10^6$, $(10-16)\cdot10^6$; 4) heating of fluid for $(GrPr)_{zh} = (6-9\cdot10^6$. a) Isothermal flow.
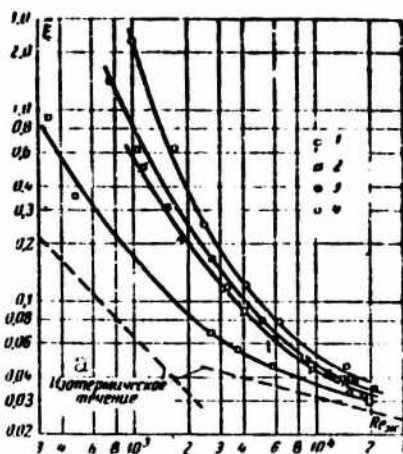
Fig. 16-21. Resistance coefficient in vertical tube with free and forced components opposite in direction at wall. 1, 2, 3) Upward flow with cooling $(GrPr)_{zh} = (2-4)\cdot10^6$, $(6-9)\cdot10^6$, $(12-16)\cdot10^6$; 4) downward flow with heating, $(GrPr)_{zh} = (5-9)\cdot10^6$. a) Isothermal flow.

For $Re_{zh} < 2300$, the experimental data on resistance in horizontal tubes, shown in Figs. 16-9 and 16-20, are satisfactorily described by the equation proposed by M.A. Mikheyev [13]:

20/441

$$\bar{\xi} = \frac{64}{Re_{_{\textbf{ж}}}} \left(\frac{Pr_{c}}{Pr_{_{\textbf{ж}}}}\right)^{1/3} \left[1 + 0.22\left(\frac{Gr\,Pr}{Re}\right)_{_{\textbf{ж}}}^{0.15}\right]. \qquad (16\text{-}14)$$

This equation is valid for $(Gr\,Pr)_{_{\textbf{ж}}} < 15 \cdot 10^{6}$. The ratio $\frac{Pr_{c}}{Pr_{_{\textbf{ж}}}} \approx \frac{\mu_{c}}{\mu_{_{\textbf{ж}}}}$ allows for the influence of the variable viscosity on $\bar{\xi}$.

Figure 16-21 shows the results of resistance measurements for water flowing in a vertical tube with opposite directions of the free and forced convections at the wall. The resistance coefficient rises sharply as Re_{zh} decreases, and depends substantially on $Gr\,Pr$. Here $\bar{\xi}$ may have ten times the values corresponding to isothermal flow. This sort of relationship is explained by the fact that here even at small Re_{zh} (about 250 or more), the flow becomes turbulent under the influence of free convection (see §16-1, and §16-3, paragraph 3).

When the forced and free convections coincide at the wall, the resistance coefficient in vertical tubes will be significantly lower than for horizontal tubes; this is even truer for vertical tubes with oppositely directed forced and free convections. Moreover, in this case there will be an abrupt increase in $\bar{\xi}$, as for $\overline{Nu}$, during the transition through Re_{kr}. The data available on resistance in vertical tubes is still inadequate to permit generalized relationships to be obtained.

16-4. FLOW AND HEAT EXCHANGE IN ROUND VERTICAL TUBE FAR FROM ENTRANCE UNDER BOUNDARY CONDITIONS OF THE SECOND KIND WITH AND WITHOUT HEAT SOURCES IN THE FLOW

An exact solution has been obtained for this problem, so that it presents special interest. The solution was first given by G.A. Ostroumov [1, 14] (in the absence of heat sources), and was later generalized by Hallman [15] to the case of internal heat sources distributed uniformly in the flow.[21]

Fig. 16-22. Problem of flow and heat exchange in round tube with combined action of forced and free convection.

Thus fluid flow and heat exchange is considered in a vertical tube for constant heat-flux density at the wall and unfirom heat release in the flow owing to the internal sources. The physical properties of the fluid, other than the density, are assumed to be constant. The variation in density as a function of temperature is assumed to be linear, and enters only into the term in the equation of motion that represents the lift force. Here, therefore, the fluid motion results from interaction of free and forced convection. Here the velocity and temperature profiles will be axisymmetric.

We shall only consider the flow at a sufficient distance from the entrance, i.e., in the region with incipient thermal and hydrodynamic flow stabilization. Within this region, the velocity and temperature profiles (measured from the wall temperature) will not vary with the length, nor will they vary with azimuth, in virtue of the axial symmetry, i.e., $w_x = w_x(r)$, $w_r = w_\varphi = 0$, $t - t_c = \vartheta(r)$. Moreover, at each point in the flow, including the wall, the longitudinal temperature gradient will be constant:

$$\frac{\partial t}{\partial x} = \frac{2q_r + q_v r_0}{\rho c_p \bar{w} r_0} = A = \text{const},\tag{16-15}$$

which follows from the constant heat-flux density at the wall q_S and the constant power of the internal heat sources q_v.

As a result, the initial equations can be simplified substantially. In the coordinate system shown in Fig. 16-22, the equations describing flow and heat exchange under the foregoing conditions will look like this:

$$w_x \frac{\partial t}{\partial x} = a\left(\frac{\partial^2 t}{\partial r^2} + \frac{1}{r} \cdot \frac{\partial t}{\partial r}\right) + \frac{q_v}{\rho c_p},\tag{16-16}$$

$$-\rho g - \frac{\partial p}{\partial x} + \mu\left(\frac{\partial^2 w_x}{\partial r^2} + \frac{1}{r} \cdot \frac{\partial w_x}{\partial r}\right) = 0,\tag{16-17}$$

$$\frac{\partial p}{\partial r} = 0,\tag{16-18}$$

$$\rho = \rho_c\left[1 - \beta_\rho(t - t_c)\right],\tag{16-19}$$

where β_ρ and ρ_S are the coefficient of volume expansion and the fluid density at the wall temperature (they are constants).[22]

Using (16-15), (16-18) and (16-19), we can reduce (16-16) and (16-17) to the form

$$\frac{d^2\vartheta}{dr^2} + \frac{1}{r} \cdot \frac{d\vartheta}{dr} = \frac{A}{a} w_x - \frac{q_v}{\lambda},\tag{16-20}$$

$$\beta_\rho g \vartheta - \frac{1}{\rho_c} \cdot \left(\frac{dp}{dx} + \rho_c g\right) + \nu\left(\frac{d^2 w_x}{dr^2} + \frac{1}{r} \cdot \frac{dw_x}{dr}\right) = 0,\tag{16-21}$$

where $\vartheta = t - t_c$; $\nu = \frac{\mu}{\rho_c}$.

Thus the problem is reduced to solution of these equations under the following boundary conditions:

$$\text{for } r = r_0, \ \vartheta = 0 \text{ and } \omega_x = 0,$$
$$\text{for } r = 0, \frac{d\vartheta}{dr} = 0 \text{ and } \frac{d\omega_x}{dr} = 0. \Bigg\} \tag{16-22}$$

For convenience in subsequent computation, we write (16-20) and (16-21) in dimensionless form:

$$\frac{d^2\theta}{dR^2} + \frac{1}{R} \cdot \frac{d\theta}{dR} = 4(KW_x - 1); \tag{16-23}$$

$$\frac{Ra}{4K}\theta + \frac{d^2W_x}{dR^2} + \frac{1}{R} \cdot \frac{dW_x}{dR} = -8P. \tag{16-24}$$

Here we let

$$R = \frac{r}{r_0}; \ \theta = \frac{16\lambda\vartheta}{q_0 d^2}; \ W_x = \frac{w_x}{\bar{w}}; \ K = \frac{\rho c_p \bar{w} A}{q_0} = \frac{2q_c}{q_0 r_0} + 1;$$

$$Ra = \frac{g\beta_r d^4 A}{16\nu a} = \frac{g\beta_r d^4 A}{16\nu^2} \cdot \frac{\nu}{a} = Gr \, Pr$$

is the Rayleigh number (the temperature difference $\Delta t = Ad/2$ is used to compute Ra and Gr);

$$P = -\frac{d^2}{32\mu\bar{w}}\left(\frac{dp}{dx} + \rho_c g\right).$$

Since P does not depend on R, differentiating (16-24) twice with respect to R and combining the results, we obtain

$$\frac{Ra}{4K}\left(\frac{d^2\theta}{dR^2} + \frac{1}{R} \cdot \frac{d\theta}{dR}\right) + \frac{d^4W_x}{dR^4} + \frac{2}{R} \cdot \frac{d^3W_x}{dR^3} - \frac{1}{R^2} \cdot \frac{d^2W_x}{dR^2} + \frac{1}{R^3} \cdot \frac{dW_x}{dR} = 0.$$

Substituting (16-23) into this equation and going from the variable R to the new variable $Z = \sqrt{Ra}\,R$, we obtain

$$\frac{d^4W_x}{dZ^4} + \frac{2}{Z} \cdot \frac{d^3W_x}{dZ^3} - \frac{1}{Z^2} \cdot \frac{d^2W_x}{dZ^2} + \frac{1}{Z^3} \cdot \frac{dW_x}{dZ} \pm \left(W_x - \frac{1}{K}\right) = 0. \tag{16-25}$$

We can distinguish two cases in our problem:

1) positive longitudinal temperature gradient, i.e., $\frac{\partial t}{\partial x} > 0$;

2) negative longitudinal temperature gradient, i.e., $\frac{\partial t}{\partial x} < 0$.

If the absolute value of the temperature gradient is used in the expression for Ra (so that Ra will always be positive), the first case will correspond to a plus sign on the last term of (16-25), and the second case to a minus sign.

The linear inhomogeneous fourth-order equation (16-25) can be solved in Bessel functions.

Solving Eq. (16-25) and determining the velocity field, we can then use Eq. (16-23) to determine the temperature field.[23]

1. *Case in which* $\frac{\partial t}{\partial x} \geqslant 0$. Here the general solution of (16-25) has the form

$$W_x = c_1 J_0(\sqrt{i}\,Z) + c_2 Y_0(\sqrt{i}\,Z) + c_3 I_0(\sqrt{i}\,Z) + c_4 K_0(\sqrt{i}\,Z).$$

where

$$J_0(x), \ Y_0(x), \ I_0(x) \ \text{and} \ K_0(x)$$

are zero-order Bessel functions of the ordinary and modified first and seconds kinds; c_1, c_2, c_3, and c_4 are constants.

Here, however, from the computational viewpoint it is more convenient to use the Kelvin functions $\text{ber}(x)$, $\text{bei}(x)$, $\text{ker}(x)$ and $\text{kei}(x)$, which are associated with the Bessel functions by familiar relationships.[24] These are functions of a real argument, and are themselves real numbers. Like the Bessel function, they have been tabulated.

The general solution of (16-25) in Kelvin functions is written as

$$w_x = C_1 \text{ber}(Z) + C_2 \text{bei}(Z) + C_3 \text{ker}(Z) + C_4 \text{kei}(Z). \tag{16-26}$$

The constants C_1, C_2, C_3, and C_4 differ from the constants in the preceding equation, although they are related to them.

Using (16-24), we can represent the boundary conditions (16-22) in the form

$$\left. \begin{array}{l} \text{for } R = 1, \ W_x = 0 \ \text{and} \ \dfrac{d^2 W_x}{dR^2} + \dfrac{1}{R} \cdot \dfrac{dW_x}{dR} = -8P; \\[3mm] \text{for } R = 0, \ \dfrac{dW_x}{dR} = 0 \ \text{and} \ \dfrac{d}{dR}\left(\dfrac{d^2 W_x}{dR^2} + \dfrac{1}{R} \cdot \dfrac{dW_x}{dR} \right) = 0. \end{array} \right\} \tag{16-27}$$

Determining the constants from the boundary conditions and using the selfevident relationship $2 \int_0^1 W_x R \, dR = 1$, we obtain an equation for the velocity field:

$$W_x = \frac{w_x}{\bar{w}} = \frac{\omega}{2}\left[\frac{\text{ber}(Z)\,\text{bei}(\omega) - \text{ber}(\omega)\,\text{bei}(Z)}{\text{ber}(\omega)\,\text{ber}'(\omega) + \text{bei}(\omega)\,\text{bei}'(\omega)} \right] +$$
$$+ \frac{1}{K}\left\{ 1 - \frac{\left[\text{ber}'(\omega) + \frac{\omega}{2}\text{bei}(\omega)\right]\text{ber}(Z) + \left[\text{bei}'(\omega) - \frac{\omega}{2}\text{ber}(\omega)\right]\text{bei}(Z)}{\text{ber}(\omega)\,\text{ber}'(\omega) + \text{bei}(\omega)\,\text{bei}'(\omega)} \right\}. \tag{16-28}$$

where $\omega = \sqrt{K}$ equals Z when $R = 1$; $\text{ber}'(\omega)$ and $\text{bei}'(\omega)$ are the derivatives of $\text{ber}(Z)$ and $\text{bei}(Z)$ with respect to Z when $Z = \omega$ (i.e., when $R = 1$).

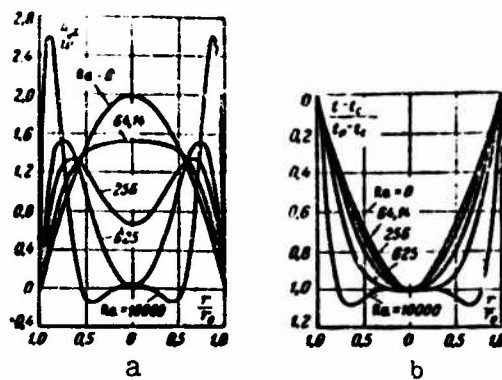Knowing the velocity distribution, we can use (16-23) to find the temperature distribution:

Fig. 16-23. Radial distributions of velocity (a) and temperature (b) when there are no internal heat sources in flow ($K = \infty$), for case in which $\frac{\partial t}{\partial x} > 0$.
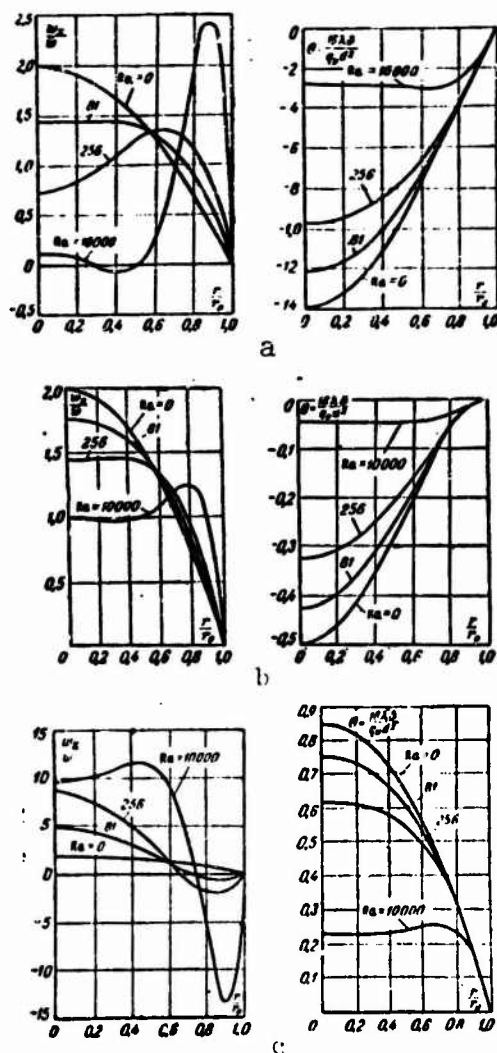

Fig. 16-24. Radial distributions of velocity and temperature for case in which $\frac{\partial t}{\partial x} > 0$. a) $K = 10$; b) $K = 1$; c) $K = 0.1$.

$$\theta = \frac{16\lambda\theta}{q_v d^2} = \frac{2K}{\omega} \left\{ \frac{[\text{ber}(Z)\,\text{ber}(\omega) + \text{bei}(Z)\,\text{bei}(\omega)] - [\text{ber}^2(\omega) + \text{bei}^2(\omega)]}{\text{ber}(\omega)\,\text{ber}'(\omega) + \text{bei}(\omega)\,\text{bei}'(\omega)} \right\} +$$

$$+ \frac{2}{\omega^2} \left[\frac{2\left\{\left[\text{bei}'(\omega) - \frac{\omega}{2}\text{ber}(\omega)\right]\text{ber}(Z) - \left[\text{ber}'(\omega) + \frac{\omega}{2}\text{bei}(\omega)\right]\text{bei}(Z)\right\} + B(\omega)}{\text{ber}(\omega)\,\text{ber}'(\omega) + \text{bei}(\omega)\,\text{bei}'(\omega)} \right]. \quad (16\text{-}29)$$

where

$$B(\omega) = \omega\,[\text{ber}^2(\omega) + \text{bei}^2(\omega)] - 2\,[\text{ber}(\omega)\,\text{bei}'(\omega) - \text{bei}(\omega)\,\text{ber}'(\omega)].$$

Let us analyze Eqs. (16-28) and (16-29) from the viewpoint of their dependence on the dimensionless parameter

$$K = \frac{\rho c_p \bar{w} A}{q_v} = \frac{q_c 2\pi r_0 + q_v \pi r_0^2}{q_v \pi r_0^2}.$$

The numerator of this expression equals the amount of heat supplied to the fluid through the wall and by the action of the internal sources (this same amount of heat is removed by convection along the axis), while the denominator equals the amount of heat transmitted to the fluid by the internal sources alone.

When $K \to \pm\infty$, there are no internal sources ($q_v = 0$), and all heat is delivered or removed through the wall. Here, as we can see without difficulty, the second terms in (16-28) and (16-29) should be omitted. In particular, (16-29) takes the form

$$\theta_* = \frac{\theta\lambda}{q_c d} =$$

$$= \frac{1}{2\omega} \left\{ \frac{[\text{ber}(Z)\,\text{ber}(\omega) + \text{bei}(Z)\,\text{bei}(\omega)] - [\text{ber}^2(\omega) + \text{bei}^2(\omega)]}{\text{ber}(\omega)\,\text{ber}'(\omega) + \text{bei}(\omega)\,\text{bei}'(\omega)} \right\}. \quad (16\text{-}30)$$

Figure 16-23 shows the velocity and temperature profiles when there are no internal heat sources in the flow (here t_0 is the temperature on the tube axis).[25] Since heat is supplied only through the wall, when Ra is sufficiently large, the principal change in the temperature and, consequently, the principal increase in velocity (as Ra becomes larger) will occur in the region near the wall. The velocity in the flow core decreases as Ra increases. In the Ra range between 0 and 64.14, the velocity profile becomes convex. When Ra > 64.14, a concavity appears near the axis; its further development leads to a change in the direction of flow in the core (for Ra = 630).

When $1 < K < \infty$, heat is supplied to the fluid both by the internal sources and through the wall. Figure 16-24a shows the velocity and temperature profiles for $K = 10$. They differ little from the profiles shown in Fig. 16-23, since the fraction of heat delivered to the fluid by the internal sources is not large $\left(\frac{q_c 2\pi r_0}{q_v \pi r_0^2} = 9\right)$.

When $K = 1$, heat is delivered to the fluid solely by the internal sources (Fig. 16-24b), so that the heat-flux density and the temperature gradient at the wall will equal zero (the wall is heat-insulated). For the same values of Ra, we find far less radial

variation in the temperature and velocity than for the preceding case.

When $0 < K < 1$, heat is supplied to the fluid by the internal sources and removed through the wall. Figure 16-24c shows the velocity and temperature profiles for $K = 0.1$. The temperature gradient at the wall is negative in this case, so that as Ra increases, the fluid velocity decreases near the wall but rises in the flow core. At a certain relatively small value of Ra, the fluid velocity near the wall changes sign, and the flow in the layer near the wall becomes opposite in direction to the flow in the core.
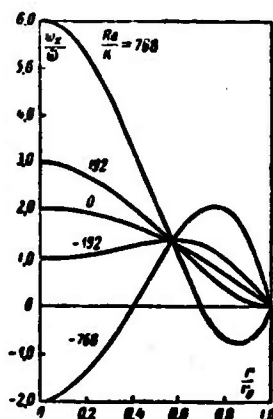
Fig. 16-25. Radial velocity distribution in tube with $K =$
$= 0$ $\left(\frac{\partial t}{\partial x} = 0, t_e = \text{const}\right)$.
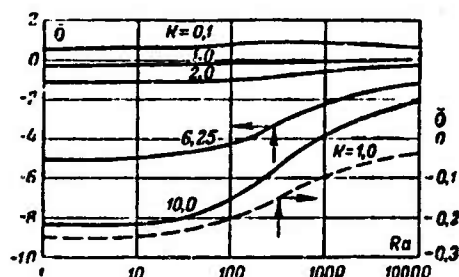
Fig. 16-26. Dimensionless difference between mean mass temperature of fluid and wall temperature as function of Ra.

When $K = 0$, the amount of heat delivered by the sources equals the amount removed through the wall. Here the fluid and wall temperatures will not vary with the length $\left(A = \frac{\partial t}{\partial x} = 0, t_s = \text{const}\right)$. Integrating Eq. (16-23) twice for $K = 0$, we obtain the temperature distribution

$$\theta = \frac{16\lambda\vartheta}{q_v d^2} = 1 - R^2. \tag{16-31}$$

- 422 -

Substituting this value of Θ into (16-24), and integrating, we find the velocity distribution:

$$W_x = \frac{w_x}{\bar{w}} = 2(1-R^2) - \frac{1}{4} \cdot \frac{Ra}{K} \left(\frac{1}{12} R^2 - \frac{1}{16} R^4 - \frac{1}{48} \right),$$ (16-32)

where

$$\frac{Ra}{K} = \frac{g\beta_p d^4 q_v}{16\lambda v \bar{w}}.$$

Figure 16-25 shows the velocity profiles for $K = 0$ and various values of Ra/K.[26]

Naturally, we should remember that not all of the flow cases predicted by the theory will be stable or capable of existing under actual conditions. Thus, for example, it is improbable that the flow will be stable for $K = 0.1$ and large Ra (Fig. 16-24c), or when $K \to 0$ and Ra/K is large.

Let us now determine the difference between the mean mass temperature of the fluid and the wall temperature $\bar{\vartheta} = \bar{t} - t_s$. Going over to dimensionless variables, we obtain

$$\bar{\theta} = \frac{16\lambda\bar{\vartheta}}{q_v d^2} = 2 \int_0^1 \theta W_x R\, dR.$$

Substituting the value of Θ and W_x from (16-28) and (16-29) into this expression, we find

$$\bar{\theta} = -\frac{64}{\omega^4} P + \frac{1}{\omega^4} \left(\frac{1}{K} - \frac{64K}{\omega^4} P^2 \right) \left[\frac{2\omega^2}{F^2}(D^2 - E^2) + \frac{8\omega D}{F} \right] + \\ + \frac{64}{\omega^4} \cdot \frac{PE}{F} \left(\frac{D}{F} + \frac{2}{\omega} \right),$$ (16-33)

where

$$P = \frac{\omega^2}{16D} \left[\omega F + \frac{1}{K}(2E - \omega F) \right];$$ (16-34)

$$D = \text{ber}(\omega)\,\text{ber}'(\omega) + \text{bei}(\omega)\,\text{bei}'(\omega);$$
$$E = \text{ber}(\omega)\,\text{bei}'(\omega) - \text{bei}(\omega)\,\text{ber}'(\omega);$$
$$F = \text{ber}^2(\omega) + \text{bei}^2(\omega).$$

Figure 16-26[27] shows $\bar{\theta}$ as a function of Ra for values of K from 0.1 to 10. The curves show that in most cases $\bar{\theta}$ increases as Ra becomes larger. Consequently, for a given value of $\bar{t}$, the wall temperature t_s will decrease. For Ra = 0 and 10^4, $\bar{\theta}$ will equal zero at $K = 0.73$ and 0.93, respectively.

When there are no internal heat sources in the flow ($1/K = 0$), Eq. (16-33) will take the following form, if we divide it by $4K$:

$$\bar{\theta}_* = \frac{\lambda\bar{\vartheta}}{q_c d} = -\frac{3}{\omega^4} P^2 \left(\frac{D^2 - E^2}{F^2} + \frac{4D}{\omega F} \right),$$ (16-35)

where for our case

$$P = \frac{\omega \, \Gamma}{16 D}.$$ (16-36)

The remaining notation is the same as for (16-33).

Since by the very formulation of the problem, the mean mass temperature $\bar{t}$ of the fluid is specified while the wall temperature t_s is unknown, Eq. (16-33) and (16-35) must be treated as expressions for the wall temperature. They also permit us to determine the limiting Nusselt number

$$Nu_\infty = \frac{\alpha_\infty d}{\lambda} = -\frac{q_c d}{\theta \lambda}.$$

In the absence of internal heat sources[20]

$$Nu_\infty = -\frac{1}{\theta_\bullet} = \frac{\omega^\bullet F^2}{32 P^2 \left(D^2 - E^2 + \frac{4}{\omega} DF \right)}.$$ (16-37)

The relationship between Nu_∞ and Ra in accordance with (16-37) is given in Fig. 16-27 (upper curve). As Ra increases, so does Nu_∞, while when Ra $\to 0$, it approaches a constant value characteristic of pure forced convection ($Nu_\infty \approx 4.36$). For $10^2 \leqslant Ra \leqslant 10^7$, this relationship can be represented by the simple interpolation equation [15]

$$Nu_\infty = 1.45 Ra^{0.27}.$$ (16-38)

The same figure shows the experimental data of Hallman on heat transfer with water flowing in vertical tubes. The data were obtained for Re $\leq$ 3300 and 30 $<$ Ra $\leq$ 2500 when the free and forced convections coincide at the wall. As we can see, there is good agreement between theory and experiment. The similar measurements of Brown [17], covering the 20 $\leq$ Re $\leq$ 60 and 1300 $\leq$ Ra $\leq$ 11·10⁴ regions were in just as good agreement with theory.
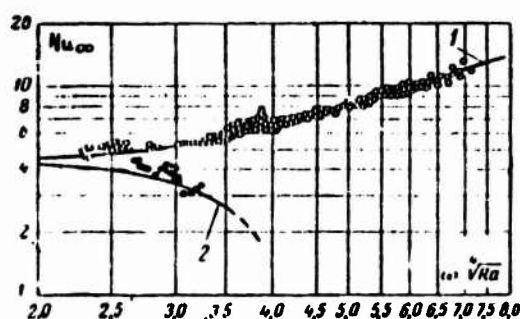
Fig. 16-27. Nusselt number from data of theoretical computation (curves) and experiment (circles). $1 - \frac{\partial t}{\partial x} > 0$; $2 - \frac{\partial t}{\partial x} < 0$.

Since the calculated and experimental values of Nu_∞ agree so well, we can conclude that the flow will remain laminar when $\partial t / \partial x > 0$, there are no internal heat sources in the flow, $Ra < 11 \cdot 10^4$ and $Re \le 3300$. Consequently, the presence of points of inflection in the velocity profile and even the appearance of a reverse stream in the flow core (see Fig. 16-23) will not disturb the stability of the flow near the wall.

As direct measurements have shown [17], for $Ra > 200$-600 and $Re > 30$-50, small irregular temperature fluctuations will appear in the flow core, while when $Ra > 1000$ and $Re > 130$, the temperature distribution in the core will begin to depart noticeably from the theoretical picture considered. These measurements are in qualitative agreement with visual observations of ink streams moving in a flow (see §16-1). Since these stability disturbances in the flow core do not change the nature of heat transfer they obviously cannot be treated as a transition to turbulent flow. The lack of experimental data still prevent us from evaluating the stability for other flow cases or from specifying the values of Re at which the transition to turbulent flow occurs.

To conclude, let us compute the pressure drop. The dimensionless parameter P, which contains the pressure gradient, is easily found from Eq. (16-24) with $R = 1$:

$$P = -\frac{d^2}{32\mu\bar{w}}\left(\frac{dp}{dx} + \rho_c g\right) = -\frac{1}{8}\left[\frac{d^2 W_x}{dR^2} + \frac{1}{R}\cdot\frac{dW_x}{dR}\right]_{R=1}.$$

Substituting in W_x from (16-28), we obtain the previous equation (16-34), representing P as a function of $\bullet = \sqrt[4]{Ra}$. When there are no internal heat sources ($1/K = 0$), this equation takes the form (16-36).

For the special case in which $K = 0$ (and, consequently, $A = 0$ and $t_s = \text{const}$), using Expression (16-32) for W_x, we obtain

$$P = 1 - \frac{1}{48}\cdot\frac{Re}{K}. \tag{16-39}$$

Figure 16-28 shows P as a function of Ra for several values of K. When $Ra = 0$, $P = 1$. As Ra increases as a function of K, P rises or falls, taking on negative values in the latter case. There are two limiting cases in which $P \ge 1$: $q_v = 0$ ($K = \infty$) and $q_s = 0$ ($K = 1$).

If we know the way in which P depends on Ra, it is not difficult to determine the pressure drop. It follows from the definition of P that

$$\frac{dp}{dx} = -\rho_c g - \frac{32\mu\bar{w}}{d^2}P.$$

Integrating this expression between $x = 0$ and x (where $x = 0$ corresponds to the section beginning with which the flow and heat exchange are stabilized), and letting $\Delta p = p_{x=0} - p$, we have

$$\Delta p = \rho_c g x + P\frac{32\mu\bar{w}x}{d^2},$$
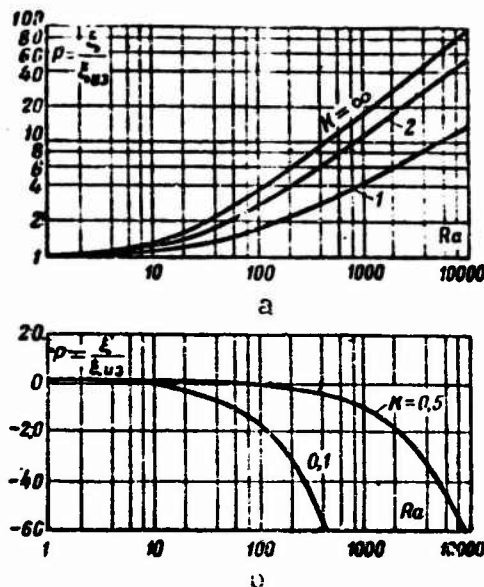
Fig. 16-28. The parameter P as
a function of Ra. a) $K = \infty$, 2,
and 1; b) $K = 0.5$ and 0.1.

or

$$\Delta p = \overline{\rho}_r g x + \xi \, \frac{\rho \overline{w}^2}{2} \cdot \frac{x}{d}, \qquad (16\text{-}40)$$

where $\xi = P\xi_{1z}$ is the friction-resistance coefficient for flow with
heat exchange; $\xi_{1z} = 64/Re$ is the same, for isothermal flow; $\overline{\rho}_s$ is
the mean density ρ_s over the segment from $x = 0$ to x.

Thus the quantity P can be interpreted as the ratio of fric-
tion-resistance coefficients for viscous-gravitational and viscous
isothermal loads. The first term in (16-40) characterizes the var-
iation in hydrostatic pressure, and the second the variation in
pressure caused by friction.

2. *Case in which* $\partial t/\partial x < 0$ *for* $q_y = 0$. Here the forced and
free convections at the wall are opposite in direction. The problem
reduces to solving (16-25) with a minus sign on the last term and
a value $1/K = 0$. The general solution of such an equation has the
form

$$W_x = C_1 I_0(Z) + C_2 Y_0(Z) + C_3 I_0(Z) + C_4 K_0(Z),$$

where

$$Z = \sqrt[4]{Ra} \, R.$$

Calculating the constants with the aid of boundary condition
(16-27) (in particular, it follows from the $R = 0$ condition that
$C_2 = C_4 = 0$), and using the relationship $2\int_0^1 W_x R\,dR = 1$, we obtain an

- 426 -

equation for the velocity distribution:

$$W_x = \frac{w_x}{\overline{w}} = \frac{\omega}{2}\left[\frac{J_0(Z)I_0(\omega) - J_0(\omega)I_0(Z)}{J_1(\omega)I_0(\omega) - J_0(\omega)I_1(\omega)}\right].$$ (16-41)

where

$$\omega = \sqrt[4]{\overline{Ra}}.$$

Substituting this expression for w_x into (16-20), letting $q_v = 0$, and integrating (16-20) twice, we find the temperature distribution:

$$\theta_0 = \frac{\theta\lambda}{q_c d} = \frac{1}{2\omega}\left[\frac{J_0(Z)I_0(\omega) + J_0(\omega)I_0(Z) - 2J_0(\omega)I_0(\omega)}{J_1(\omega)I_0(\omega) - J_0(\omega)I_1(\omega)}\right].$$ (16-42)
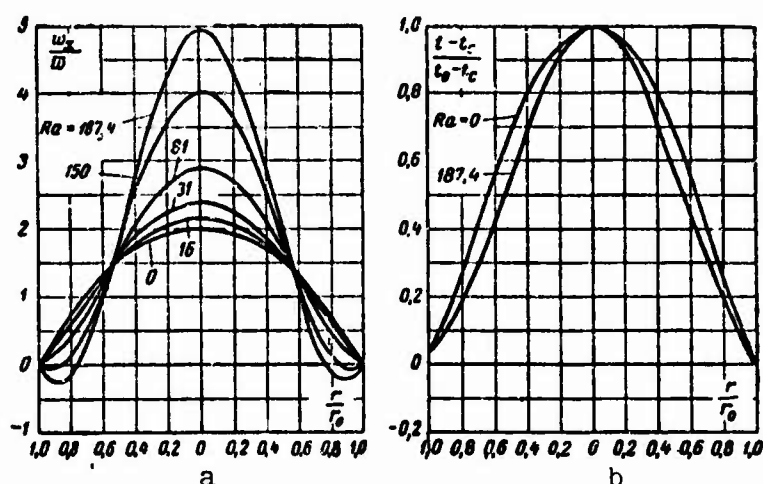
Fig. 16-29. Radial distributions of velocity (a) and temperature (b) for case in which $\frac{dt}{dx} < 0$ and $K = \infty$.

Figure 16-29 shows the velocity and temperature profiles calculated from Eqs. (16-41) and (16-42). Here, in contrast to the preceding case (compare with Fig. 16-23), the fluid velocity increases at the center of the tube, while near the wall it decreases as Ra becomes larger. At Ra = 104.9, a reverse flow appears at the wall; by Ra ≥ 168, stability is lost.

Using the expressions found for the velocity and temperature, we have no difficulty in determining the limiting Nusselt number:

$$Nu_\infty = \frac{[J_1(\omega)I_0(\omega) - J_0(\omega)I_1(\omega)]^2}{\frac{1}{4}[J_1^2(\omega)I_0^2(\omega) + J_0^2(\omega)I_1^2(\omega)] + \frac{J_0(\omega)I_0(\omega)}{\omega}[J_0(\omega)I_1(\omega) - J_1(\omega)I_0(\omega)]}.$$ (16-43)

Figure 16-27 shows the way in which Nu_∞ depends on Ra (lower

curve). When Ra → 0, $Nu_\infty = 4.36$, which corresponds to pure forced convection; as Ra increases, Nu_∞ decreases. The same figure shows experimental data for $\omega \leq 3.3$ ($Ra \leq 119$). They are in satisfactory agreement with theory. Measurements of temperature fields and heat transfer [17] show that at $Ra \geq 168$ stability is lost, while when $Ra > 250$, the flow becomes turbulent. These results are in qualitative agreement with observations of ink-stream motion (see §16-1), as well as with data on heat transfer at constant wall temperature (see §16-3). Thus the theory is valid only for $Ra < 168$.

Everything said in this section holds only for stabilized flow and heat exchange. Unfortunately, there are still no data available that would permit us to find the distance from the entrance at which stabilization of the velocity and temperature profiles set in.

Some information has been published on heat exchange and resistance in the thermal initial segment of a round tube for gas flowing with variable physical parameters when the forced and free convections coincide at the wall [11] (see References for Chapter 7).

16-5. FLOW AND HEAT EXCHANGE IN FLAT AND PRISMATIC VERTICAL TUBES FAR FROM THE ENTRANCE UNDER BOUNDARY CONDITIONS OF THE SECOND KIND WITH AND WITHOUT HEAT SOURCES IN THE FLOW

1. Let us consider viscous-gravitational flow and heat exchange in a flat vertical tube. Let the heat-flux densities be identical at the two walls and constant over the surface, and let heat be released uniformly in the flow by the internal heat sources. All remaining conditions are the same as in the preceding sections.

If the fluid moves upward with heating   ($\partial t/\partial x > 0$, the x axis has the direction of the velocity vector), then for fully developed flow and heat exchange, the motion and energy equations will have the form

$$\beta_p g \vartheta - \frac{1}{\rho_c}\left(\frac{dp}{dx} + \rho_c g\right) + \nu \frac{d^2 W_x}{dy^2} = 0,$$

$$\frac{d^2 \vartheta}{dy^2} = \frac{A}{a} w_x - \frac{q_\ast}{\lambda},$$

where

$$\vartheta = t - t_c;$$

$$A = \frac{\partial t}{\partial x} = \frac{dt_c}{dx} = \frac{q_c + q_\ast r_\ast}{\rho c_p w r_\ast} = \text{const};$$

here $2r_0$ is the width of the tube.

These equations can be written in dimensionless form:

$$\frac{d^2 W_x}{dY^2} + Ra\,\vartheta = P, \tag{16-44}$$

$$\frac{d^2 \vartheta}{dY^2} - W_x = -F, \tag{16-45}$$

where

$$Y = \frac{y}{r_0}; \quad W_x = \frac{w_x}{u}; \quad \theta = \frac{\theta_0}{\Delta \omega T};$$

$$Ra = \frac{g\beta_1 \Delta r_0^4}{a\nu};$$

$$P = \frac{r_0^2}{\mu\omega}\left(\frac{dp}{dx} + \rho_0 g\right);$$

$$F = \frac{q_0}{\Delta \omega c_p}.$$

Thus the problem reduces to solving Eqs. (16-44) and (16-45) under the boundary conditions

$$W_x = 0 \text{ and } \theta = 0 \text{ for } Y = \pm 1.$$

This problem (see [1, 20, 21]) can be solved by the method used in the preceding case (see §16-4). However, we shall use another method proposed by Tao [20]. This method is valid only when Ra is positive. Thus the entire discussion pertains to Ra > 0.

We introduce the complex function

$$\Phi = W_x + i \cdot \theta \text{ and } G = F + i\omega^{-2}P,$$

where

$$\omega = Ra^{1/4}.$$

Then Eqs. (16-44) and (16-45) are combined into a single equation:

$$\frac{d^2\Phi}{dY^2} - i\omega^2\Phi = i\omega^2 G, \tag{16-46}$$

while the boundary conditions take the following form: when $Y = \pm 1$, $\Phi = 0$. By introducing the function $\Psi = \Phi - G$, we transform the inhomogeneous equation (16-46) into the homogeneous equation

$$\frac{d^2\Psi}{dY^2} - i\omega^2\Psi = 0 \tag{16-47}$$

with inhomogeneous boundary conditions: when $Y = \pm 1$ $\Psi = -G$. The general solution of (16-47) is written as

$$\Psi = C_1 \operatorname{ch}(i^{1/2}\omega Y) + C_2 \operatorname{sh}(i^{1/2}\omega Y).$$

Using the boundary conditions, we find

$$\Psi = -\frac{\operatorname{ch}(i^{1/2}\omega Y)}{\operatorname{ch}(i^{1/2}\omega)} G$$

or

$$\Phi = G\left[1 - \frac{\operatorname{ch}(i^{1/2}\omega Y)}{\operatorname{ch}(i^{1/2}\omega)}\right]. \tag{16-48}$$

The velocity and temperature will evidently equal

$$W_x = \operatorname{Reel}(\Psi) \text{ and } \theta = \omega^{-2}\operatorname{Im}(\Psi)^{2}. {}^{9}$$

For clarity and convenience, we represent these solutions as functions of a real variable. As a result of our manipulations, we obtain

$$W_x = \text{Reel}\,(\Psi) = F\zeta_r - \omega^{-2}P\zeta_i, \qquad (16\text{-}49)$$

$$\theta = \omega^{-2}\,\text{Im}\,(\Psi) = \omega^{-2}(\omega^{-2}P\zeta_r + F\zeta_i), \qquad (16\text{-}50)$$

where

$$\zeta_r = 1 - \frac{\operatorname{ch} k(1+Y)\cos k(1-Y) + \cos k(1+Y)\operatorname{ch} k(1-Y)}{\operatorname{ch} 2k + \cos 2k};$$

$$\zeta_i = \frac{\operatorname{sh} k(1+Y)\sin k(1-Y) + \sin k(1+Y)\operatorname{sh} k(1-Y)}{\operatorname{ch} 2k + \cos 2k};$$

$$k = \frac{\omega}{\sqrt{2}}.$$

The parameter P, i.e., the dimensionless pressure gradient, can be found from the constant-flow-rate equation,

$$\int_{-1}^{+1} W_x\,dY = 2,$$

or

$$\text{Reel}\left[\int_{-1}^{+1} \Phi\,dY\right] = 2.$$

Integrating this expression, we find

$$\text{Reel}\left\{G\left[1 - \frac{\operatorname{th}(i^{1/2}\omega)}{i^{1/2}\omega}\right]\right\} = 1$$

or

$$F\xi_r - \omega^{-2}P\xi_i = 1,$$

where

$$\xi_r = 1 - \frac{1}{2k}\left[\frac{\operatorname{sh} 2k + \sin 2k}{\operatorname{ch} 2k + \cos 2k}\right];$$

$$\xi_i = \frac{1}{2k}\left[\frac{\operatorname{sh} 2k - \sin 2k}{\operatorname{ch} 2k + \cos 2k}\right].$$

Thus

$$P = \frac{\omega^2}{\xi_i}(F\xi_r - 1). \qquad (16\text{-}51)$$

The dimensionless mean mass temperature of the fluid is

$$\bar{\theta} = \frac{\bar{\vartheta}a}{A\bar{\omega}r_0^2} = \frac{1}{2}\int_{-1}^{+1}\theta W_x\,dY = \frac{1}{4\omega^2}\,\text{Im}\left[\int_{-1}^{+1}\Psi^2\,dY\right] =$$

$$= \frac{1}{4\omega^2}\,\text{Im}\left\{G\left[3 - \frac{3\operatorname{th}(i^{1/2}\omega)}{i^{1/2}\omega} - \operatorname{th}^2(i^{1/2}\omega)\right]\right\}$$

and, finally,

$$\ddot{\theta}=\frac{1}{4\omega^{2}}\left[\left(F^{2}-\frac{P^{2}}{\omega^{4}}\right)\eta_{i}+\frac{2PF}{\omega^{2}}\eta_{r}\right]. \tag{16-52}$$

where

$$\eta_{r}=3\xi_{r}-\frac{sh^{2}2k-\sin^{2}2k}{(ch\,2k+\cos 2k)^{2}};$$

$$\eta_{i}=3\xi_{i}-\frac{2\,sh\,2k\,\sin 2k}{(ch\,2k+\cos 2k)^{2}}.$$

The Nusselt number, defined in the usual way, equals

$$Nu_{\infty}=\frac{q_{c}2r_{0}}{\theta\lambda}=\frac{2(1-F)}{\bar{\theta}}. \tag{16-53}$$

When there are no internal heat sources in the flow ($F = 0$),

$$Nu_{\infty}=\frac{2}{\bar{\theta}}, \tag{16-54}$$

and

$$\bar{\theta}=\frac{4k\,sh\,2k\,\sin 2k-3\,(sh\,2k-\sin 2k)\,(ch\,2k+\cos 2k)}{4k\,(sh\,2k-\sin 2k)^{2}}. \tag{16-55}$$

Figure 16-30 shows the way in which Nu_{∞} depends on Ra when $F = 0$. As Ra decreases, Nu_{∞} approaches the value corresponding to pure forced convection ($Nu_{\infty}=\frac{70}{17}\approx 4.12$, see §8-2).

The method used here to solve the problem had certain advantages as compared with the usual approach (see §16-4). They lie in the fact that the basic equation is of order two (rather than four), while the solution simultaneously gives the velocity and temperature distributions. The method is particularly convenient for solution of two-dimensional problems. There have been several studies of flow and heat exchange in prismatic tubes for viscous-gravitational flow with $\partial t/\partial x > 0$. A solution has been obtained in [20, 22] for a rectangular tube, and in [19, 23] for tubes with cross sections in the form of ring sectors and complete circular sectors. All calculations were carried out for fully developed flow and heat exchange with the wall temperature constant over the perimeter and the heat-flux density constant over the length (but variable along the perimeter), with and without internal heat sources in the fluid flow.

To conclude, we give the mean values over the perimeter of the limiting Nusselt numbers for a square tube as a function of Ra, according to the data of [22]:

Ra	0	97.4	974	9740
Nu_{∞}	3.61	3.69	4.27	9.46

The values of Ra and Nu_{∞} in this table were calculated by means of the equivalent diameter.
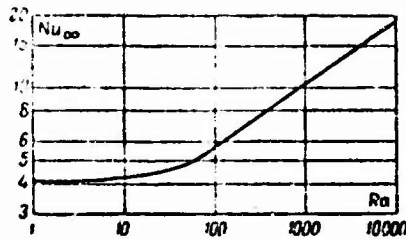
Fig. 16-30. Dependence of Nu_∞
on Ra for $F = 0$ in flat verti-
cal tube for $\frac{\partial t}{\partial x} > 0$.

16-6. FLOW AND HEAT EXCHANGE IN A ROUND HORIZONTAL TUBE UNDER BOUNDARY CONDITIONS OF THE SECOND KIND

An approximate theoretical analysis of this problem for fully developed velocity and temperature fields with $\overline{q}_s$ = const[30] along the length and t_s = const along the perimeter has been given by Morton [24]. The solution was obtained as a series in powers of the Rayleigh number, and it holds only for small values of this number. It is interesting since it makes it possible to form a qualitatively correct picture of the flow under these conditions.[31]

Figure 16-31 shows the theoretically calculated streamlines
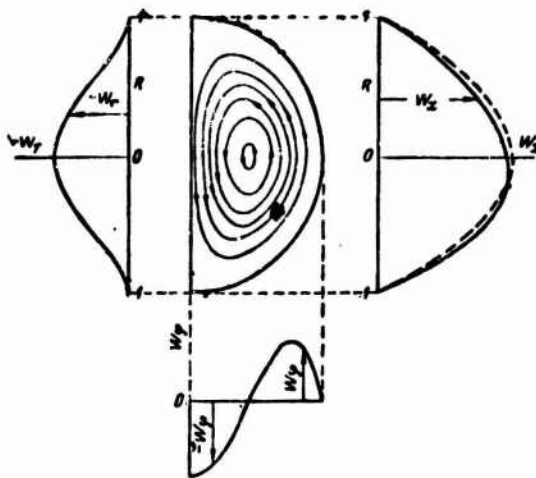
Fig. 16-31. Streamlines in right half of section through horizontal tube (projection onto plane normal to axis). Distribution of dimensionless velocity components $W_x = \frac{w_x}{2w}$, $W_r = \frac{w_r r_0}{v}$ and $W_\varphi = \frac{w_\varphi r_0}{v}$ for RaRe = 1000 and Pr = 0.73 (the dashed line corresponds to isothermal flow).

(projected onto the vertical plane perpendicular to the tube axis); their nature is determined by the interaction of the free and forced convections. The same figure shows the components of the velocity

vector in the axial (w_x), radial (w_r), and tangential (w_φ) directions for RaRe = 1000 and Pr = 0.73. All velocity components are given in dimensionless form, and refer to the same tube cross section. The distributions of w_x and w_r along the diameter, which lies in the vertical plane, are shown at the right and left of Fig. 16-31, while the distribution of w_φ along the radius in the horizontal plane is shown at the bottom). Free convection causes the profile of the longitudinal velocity component to become asymmetric; the velocity maximum for heating of the fluid shifts downward.

Fig. 16-32. Distribution of $t_s - \bar{t}$ over tube perimeter for Ra = $(1.8-3.0)\cdot10^7$, Re = 1400-1700. The values of $\frac{1}{\mathrm{Pr}}\frac{x}{d}\cdot10^3$ are: 1) 0.43; 2) 0.75; 3) 1.2; 4) 2.3; 5) 3.9; 6) 6.1; 7) 9.5 (the curves are displaced with respect to one another, so that the scale is shown on each of them; the angle φ = 0 corresponds to the upper generatrix).

The results of [24] do not give an adequate notion of the heat-exchange laws. Thus we turn directly to the experimental data. A.F. Polyakov and the author have carried out an experimental investigation into heat exchange for viscous-gravitational flow in a horizontal tube with the heat release at the wall constant along the circumference and the length [26, 27]. Heat exchange was studied for water in a tube heated by an electric current. The tube, made from 1X18H9T steel, had an inside diameter $d \approx 19$ mm and a wall thickness 0.36 mm; the heated and stilling segments equaled roughly 100d each.

The experiments disclosed significant nonuniformity in the distribution of wall temperature and local heat-transfer coefficient over the circumference; this is naturally associated with the existence of the tangential free-convection flows.[32]

Figure 16-32 shows the distribution of wall temperature t_s (measured from $\bar{t}$ in the same section) over the circumference for various values of the reduced length; Fig. 16-33 shows the variation in the dimensionless wall temperature T_s on the upper and lower generatrices as a function of the reduced length. Figure 16-34 gives some idea as to the nature of the circumferential and length distributions of the local Nu number for certain values of Re and Ra. Here

$$T_c = \frac{(t_c - \bar{t})\lambda}{q_c d};$$

$$\mathrm{Nu} = \frac{q_c d}{(t_c - \bar{t})\lambda}; \quad \mathrm{Re} = \frac{\bar{w}d}{\nu};$$

$$\mathrm{Ra} = \mathrm{GrPr} = \frac{g\beta\bar{q}_c d^4}{\nu a \lambda},$$

where q_s is the local heat-flux density at the wall at a given point on the tube perimeter; $\bar{q}_s$ is the heat-flux density averaged over the perimeter (owing to spreading of the heat, q_s will vary noticeably over the perimeter).
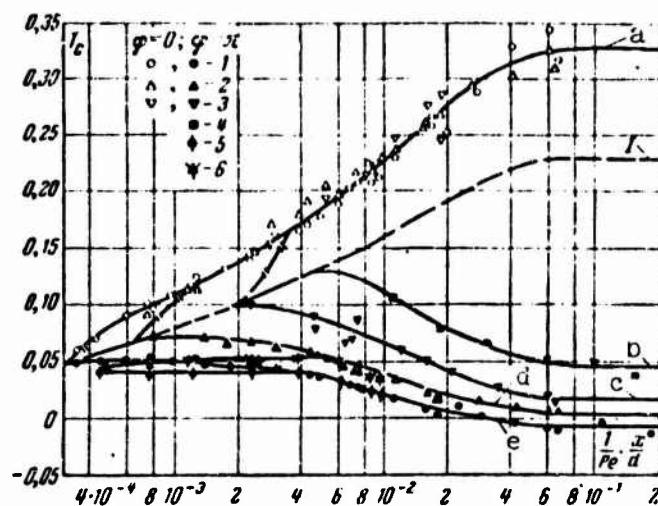
Fig. 16-33. Variation of T_s on upper (a) and lower (b, c, d, e) generatrices as function of reduced length for Re = 50-2400. The values of Ra·10⁶: 1) (15-30); 2)(5.5-7); 3) (1.4-1.8); 4) 0.3; 5) (18-25); 6) (5.5-6.4). I) Viscous flow with constant physical properties.

In the expressions for T_s, Nu, Re, and Ra, the physical properties of the fluid were selected for the mean mass temperature $\bar{t}$ of the fluid at the given cross section.

It is clear from the figures that the wall temperature varies substantially along the circumference. In the upper part of the

tube, T_s is substantially greater and Nu substantially less than
in the lower part. As the reduced length increases, the distribu-
tions of T_s and Nu over the circumference become less uniform. Thus,
for $\frac{1}{Pe}\cdot\frac{x}{d} \geqslant 10^{-1}$, the value of Nu on the lower generatrix is roughly
10 times the value on the upper generatrix.

At sections close to the beginning of the heated segment,
there is a local reduction in wall temperature and a corresponding
increase of Nu near the lower generatrix. As we move away from the
entrance to the heated section, the drop in $t_s - \bar{t}$ and the increase
in Nu gradually vanish.

The way in which $T_s = Nu^{-1}$ varies with the length differs from
the variation with Ra at different points.

When Ra is small, the wall temperature T_s does not depend on
Ra, but corresponds to the values of T_s for pure viscous flow (curve
I of Fig. 16-33). For sufficiently large Ra, the $T_s(X)$ curves for the
uppwer and lower generatrices deviate from the curve for viscous
flow at values of X that are smaller the larger Ra. On the upper
generatrix, T_s first rises as Ra increases, and then remains con-
stant; on the lower generatrix, T_s decreases as Ra increases. As
Fig. 16-33 shows, the $T_s(Ra)$ curves differ substantially for the
upper and lower generatrices. As we can see from the same figure,
however, the length of the thermal initial segment for local val-
ues of T_s or Nu will be roughly the same for viscous-gravitational
flow or viscous flow.

This type of variation in wall temperature and Nu over the
tube surface is caused by the specific motion of the fluid. The
latter results from the interaction of the tangential free-convec-
tion currents and the longitudinal forced flow. The intensity of
the free-convection currents rises with the length, which leads
to a significant increase in heat transfer and a corresponding
reduction in wall temperature near the lower generatrix of the
tube as compared with pure viscous flow. Here the heat exchange
not only does not increase near the upper generatrix, but it even
decreases as compared with viscous flow. This is apparently ex-
plained by the fact that comparatively hot fluid within which the
free-convection currents do not penetrate, concentrates near the
upper generatrix, so that this fluid moves only in the axial di-
rection.

These features of heat exchange have been confirmed, in
particular, by measurements of the temperature field in a flow.
The measurements were carried out in the horizontal and vertical
diametral planes for various values of x/d. The measurement results
are shown in Fig. 16-35, where $\theta = \frac{t - t_0}{\frac{qd}{\lambda}}$; $R = r/r_0$; t_0 is the temperature
of the fluid at the entrance.

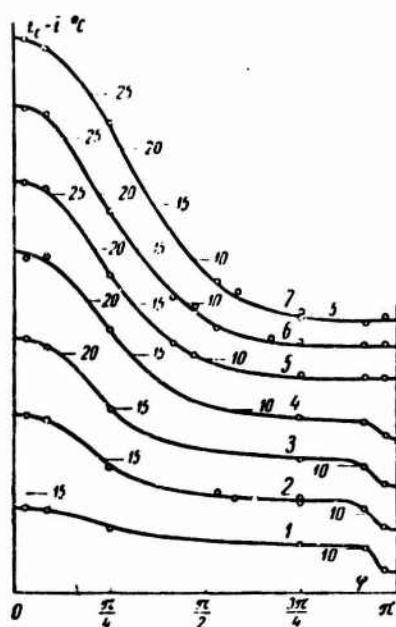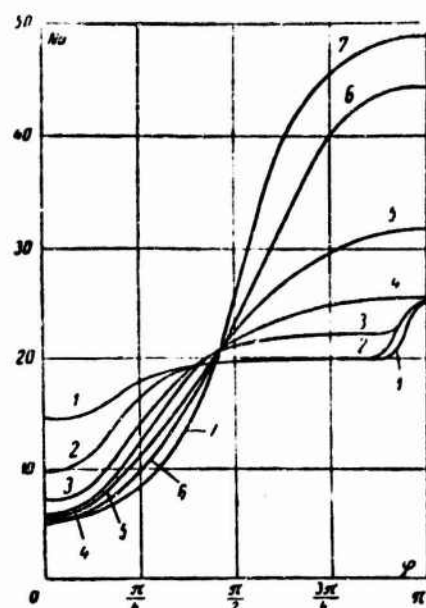Fig. 16-34. Distribution of local Nu number over tube perimeter for
Ra = $(1.8-3.0) \cdot 10^7$, Re = 1400-1700. The values of $\frac{1}{Pe} \cdot \frac{x}{d} \cdot 10^4$ are: 1)
0.43; 2) 0.75; 3) 2.3; 4) 3.9; 5) 6.1; 6) 8.5; 7) 9.5.

a

b
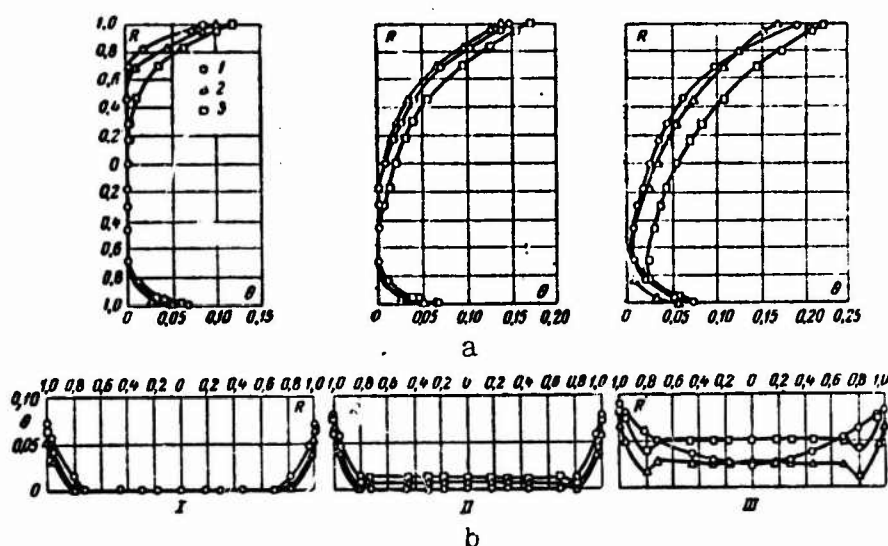
Fig. 16-35. Distribution of temperature in flow in
vertical (a) and horizontal (b) diametral planes.

$I - \frac{x}{d} = 8.5$; $II - \frac{x}{d} = 32.5$; $III - \frac{x}{d} = 76.0$; $1 - Ra = (5.5-6.4) \cdot 10^6$; $Re = 1\,400-1\,700$; $2 - Ra = (1.8-3.0) \cdot 10^7$;
$Re = 1\,400-1\,500$; $3 - Ra = (1.6-2.8) \cdot 10^7$; $Re = 760-960$.

The value of Ra at which T_s or Nu begins to deviate from the
corresponding value for pure viscous flow can be said to be the
limiting value. We represent it by Ra_0.

It is clear from Fig. 16-33 that within the thermal initial

Fig. 16-36. Comparison of Eq. (16-56) (solid lines) with experimental data (points) for Ra = $2 \cdot 10^5 - 4 \cdot 10^7$ and Re = 50-2400.

segment, Ra_0 decreases as X increases, while when $X \to \infty$ [in practice when $X > (1/Pe)(l_{n.t}/d)$] it approaches a certain constant value. When $Ra \le Ra_0$, the value of T_s (or Nu) corresponds to the values for pure viscous flow, and depends solely on X. For $Ra > Ra_0$, T_s depends on X and Ra.

For the dimensionless wall temperature T_s or the local Nusselt number (Nu = T_s^{-1}), the interpolation equation

$$T_c = T_{c\pi} + (T_{c0} - T_{c\pi})\left(\cos\frac{\varphi}{2}\right)^{2k},$$ (16-56)

is used, where T_{s0} and $T_{s\pi}$ are the values of T_s at the upper ($\varphi = 0$) and lower ($\varphi = \pi$) generatrices,

$$\frac{T_{c0}}{T_{c.e}} = 1.4 - \frac{0.4}{1 + 0.2\,(Ra/Ra_0)^4};$$ (16-57)

$$\frac{T_{c\pi}}{T_{c.e}} = -0.15 + \frac{1.15}{[1 + (Ra/Ra_0)^4]^{1/16}};$$ (16-58)

here $T_{s.v} = Nu_v^{-1}$ is the dimensionless wall temperature for viscous flow of a fluid with constant physical properties; Nu_v is the local Nusselt number under the same conditions [$T_{s.v}(X)$ or $Nu_v(X)$ can be computed from Eqs. (8-13) or (8-15)]; Ra_0 is the limiting value of Ra for local heat transfer:[33]

$$Ra_0 = 3.8 \cdot 10^9 X^{-1} \text{ (for } X < 2 \cdot 10^{-3});$$

$$Ra_0 = (2300 + 7.8\,X^{-1})\left(1 - \frac{150\,X^2}{1 + 55 \cdot 10^6 X^4}\right) \text{ (for } X > 2 \cdot 10^{-3});$$

$$X = \frac{1}{Pe}\frac{x}{d}.$$

Fig. 16-37. Nusselt number averaged over perimeter as function of reduced length (Re = 300-800). The values of Ra are:

$1 - 2,5 \cdot 10^5$; $2 - 1,2 \cdot 10^6$; $3 - 6 \cdot 10^6$; $4 - 1,6 \cdot 10^7$; $5 - 3,5 \cdot 10^7$.

The parameter k in (16-56) equals

$$k = \frac{1 + 5.2 \cdot 10^{-8} Ra}{1 + 3 \cdot 10^{-7} Ra}.$$

The physical properties in Eq. (16-56) are selected for the mean mass temperature of the fluid in the given section.

In Fig. 16-36, Eq. (16-56) is compared with experimental data for values of the angle φ = 0, $\pi/4$, and π. The figure clearly shows the way in which T_s depends on Ra for various values of φ. As we have already noted, an interesting fact is observable here. On the upper generatrix, T_s first rises rapidly (as a consequence, Nu decreases) as Ra increases, and then remains constant; on the bottom and intermediate generatrices (for φ between $\pi/4$ and π), T_s decreases while Nu increases as Ra increases.

Equation (16-56) holds for values of $50 \leqslant Re \leqslant 2400$. $2 \cdot 10^5 \leqslant Ra \leqslant 4 \cdot 10^7$ $2 < Pr < 10$ and $4 \cdot 10^{-2} < X < 0.2$ for heating of the fluid.

Figure 16-37 shows the change in the Nusselt number $\overline{Nu}$ averaged over the perimeter at a given tube cross section as a function of the reduced length for various Rayleigh numbers. Here

$$\overline{Nu} = \frac{\overline{q_c} d}{(\overline{t_c} - \overline{t}) \lambda},$$

where $\overline{t_c} = \frac{1}{\pi} \int_0^\pi t_c \, d\varphi$ is the mean integral value of wall temperature at the given section. The lower (limiting) curve of Fig. 16-37 corresponds to Eq. (8-13) for pure viscous flow at q_s = const. For a given value of Ra, $\overline{Nu}$ for viscous-gravitational flow first coincides with the corresponding values for pure viscous flow (for sufficiently small X) and, consequently, depends solely on the reduced length;[34] it then takes on a constant value, which is greater the larger Ra.

These aspects of the behavior of $\overline{Nu}$ for viscous-gravitational flow in horizontal tubes are well reflected by the interpolation equation

$$\frac{\overline{Nu}}{Nu_0} = \left[1 + \left(\frac{Ra}{Ra_0} \right)^4 \right]^{0.044}. \tag{16-59}$$

where $Nu_0(X)$ is the value of the Nusselt number for viscous flow, while $\overline{Ra}_0$ is the limiting value of Ra for the mean heat transfer, determined from the condition requiring that for viscous-gravitational flow $\overline{Nu}$ not differ by more than 5% from Nu_v. The following equations are used for $\overline{Ra}_0$:

$$\overline{Ra}_0 = 5 \cdot 10^3 X^{-1} \quad (\text{for } X < 1.7 \cdot 10^{-3});$$

$$\overline{Ra}_0 = 1.8 \cdot 10^4 + 55 X^{-1.7} \quad (\text{for } X > 1.7 \cdot 10^{-3}).$$
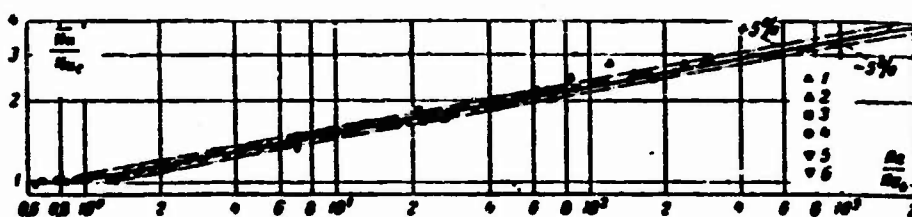
Fig. 16-38. Comparison of Eq. (16-59) (solid line) with experimental data (points). Re values:
1 — 50- 80; 2 — 200-300; 3 — 750-900; 4 — 1400-1700; 5 — 1800-2000; 6 — 2300-2400.
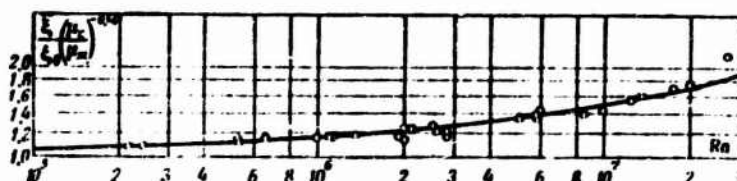
Fig. 16-39. Resistance coefficient as a function of Ra for viscous-gravitational flow in a horizontal tube, q_s = const.

The physical properties in Eq. (16-59) are selected for the mean mass temperature of the fluid in the given section.

As Fig. 16-38 shows, Eq. (16-59) describes the experimental data to within ±5%. It is valid within the same limits of variation of the controlling parameters as Eq. (16-56).

When $X \to \infty$ $\overline{Ra}_0 = 1.8 \cdot 10^4$, and $Nu_0 = 4.36$. Here on the basis of (16-59), we have

$$\overline{Nu} = \overline{Nu}_\infty = 4.36 \left[1 + \left(\frac{Ra}{1.8 \cdot 10^4} \right)^6 \right]^{0.045} \tag{16-60}$$

As we can see from Fig. 16-37, for viscous-gravitational flow in horizontal tubes, $\overline{Nu}$ becomes constant over the length at lower values of X than for pure viscous flow. Thus (16-60) will be valid when $X \geqslant 1.7 \cdot 10^{-3}$ and $Ra \geqslant 1.8 \cdot 10^4 + 55 X^{-1.7}$

Mori and his associates [28] have measured heat transfer for air flowing in a horizontal tube with q_s = const over the length and t_s = const over the circumference.[35] They only measured the heat-transfer coefficients averaged over the circumference at a section far from the entrance, i.e., for stabilized flow and heat exchange. The results of these measurements agree very well with our data (for the region of stabilized heat exchange), and are described by Eq. (16-60) with the same accuracy as are our data. Thus we can conclude that a nonuniform distribution of t_s over the circumference has no noticeable influence on $\overline{Nu}$, and that (16-59) and (16-60), or the latter in any case, are valid for values $0.7 \leqslant Pr \leqslant 10$.

According to the data of [29], the resistance coefficient averaged over the tube length rises as Ra increases. The following approximate equation holds for it:

$$\frac{\xi}{\xi_0} = \left(1 + 0.5\sqrt{\frac{Ra}{10^7}}\right)\left(\frac{\mu_c}{\mu_s}\right)^{0.14}. \qquad (16\text{-}61)$$

where $\xi_0 = 64/Re$ is the resistance coefficient for isothermal flow. The physical properties in (16-61) are chosen for a mean fluid temperature $t_{zh} = (t_0 + \overline{t}_l)/2$, with the exception of μ_s (the viscosity at the wall).

In Fig. 16-39, Eq. (16-61) is compared with experimental data [29]. It is valid for values $Re < 2300$, $Ra < 5 \cdot 10^7$ $3 \leqslant Pr \leqslant 10$ for heating of the fluid.

Manu-script Page No.	Footnotes
394	[1]This case is not considered here. Gravitational free convection within tubes and chambers of various shapes has been investigated by G.A. Ostroumov; his results are reported in [1].
396	[2]For simplicity, we shall still assume that there are no internal heat sources in the fluid flow.
396	[3]The profiles correspond to fully developed (stabilized) flow and heat exchange at q_s = const.
39?	[4]On Figs. 16-1, 16-3, and 16-5, Gr and Re have been calculated for the tube diameter; the temperature drop in the expression for Gr is found as the difference between the wall temperature and the temperature at the tube axis.
97	[5]No observations were made for large Re.

35/443

398   [6]The experiments were carried out at $T_s = $ const; for more details, see §16-3. See also [4].

398   [7]The values of Re_{kr} and G were computed over the tube diameter; in the expression for Gr, in the temperature for Gr, the temperature head is found as the arithmetic mean; the physical properties of the fluid in the Re_{kr} calculation were taken for a mean flow temperature $t_{zh} = $
$$= (t_{vkh} + t_{vykh})/2, \text{ and for GrPr at } t_g = (t_{zh} + t_s)/2.$$

399   [8]See the first footnote to page   .

399   [9]That is, the curvature of the ink stream and its subsequent disruption when Re decreases and Gr remains constant.

401   [10]The first equation is for a flat tube and the second for a round tube.

404   [11]After the + sign under the radical has been replaced by a − sign, Eq. (16-6) is recommended for flow in vertical tubes when the free and forced convections are opposite in direction at the wall. There is no basis for this, as we shall see later.

405   [12]So far as we know, there have been no measurements of local heat transfer for constant wall temperature.

406   [13]This naturally does not imply that Nu is totally independent of GrPr in turbulent flow. We only mean that such a relationship was not observed within the limits of GrPr variation used in the given experiments.

407   [14]See [4].

408   [15]The points on the asymptote are not shown in Fig. 16-11. The points corresponding to viscous flow are not shown in Fig. 16-12.

409   [16]Unfortunately, it is difficult to use the data of [10] owing to their inadequate accuracy and the lack of information on the properties of the oils.

411   [17]In this equation, the heat-transfer coefficient refers to the arithmetic mean temperature head.

412   [18]The coördinates on Fig. 16-15 are the same as for Figs. 16-9 and 16-13.

     [19]The coefficient $\bar{\xi}$ has been determined from experimental data on the basis of Eq. (7-85). See also the footnote to page   .

415   [20]In Fig. 16-20, a relationship between $\bar{\xi}$ and GrPr is found only for fairly small values of Re_{zh}, since the   .

experiments carried out over a relatively narrow range of Δt (from 20 to 50°C).

416 [21]A solution is given for this problem in other studies, such as [16, 17, 18, 19]. A different method was used to obtain the solution in the last paper cited.

417 [22]The quantity β_ρ, which we have rather arbitrarily called the coefficient of volume expansion ($\beta_\rho = (\rho/\rho_s)\beta$, where β is the coefficient of volume expansion, see §3-2) is temperature-dependent, generally speaking. Thus the assumption of constancy is an additional assumption that is truer the less the temperature difference in the flow.

418 [23]Another method for solving the problem has been proposed by Tao [19, 20]. By introducing a complex function whose real and imaginary parts depend on the velocity and temperature, respectively, he reduces the energy and motion equations to a single second-order differential equation. Solving this equation by a method of mathematical physics, he finds the velocity and temperature fields simultaneously. For two-dimensional problems (for example, flow in a rectangular tube), this method offers certain advantages. It can only produce a solution for $dt/dx > 0$, however.

419 [24]For example, $\mathrm{ber}(x) + i\,\mathrm{bei}(x) = I_0(i\sqrt{ix}) = I_0(\sqrt{ix})$. $\mathrm{ker}(x) + i\,\mathrm{kei}(x) = K_0(\sqrt{ix})$. (see G. Watson, Theory of Bessel Functions, Foreign Literature Press, 1949).

421 [25]For Ra = 0, the velocity and temperature profiles are constructed from the corresponding equations for pure forced convection.

423 [26]The values of q_v and $\bar{w}$ in the expression for Ra/K may be either positive or negative.

423 [27]The dashed line shows the curve for K_1 in a larger scale.

424 [28]If there are internal sources in the flow, then Nu_∞ becomes inconvenient and unclear (for example, when = 0, Nu_∞ has a discontinuity). In such case, it is more convenient to use Eq. (16-33) to determine the wall temperature.

429 [29]The symbols Reel and Im represent the real and imaginary parts of a complex function.

432 [30]Here $\bar{q}_s$ is the heat-flux density at the wall, averaged over the perimeter.

432 [31]An analogous problem for inclined tubes (inclined at from 0 to 90° with respect to the horizontal) has been

433 [32]Since the wall thickness and thermal-conductivity coefficient are fairly small, heat transfer by conduction

will not equalize the wall temperature over the circumference.

437   [33]The values of Ra_0 are so selected that the measured values of T_s will differ by no more than 10% from the values computed from Eqs. (16-57) and (16-58). Naturally, the selected values of Ra_0 may differ considerably from the actual values.

438   [34]Here the local values of Nu in the upper and lower tube sections may differ considerably from one another and from $\overline{Nu}$.

440   [35]Brass tube; wall thickness 1.2 mm; $d = 35.6$ mm; $l_{usp} = l_{obog} = 7$ m.

Manu-script Page No.	Transliterated Symbols
397	кр = kr = kriticheskiy = critical
397	г = g = granitsa = limit
403	ж = zh = zhidkost' = fluid, liquid
403	c = s = stenka = wall
403	л = l = logarifmicheskiy = logarithmic
408	н = n = narushnyy = outside
408	к = k = kol'tsevoy = annular
411	ас = as = asimptoticheskiy = asymptotic
426	из = iz = izotermicheskiy = isothermal
437	н.т = n.t = nachal'nyy termicheskiy = thermal initial
437	c.в = s.v = vyazkostnaya stenka = viscous wall
439	в = v = vozdushnyy = air
441	вх = vkh = vkhod = entrance
441	зых = vykh = vykhod = exit
443	усп = usp = uspokoitel'nyy = damping
443	обог = obog = obogrevayemyy = heated

Chapter 17

HEAT EXCHANGE IN TUBES UNDER NONSTATIONARY CONDITIONS

17-1. PRELIMINARY REMARKS

Recently, much attention has been devoted to the study of convective heat exchange under nonstationary conditions. This problem is interesting chiefly in connection with regulation and control of heat-exchange equipment operating at high thermal loads. A nuclear reactor is an example. Reactor control requires a knowledge of its characteristics for both stationary and transient regimes (startup, shutdown, change in power), as well as emergency regimes (for example, reduction or interruption in coolant supply owing to a pump fault). In a word, it is important to know the dynamic behavior of the equipment. Naturally, this requires development of methods for determining heat-exchange processes in reactor cooling-system channels in nonstationary operation.

In other cases, the operating principle of a heat exchanger or the associated equipment supplying coolant determines equipment operation under nonstationary conditions. Examples are certain types of regenerative heat exchangers, as well as equipment in which the coolant is supplied by piston pumps, compressors, internal-combustion engines, etc.

In the general case, heat-exchange calculations consist in determining the temperature field in the flow and in the wall washed by the flow and calculating the heat flux at the fluid-wall boundary. This requires joint consideration of the process of convective heat exchange in the fluid flow and the heat-conduction process in the wall, i.e., the combination problem must be solved (see §1-4). The solution of combination nonstationary problems involves great mathematical difficulty. No analytic methods have as yet been devised for solving such problems. Thus studies are usually limited to nonstationary convective heat exchange in a fluid flow, with heat conduction in the wall ignored; this is done by specifying appropriate thermal boundary conditions at the inside surface. Naturally, this limits the generality of the results obtained; they become suitable only for very thin walls or walls with very high thermal diffusivity. Nonetheless, the solution of such problems is very interesting, since the foregoing conditions hold, in approximation, for many cases of practical importance. By analyzing such problems, it is also possible to determine the physical pattern for development of the nonstationary heat-exchange process.

From the viewpoint of the factors responsible for nonstationarity, problems of convective heat exchange under nonstationary conditions can be divided into three groups. The first includes problems in which the fluid flow is stationary while the thermal boundary conditions vary with time (see §17-2, 17-3, and 17-4); the second includes problems of heat exchange with nonstationary flow and boundary conditions that are constant in time (§17-5, 17-6); the third includes problems in which both the fluid flow and the thermal boundary conditions are nonstationary (§17-7).

The theoretical investigation of convective heat-exchange processes under nonstationary conditions is quite difficult. Thus the analysis is frequently carried out with the aid of simplified models and approximate methods.

The simplest approach to determination of heat exchange under nonstationary conditions consists in assuming that quasistationarity obtains. In this approach, we assume that the same relationships are valid for heat transfer under nonstationary conditions as under stationary conditions, provided we substitute the instantaneous values of the parameters $(\bar{t}, \bar{w}, t_s, q_s)$ that characterize the nonstationary process. The time and length variation of these parameters can be found by solving the problem in the one-dimensional approximation, i.e., the values of the corresponding parameters averaged over the cross section are considered. This computational method can be used (as has been confirmed by comparison of theory and experiment) only when the parameters characteristic of the process vary slowly enough in time.

Another simplified approach consists in assuming bar flow (the fluid velocity is assumed to be constant over the cross section and length, but it can vary in time); in many cases, this permits us to solve the problem with no additional simplifications. Calculations based on this approach yield a qualitatively correct pattern for the process, so that many interesting features can be determined. The quantitative data may depart noticeably from the actual values, however.

In many cases, in place of the differential equation for the energy we use the energy equation in an integral form, obtained from the differential equation by integration over the tube cross section. As a rule, this approach yields quite satisfactory results. Finally, we might also mention the application of approximate methods of boundary-layer theory and numerical computation methods to nonstationary problems of convective heat exchange.

In the ensuing discussion, we shall use a fairly exact method based on solution of the energy equation in integral form. The computational results obtained by this method are usually compared with results obtained by other methods, so that the limits of applicability of the latter can be estimated.

17-2. HEAT EXCHANGE IN ROUND AND FLAT TUBES WHEN THE WALL TEMPERATURE VARIES IN TIME

We shall consider nonstationary heat exchange in round and flat

t bes for stationary stabilized flow of the fluid with a parabolic velocity profile. We assume that the wall temperature at any time is constant over the surface. At the initial instant, let the temperature field in the fluid flow be uniform and let the wall temperature equal the fluid temperature t_0 at the entrance, so that there

is no heat exchange. At the next instant, the wall temperature changes abruptly, taking on a new constant value $t_s \neq t_0$. Here a

nonstationary temperature field will appear in the flow together with a nonstationary heat-exchange process; these are the subjects of investigation. Siegel [1] has solved this problem for round and flat tubes, and subsequently generalized it to more complicated conditions.

We shall henceforth assume that the physical properties of the fluid are constant, that there are no internal heat sources or energy dissipation in the flow, and that the variation in heat flow along the axis owing to conduction is negligibly small.

1. We first consider the problem of heat exchange in a round tube. Here the energy equation has the form

$$\frac{\partial t}{\partial \tau} + w_x \frac{\partial t}{\partial x} = a \frac{1}{r} \frac{\partial}{\partial r} \left(r \frac{\partial t}{\partial r} \right)$$

Substituting $w_x = 2\bar{w} \left(1 - \frac{r^2}{r_0^2} \right)$ into this equation and introducing the dimensionless variables

$$T = \frac{t - t_0}{t_c - t_0}, \quad Fo = \frac{a\tau}{r_0^2},$$

$$X = \frac{1}{Pe} \frac{x}{r_0}, \quad Pe = \frac{\bar{w} 2 r_0}{a} \text{ and } R = \frac{r}{r_0},$$

we obtain

$$\frac{\partial T}{\partial Fo} + (1 - R^2) \frac{\partial T}{\partial X} = \frac{1}{R} \frac{\partial}{\partial R} \left(R \frac{\partial T}{\partial R} \right), \tag{17-1}$$

where Fo is the Fourier number, which has the meaning of the dimensionless time.

The initial condition is

$$T(X, R, 0) = 0. \tag{17-2}$$

The boundary conditions at the entrance, on the tube axis, and at the wall are

$$\begin{aligned} &T(0, R, Fo) = 0; \\ &\left(\frac{\partial T}{\partial R} \right)_{R=0} = 0; \\ &T(X, 1, Fo) = 1. \end{aligned} \right\} \tag{17-3}$$

A solution of the corresponding stationary problem, i.e., Eq. (17-1) for the case $\partial T / \partial Fo = 0$ under boundary conditions (17-3), will be found in §6-1. This solution has the form

$$T_e = 1 - \sum_{n=0} A_n \psi_n(R) e^{-\varepsilon_n^2 X}, \qquad (17\text{-}4)$$

where ε_n and $\psi_n(R)$ are the eigenvalues and eigenfunctions of the Sturm–Liouville problem for Eq. (6-7) under the boundary conditions $\psi'(0) = 0$ and $\psi(1) = 0$. The A_n are constants determined from Eqs. (6-16) or (6-19). The values of ε_n^2 and A_n are given in Table 6-2.

We seek a solution of the nonstationary problem in the form

$$T = 1 - \sum_{n=0}^{\infty} A_n \psi_n(R) \varphi_n(X, \text{Fo}). \qquad (17\text{-}5)$$

When Fo (or τ) is sufficiently large, the unknown function $\varphi_n(X, F_0)$ will obviously take the form

$$\varphi_n = e^{-\varepsilon_n^2 X}.$$

In general, (17-5) must satisfy (17-1). We confine the discussion to the approximate solution of the problem, however, only requiring that it satisfy the energy equation in integral form, which can be obtained from (17-1) if we multiply it by $R\,dR$ and integrate between $R = 0$ and $R = 1$:

$$\int_0^1 R \frac{\partial T}{\partial \text{Fo}} dR + \int_0^1 R(1 - R^2) \frac{\partial T}{\partial X} dR = \left(\frac{\partial T}{\partial R}\right)_{R=1}. \qquad (17\text{-}6)$$

We then obtain the following partial differential equation for φ_n:

$$\frac{\partial \varphi_n}{\partial \text{Fo}} \int_0^1 \psi_n R\,dR + \frac{\partial \varphi_n}{\partial X} \int_0^1 \psi_n (1 - R^2) R\,dR - \varphi_n \left(\frac{d\psi_n}{dR}\right)_{R=1} = 0. \qquad (17\text{-}7)$$

Using the method of characteristics[1] to solve this equation, we write the characteristic system of ordinary differential equations corresponding to (17-7):

$$\frac{d\text{Fo}}{\int_0^1 \psi_n R\,dR} = \frac{dX}{\int_0^1 \psi_n (1-R^2) R\,dR} = \frac{d\varphi_n}{\varphi_n \left(\frac{d\psi}{dR}\right)_{R=1}}. \qquad (17\text{-}8)$$

Integrating the equation formed by the last two expressions of (17-8) with respect to X, under the condition that $\varphi_n = 1$ when $X = 0$, we have

$$\varphi_n = \exp\left[\frac{\left(\frac{d\psi_n}{dR}\right)_{R=1}}{\int_0^1 \psi_n (1 - R^2) R\,dR} X \right]. \qquad (17\text{-}9)$$

After integration with respect to Fo under the condition that $\varphi_n = 1$ when Fo $= 0$, the equation formed by the first and third ex-

pressions of (17-8) yields

$$\varphi_n = \exp\left[\frac{\left(\frac{d\psi_n}{dR}\right)_{R=1}}{\int_0^1 \psi_n R\, dR} \text{Fo}\right]. \qquad (17\text{-}10)$$

According to (17-9), φ_n is a function of X alone, while according to (17-10), φ_n depends on Fo alone. The method of characteristics shows that the two equations join along the limiting characteristic line, which passes through the origin in the X-Fo plane. The equation of this line is easily obtained by integrating the first equation of (17-9):

$$\text{Fo} = \left[\frac{\int_0^1 \psi_n R\, dR}{\int_0^1 \psi_n (1-R^2) R\, dR}\right] X = a_n X, \qquad (17\text{-}11)$$

where a_n is the ratio of the integrals in brackets. Equation (17-9) is valid along characteristics cutting the positive Fo axis in the Fo-X plane, while (17-10) is valid along characteristics cutting the positive X axis in this same plane.

After multiplication by $R\, dR$ and integration between $R = 0$ and $R = 1$, we find from (6-7) (see §6-1):

$$\epsilon_n^2 = -\frac{\left(\frac{d\psi_n}{dR}\right)_{R=1}}{\int_0^1 \psi_n (1-R^2) R\, dR}.$$

In addition,

$$\frac{\epsilon_n^2}{a_n} = -\frac{\left(\frac{d\psi_n}{dR}\right)_{R=1}}{\int_0^1 \psi_n R\, dR}.$$

Comparing this expression with (17-9) and (17-10) and considering what has been said previously, we find

$$\varphi_n = \exp(-\gamma_n \text{Fo}) \text{ for } \text{Fo} \leq a_n X,$$
$$\varphi_n = \exp(-\epsilon_n^2 X) \text{ for } \text{Fo} \geq a_n X,$$

where $\gamma_n = \frac{\epsilon_n^2}{a_n}$.

Substituting these values of φ_n into (17-5), we obtain

$$T = \sum A_n \psi_n(R) \times \begin{cases} e^{-\gamma_n \text{Fo}}, & \text{Fo} \leq a_n X; \\ e^{-\epsilon_n^2 X}, & \text{Fo} \geq a_n X. \end{cases} \qquad (17\text{-}12)$$

It is not difficult to verify that (17-12) also satisfies initial condition (17-2) and the boundary conditions (17-3) and, consequently, is a solution of the problem. When Fo is sufficiently large, (17-12) goes over to Eq. (17-4) for stationary heat exchange. The eigenfunctions ψ_n and constants ε_n^2 and A_n in (17-12), as we have already noted, have the same values as in the solution for the stationary problem (see Tables 6-1 and 6-2). Table 17-1 gives the first seven values of the constants γ_n and a_n required for calculations using (17-12) and the subsequent equations.

Using the Fourier law and Eq. (17-12), we obtain an expression for the dimensionless heat-flux density at the wall:

$$\frac{q \cdot r_0}{\lambda(t_c - t_0)} = -\sum_{n=0}^{\infty} A_n \left(\frac{d\psi_n}{dR}\right)_{R=1} \times \left\{ \begin{array}{l} e^{-\gamma_n \, Fo}, \ Fo < a_n X; \\ e^{-\varepsilon_n^2 X}, \ Fo > a_n X. \end{array} \right\} \quad (17\text{-}13)$$

The values of the constant $B_n = -\frac{1}{2} A_n \left(\frac{d\psi_n}{dR}\right)_{R=1}$ are given in Table 6-2.

TABLE 17-1

Values of Constants γ_n and a_n in Problem of Nonstationary Heat Exchange in a Round Tube Under an Abrupt Change in Wall Temperature

n	γ_n	a_n
0	5,1540	1,4190
1	16,262	2,7432
2	29,918	3,8078
3	45,392	4,7418
4	62,327	5,5925
5	80,324	6,3963
6	99,592	7,1403
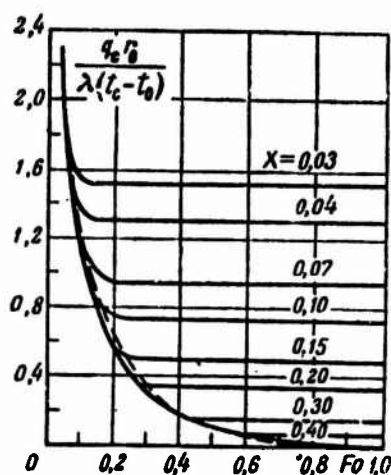
Fig. 17-1. Heat-flux density at wall of round tube under abrupt change in wall temperature.

As we can see, the left side of the equation is the local Nusselt number, in which the heat-transfer coefficient refers to the initial temperature head.

The solid lines on Fig. 17-1 show curves computed from Eq. (17-13). The nature of the curves becomes clear when we look at the heat-exchange process during the time directly following the wall-temperature jump. At those tube cross sections that have not been reached by fluid located outside the heated segment of the tube prior to the jump, the temperature will change only in time and along

the radius, remaining constant along the length $[(\partial T/\partial X)=0]$. At these sections, the heat transfer will be independent of the conditions at the entrance, and will vary only in time, in accordance with the top line of Eq. (17-13). In other words, here heat transfer takes place as if the fluid were stationary, i.e., in accordance with pure heat conduction. Actually, when $\partial T/\partial X = 0$, the energy equation (17-1) goes over to the heat-conduction equation, which has a familiar solution for the case in which there is an abrupt change in the wall temperature, which is constant along the surface [3]. This solution leads to the following equation for the heat-flux density at the wall:

$$\frac{q_c r_0}{\lambda\,(t_c - t_0)} = 2 \sum_{n=0}^{\infty} e^{-\mu_n^2\,Fo},$$

(17-14)

where the μ_n are roots of a zero-order Bessel function of the first kind.[2]

Equation (17-14), obtained by solving the exact differential equation, is in good agreement with (17-13) (top line), which was obtained by solving the integral relationship. This is quite clear from Fig. 17-1, where Eq. (17-14) is represented by the dashed line.

In tube cross sections that have been reached by fluid located outside the heating segment prior to the jump in t_s, the heat transfer varies both along the X coordinate and in time. This type of relationship is maintained until stationary conditions set in.

Fig. 17-2. Time at which stationary regime sets in for round tube under abrupt change in wall temperature. 1) Eq. (17-13); 2) $Fo_s = 2X$; 3) $Fo_s = X$.
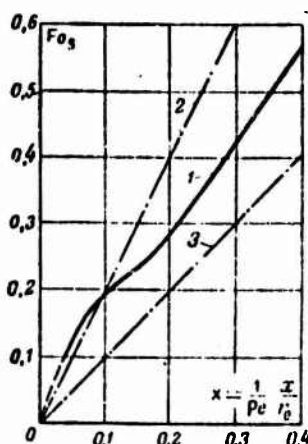
The time τ_s (or $Fo_s = a\tau_s/r_0^2$ in dimensionless form) at which the stationary regime sets in can be determined as the time that must elapse for the heat flux at the wall to differ by no more than

[2]/496

5% from its value at $\tau \to \infty$. Figure 17-2 shows the relationship between Fo_s and X, found with the aid of (17-13). The same figure shows the approximate relationships $Fo_s = 2X$ and $Fo_s = X$, obtained from the selfevident relationships $\tau_s = x/\bar{w}$ and $\tau_s = x/w_0$ (where $w_0 = 2\bar{w}$ is the velocity on the tube axis) after conversion to dimensionless form.

Example. Consider isothermal flows in a tube with diameter $d = 5$ mm of transformer oil ($a = 2.5 \cdot 10^{-4}$ m²/h), water ($a = 5.63 \cdot 10^{-4}$ m²/h), or air ($a = 9.0 \cdot 10^{-2}$ m²/h) at Pe = 1000. At a certain time, the wall temperature changes abruptly. We are to determine the time that has elapsed after the jump when the stationary state sets in at a distance $x = 50d$ from the entrance.

In this case, $\frac{1}{Pe} \cdot \frac{x}{r_0} = 0,1$. As we can see from Fig. 17-2, this value corresponds to $Fo_x = \frac{a\tau_s}{r_0^2} \approx 0,2$. Thus we find that for transformer oil the stationary regime commences after $\tau_s = 18$ s, for water after 8 s, and for air after 0.05 s.

———

The solution for a single wall-temperature jump can be generalized to an arbitrary variation in t_s with time. Let $\vartheta_s = t_s - t_0$ be be a certain arbitrary time function, as shown in Fig. 17-3a, and let $t_0 = $ const. We represent the curve for ϑ_s(Fo) as a set of infinitesimal temperature jumps $d\vartheta_s$. For each such jump occurring at time Fo_*, we can determine the change in heat-flux density at the wall, using Eq. (17-13):

$$dq_c = -\frac{\lambda}{r_0} \sum_{n=0}^{\infty} A_n \left(\frac{d\psi_n}{dR}\right)_{R=1} \times$$
$$\times \left\{ \begin{array}{l} \exp[-\gamma_n(Fo - Fo_*)], \ 0 < (Fo - Fo_*) \leqslant a_n X \\ \exp[-\varepsilon_n^2 X], \ (Fo - Fo_*) \ a_n X \end{array} \right\} d\vartheta_c. \qquad (17\text{-}15)$$

Since the energy equation is linear, we can obtain an expression for q_s with an arbitrary change in ϑ_s in time by summation of the elementary step changes in dq_s or, in the limit, by integrating (17-15) over the ϑ_s curve.[3] Integrating, after certain manipulations we obtain

$$\frac{q_c r_0}{\lambda}(Fo, X) = \sum_{n=0}^{n=N-1} -A_n \left(\frac{d\psi_n}{dR}\right)_{R=1} \left\{ \exp(-\varepsilon_n^2 X)(\vartheta_c)_{Fo - a_n X} + \int_{Fo - a_n X}^{Fo} \right.$$
$$\left. -\gamma_n \exp[-\gamma_n(Fo - Fo_*)]\vartheta_c(Fo_*)\,dFo_* \right\} + \qquad (17\text{-}16)$$
$$+ \sum_{n=N}^{\infty} \gamma_n A_n \left(\frac{d\psi_n}{dR}\right)_{R=1} \int_0^{Fo} \exp[-\gamma_n(Fo - Fo_*)]\vartheta_c(Fo_*)\,dFo_*,$$

where for a given value of Fo, N is found from the relationship

$$a_{N-1} X < Fo \leqslant a_N X. \qquad (17\text{-}17)$$

For $N = 0$, the first sum $\sum_{n=0}^{-1} = 0$, while the constant $a_{-1} = 0$.
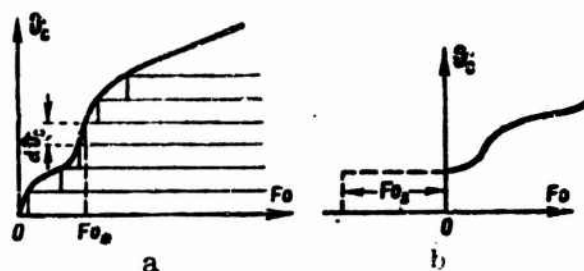
Fig. 17-3. Time variation in wall temperature. a) Case in which $\vartheta_s = 0$ at Fo = 0; b) case in which $\vartheta_s \neq 0$ at Fo = 0.

The heat-flux density q_s is calculated as a function of time for a particular value of X, for example, for $X = X_i$. As long as the time that has elapsed since the beginning of the process is short, Fo will be less than any value of $a_n X_i$ $(n=0, 1, ..., i)$; consequently $N = 0$, and only the term containing the second sum from $n = 0$ to ∞ remains in Eq. (17-16). As the time increases, an ever greater number of terms is associated with the first sum. For the given problem, we need only consider seven terms of the series, since when the time is so great that Fo > $a_6 X_i$, only the term containing the first sum will remain in (17-16).

The preceding calculations were carried out on the assumption that at the initial instant, the temperature field in the fluid flow is uniform ($\vartheta_s = 0$ and, consequently, there is no heat exchange). If there is a stationary heat-exchange process at the initial instant ($\vartheta_s \neq 0$, see Fig. 17-3b), and the wall temperature later changes abruptly, the calculations should be carried out as if there had been no heat exchange ($\vartheta_s = 0$) at a certain time preceding the initial instant; the wall-temperature jump occurred later, and during a certain sufficiently long time, this temperature remained constant, so that at $\tau = 0$ a stationary state was reached; subsequently, the wall temperature again began to vary in accordance with the specified law. Using this scheme and the method discussed above, we can determine the nonstationary heat exchange for transition from one stationary state to another.

2. We turn to the problem of nonstationary heat exchange in a flat tube under an abrupt change in wall temperature, on the assumption that the temperature field is uniform at the initial instant ($t_s = t_0$). In this case, the energy equation can be written in the following form after substitution of Expression (5-11) for the velocity profile:

$$\frac{\partial T}{\partial \text{Fo}} + (1 - Y^2)\frac{\partial T}{\partial X} = \frac{\partial^2 T}{\partial Y^2}. \qquad (17-18)$$

where $T = \frac{t - t_o}{t_* - t_o}$; $Fo = \frac{a\tau}{r_o^2}$; $X = \frac{4}{3}\frac{1}{Pe}\frac{x}{r_o}$; $Pe = \frac{\bar{w}2r_o}{a}$; $Y = \frac{y}{r_o}$; $2r_o$ is the width of the flat tube.

TABLE 17-2

Values of Constants ζ_n, η_n, and f_n in the Problem of Nonstationary Heat Exchange in a Flat Tube with Abrupt Change in Wall Temperature (Approximation Using five Terms of Series)

n	ζ_n	η_n	f_n
0	2.30858	2.82948	1.22564
1	11.9441	32.3656	2.70975
2	24.9156	95.2824	3.82421
3	37.4251	178.074	4.75764
4	92.5892	608.811	6.57754

The initial and boundary conditions have the form

$$\left.\begin{array}{l} T(X, Y, 0) = 0; \\ T(0, Y, Fo) = 0; \\ \left(\frac{\partial T}{\partial Y}\right)_{Y=0} = 0; \\ T(X, \pm 1, Fo) = 1. \end{array}\right\} \quad (17\text{-}19)$$

As in the round-tube case, to solve this nonstationary problem we use Solution (6-47), corresponding to the stationary problem. If we go from the temperature θ to the temperature T, this solution will have the form

$$T_* = 1 - \sum_{n=0}^{4} b_{n\circ} e^{-\epsilon_n^2 X}\left[\cos\frac{\pi Y}{2} + \sum_{m=1}^{4} \frac{b_{nm}}{b_{n\circ}}\cos\frac{(2m+1)\pi Y}{2}\right]. \quad (17\text{-}20)$$

where ϵ_n^2 and b_{nm} are constants (see Table 6-5).

We represent the solution of the nonstationary problem in the form

$$T = 1 - \sum_{n=0}^{4} b_{n\circ} G_n(X, Fo)\left[\cos\frac{\pi Y}{2} + \sum_{m=1}^{4} \frac{b_{nm}}{b_{n\circ}}\cos\frac{(2m+1)\pi Y}{2}\right]. \quad (17\text{-}21)$$

Substituting this expression into the integral equation for the energy

$$\frac{\partial}{\partial Fo}\int_0^1 T\,dY + \frac{\partial}{\partial X}\int_0^1 (1 - Y^2)T\,dY = -\left(\frac{\partial T}{\partial Y}\right)_1,$$

which can be obtained from (17-18), we find the partial differential equation for the function G_n; it is similar in form to Eq. (17-7). Solving this equation by the method of characteristics, we arrive at the final expression for the temperature:

$$T = 1 - \sum_{n=0}^{4} b_{n\circ}\left[\cos\frac{\pi Y}{2} + \sum_{m=1}^{4} \frac{b_{nm}}{b_{n\circ}}\cos\frac{(2m+1)\pi Y}{2}\right] \times$$

$$\times \left\{\begin{array}{l} \exp(-\zeta_n Fo), \quad Fo \lesssim f_n X \\ \exp(-\eta_n X), \quad Fo \gtrsim f_n X \end{array}\right\}. \quad (17\text{-}22)$$

where

- 453 -

$$\zeta_n = \frac{\pi^2}{4} \frac{\left[1 + \sum_{m=1}^{4} (2m+1)(-1)^m \frac{b_{nm}}{b_{n0}}\right]}{\left[1 + \sum_{m=1}^{4} \frac{1}{(2n+1)} (-1)^m \frac{b_{nm}}{b_{n0}}\right]},$$

$$\eta_n = \frac{\pi^4}{32} \frac{\left[1 + \sum_{m=1}^{4} (2m+1)(-1)^m \frac{b_{nm}}{b_{n0}}\right]}{\left[1 + \sum_{m=1}^{4} \frac{1}{(2m+1)^3} (-1)^m \frac{b_{nm}}{b_{n0}}\right]}$$

TABLE 17-3

Values of Constants in Problem of Nonstationary Heat Exchange in Flat Tube Under Abrupt Change in Wall Temperature (Approximation Using Three Terms of Series)

n	b_{n0}	$\frac{b_{n1}}{b_{n0}}$	$\frac{b_{n2}}{b_{n0}}$	ϵ_n^2	ζ_n	η_n	l_n
0	1,18025	0,0211847	—0,00114101	2,82777	2,31337	2,83546	1,22568
1	0,0589906	—5,37097	—0,842957	32,1508	12,1389	32,9332	2,71304
2	0,0339989	—3,89954	8,99210	104,683	34,7142	144,296	4,15668
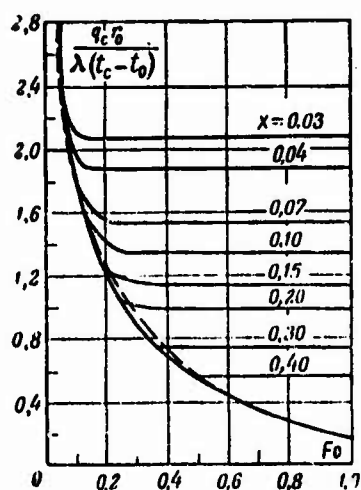
Fig. 17-4. Heat-flux density at wall of flat tube under abrupt change in wall temperature.
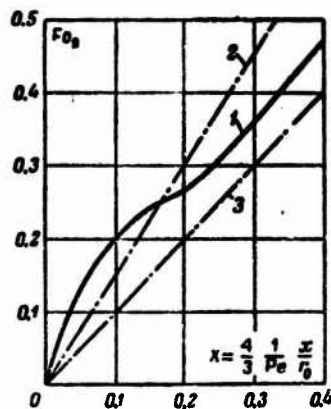
Fig. 17-5. Time at which stationary regime sets in for flat tube under abrupt change in wall temperature. 1) Eq. (17-23); 2) $Fo_s = 3X/2$; 3) $Fo_s = X$.

and

$$f_n = \frac{\eta_n}{\zeta_n}.$$

Using the Fourier law and Eq. (17-22), we obtain an expression for the dimensionless heat-flux density at the wall:

$$\frac{q_c r_0}{\lambda (t_c - t_0)} = \frac{\pi}{2} \sum_{n=0}^{4} b_{n_0} \left[1 + \sum_{m=1}^{4} \frac{b_{nm}}{b_{n_0}} (-1)^m (2m+1) \right] \times$$

$$\times \left\{ \begin{array}{l} \exp(-\zeta_n Fo), \ Fo \leqslant f_n X \\ \exp(-\eta_n X), \ Fo > f_n X \end{array} \right\}.$$

(17-23)

The constants in (17-20), (17-22), and (17-23) were determined by computer. Their values are given in Tables 6-5 and 17-2 for approximation by five terms of the series, and in Table 17-3 for approximation by three terms.

The curves calculated from Eq. (17-23) are shown in Fig. 17-4 by the solid line. The same figure uses the dashed line to show the curve corresponding to the equation

$$\frac{q_c r_0}{\lambda (t_c - t_0)} = 2 \sum_{n=0}^{\infty} \exp \left[-(2n+1)^2 \frac{\pi^2}{4} Fo \right],$$

(17-24)

obtained from the familiar solution to the problem of nonstationary heat conduction in an infinite plate of thickness $2r_0$ under boundary conditions of the first kind.
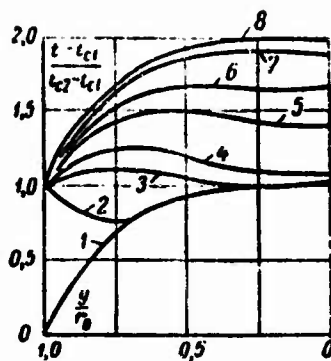
Fig. 17-6. Temperature distribution in fluid flow in flat tube for values of Fo $= a/r_0^2$ equaling: $1 - 0;\ 2 - 0.01;\ 3 - 0.05;\ 4 - 0.1;\ 5 - 0.3;\ 6 - 0.5;\ 7 - 1.0;\ 8 - \infty$

Figure 17-5 shows the time Fo_s required for the stationary regime to set in as a function of X, calculated from Eq. (17-23) under the condition that $(q_c)_{\tau=\tau_s} = 1.05(q_c)_{\tau=\infty}$. For comparison, the same fig re gives $Fo_s = \frac{3}{2}X$ and $Fo_s = X$. The curves of Figs. 17-4 and 17-5 are the same in nature as for heat exchange in a round tube.

The solution given here to the problem can be generalized to the case of an arbitrary variation in wall temperature with time (both for $t_s = t_0$ and for $t_s \neq t_0$ when $\tau = 0$), as was done for the round tube in paragraph 1.

Sadikov [5] has considered certain problems involving heat exchange in round and flat tubes under an abrupt variation for harmonic oscillation in wall temperature with time. All of these problems pertain to the case in which the heat appearing in the flow owing to energy dissipation is completely removed through the walls, while the velocity and temperature profiles are developed, so that the velocity and temperature do not vary with the length.[4] In this case, the energy equation reduces to the equation for heat conduction with heat sources. As an example, Fig. 17-6 shows temperature profiles in a fluid flow in a flat tube at various times after the stationary state was disturbed by an instantaneous change in wall temperature from t_{s1} to t_{s2}.

17-3. HEAT EXCHANGE IN THERMAL INITIAL SEGMENT OF FLAT AND ROUND TUBES WHEN WALL TEMPERATURE VARIES IN TIME

In this section, we shall consider the same problem as in the preceding section, but for the region of the thermal initial segment.[5] Adopting this restriction and using the approximate method of bound. ry-layer theory in conjunction with the method of characteristics, we can obtain simple analytic expressions for the heat transfer under nonstationary conditions.

1. As the initial problem, let us analyze heat exchange in a flat tube for the case in which there is no heat exchange at the initial instant ($t_s = t_0$), while the wall temperature later changes abruptly, taking on a constant value $t_s \neq t_0$.
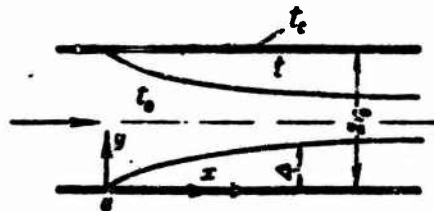
Fig. 17-7. Problem of nonstationary heat exchange in the thermal initial segment of a flat tube.

Under these conditions, the energy equation for the nonstationary temperature field will have the form

$$\frac{\partial t}{\partial \tau} + w_x \frac{\partial t}{\partial x} = a \frac{\partial^2 t}{\partial y^2}. \qquad (17\text{-}25)$$

The flow in the tube can be divided into two regions (Fig. 17-7): a thermal boundary layer of thickness Δ that depends on X and τ, and a core whose temperature is constant and equal to the entrance temperature t_0.

Integrating (17-25) with respect to y between 0 and Δ (for details, see §12-4), we obtain

$$\frac{\partial}{\partial \tau} \int_0^\Delta (t - t_0) \, dy + \frac{\partial}{\partial x} \int_0^\Delta w_x (t - t_0) \, dy = -a \left[\frac{\partial (t - t_0)}{\partial y} \right]_{y=0}. \qquad (17\text{-}26)$$

To solve this equation, we specify the temperature distribution over the boundary-layer thickness as the polynomial $t = b_0 + b_1 y + b_2 y^2 + b_3 y^3$, whose coefficients can be found from the boundary conditions

$$\text{For } \tau > 0 \text{ and } y = 0 \quad t = t_c, \quad \frac{\partial^2 t}{\partial y^2} = 0;$$

$$\text{For } \tau > 0 \text{ and } y = \Delta \quad t = t_0, \quad \frac{\partial t}{\partial y} = 0.$$

With allowance for the first boundary condition, the second boundary condition follows from (17-25) when $y = 0$.

As a result, we obtain

$$\frac{t - t_0}{t_s - t_0} = 1 - \frac{3}{2} \left(\frac{y}{\Delta} \right) + \frac{1}{2} \left(\frac{y}{\Delta} \right)^3 \quad (\tau > 0, \; 0 \leqslant y \leqslant \Delta). \qquad (17\text{-}27)$$

We have a Poiseuille velocity distribution:

$$\frac{w_x}{w} = \frac{3}{2} \left[2 \left(\frac{y}{r_0} \right) - \left(\frac{y}{r_0} \right)^2 \right]. \qquad (17\text{-}28)$$

- 457 -

Substituting (17-27) and (17-28) into (17-26) and integrating, we obtain the partial differential equation for the thickness Δ of the thermal boundary layer, depending on x and τ. In dimensionless form, this equation looks like this:

$$\frac{\tilde{\Delta}}{4}\frac{\partial\tilde{\Delta}}{\partial Fo}+\left(\frac{4}{15}\tilde{\Delta}^2-\frac{1}{12}\tilde{\Delta}^3\right)\frac{\partial\tilde{\Delta}}{\partial X}=1. \tag{17-29}$$

where

$$\tilde{\Delta}=\frac{\Delta}{r_0}; \quad Fo=\frac{a\tau}{r_0^2}; \quad X=\frac{4}{3}\frac{1}{Pe}\frac{x}{r_0}; \quad Pe=\frac{\bar{w}2r_0}{a}.$$

Solving (17-29) by the method of characteristics, we write the characteristic system of ordinary differential equations corresponding to (17-29):

$$\frac{dFo}{\frac{1}{4}\tilde{\Delta}}=\frac{dX}{\frac{4}{15}\tilde{\Delta}^2-\frac{1}{12}\tilde{\Delta}^3}=d\tilde{\Delta}. \tag{17-30}$$

or

$$\left(\frac{16}{15}\tilde{\Delta}-\frac{1}{3}\tilde{\Delta}^2\right)dFo=dX, \tag{17-30a}$$

$$\frac{1}{4}\tilde{\Delta}d\tilde{\Delta}=dFo, \tag{17-30b}$$

$$\left(\frac{4}{15}\tilde{\Delta}^2-\frac{1}{12}\tilde{\Delta}^3\right)d\tilde{\Delta}=dX. \tag{17-30c}$$

Integrating (17-30b) under the condition that $\tilde{\Delta}=0$ for $Fo=0$ (for any X), we find

$$\tilde{\Delta}=(8Fo)^{1/2}. \tag{17-31}$$

Integrating (17-30c) under the condition that $\tilde{\Delta}=0$ for $X=0$ (for any Fo), we obtain

$$\frac{4}{45}\tilde{\Delta}^3-\frac{1}{48}\tilde{\Delta}^4=X. \tag{17-32}$$

Equation (17-31) is valid along characteristics intersecting the positive X axis on the X-Fo plane. Along these characteristics, Δ depends solely on Fo. Equation (17-32) is valid along characteristics intersecting the positive Fo axis on the same plane. Along these lines, Δ depends solely on X and, consequently, Eq. (17-32) corresponds to the limiting case of stationary heat exchange. The two equations join along the limiting characteristic, which passes through the origin and divides the X-Fo plane into two regions (Fig. 17-8). The region lying below the limiting characteristic correspond to nonstationary heat exchange, and the region lying above to stationare exchange. Consequently, the equation of the limiting characteristic determines the time Fo_s required for the stationary state to be reached for any value of X. Substituting the value of $\tilde{\Delta}$ from (17-31) into (17-30a) and integrating, we find this equation:

$$\frac{64}{45}\sqrt{2}Fo_s^{3/2}-\frac{4}{3}Fo_s^2=X. \tag{17-33}$$

Figure 17-9 illustrates the relationship between Fo_s and X (curve 1).

Using the Fourier law and Eq. (17-27), we find an expression for the heat-flux density at the wall (or the local Nusselt number):

$$\frac{q_c 2r_0}{(t_c - t_s)\lambda} = \frac{3}{\tilde{\Delta}}. \tag{17-34}$$

Substituting in the value of $\tilde{\Delta}$ from (17-31), we finally obtain

$$\left.\begin{array}{l} \frac{q_c 2r_0}{(t_c - t_s)\lambda} = \frac{3}{2\sqrt{2}} Fo^{-1/2}, \quad Fo < Fo_s; \\[2mm] \frac{q_s 2r_0}{(t_c - t_s)\lambda} = \frac{3}{2\sqrt{2}} Fo_s^{-1/2}, \quad Fo > Fo_s. \end{array}\right\} \tag{17-35}$$

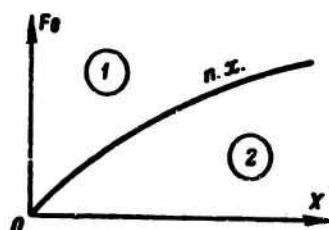Fig. 17-8. Limiting characteristic [l.c.] (п.х.) on X-Fo plane. 1) Steady-state region; 2) nonsteady-state region.
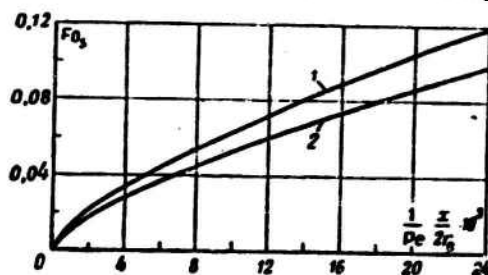
Fig. 17-9. Time of onset of steady-state regime in thermal initial segment of flat (1) and round (2) tubes with jumpwise changes in wall temperature.

Here Fo_s depends on X, and is found from Eq. (17-33) for Fig. 17-9.

An expression for q_s when $Fo > Fo_s$, i.e., under stationary con-

d'tions, can also be obtained if we substitute the value of $\tilde{\Delta}$ from (17-32) into (17-34). If in (17-32), we neglect the second term c the left side, which is permissible when $\tilde{\Delta} \ll 1$, we obtain the following equation for q_s:

$$\frac{q_c 2r_0}{(t_s - t_0)\lambda} = 0.965 \left(\frac{1}{Pe} \cdot \frac{x}{2r_0} \right)^{-1/3}.$$

This is nearly the same as the Leveque equation (6-57) for a flat tube (the constants differ by only 1.3%).

Compar:n the results of heat-transfer calculations using the method of characteristics with results obtained by direct numerical integration cf Eq. (17-25), we see that the discrepancy between them does not exceed 5%. Just as good agreement is obtained for the time required to establish the stationary state.

Equation (17-35) representing the response of the heat flux to a single jump in wall temperature (when there is no heat exchange at the initial instant), can be generalized to the case of arbitrary variation in wall temperature with time. As we have already noted, this generalization is possible in virtue of the linearity of the energy equation.

The change in heat-flux density dq_s caused by an elementary wall-temperature jump at time Fo* (see Fig. 17-3a) will equal

$$dq_c = \frac{3}{4\sqrt{2}} \frac{\lambda}{r_0} (Fo - Fo_*)^{-1/2} d\vartheta_c, \quad Fo - Fo_* < Fo_s; \\ dq_c = \frac{3}{4\sqrt{2}} \frac{\lambda}{r_0} Fo_*^{-1/2} d\vartheta_c, \quad Fo - Fo_* \geqslant Fo_s,$$

(17-36)

where $\vartheta_c = t_c - t_0$; $t_0 = \text{const}$.

For an arbitrary variation in ϑ_s with time, the response of the heat-flux density at the wall is found by integrating Eq. (17-36):

$$q_c(X, Fo) = \frac{3}{4\sqrt{2}} \frac{\lambda}{r_0} \int_0^{Fo} \frac{d\vartheta_c}{dFo_*} (Fo - Fo_*)^{-1/2} dFo_*, \quad Fo < Fo_s; \\ q_c(X, Fo) = \frac{3}{4\sqrt{2}} \frac{\lambda}{r_0} \left[Fo_*^{-1/2} (\vartheta_c)_{Fo - Fo_s} + \right. \\ \left. + \int_{Fo - Fo_s}^{Fo} \frac{d\vartheta_c}{dFo_*} (Fo - Fo_*)^{-1/2} dFo_* \right], \quad Fo \quad Fo_s.$$

(17-37)

For example, let the wall temperature vary linearly in time, i.e., $\vartheta_c = AFo$, where $A = \text{const}$. Substitution of this expression into (17-37) yields

$$q_c = \frac{3}{2\sqrt{2}} \frac{\lambda}{r_0} AFo^{1/2}, \quad Fo < Fo_s; \\ q_c = \frac{3}{4\sqrt{2}} \frac{\lambda}{r_0} AFo_s^{-1/2} (Fo + Fo_s), \quad Fo \quad Fo_s.$$

Equations (17-37) are also valid when the specified variation

in $_s$ contains jumps. Let us assume that there is a jump equaling $\Delta_{s,i}$ at $Fo = Fo_i$. In such case, we use the ordinary method to evaluate the integrals everywhere except for Fo_i, where we add the additional term

$$\frac{3}{4\sqrt{2}} \cdot \frac{\lambda}{r_*} (Fo - Fo_i)^{-1/2} \Delta \vartheta_{ci}.$$

If $Fo_i < Fo - Fo_s$, we do not add this term to the second equation of (17-37), since here the first term on the right side of this equation automatically allows for the influence of the jump.

Let us look at the case in which there is stationary heat exchange in the system at the initial instant (i.e., $\tau = 0$ $t_c \neq t_0$), and the wall temperature then begins to vary arbitrarily in time (see Fig. 17-3b). In this case, we proceed from the assumption that during the time preceding the initial instant (i.e., for $Fo < 0$), there exists a certain fictitious transient, appearing when $t_c = t_0$ and terminating in the stationary state at $Fo = 0$. For this state to be attained, the duration of the transient must obviously equal Fo_s. Considering the fictitious and actual processes jointly, and using the results of the preceding analysis, we can write

$$
\left.
\begin{aligned}
q_c(X, Fo) &= \frac{3}{4\sqrt{2}} \frac{\lambda}{r_*} \left[Fo_*^{-1/2} (\theta_c)_{Fo=0} + \right. \\
&\quad + \left. \int_0^{Fo} \frac{d\vartheta_c}{dFo_*} (Fo - Fo_*)^{-1/2} d Fo_* \right], \ Fo < Fo_s; \\
q_c(X, Fo) &= \frac{3}{4\sqrt{2}} \frac{\lambda}{r_*} \left[Fo_*^{-1/2} (\theta_c)_{Fo-Fo_s} + \right. \\
&\quad + \left. \int_{Fo-Fo_*}^{Fo} \frac{d\vartheta_c}{dFo_*} (Fo - Fo_*)^{-1/2} d Fo_* \right], \ Fo \ Fo_s.
\end{aligned}
\right\}
\qquad (17\text{-}38)
$$

2. For a nonstationary regime in the thermal initial segment of a round tube, the heat exchange can be determined by the same method used in the initial segment of a flat tube.

We take as the basic case the situation in which there is no heat exchange at the initial instant ($t_c = t_0$), and at a subsequent instant the wall temperature varies abruptly, taking on a constant value $t_c \neq t_0$.

The energy equation for the nonstationary temperature field will have the following form in this case:

$$\frac{\partial t}{\partial \tau} + w_x \frac{\partial t}{\partial x} = a \frac{1}{r} \frac{\partial}{\partial r} \left(r \frac{\partial t}{\partial r} \right). \qquad (17\text{-}39)$$

Going from the variable r to the variable $y = r_0 - r$ and integrating (17-39) between 0 and Δ, where Δ is a function of x and τ, we obtain

$$\frac{\partial}{\partial \tau} \int_0^\Delta (r_\bullet - y)(t - t_\bullet)\,dy + \frac{\partial}{\partial x} \int_0^\cdot (r_\bullet - y)\,w_x(t - t_\bullet)\,dy =$$

$$= -ar_\bullet \left[\frac{\partial(t - t_\bullet)}{\partial y}\right]_{y=0}.$$

(17-40)

To solve this equation, we must know the distributions of w_x and t over the cross section of the thermal boundary layer Δ.

We know the distribution of w_x

$$\frac{w_w}{w} = 2\left(2\frac{y}{r_0} - \frac{y^2}{r_0^2}\right).$$

(17-41)

The distribution of t is represented as the polynomial

$$t = b_0 + b_1 y + b_2 y^2 + b_3 y^3,$$

whose coefficients are determined from the boundary conditions:

$$\text{for } \tau > 0 \text{ and } y = 0 \quad t = t_c, \quad \frac{\partial}{\partial y}\left[(r_\bullet - y)\frac{\partial t}{\partial y}\right] = 0;$$

$$\text{for } \tau > 0 \text{ and } y = \Delta \quad t = t_\bullet, \quad \frac{\partial t}{\partial y} = 0.$$

The second boundary condition follows from Eq. (17-39) when we consider that $w_x = 0$ и $\frac{\partial t}{\partial \tau}$ 0 при $y = 0$; the remaining conditions are self-evident.

As a result we obtain

$$\frac{t - t_\bullet}{t_c - t_\bullet} = 1 - \frac{6}{4r_\bullet\Delta + \Delta^2}\left[r_\bullet y + \frac{1}{2}y^2 - \frac{r_\bullet + \Delta}{3\Delta^2}y^3\right].$$

(17-42)

Substituting the values of w_x and t from (17-41) and (17-42) into (17-40), we obtain a partial differential equation for $\Delta(x, \tau)$:

$$\frac{\partial I_1}{\partial \mathrm{Fo}} + \frac{\partial I_2}{\partial X} = \frac{6}{\tilde{\Delta}^2 + 4\tilde{\Delta}},$$

(17-43)

where

$$I_1 = \tilde{\Delta} - \frac{\tilde{\Delta}^2}{2} - \frac{1}{\tilde{\Delta} + 4}\left(\frac{5}{2}\tilde{\Delta} - \frac{11}{10}\tilde{\Delta}^2 - \frac{7}{20}\tilde{\Delta}^3\right);$$

$$I_2 = 2\tilde{\Delta}^2 - 2\tilde{\Delta}^3 + \frac{\tilde{\Delta}^4}{2} + \frac{1}{\tilde{\Delta} + 4}\left(-\frac{32}{5}\tilde{\Delta}^2 + \frac{28}{5}\tilde{\Delta}^3 - \frac{8}{35}\tilde{\Delta}^4 - \frac{3}{7}\tilde{\Delta}^5\right);$$

$$\tilde{\Delta} = \frac{\Delta}{r_\bullet}; \quad \mathrm{Fo} = \frac{a\tau}{r_0^2}; \quad X = 2\frac{1}{\mathrm{Pe}}\frac{x}{r_\bullet}; \quad \mathrm{Pe} = \frac{\bar{w}2r_\bullet}{a}.$$

Solving Eq. (17-43) by the method of characteristics, we obtain:

for the region of nonstationary heat exchange $(\mathrm{Fo} \leqslant \mathrm{Fo}_s)$

$$-\frac{13}{15}\tilde{\Delta} + \frac{7}{30}\tilde{\Delta}^2 - \frac{1}{36}\tilde{\Delta}^3 - \frac{1}{80}\tilde{\Delta}^4 + \frac{52}{15}\ln\left(\frac{\tilde{\Delta}}{4} + 1\right) = \mathrm{Fo};$$

(17-44)

for the region of stationary heat exchange $(\mathrm{Fo} \geqslant \mathrm{Fo}_s)$

$$\frac{1408}{105}\tilde{\Delta} - \frac{176}{105}\tilde{\Delta}^2 + \frac{16}{35}\tilde{\Delta}^3 - \frac{5}{42}\tilde{\Delta}^4 - \frac{1}{75}\tilde{\Delta}^5 + \frac{1}{126}\tilde{\Delta}^6 - \frac{5632}{105}\ln\left(\frac{\tilde{\Delta}}{4}+1\right) = X. \quad (17\text{-}45)$$
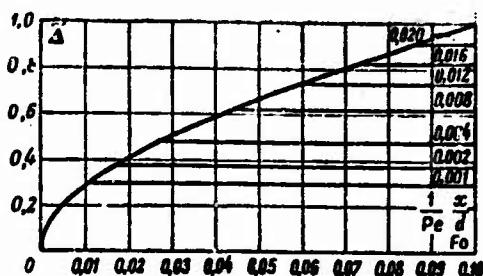
Fig. 17-10. Dependence of $\tilde{\Delta}$ on Fo and $\frac{1}{\mathrm{Pe}}\frac{x}{d}$ for the thermal initial segment of a round tube with an abrupt variation in t_s.

Figure 17-10 shows $\tilde{\Delta}$ as a function of Fo for various values of $\frac{1}{\mathrm{Pe}}\cdot\frac{x}{d}$; the relationship was found from Eqs. (17-44) and (17-45).

The time required for the stationary state $\mathrm{Fo}_s(X)$ to set in is easily found by solving (17-44) and (17-45) simultaneously for each specified value of $\tilde{\Delta}$, since both of these equations are valid along the limiting characteristic. The results of such a computation are shown in Fig. 17-9 (curve 2).

Using the Fourier law and Eq. (17-42), we find the expression for the heat-flux density at the wall:

$$q_c = \frac{\lambda}{r_0}(t_c - t_0)\frac{6}{4\tilde{\Delta} + \tilde{\Delta}^2}. \quad (17\text{-}46)$$

This expression is valid for both nonstationary and stationary conditions. The values of $\tilde{\Delta}$ are found from (17-44) and (17-45) or from the graph of Fig. 17-10.

Repeating the arguments of paragraph 1, we can generalize Eq. (17-46) to the case of an arbitrary variation of $\vartheta_c = t_c - t_0$ in time. We can at once write an expression for q_s when for $\tau = 0$ there is a stationary heat-exchange process $(\vartheta_c \neq 0)$ and for $\tau > 0$ the quantity ϑ_s is an arbitrary function of the time:

$$q_c(X, \text{Fo}) = 6\frac{\lambda}{r_0}\left[\frac{1}{4\tilde{\Delta}_{\text{Fo}_s} + \tilde{\Delta}_{\text{Fo}_s}^2}(\vartheta_c)_{\text{Fo}=0} + \right.$$

$$+\int_0^{\text{Fo}}\frac{d\vartheta_c}{d\text{Fo}_*}\frac{1}{4\tilde{\Delta}_{\text{Fo}-\text{Fo}_*} + \tilde{\Delta}_{\text{Fo}-\text{Fo}_*}^2}\,d\text{Fo}_*\bigg], \quad 0 < \text{Fo} < \text{Fo}_s;$$

$$q_c(X, \text{Fo}) = 6\frac{\lambda}{r_0}\left[\frac{1}{4\tilde{\Delta}_{\text{Fo}_s} + \tilde{\Delta}_{\text{Fo}_s}^2}(\vartheta_c)_{\text{Fo}-\text{Fo}_s} + \int_{\text{Fo}-\text{Fo}_s}^{\text{Fo}}\frac{d\vartheta_c}{d\text{Fo}_*}\times\right.$$

$$\left.\times\frac{1}{4\tilde{\Delta}_{\text{Fo}-\text{Fo}_*} + \tilde{\Delta}_{\text{Fo}-\text{Fo}_*}^2}\,d\text{Fo}_*\right], \quad \text{Fo} \gtrless \text{Fo}_s.$$

(17-47)

Here when $\tilde{\Delta}$ has a subscript containing Fo, it corresponds to the nonstationary regime, while when the subscript contains Fo_s, it corresponds to stationary conditions. The subscript $\text{Fo}-\text{Fo}_*$ means that $\tilde{\Delta}$ is a function of $\text{Fo}-\text{Fo}_*$, i.e., it depends on the time that has elapsed since the instant at which the wall temperature began to change. Thus for the period of variation in ϑ_s beginning with Fo_*, in Fig. 17-10, the variable along the axis of abscissas will be $\text{Fo}-\text{Fo}_*$, and the stationary state will be reached when $\text{Fo}-\text{Fo}_* = \text{Fo}_s$.

If there is no heat exchange at the initial instant, $(\vartheta_c)_{\text{Fo}=0} = 0$, then in the first equation of (17-47), the first term in brackets vanishes. The specified variation in ϑ_s may also include jumps (i.e., a step variation in ϑ_s). In such case, Eqs. (17-47) will still remain valid. For example, let there be a jump equaling $\Delta\vartheta_{si}$ at time Fo_i. Here the integrals are determined in the usual method everywhere except for Fo_i, where we add the additional term

$$6\frac{\lambda}{r_0}\cdot\frac{1}{4\tilde{\Delta}_{\text{Fo}-\text{Fo}_i} + \tilde{\Delta}_{\text{Fo}-\text{Fo}_i}^2}\Delta\vartheta_{ci}.$$

An exception to this rule occurs for the second equation of (17-47), when $\text{Fo}_i < \text{Fo} - \text{Fo}_s$. Here the additional term is not added, since the first term on the right side of the equation allows for the jump.

17-4. HEAT EXCHANGE IN THE THERMAL INITIAL SEGMENT OF FLAT AND ROUND TUBES WHEN THE HEAT-FLUX DENSITY AT THE WALL VARIES IN TIME

The problem of heat exchange in the thermal initial segment of a flat or round tube for a specified time variation in the heat-flux density at the wall has been solved elsewhere [6, 7]. The solution method is similar to that used for problems considered in the preceding section. Thus we shall only give the principal steps in the solution and the final results.

1. We consider heat exchange in a flat tube at whose walls the ...at-flux density is constant over the surface, but capable of vary-

ing in time.

Since q_s is specified while $a\left(\frac{\partial t}{\partial y}\right)_{y=0} = -\frac{q_c}{\kappa_p}$, in accordance with (17-26), the energy equation is more conveniently written in integral form as

$$\frac{\partial}{\partial \tau}\int_0^\Delta (t-t_0)\,dy + \frac{\partial}{\partial x}\int_0^\Delta w_x(t-t_0)\,dy = \frac{q_c}{\kappa_p}.$$
(17-48)

We specify the temperature distribution over the thickness of the thermal boundary layer in the form

$$t-t_0 = \frac{q_c\Delta}{2\lambda}\left(1-\frac{y}{\Delta}\right)^2.$$
(17-49)

while the Poiseuille distribution (17-28) is used for the velocity.

After substituting (17-49) and (17-28) into (17-48) and integrating, we obtain a partial differential equation for the thickness of the thermal boundary layer $\Delta(x, \tau)$. We write it in dimensionless form:

$$\frac{1}{3}\tilde{\Delta}\frac{\partial\tilde{\Delta}}{\partial \mathrm{Fo}} + \left(\frac{1}{4}\tilde{\Delta}^2 - \frac{1}{15}\tilde{\Delta}^3\right)\frac{\partial\tilde{\Delta}}{\partial X} = 1.$$
(17-50)

Here the notation is the same as in (17-29).

Equation (17-50) can be solved by the method used for (17-29).

If at the initial instant the fluid temperature is the same everywhere and equal to t_0 (i.e., there is no heat exchange), while at a subsequent time the heat-flux density at the wall abruptly rises from zero to q_s, we obtain the following final results.

The initial nonstationary increase in the thermal boundary layer is determined by the equation

$$\tilde{\Delta} = (6\,\mathrm{Fo})^{1/2};$$
(17-51)

the solution for the stationary state has the form

$$\frac{1}{12}\tilde{\Delta}^3 - \frac{1}{60}\tilde{\Delta}^4 = X;$$
(17-52)

the time required to reach the stationary state is determined by the equation

$$\frac{1}{2}\sqrt{6}\,\mathrm{Fo}_s^{3/2} - \frac{3}{5}\mathrm{Fo}_s^2 = X.$$
(17-53)

Figure 17-11 shows Fo_s as a function of X (curve 1).

The response of the wall temperature to a single jump q_s is

- 465 -

$$t_c - t_e = \frac{\sqrt{6}}{2} \cdot \frac{q_c r_e}{\lambda} Fo^{1/2}, \quad Fo \leqslant Fo_s;$$

$$t_c - t_e = \frac{\sqrt{6}}{2} \cdot \frac{q r_e}{\lambda} Fo_s^{1/2}, \quad Fo \geq Fo_s, \tag{17-54}$$

where $Fo_s(X)$ is found from (17-53) or Fig. 17-11.
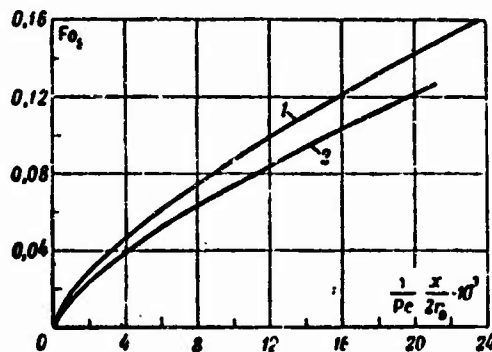
Fig. 17-11. Time at which stationary regime sets in for thermal initial segment of flat (1) and round (2) tube under abrupt change in heat flux at wall.

Using the same method as before, we can generalize Eq. (17-54) to the case of an arbitrary time variation in q_s.

If at the initial instant there is a stationary heat-exchange process ($q_c \neq 0$ for $\tau = 0$), and during the succeeding period ($\tau > 0$), $q_s(\tau)$ varies in time in accordance with the specified law, we have the following equations for the wall temperature:

$$t_c(X, Fo) - t_e = \frac{\sqrt{6}}{2} \cdot \frac{r_e}{\lambda} \left[Fo_e^{1/2} (q_c)_{Fo=0} + \right.$$

$$\left. + \int_0^{Fo} \frac{dq_c}{d Fo_*} (Fo - Fo_*)^{1/2} d Fo_* \right], \quad Fo \leqslant Fo_s;$$

$$t_c(X, Fo) - t_e = \frac{\sqrt{6}}{2} \cdot \frac{r_e}{\lambda} \left[Fo_e^{1/2} (q_c)_{Fo-Fo_s} + \right. \tag{17-55}$$

$$\left. + \int_{Fo-Fo_s}^{Fo} \frac{dq_c}{dFo_*} (Fo - Fo_*)^{1/2} dFo_* \right], \quad Fo > Fo_s.$$

When there is no heat exchange at the initial instant $[(q_c)_{Fo=0} = 0]$ the corresponding term in the first equation of (17-55) drops out. If at a certain value $Fo = Fo_i$, the relationship $q_s(Fo)$ has a jump in q_s equaling Δq_{si}, then the integrals are evaluated by the usual method and, in addition, we add the term

$$\frac{\sqrt{6}}{2} \cdot \frac{r_e}{\lambda} (Fo - Fo_i)^{1/2} \Delta q_{ci}.$$

- 466 -

We do not add this term to the second equation of (17-55) if $Fo_i < Fo - Fo_s$.

2. We shall now consider heat exchange in the thermal initial segment of a round tube at whose walls the heat-flux density is constant along the surface, but variable in time. In such case, the energy equation in integral form looks like this:

$$\frac{\partial}{\partial \tau}\int_0^\Delta (r_0 - y)(t - t_0)\,dy + \frac{\partial}{\partial x}\int_0^\Delta (r_0 - y)\,w_x\,(t - t_0)\,dy = r_0\frac{q_c}{\kappa_0}. \qquad (17\text{-}56)$$
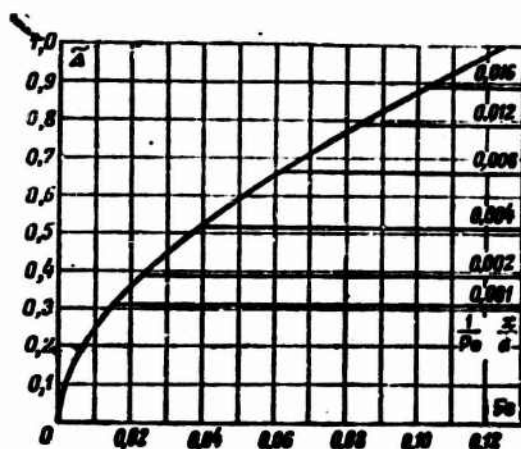
Fig. 17-12. Dependence of $\tilde{\Delta}$ on Fo and $\frac{1}{Pe}\frac{x}{d}$ for thermal initial segment in round tube when q_s varies.

Using Relationships (17-41) and (17-49)[6] for the velocity and temperature distributions over the cross section of the boundary layer, and integrating, we obtain

$$\frac{\partial}{\partial Fo}\left(\frac{1}{6}\tilde{\Delta}^2 - \frac{1}{24}\tilde{\Delta}^3\right) + \frac{\partial}{\partial X}\left(\frac{1}{6}\tilde{\Delta}^3 - \frac{1}{10}\tilde{\Delta}^4 + \frac{1}{60}\tilde{\Delta}^5\right) = 1. \qquad (17\text{-}57)$$

Solution of this equation by the method of characteristics leads to the following results.

For a single jump in heat-flux density from zero to q_s (when there is no heat exchange at the initial instant), we have:

a) for the region of nonstationary heat exchange ($Fo \leq Fo_s$),

$$\frac{1}{6}\tilde{\Delta}^2 - \frac{1}{24}\tilde{\Delta}^3 = Fo; \qquad (17\text{-}58)$$

b) for the stationary state ($Fo \geq Fo_s$),

$$\frac{1}{6}\tilde{\Delta}^3 - \frac{1}{10}\tilde{\Delta}^4 + \frac{1}{60}\tilde{\Delta}^5 = X. \qquad (17\text{-}59)$$

- 467 -

Figure 17-12 shows $\tilde{\Delta}$ as a function of Fo and X, with the relationship computed from Eqs. (17-58) and (17-59).

Solving (17-58) and (17-59) simultaneously for each specified valud of $\tilde{\Delta}$, we have no difficulty in finding the time required for the stationary state to set in. Figure 17-11 shows the dependence of Fo_s on X (curve 2).

The variation in wall temperature produced by the single jump q_s is found from (17-49):

$$t_c - t_s = \frac{q_r}{2} \cdot \frac{r_0}{\lambda} \tilde{\Delta},$$

(17-60)

where $\tilde{\Delta}$ is found from (17-58) and (17-59), or from the graph (Fig. 17-12).

If there is a stationary heat-exchange process at the initial instant, and during the subsequent period q_s varies in time according to the specified law, then the wall-temperature variation can be determined from the results for a single jump q_s and the method which we have employed several times previously. As a result, we obtain

$$
\begin{aligned}
t_c (X, \text{Fo}) - t_s &= \frac{r_0}{2\lambda} \left[\tilde{\Delta}_{\text{Fo}_s}(q_c)_{\text{Fo}=0} + \right. \\
&\left. + \int_0^{\text{Fo}} \frac{dq_r}{d\text{Fo}_s} \tilde{\Delta}_{\text{Fo}-\text{Fo}_s} d\text{Fo}_s \right], \text{Fo} \leqslant \text{Fo}_s; \\
t_c (X, \text{Fo}) - t_s &= \frac{r_0}{2\lambda} \left[\tilde{\Delta}_{\text{Fo}_s}(q_c)_{\text{Fo}-\text{Fo}_s} + \right. \\
&\left. + \int_{\text{Fo}-\text{Fo}_s}^{\text{Fo}} \frac{dq_r}{d\text{Fo}_s} \tilde{\Delta}_{\text{Fo}-\text{Fo}_s} d\text{Fo}_s \right], \text{Fo} \geqslant \text{Fo}_s.
\end{aligned}
$$

(17-61)

Here the notation is the same as in (17-47).

When there is no heat exchange at the initial instant (when Fo = 0), the corresponding term in the first equation of (17-61) vanishes. If the function q_s(Fo) has a jump Δq_{si} at Fo = Fo_i, then evaluating the integrals in the usual way, we add the term

$$\frac{r_0}{2\lambda} \tilde{\Delta}_{\text{Fo}-\text{Fo}_i} \Delta q_{ci}.$$

This term is not added to the second equation of (17-61) if $\text{Fo}_i < \text{Fo} - \text{Fo}_s$.

Example. A fluid for which λ = 0.1 kW/m·deg and a = 2.47·10^{-4} m^2/h flows in a tube of diameter d = 20 mm at a velocity $\bar{w}$ = 0.06 m/s. heat-flux density q_s = 1500 kW/m^2 is maintained for a long period at the tube wall: the stationary heat-exchange process is disrupted by an instantaneous increase in the heat flux by a factor of 2. We are to determine: 1) the time interval after which the new

stationary regime sets in at a distance $x = 140d$ from the beginning of the heated segment; 2) the wall temperature at this distance 30 s after the instantaneous increase in the heat flux and after the stationary state has been established.

The number $\frac{1}{Pe} \cdot \frac{x}{d} = \frac{a}{\bar{w}d} \cdot \frac{x}{d} = 0.008$. Here the value of X (see Fig. 17-11) is $Fo_s = \frac{a\tau_s}{r_0^2} = 0.062$. Thus the time after which the new stationary regime sets in is $\tau_s \approx 91.2$ s.

To determine the wall temperature for $\tau < \tau_s$, we use the first equation of (17-61). With allowance for the rule used above to allow for the jump Δq_{si}, in our case we have

$$t_c - t_o = \frac{r_0}{2\lambda} \left[\tilde{\Delta}_{Fo_s}(q_c)_{Fo=0} \right] + \frac{r_0}{2\lambda} \tilde{\Delta}_{Fo-Fo_i} \Delta q_{ci}.$$

By hypothesis, $(q_c)_{Fo=0} = \Delta q_{ci} = q_c = 1500 \text{kW/mm}^2$, while $Fo_i = 0$. Consequently,

$$t_c - t_o = \frac{r_0 q_c}{2\lambda} \left[\tilde{\Delta}_{Fo_s} + \tilde{\Delta}_{Fo} \right].$$

30 s after the instantaneous increase in the heat flux, $Fo = \frac{a\tau}{r_0^2} = 0.020$. Using (17-58) or Fig. 17-12, we find $\tilde{\Delta}_{Fo_s} = 0.67$ and $\tilde{\Delta}_{Fo} = 0.37$. Using the last equation for $(t_c - t_o)$, we find the wall temperature: 30 s after the increase in the heat flux, $t_c - t_0 = 78°$ C; after the stationary state has been established (Fo = Fo_s), $t_c - t_0 = 100°$ C.

17-5. HEAT EXCHANGE IN A FLAT TUBE WITH PULSATING FLOW

In many cases, the heat-exchange process is nonstationary owing to the nonstationary nature of the flow. In such case, the thermal boundary conditions may remain stationary. An example is heat exchange with a pulsating fluid flow.

1. Let pulsating flow take place in a flat tube whose wall temperature is maintained constant and different from the fluid entrance temperature. The flow pulsations are produced by sinusoidal oscillations superposed on the stationary (time-averaged) pressure gradient, so that the instantaneous pressure gradient is a periodic time function:

$$\frac{\partial p}{\partial x} = \left(\frac{dp}{dx} \right)_s \left(1 + \frac{\gamma}{2} \cos \omega\tau \right).$$

(17-62)

where $\left(\frac{dp}{dx} \right)_s = -3 \frac{\mu\bar{w}}{r_0^2}$ is the stationary component of the pressure gradient; $\bar{w}$ is the average (over the cross section and the time) flow velocity; γ the dimensionless amplitude of pressure oscillations; $\omega = 2\pi/\tau_0$ is the oscillation frequency; τ_0 is the oscillation period; τ is the time.

The fluid arrives at the heated tube segment from the stilling segment, so that the flow is stabilized in the heated segment and, consequently, the velocity is independent of the longitudinal coor-

ilinate. We assume that the fluid is incompressible, and that its physical properties are constant; we also ignore the energy dissipation in the flow and the variation in heat flux along the axis owing to conduction.

A solution is known for the problem of fluid moving under such conditions. The velocity distribution has been given in §5-7. Thus we turn directly to the heat-exchange problem, which has been solved in approximation by Siegel and Perlmutter [8]. Taking the conditions formulated into account and assuming that the flow contains no internal heat sources, we write the energy equation in the form

$$\frac{\partial t}{\partial \tau} + w_x \frac{\partial t}{\partial x} = a \frac{\partial^2 t}{\partial y^2}. \tag{17-63}$$

For w_x we have the equation

$$w_x = \frac{3}{2} \bar{\bar{w}} \left[\left(1 - \frac{y^2}{r_0^2} \right) + \gamma U \right]. \tag{17-64}$$

where $U(Y, \omega\tau, M)$ is a periodic function depending on $\omega\tau = 2\pi \frac{\tau}{\tau_0}$, $Y = y/r_0$ and the parameter $M = \left(\frac{\omega r_0^2}{2\nu} \right)^{1/2}$. An expression for U is given in §5-7.

We substitute (17-64) into (17-63), and write the energy equation in dimensionless form:

$$\frac{\partial T}{\partial \mathrm{Fo}} + (1 - Y^2 + \gamma U) \frac{\partial T}{\partial X} = \frac{\partial^2 T}{\partial Y^2}. \tag{17-65}$$

Here $T = \frac{t - t_0}{t_c - t_0}$, $\mathrm{Fo} = \frac{a\tau}{r_0^2}$,

$$X = \frac{8}{3} \frac{1}{\mathrm{Pe}} \cdot \frac{x}{2r_0} \text{ and } \mathrm{Pe} = \frac{\bar{\bar{w}} 2 r_0}{a}.$$

We note that $\omega\tau$ and Fo are connected by the relationship $\omega\tau = 2M^2 \mathrm{Pr} \mathrm{Fo}$.

Equation (17-65) is solved under the following boundary conditions:

$$T(0, Y, \mathrm{Fo}) = 0; \tag{17-66a}$$
$$T(X, \pm 1, \mathrm{Fo}) = 1; \tag{17-66b}$$
$$\left(\frac{\partial T}{\partial Y} \right)_{Y=0} = 0. \tag{17-66c}$$

To satisfy the first boundary condition, we must impose a restriction on the pressure-gradient fluctuations. They must not be so large as to produce a reverse flow of fluid from the center portion of the tube toward the entrance to the heated section.

It is clear that T will vary periodically in time. For very ill pressure oscillations, the expression for T should reduce to solution of the stationary problem (see §6-2):

$$T_s = 1 - \sum_{n=0}^{4} b_{n0} \psi_n(Y) \exp(-\epsilon_n^2 X). \qquad (17\text{-}67)$$

Each eigenfunction ψ_n is a series in cosines,

$$\psi_n = \sum_{m=0}^{4} \frac{b_{nm}}{b_{n0}} \cos E_m Y,$$

where $E_m = \left(m + \frac{1}{2}\right)\pi$; the values of $b_{n0}, b_{nm}/b_{n0}$ and ϵ_n^2 are given in Table 6-5.

We seek a solution for the nonstationary state in a form analogous to (17-67):

$$T = 1 - \sum_{n=0}^{4} b_{n0} \psi_n(Y) F_n(X, \text{Fo}). \qquad (17\text{-}68)$$

where F_n is the unknown function.

The dependence on Y in (17-68) satisfies the boundary condition (17-66b) and (17-66c). The function F_n should be a periodic time function, and should satisfy the boundary condition at the entrance (17-6a). In addition, for small velocity oscillations, F_n should approach the expression for the stationary state, $\exp(-\epsilon_n^2 X)$, which appears in (17-67).

To determine F_n, we use an integral form of the energy equation, which can be obtained by integrating (17-65) over the tube cross section:

$$\frac{\partial}{\partial \text{Fo}} \int_0^1 T \, dY + \frac{\partial}{\partial X} \int_0^1 (1 - Y^2 + \gamma U) T \, dY = \left(\frac{\partial T}{\partial Y}\right)_{Y=1}. \qquad (17\text{-}69)$$

Substituting (17-68) into (17-69), we find a partial differential equation for F_n:

$$\frac{\partial F_n}{\partial \text{Fo}} \int_0^1 \psi_n \, dY + \frac{\partial F_n}{\partial X} \int_0^1 (1 - Y^2 + \gamma U) \psi_n \, dY = F_n \left(\frac{d\psi_n}{dY}\right)_{Y=1}. \qquad (17\text{-}70)$$

An equation of this type is solved by the method of characteristics. If we use the abbreviated notation $\int_0^1 g(Y, \text{Fo}) dY = \bar{g}(\text{Fo})$ to write the integral coefficients in (17-70), where g is the integrand, then the characteristic system of ordinary differential equations corresponding to (17-70) is written as

$$\frac{d\text{Fo}}{\bar{\psi}_n} = \frac{dX}{\overline{(1 - Y^2 + \gamma U)\psi_n}} = \frac{dF_n}{F_n \left(\frac{d\psi_n}{dY}\right)_{Y=1}}. \qquad (17\text{-}71)$$

We integrate the equation formed by the first two expressions of (17-71) from a certain arbitrary point with coordinates X_0, Fo_0. As a result, we obtain the relationship between X and Fo, which is the characteristic equation with origin at X_0 and Fo_0. We are interested only in the characteristic with origin at $X = 0$, since this will satisfy boundary condition (17-66a). Letting $X_0 = 0$, we thus obtain

$$\int_{Fo_0}^{Fo} \frac{\overline{(1-Y^2+YU)\psi_n}}{\psi_n} \, dFo = \int_0^X dX. \tag{17-72}$$

After substituting the values of U and ψ_n, and integrating, we have

$$X = \frac{Fo - Fo_0}{I_n} - \frac{\gamma}{4M^2 \, Pr} \varphi_n (\cos 2M^2 \, Pr \, Fo - \cos 2M^2 \, Pr \, Fo_0) +$$

$$+ \frac{\gamma}{2M^2 \, Pr} \chi_n (\sin 2M^2 \, Pr \, Fo - \sin 2M^2 \, Pr \, Fo_0), \tag{17-73}$$

where

$$I_n = \frac{\overline{\psi_n}}{(1-Y^2)\psi_n} = \frac{\sum_{m=0}^{4} \frac{b_{nm}}{b_{n0}} \cdot \frac{(-1)^m}{E_m}}{2 \sum_{m=0}^{4} \frac{b_{nm}}{b_{n0}} \cdot \frac{(-1)^m}{E_m^3}};$$

$$\varphi_n(M) = 1 - \frac{\sum_{m=0}^{4} \frac{b_{nm}}{b_{n0}} \cdot \frac{(-1)^m E_m^3}{4M^4 + E_m^4}}{\sum_{m=0}^{4} \frac{b_{nm}}{b_{n0}} \cdot \frac{(-1)^m}{E_m}};$$

$$\chi_n(M) = \frac{\sum_{m=0}^{4} \frac{b_{nm}}{b_{n0}} \cdot \frac{(-1)^m E_m}{4M^4 + E_m^4}}{\sum_{m=0}^{4} \frac{b_{nm}}{b_{n0}} \cdot \frac{(-1)^m}{E_m}}.$$

Now that we have found the equation for the characteristics, let us see how F_n varies along these lines. Equating the first and last expressions of (17-71) and integrating, we find

$$\int_1^{F_n} \frac{dF_n}{F_n} = \frac{1}{\psi} \left(\frac{d\psi}{dY} \right)_{Y=1} \int_{Fo_0}^{Fo} dFo. \tag{17-74}$$

The lower limit of integration corresponds to the boundary condition $F_n = 1$ at $Fo = Fo_0$. Since Fo_0 is located at the origin of the

characteristic line, where $X=0$, this boundary condition is equivalent to the condition $F_n=1$ at $X=0$ for any Fo_0. If $F_n=1$, then (17-68) takes the same form as Solution (17-67) for the stationary state at $X=0$. Since $T_s=0$ when $X=0$, boundary condition (17-66a) is satisfied.

Integrating (17-74), we find

$$\ln F_n = -\zeta_n(Fo - Fo_0),$$ (17-75)

where

$$\zeta_n = -\frac{1}{\psi_n}\left(\frac{d\psi_n}{dY}\right)_{Y=1} = \frac{\sum_{m=0}^{4}\frac{b_{nm}}{b_{n0}}(-1)^m E_m}{\sum_{m=0}^{4}\frac{b_{nm}}{b_{n0}}\cdot\frac{(-1)^m}{E_m}}.$$

To eliminate Fo_0, we solve (17-73) and (17-75) simultaneously. As a result, we obtain a relationship for F_n that is valid for every X and Fo:

$$X = -\frac{\ln F_n}{\eta_n} - \frac{\gamma\psi_n}{4M^4 Pr}\left[\cos 2M^2 Pr\, Fo - \cos 2M^2 Pr\left(Fo + \frac{1}{\zeta_n}\ln F_n\right)\right] +$$
$$+ \frac{\gamma\chi_n}{2M^2 Pr}\left[\sin 2M^2 Pr\, Fo - \sin 2M^2 Pr\left(Fo + \frac{1}{\zeta_n}\ln F_n\right)\right].$$ (17-76)

where $\eta_n = \int_n \zeta_n$. The numerical values of $\int_n, \zeta_n$ и η_n are given in Table 17-2.[7]

When the flow fluctuations are small ($\gamma \rightarrow 0$), the terms containing the ordinary sine and cosine drop out of (17-76) and the function F_n takes on the limiting value

$$F_n = \exp(-\eta_n X).$$

If this limiting value is to correspond to the stationary state for which $F_n = \exp(-\varepsilon^2_n X)$, in accordance with (17-67), the values of η_n must coincide with the values of ε^2_n. It is clear from Tables 6-5 and 17-2 that there is good agreement, except for large n. This discrepancy is explained by the fact that when we analyzed nonstationary flow, we represented the eigenfunctions as series with a limited number of terms. If we use the exact values of the eigenfunctions or, in other words, more terms of the series, then as was shown in [1], η_n must be the same as ε^2_n. Thus within the limits of the five-term approximation used for the eigenfunction, the approximate solution obtained reduces to the exact solution for the stationary state when the oscillation amplitude approaches zero.

Since we now know the temperature field, we can use the Fourier law and Eq. (17-68) to find an expression for the heat-flux density at the wall:
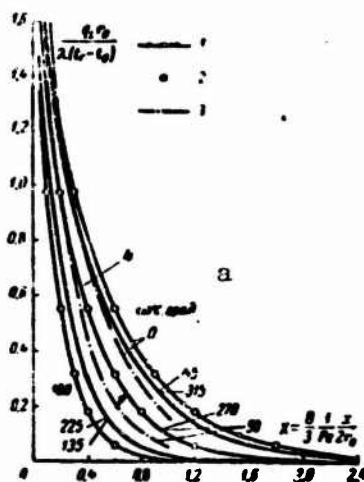
Fig. 17-13. Heat transfer for a pulsating flow with low oscillation frequency at $M=0.1$; $Pr=0.7$; $\gamma=1.0$. 1) Calculated from Eq. (17-77); 2) calculated on the assumption that heat transfer is quasistationary; 3) calculated for slug flow; 4) heat transfer for constant average velocity. a) deg.

Fig. 17-14. Difference between nonstationary and stationary values of heat flux for pulsating flow with $M=1.0$; $Pr=0.7$; $\gamma=1.0$. 1) Calculated from Eq. (17-77) for $\omega\tau = 0-135°$; 2) the same, $\omega\tau = 180-315°$. a) deg.

$$\lambda_{(t_c-t_0)}^{q_c r_0} = \sum_{n=0}^{1}\sum_{m=0}^{4} b_{n_0}\left(\frac{b_{nm}}{b_{n_0}}\right)(-1)^m F_n E_m .$$

(17-77)

Let us analyze the way in which the heat-flux density depends on the parameter M associated with the oscillation frequency, Pr, and the dimensionless pressure-fluctuation amplitude $\gamma/2$.

The influence of the parameter M can be seen on Fig. 17-13, 17-14, and 17-15. For the cases shown in these figures, a value of 0.7 was taken for Pr, while $\gamma = 1$ (i.e., the amplitude of the pressure-gradient fluctuations corresponds to half the pressure gradient the stationary state). Thus the cases selected for illustration correspond to fairly large pressure fluctuations.

Figure 17-13 shows the variation in the dimensionless heat-flux density along the tube length for $N = 0.1$ for every eighth cycle of oscillation. As we have noted in §5-7, at such a low frequency, the oscillations occur so slowly that the velocity distribution is quasistationary. This means that the velocity variations are in phase with the pressure variations, and the velocity profile at any instant will be parabolic, corresponding to the instantaneous pressure gradient. If we calculate the heat flux for specified values of $\omega\tau$, using the stationary-state equatons and the instantaneous values of mean velocity, as Fig. 17-13 shows, the results of the calculation will be in good agreement with the results of calculations using Eq. (17-77) for the nonstationary state.

Fig. 17-15. Difference between nonstationary and stationary values of heat flux for pulsating flow with $M=2.0$; $Pr=0.7$; $\gamma=1.0$. The symbols are the same as for Figs. 17-13 and 17-14. a) deg.
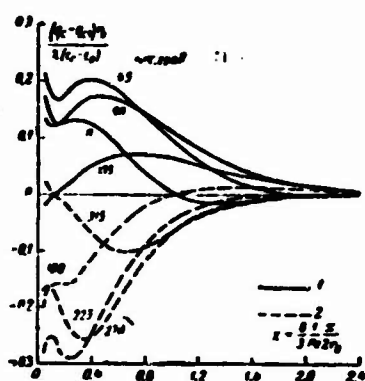

Fig. 17-16. Difference between nonstationary and stationary heat-flux values for pulsating flow with $M=1.0$; $Pr=0.01$; $\gamma=1.0$. 1) Calculated from Eq. (17-77) for $\omega\tau = 0-135°$; 2) the same, $\omega\tau = 180-315°$; 3) computed on the assumption that heat transfer is quasistationary; 4) computed for slug flow. a) deg.

Thus when $M \leq 0.1$, the heat fluxes under nonstationary conditions can be determined on the basis of the assumption that the heat-exchange process is quasistationary. In particular, when $\omega\tau = 90$ and $270°$ the pulsating velocity component equals zero. Consequently, the mean velocity of the nonstationary flow will be the same for these time values as for stationary flow. Since heat exchange is quasistationary in this case, when $\omega\tau = 90$ and $270°$, the heat fluxes calculated for the non-stationary case will coincide with those for the quasistationary approximation.

Figures 17-14 and 17-15 show the results of heat-transfer calculations for $M = 1.0$ and 2.0. Here the axis of ordinates shows the dimensionless difference between the instantaneous nonstationary heat flux and the stationary heat-flux value calculated from the mean velocity (the stationary heat flux $\frac{q_{c.} \cdot r_0}{\lambda (t_c - t_0)}$ corresponds to curve 4 on Fig. 17-13). When we compare the curves for the heat fluxes with the curves for the pulsating velocity component (Fig. 5-22 and 5-23) for the same values of M and $\omega\tau$, it is easy to see that when $M = 1$ or 2, heat transfer is still not quasistationary. For example, with $M = 1$ and $\omega\tau = 135°$, the pulsating velocity component is negative. Consequently, the instantaneous value averaged over the entire tube is less than the mean velocity under stationary conditions. In this case, the nonstationary-regime heat transfer computed from quasistationary theory should be less than under stationary conditions. But in fact, as we can see from Fig. 17-14 (the curve for $\omega\tau = 135°$), the heat transfer is greater over the entire tube length, except for a small segment near the entrance. As another example, let us look at the case in which $M = 2$ and $\omega\tau = 0$. Here the instantaneous mean velocity exceeds the mean velocity under stationary conditions, while the heat transfer is less, which also contradicts the quasistationary theory.

Comparing Figs. 17-13, 17-14, and 17-15, we note that as the oscillation frequency or, more accurately, the parameter M, increases, the change in heat transfer caused by the velocity pulsations decreases. This is explained by the fact that the velocity pulsations decrease as M becomes larger (see Fig. 5-23). Thus for $M \cdot 5$ $(\gamma = 1$ and $Pr = 0.7)$, the velocity pulsations are so small that their influence on heat transfer can be neglected.

The influence of Pr can be seen in Figs. 17-14, 17-16, and 17-17, which show the results of calculations for $M = 1$, $\gamma = 1$ and $Pr = 0.7$, 0.01, and 10. To gain a better understanding of these results, let us determine the mean distance traversed by the fluid during a complete oscillation cycle. This distance is determined by the mean stationary velocity, since the pulsating velocity component vanishes when we integrate over the entire cycle. The oscillation period $\tau_0 = 2\pi/\omega$, while the distance traversed by the fluid during an entire cycle is $x_0 = \bar{w} \frac{2\pi}{\omega}$ or, in dimensionless form,

$$X_0 = \frac{8}{3} \frac{1}{Pe} \frac{x_0}{2r_0} = \frac{2\pi}{3MPr}.$$

The distance X_0 can vary within wide limits. Thus when $M = 1$ and $Pr = 0.01$, 0.7, and 10, the corresponding values of X_0 are 210, 3.0, and 0.21.
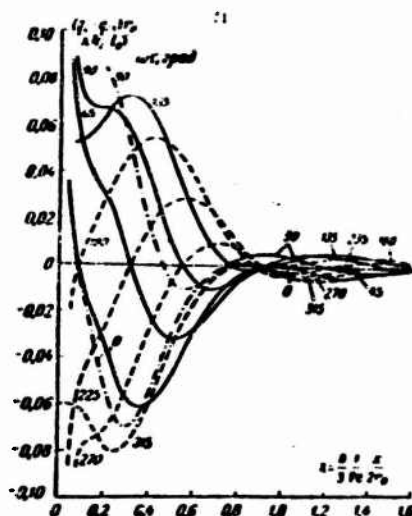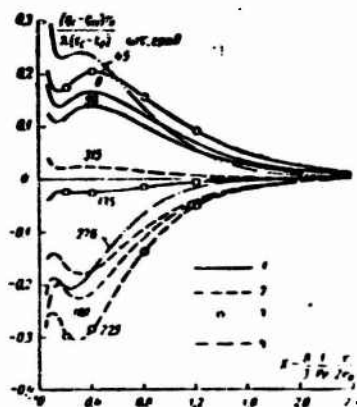
Fig. 17-17. Difference between nonstationary and stationary values of heat flux for pulsating flow at $M=1.0$; $Pr=10$; $\gamma=1.0$. The symbols are the same as on Fig. 17-16. a) deg.

For constant wall temperature, it makes sense to consider the heat transfer for tube segments with reduced length $X \leq 3$, since when X is large the heat fluxes become very small, so that the fluid temperature approaches the wall temperature (see, for example, Fig. 17-13).

When $Pr \ll 1$, for example, when $Pr = 0.01$, the reduced distance $X \approx 3$ forms a small fraction of the reduced length corresponding to the complete cycle of X_0 oscillations. In essence, this means that the time interval characterizing establishment of the stationary state, determined by the value of X, turns out to be far less than the oscillation period, characterized by X_0. Thus results calculated from Eq. (17-77) for each value of $\omega\tau$ should coincide with the solution for stationary flow with the same velocity profile as the instantaneous nonstationary velocity profile for the given values of M and $\omega\tau$. For $M \leq 1$, when the velocity profiles are nearly parabolic, the computational results should agree with quasistationary theory, which is the case in Fig. 17-16.

If Pr is sufficiently large, for example, $Pr = 10$ (see Fig. 17-17), then the reduced length corresponding to a complete cycle of X_0 forms only a part of the reduced length $X \approx 3$. Here the actual heat-transfer values will differ substantially from the values predicted by the quasistationary theory. For example, when $M = 1$ and $\omega\tau = 90°$, the pulsating velocity component is positive (see Fig. 5-22), so that in accordance with the quasistationary theory, the heat transfer should be greater for all values of X than in stationary flow. As we can see from Fig. 17-17, however, the difference between the values of the nonstationary and stationary heat flows at $\omega\tau=90°$ vary along X in accordance with an oscillating curve that takes on positive and negative values.

Figures 17-14 and 17-18 show the influence of the pressure-oscillation amplitude. On the second figure, the double amplitude $\gamma = 2$, i.e., it is 2 times the value for the first figure, while the other parameters are identical. Increasing the amplitude by a
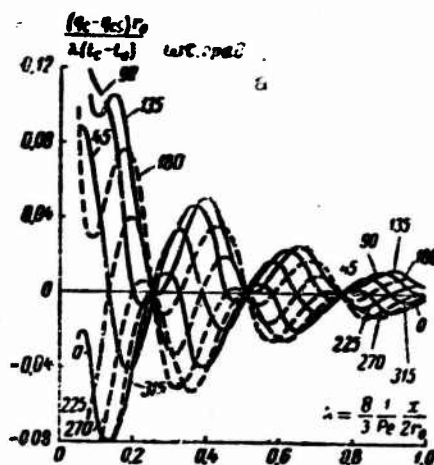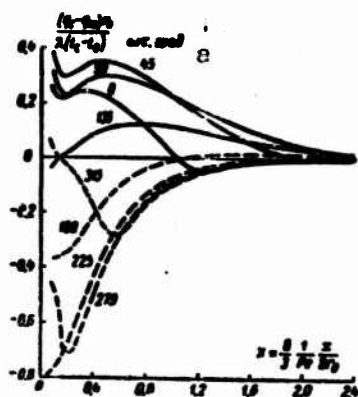
Fig. 17-18. Difference between nonstationary and stationary values of
heat fluxes for pulsating flow with $M = 1.0$; $Pr = 0.7$; $\gamma = 2.0$. The
symbols are the same as for Fig. 17-16. a) deg.

factor of 2 does not significantly change the nature of the curves,
but, as we might expect, the difference in heat transfer for the
nonstationary and stationary regimes nearly doubles. The amplitude
has the same influence in other cases: the curves are deformed some-
what, while exhibiting no new features.

We must once again emphasize that the heat-transfer calcula-
tions considered here are valid only for a combination of the para-
meters M and γ such that no reverse flows appear ($w_x \geq 0$). For
$\gamma = 2$ and $M = 1$, however, the velocity pulsations are so large as to
cause a reverse flow of the fluid. This effect will become more pro-
nounced at greater amplitudes and the same value of M.

The determination of heat exchange in pulsating flow will be
significantly simplified if we introduce the notion of the uniform
velocity distribution over a cross section, i.e., if we use the slug-
flow model. In this case, there is an exact solution for the energy
equation. Such calculations have been carried out in [9]. Certain
of the computational results are shown in Figs. 17-13, 17-15, and
17-16 in the form of individual curves. The computation based on
the slug-flow model and the integral method considered here yield a
qualitatively identical kind of heat-transfer variation, but differ-
ent quantitative results.

To determine the resultant influence of velocity pulsations on
the mean heat transfer, it is necessary to integrate the instantan-
eous heat fluxes at each point in the tube over the entire oscilla-
tion cycle, and then to integrate the local values (averaged over
time) found for these quantities over the tube length. For example,
the curves of Figs. 17-15 and 17-17 are symmetric about the X axis
(the positive and negative components are identical, in the main).
Here it is obvious that we cannot obtain an increase in the mean
heat transfer as compared with the stationary regime. For nonsymme-
tric curves such as those of Figs. 17-14 and 17-18, heat transfer
will increase at certain points along the length and decrease at
others. As a rule, the absolute values for negative results will be

- 478 -

somewhat greater near the entrance. Consequently, heat transfer should decrease slightly for short tubes. For sufficiently long tubes, however, the change in average heat transfer is negligible.

Thus velocity pulsations lead to no noticeable increase or decrease in the mean heat transfer as compared with stationary flow conditions. Naturally, this condition holds provided the flow remains laminar over the entire oscillation cycle. When this condition is satisfied, the conclusion is in agreement with the experimental data. Experiments carried out for sufficiently small values of Re, where it is impossible to go over to turbulent flow, either show no pulsation influence whatsoever, or a slight increase in heat transfer [10, 14]. If the value of Re, calculated from the mean stationary velocity, is sufficiently great (although less than Re_{kr}), then during flow acceleration, the instantaneous values of mean velocity may reach values corresponding to Re > Re_{kr}. In such case, as experiment has shown [10], there will be a significant growth in heat transfer (by a factor of 2 or more) as a result of turbulence. This is an even stronger possibility, since Re_{kr} is apparently lower for pulsating flow than for stationary flow. Thus according to the data of [11], Re_{kr} is about 1500 when calculated from the mean stationary velocity, as against 2100 for stationary flow (see also §5-7).

2. The problem of heat exchange during pulsating flow in a flat tube has been solved for constant heat-flux density only on the assumption of slug flow. As in the preceding case, let the velocity variation be produced by sinusoidal oscillations in the pressure gradient in accordance with (17-62).

We take the fluid velocity, constant over the cross section, to equal the actual flow velocity averaged over the cross section, i.e., we follow Eq. (5-57) (see §5-7). Thus the instantaneous velocity depends solely on the time. All remaining problem conditions are the same as in the preceding paragraph.

After the concept of slug flow has been introduced, the problem admits of the exact solution obtained in [9]. This has the form

$$\frac{(t - t_0)\lambda}{q_c r_0} = H + \frac{1}{2} Y^2 - \frac{1}{6} - 2 \sum_{n=1}^{\infty} \frac{(-1)^n}{(n\pi)^2} \cos(\pi n Y) \exp[-(n\pi)^2 H]. \quad (17-78)$$

The function $H(X, Fo)$ is found from the equation

$$X = H - \frac{C_1}{2M^2 \Pr} [\cos 2M^2 \Pr Fo - \cos 2M^2 \Pr (Fo - H)] +$$
$$+ \frac{C_2}{2M^2 \Pr} [\sin 2M^2 \Pr Fo - \sin 2M^2 \Pr (Fo - H)], \quad (17-79)$$

where

$$C_1 = \frac{3\gamma}{4M^2}\left[1 - \frac{\sh 2M + \sin 2M}{4M(A^2 + B^2)}\right];$$

$$C_2 = \frac{3\gamma}{4M^2}\left[\frac{\sh 2M - \sin 2M}{4M(A^2 + B^2)}\right];$$

$$A = \sh M \sin M; \quad B = \ch M \cos M; \quad X = \frac{4}{\mathrm{Pe}} \cdot \frac{x}{2r_0}.$$

The remaining definitions are the same as in the preceding paragraph. Since in this case the heat-flux density q_s at the wall is specified and we are required to determine the wall temperature, letting $Y = 0$ in (17-78), we obtain

$$\frac{(t_c - t_0)\lambda}{q_s r_0} = H + \frac{1}{3} - 2\sum_{n=1}^{\infty}\frac{1}{(n\pi)^2}\exp[-(n\pi)^2 H]. \qquad (17\text{-}80)$$

When the velocity pulsations are very small ($\gamma \to 0$), the function $H = X$ and Eqs. (17-78) and (17-80) take on the form corresponding to the limiting case of stationary slug flow in a flat tube.
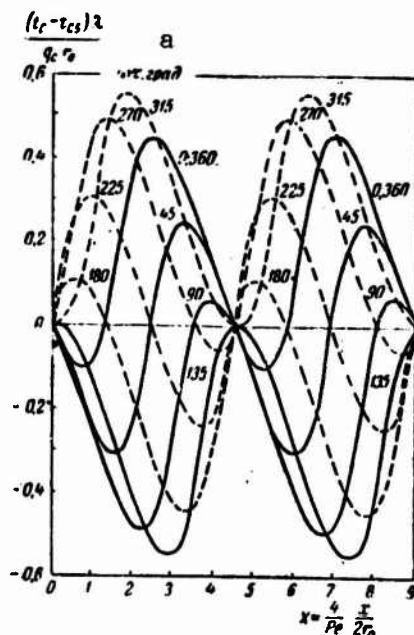

Fig. 17-19. Difference in wall temperatures for pulsating and stationary flows at $M = 1.0$; $\mathrm{Pr} = 0.7$; $\gamma = 1$. a) deg.

When the heat-flux density is constant at the wall, the velocity pulsations produce periodic oscillations in wall temperature; is important to know these if we are to evaluate the operating reliability of a heat-exchange system. As an example, Fig. 17-19

shows the variation in wall temperature along tube length at various times during the complete oscillation cycle for $M=1$, $\mathrm{Pr}=0.7$ and $\gamma=1$. The axis of ordinates gives the dimensionless difference in wall temperatures for pulsating (t_s) and stationary (t_{ss}) flows with identical average (over time and over cross section) velocities $\bar{w}$.

As we see, the wall temperature may deviate very significantly from the values corresponding to stationary flow. The deviations equal zero at node points with coordinates X equal to or multiples of the dimensionless length of a complete cycle of oscillation in X_0 (in this case $X_0=\pi/\bar{M}^2\mathrm{Pr}$). Thus the larger Pr or M, the more node points will fit within a given tube segment. Under the conditions corresponding to Fig. 17-19, therefore, $X_0 = 4.49$, and three node points will fit within a tube segment of length $X = 9$. As M increases, the deviation of the wall temperature from the values corresponding to the stationary state will decrease.

To conclude, we note that the results given here are valid only for an infinitely thin wall whose heat capacity is zero. If the wall has finite thickness and heat capacity, these will smooth the temperature fluctuation.

17-6. HEAT EXCHANGE IN A FLAT TUBE FOR STEP VARIATION IN PRESSURE GRADIENT WITH TIME

Let a fluid be in stationary motion within a flat tube at a mean velocity $\bar{w}_1$; let there be a stationary heat-exchange process at constant wall temperature. At time $\tau = 0$, the pressure gradient changes instantaneously and takes on a new constant value. As a result, a nonstationary transient process appears, during which the fluid velocity changes from $\bar{w}_1$ to the new constant value $\bar{w}_2$; here the wall temperature is maintained constant. All other conditions are the same as for the problem considered in the preceding section.

Let us investigate the nonstationary heat exchange during the transient period. For this case, the energy equation will have the same form as (17-63). The velocity distribution during the transient is also known, and is found from Eq. (5-48). Thus, going over to dimensionless variables, we have

$$\frac{\partial T}{\partial \mathrm{Fo}} + \frac{2}{3}\,W_x\,\frac{\partial T}{\partial X} = \frac{\partial^2 T}{\partial Y^2}, \qquad (17\text{-}81)$$

where

$$W_x = \frac{w_x}{\overline{w}_2} = \frac{3}{2}\left[1 - Y^2 - 4\left(1 - \frac{\overline{w}_1}{\overline{w}_2}\right)\sum_{i=0}^{\infty}\frac{(-1)^i}{E_i^3}\cos E_i Y \exp(-E_i^2 \mathrm{Pr\,Fo})\right]. \qquad (17\text{-}82)$$

Here we let

$$T = \frac{t-t_0}{t_c-t_0}; \quad \mathrm{Fo} = \frac{a\tau}{r_0^2}; \quad X = \frac{8}{3}\cdot\frac{1}{\mathrm{Pe}}\cdot\frac{x}{2r_0}; \quad \mathrm{Pe} = \frac{\overline{w}_2 2 r_0}{a}; \quad Y = \frac{y}{r_0}.$$

Equation (17-81) must be solved under the initial condition

$$T(X, Y, 0) = T_{s1} \qquad (17\text{-}83\text{a})$$

and the boundary condition

$$
\begin{aligned}
&T(0, Y, \text{Fo}) = 0, \\
&T(X, \pm 1, \text{Fo}) = 1, \\
&\left(\frac{\partial T}{\partial Y}\right)_{Y=0} = 0,
\end{aligned}
\right\} \qquad (17\text{-}83\text{b})
$$

where T_{s1} is the stationary temperature distribution at the initial instant.

The solution of this nonstationary problem can be represented in a form analogous to Solution (17-67) for the stationary case:

$$T = 1 - \sum_{n=0}^{\infty} b_{n0} \psi_n(Y) G_n(X, \text{Fo}), \qquad (17\text{-}84)$$

where G_n is the unknown function, which depends both on X and Fo.

Equation (17-84) already satisfies the second and third boundary conditions. The initial condition requires that

$$G_n(X, 0) = \exp\left(-\varepsilon_n^2 \frac{\overline{w}_1}{\overline{w}_1} X\right) \qquad (17\text{-}85)$$

($\overline{w}_2/\overline{w}_1$ appears since X contains $\overline{w}_2$, and at the initial instant the fluid velocity averaged over the cross section equals $\overline{w}_1$).

The function G_n must also satisfy the boundary condition at the entrance: for sufficiently large Fo, it approaches the new stationary value

$$G_n(X, \infty) = \exp\left(-\varepsilon_n^2 X\right).$$

As in the preceding cases, G_n can be found from the energy equation in integral form, which is solved by the method of characteristics. The calculations lead to the following results [12].

For each value of n there is a characteristic curve that divides the Fo-X plane into two regions, and passes through the origin. This curve is described by the equation

$$X = \frac{\text{Fo}}{I_n} + \frac{2\left(1 - \frac{\overline{w}_1}{\overline{w}_2}\right)}{\text{Pr}\,\overline{\psi}_n} \sum_{m=0}^{4} \frac{b_{nm}}{b_{n0}} \frac{(-1)^m}{E_m^5} \left[\exp\left(-E_m^2 \text{Pr}\,\text{Fo}\right) - 1\right]. \qquad (17\text{-}86)$$

For the region below the characteristic curve (small values of Fo), G_n is determined from the equation
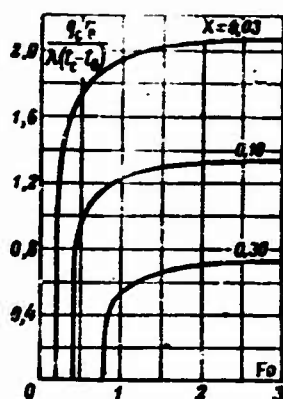
Fig. 17-20. Heat transfer in a
flat tube with step variation
in pressure gradient and con-
stant wall temperature ($\overline{w}_1 = 0$,
Pr = 0.7).

$$\frac{1}{\epsilon_n^2} \cdot \frac{\overline{w}_1}{\overline{w}_2} \ln G_n = -X + \left(\frac{1}{l_n} - \frac{\zeta_n}{\epsilon_n^2} \cdot \frac{\overline{w}_1}{\overline{w}_2} \right) Fo +$$

$$+ \frac{2 \left(1 - \frac{\overline{w}_1}{\overline{w}_2} \right)}{Pr \, \overline{\psi}_n} \sum_{m=0}^{4} \frac{b_{nm}}{b_{n0}} \frac{(-1)^m}{E_m^5} [\exp(-E_m^2 \, Pr \, Fo) - 1]; \qquad (17\text{-}87)$$

for the region lying above the characteristic curve (large values of
Fo) G_n is found from the equation

$$X = -\frac{1}{\tau_{in}} \ln G_n + \frac{2 \left(1 - \frac{\overline{w}_1}{\overline{w}_2} \right)}{Pr \, \overline{\psi}_n} \sum_{m=0}^{4} \frac{b_{nm}}{b_{n0}} \cdot \frac{(-1)^m}{E_m^5} \exp(-E_m^2 \, Pr \, Fo) \times$$

$$\times \left[1 - \exp \left(-E_m^2 \, Pr \, \frac{\ln G_n}{\zeta_n} \right) \right]. \qquad (17\text{-}88)$$

Here ψ_n, E_m, b_{n0}, b_{nm}/b_{n0} and ϵ_n have the same values as in (17-67);

$\psi_n - \int_0^1 \psi_n \, dY$. The constants l_n and ζ_n are found with the aid of the same

relationships as the similar constants in (17-73) and (17-75);
$\eta_n = l_n \zeta_n$. Their values are given in Table 17-2.

When Fo $\rightarrow \infty$, the exponential term in (17-88) vanishes, and
then

$$G_n = \exp(-\eta_n X).$$

Since the values of η_n are in good agreement with the values of
ϵ_n^2 (except for large n), we see that for sufficiently large Fo, ap-

- 483 -

proximate solution (17-84) reduces to the exact solution for the stationary state. Thus we can use (17-86)-(17-88) to determine q_n in (17-84). Using the Fourier law and Eq. (17-84), we find the expression for the heat-flux density at the wall:

$$\frac{q_c r_0}{\lambda (t_c - t_0)} = \sum_{n=0}^{4} \sum_{m=0}^{4} b_{n_0} \left(\frac{b_{n m}}{b_{n_0}} \right) (-1)^m E_m G_n. \tag{17-89}$$

As an example, let us consider the case in which the pressure gradient is initially zero, and then abruptly takes on a constant value. This is the sharpest possible change in the pressure gradient, so that this case illustrates the maximum influence that flow nonstationarity can have on heat exchange. Thus the fluid is first motionless and, consequently, its temperature in the heated segment of the tube will equal the wall temperature, thus differing from the temperature of the fluid at the entrance (i.e., there is no heat exchange in the heated segment). Figure 17-20 shows the change in heat-flux density at the wall with time for Pr = 0.7 and several values of X. At the beginning of the nonstationary period, when fluid motion arises, the heat transfer in a certain cross section X will remain equal to zero until the fluid at temperature t_0 reaches this section. During the subsequent period, the heat flux will rise rapidly, and will then take on a constant (stationary) value corresponding to the velocity distribution that has been established.

17-7. HEAT EXCHANGE IN A FLAT TUBE WITH SIMULTANEOUS TIME VARIATION IN PRESSURE GRADIENT AND BOUNDARY CONDITIONS AT THE WALL

In this case, the heat-exchange process is nonstationary owing both to the nonstationary nature of flow and the time variation in the boundary condition at the wall; these two factors act simultaneously.

1. Let a fluid be in stationary motion at an average velocity $\bar{w}_1$ in a flat tube. The fluid and wall temperatures are identical everywhere, and equal to the fluid temperature at the entrance $(t = t_c = t_0)$, so that there is no heat exchange. At a certain time ($\tau = 0$), the pressure gradient and the wall temperature at the heated segment change instantaneously, taking on new constant values. These disturbances produce a nonstationary transient process; with the course of time, this process leads to a new stationary state of flow and heat exchange with mean velocity $\bar{w}_2$ and wall temperature t_{s_2}.

This nonstationary problem resembles the one considered in the preceding section. If we define the dimensionless temperature in the form

$$T = \frac{t - t_0}{t_{c2} - t_0},$$

then the energy equation (17-81) and the boundary conditions (17-83b) also apply to this case. The initial condition will differ, however. In place of (17-83a), we must write

$$T(X, Y, 0) = 0.$$

The solution of this problem has the same form as for the preceding one:

$$T = 1 - \sum_{n=0}^{\infty} b_n \psi_n (Y) H_n (X, Fo).$$ (17-90)

where H_n is an unknown function.

The function H_n is determined from the energy equation in integral form, which is solved by the method of characteristics. Calculations given in [12] show that the characteristic curve, which divides the Fo-X plane into two regions and passes through the origin, as in the preceding case, is described by Eq. (17-86).

For the region lying below the characteristic curve (small values of Fo), the function H_n is found from the equation

$$H_n = \exp(-\zeta_n Fo),$$ (17-91)

where ζ_n is the same constant as in (17-75).

For the region lying above the characteristic curve (large values of Fo), the function H_n is determined with the aid of the same equation as the function G_n in the preceding section, i.e., Eq. (17-88), where we must replace G_n by H_n for the present case.
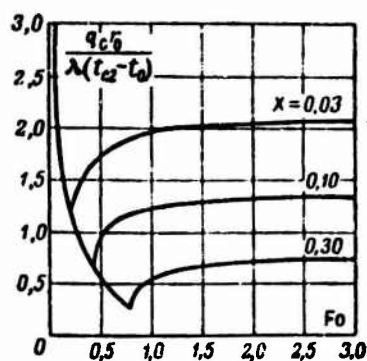
Fig. 17-21. Heat transfer in flat tube for simultaneous step variation in pressure gradient and wall temperature $(\bar{w}_1 = 0, Pr = 0.7)$.

The expression for the heat-flux density at the wall coincides with Eq. (17-89) if we replace the function G_n by the function H_n in this equation.

Figure 17-21 shows the results of heat-transfer calculations for the case in which the fluid is first motionless $(w_1 = 0)$, being everywhere at the same temperature as the wall $(t = t_{c1} = t_0)$; the pressure gradient and, simultaneously, the wall temperature change

ruptly, and then remain unknown. As we can see from Fig. 17-21, for each value of X, the heat transfer will pass through a minimum and then increase to a certain constant value corresponding to the stationary state. The minimum points correspond to the time intervals during which the fluid that had previously been in the stilling segment reaches the given tube cross section. For small Fo (less than the Fo values corresponding to the minimum points), the temperature along the tube axis will not change, and the convective term will drop out from the energy equation. Thus the curve on the left side of Fig. 17-21, corresponding to a reduction in heat transfer, essentially reflects the process of nonstationary heat conduction. For values of Fo exceeding the Fo values at the minimum points, the derivative $\partial T/\partial X$ no longer equals zero, the convective term in the energy equation has a finite value, and under the influence of the increasing velocity the heat transfer increases until the velocity reaches the constant value $\bar{w}_2$.

2. In contrast to the preceding problem, if prior to the initial time there is stationary heat exchange $(t_{c1} \neq t_0)$, while the wall temperature later changes abruptly from t_{s_1} to t_{s_2}, with a simultaneous abrupt change in the pressure gradient, a solution can be obtained to this problem by summation of the solutions applying to the two special cases considered previously. Let the following conditions obtain in each of these cases:

1 Случаи	2 Температура на входе	3 Скачок температуры стенки	4 Изменение скорости
5 Первый	$t_0 = 0$	6 От 0 до $t_{c2} - t_{c1}$ 7	6 От $\bar{w}_1$ до $\bar{w}_2$ 7
8 Второй	t_0	6 От t_{c1} до t_{c1} 7	6 От $\bar{w}_1$ до $\bar{w}_2$ 7
9 Общий	t_0	6 От t_{c1} до t_{c2}	6 От $\bar{w}_1$ до $\bar{w}_2$ 7

1) Case; 2) exit temperature; 3) jump in wall temperature; 4) velocity change; 5) first; 6) from; 7) to; 8) second; 9) total.

As we can see, summation of the temperature conditions for these two cases yields the conditions corresponding to our present problem (i.e., to the general case).

A solution can be written for the first case if we use Eq. (17-90):

$$t = (t_{c_2} - t_{c_1})\left[1 - \sum_{n=0}^{4} b_{n0}\psi_n(Y) H_n(X, \text{Fo})\right].$$

In the second case, on the basis of the results of the preceding section [see Eq. (17-84)], we have

$$t = (t_{c_1} - t_0)\left[1 - \sum_{n=0}^{4} b_{n0}\psi_n(Y) G_n(X, \text{Fo})\right] + t_0.$$

/497
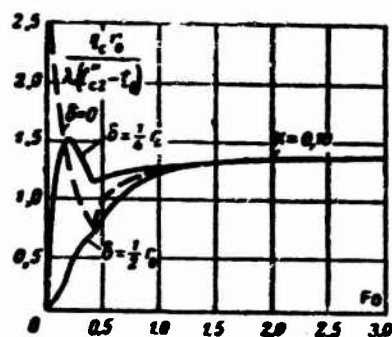
Fig. 17-22. Heat transfer in flat tube at distance X = 0.1 from the entrance with step variation in pressure gradient and temperature of outside wall surface ($\bar{w}_1$ = 0; $2r_0$ = 6.4 mm; wall of chrome-nickel steel, air as heat-transport medium).

Adding these expressions, we obtain the solution to our problem:

$$\frac{t-t_0}{t_{c2}-t_0}=\frac{t_{c2}-t_{c1}}{t_{c2}-t_0}\left[1-\sum_{n=0}^{4} b_{n_0}\psi_n(Y)H_n(X,\ \text{Fo})\right]+$$

$$+\frac{t_{c1}-t_0}{t_{c2}-t_0}\left[1-\sum_{n=0}^{4} b_{n_0}\psi_n(Y)G_n(X,\ \text{Fo})\right]. \tag{17-92}$$

When $t_{c2}=t_{c1}$, Eq. (17-92) reduces to (17-84), while when $t_{c1}=t_0$, it reduces to (17-90).

3. In studying nonstationary heat exchange under a step change in wall temperature with time, we have always assumed that the wall is either very thin, or that it possesses extremely high thermal diffusivity, so that its inside surface takes on the specified temperature almost instantaneously following a jump. To allow for the influence of finite wall thickness on heat exchange, we must specify the instantaneous change in temperature at the outside surface, and jointly consider the nonstationary conduction processes in the wall and the convective heat exchange between the wall and the fluid flow. A complete solution of this problem is very difficult, but we can give a certain amount of analysis.

During the initial period following the jump in t_s, heat is transported in the flow basically by conduction; thus to calculate the heat exchange during this period, we can make use of the solution to the problem of nonstationary heat conduction in a two-layer 1 finite plate. The first layer corresponds to the tube wall and the second to the fluid included between the wall and the tube axis. A solution of this problem under corresponding boundary conditions has been given in [13], while an expression for the heat transfer appears in [12]. This computation will be valid for values of Fo from 0 to the values at which the fluid that had previously been in the stilling segment begins to exert an influence on heat transfer

- 487 -

in the given cross section (the minimum points in Fig. 17-21, whose locations are known). For large values of Fo, corresponding to the stationary state, we can use the heat-exchange calculation method discussed in Chapter 11. For a stationary regime, however, the influence of finite wall thickness will not be great, as a rule, and it can be neglected. Interpolation must be used for intermediate values of Fo.

Figure 17-22 illustrates the influence of finite wall thickness on heat transfer in a flat tube at a distance $X = 0.1$ from the entrance when the temperature of the outside wall surface jumps from $t_{c1}'' = t_0$ to t_{c2}''. The remaining conditions are the same as for Fig. 17-21 (in particular, $\bar{w}_1 = 0$). As we see, the finite wall thickness may have a very considerable influence. While when $\delta = 0$ (the same case as in Fig. 17-21), the heat transfer drops during the initial period, and then increases to a finite stationary value, when $\delta = r_0/4$, the heat transfer first increases from 0 to a maximum, and then drops to a minimum point; only after this does it again increase to a stationary value. When $\delta = r_0/2$, the heat transfer spends the entire time rising from zero to the stationary value, i.e., there are neither maximums nor minimums.

4. The problem of heat exchange in a flat tube with simultaneous step variations in the pressure gradient and heat-flux density at the wall has been solved on the assumption of slug flow [14].[9] The fluid velocity, constant over the cross section, is taken equal to the mean velocity of the actual flow, and is determined from Eq. (5-49). All other conditions are the same as for the problem of heat exchange with step variation in $\partial p/\partial x$ and t_{s_1}, which was considered in paragraph 1.

If the flow is initially stationary, with no heat exchange $(w_x = \bar{w}_1, \ t = t_0 \text{ and } q_c = 0)$, and the pressure gradient subsequently changes abruptly while at the very same instant a heat-flux density q_s is set up at the inside wall surface, then the change in wall temperature with time and with length will be described by the equation

$$\frac{t_c - t_0}{\frac{q_c r_0}{\lambda}} = L_0(X, \text{Fo}) + \frac{1}{3} - 2 \sum_{n=0}^{\infty} \frac{1}{(n\pi)^2} L_n(X, \text{Fo}), \qquad (17\text{-}93)$$

where

$$X = \frac{4}{\text{Pe}} \cdot \frac{x}{2r_0}; \quad \text{Pe} = \frac{\bar{w}_2 2r_0}{a}; \quad \text{Fo} = \frac{a\tau}{r_0^2}.$$

The functions L_0 and L_n are determined differently, depending on which of the two regions on the Fo-X plane contains the given point. These regions are separated by the limiting characteristic, whose equation has the form

$$X = \text{Fo} - \frac{6}{\text{Pr}} \left(\frac{\bar{w}_1}{\bar{w}_2} - 1 \right) \sum_{m=0}^{\infty} \frac{1}{E_m^6} \left[\exp(-E_m^2 \text{Pr Fo}) - 1 \right], \qquad (17\text{-}94)$$

where

$$E_m = \left(m + \frac{1}{2}\right)\pi.$$

For points lying below the limiting characteristic (small values of Fo),

$$\left.\begin{array}{l} L_0 = Fo; \\ L_n = \exp\left[-(n\pi)^2 Fo\right]. \end{array}\right\} \qquad (17\text{-}95)$$

For points lying above the limiting characteristic (large values of Fo), L_0 and L_n are found from the expressions

$$\left.\begin{array}{l} X = L_0 - \dfrac{6}{Pr}\left(\dfrac{\overline{w_1}}{\overline{w_2}} - 1\right)\displaystyle\sum_{m=0}^{\infty} \dfrac{1}{E_m^6}\exp\left(-E_m^2\,Pr\,Fo\right) \times \\ \qquad\qquad \times \left[1 - \exp\left(-E_m^2\,Pr\,L_0\right)\right], \\[2mm] X = -\dfrac{1}{(n\pi)^2}\ln L_n - \dfrac{6}{Pr}\left(\dfrac{\overline{w_1}}{\overline{w_2}} - 1\right)\displaystyle\sum_{m=0}^{\infty}\dfrac{1}{E_m^6}\times \\[2mm] \qquad \times \exp\left(-E_m^2\,Pr\,Fo\right)\left[1 - \exp\left(-\dfrac{E_m^2\,Pr}{(n\pi)^2}\ln L_n\right)\right]. \end{array}\right\} \qquad (17\text{-}96)$$
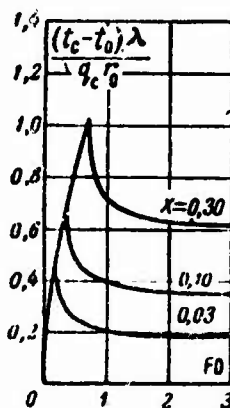
Fig. 17-23. Variation in wall temperature of flat tube under simultaneous step change in pressure gradient and heat flux at wall $\left(\overline{w_1} = 0,\ Pr = 0.7,\ Fo = \dfrac{a\tau}{r_0^2}\right)$.

Figure 17-23 shows the results of a wall-temperature calculation using Eq. (17-93) for the case in which $\overline{w_1} = 0$ and $Pr = 0.7$. During the initial period, the wall temperature increases to a maximum and then decreases to the stationary value. This value is established when the fluid velocity reaches the final value $\overline{w_2}$.

Nonstationary heat exchange in a flat tube has also been determined on the assumption of slug flow under more complicated
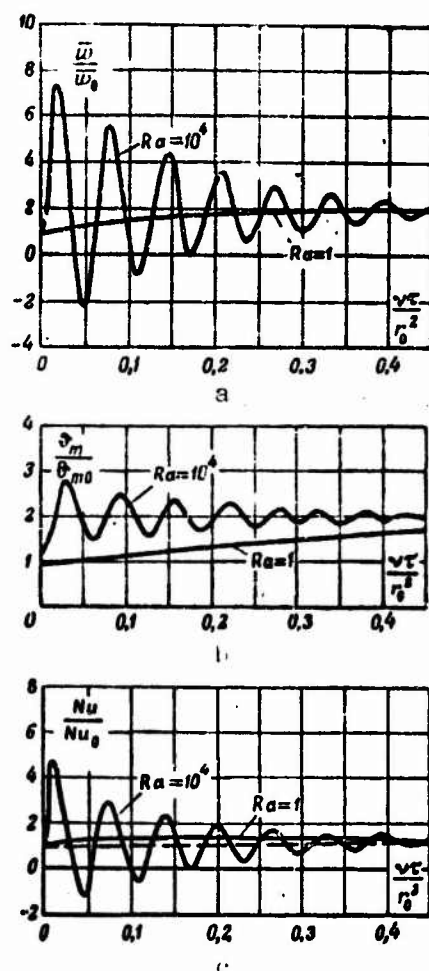
Fig. 17-24. Time variation in mean velocity (a), mean fluid temperature (b), and heat transfer (c) under double step increase in pressure gradient.

boundary conditions [16], in particular for an arbitrary variation in q_s in time and over tube length, and with a simultaneous change in velocity with time [in the latter case, just for an elementary type of relationship, $q_c = q_c(\tau, x)$ and $w = w(\tau)$] . As we have already noted, calculations based on the slug-flow model give qualitatively correct results, but the quantitative values of the unknown variables may depart substantially from the true values.

. We have so far considered nonstationary processes of convective heat exchange for pure forced motion of the fluid. Certain results pertaining to joint action of forced and free convection are of some interest, however. In [17], a study was made of nonstationary flow and heat exchange in flat tubes, and in [18] in round vertical tubes for heating of an upward-flowing fluid or cooling of a downward-flowing fluid. An analysis was carried out for fully developed (stabilized) flow and heat exchange with a linear variation in wall temperature along the length, and uniform heat release in the flow. The initial stationary state was disrupted by an arbitrary time variation in wall temperature, pressure gradient, and output

- 490 -

of internal heat sources.

The calculations show that under such conditions the time variations in velocity, fluid temperature, and heat transfer take the form of oscillations with damped amplitude. The oscillations are most noticeable when Pr = 1 and Ra or Gr are large, as is quite clear from Fig. 17-24. This figure shows the results of calculations for a nonstationary transient in a round tube when the flow contains no internal heat sources, for Pr = 1, and for two values of Ra, 1 and 10^4 (here $Ra = Gr\,Pr = \frac{g\beta A r_0^4}{v^2}\,Pr$, where $A \cdot \frac{\partial t}{\partial x} = \mathrm{const}$). The nonstationarity results from an abrupt change, by a factor of 2, in the pressure gradient while the wall temperature remains constant (in time). The figure shows curves characterizing the time variation in the mean velocity $\bar{w}$, the mean temperature ϑ_m over the cross section (measured from t_s), and Nu (which was computed with the aid of the temperature head ϑ_m). All these quantities refer to the corresponding stationary values at the initial instant. While all these variables change monotonically when Ra = 1, they oscillate when Ra = 10^4; the oscillation amplitude is damped with time.

The appearance of oscillations can be explained as follows. The increasing pressure gradient causes an increase in the fluid velocity and, consequently, in the heat transfer (since $\partial t/\partial x = dt_s/dx = \mathrm{const}$). If the wall temperature remains constant in time, this will increase the mean fluid temperature and correspondingly reduce the lift force. The latter entails a reduction in velocity, a decrease in heat transfer, and a reduction in the mean fluid temperature. This increases the lift force, which again leads to a rise in the velocity, etc. The oscillation frequency is greater the larger Ra. The oscillations are gradually damped by the viscosity and heat conduction.

17-8. SOME GENERAL LAWS GOVERNING NONSTATIONARY HEAT EXCHANGE FOR LARGE VALUES OF THE FOURIER NUMBER

In the preceding sections of this chapter, we have given solutions for individual problems of nonstationary heat exchange. Here we shall consider certain general laws governing the behavior of the nonstationary temperature field and the Nusselt number for large values of Fo. The following discussion is based on results obtained by V.D. Vilenskiy [19] with the aid of asymptotic estimates of the nonstationary temperature field.

Let us consider nonstationary heat exchange with stationary motion of a fluid in a straight tube whose cross section is arbitrary but constant along the length. If we assume that the physical properties of the fluid are constant, that the flow is stabilized, and that effects associated with energy dissipation and heat conduction along the axis are negligibly small, then the nonstationary temperature field is described by the equation

$$\frac{\partial \Theta}{\partial Fo} + W_x(Y, Z)\,\frac{\partial \Theta}{\partial X} = \frac{\partial^2 \Theta}{\partial Y^2} + \frac{\partial^2 \Theta}{\partial Z^2}, \qquad (17\text{-}97)$$

where

$$\theta=\frac{t-t_0}{t_0}; \quad \text{Fo}=\frac{i a \tau}{d_s^2}; \quad W_x=\frac{w_x}{\bar{w}};$$

$$X=\frac{4}{\text{Pe}}\frac{x}{d_s}; \quad \text{Pe}=\frac{\bar{w} d_s}{a}; \quad Y=\frac{2y}{d_s}; \quad Z=\frac{2z}{d_s};$$

here $d_s=\frac{4f}{s}$ is the equivalent diameter, f is the tube cross-section-al area; s is the perimeter; and t_0 is the fluid temperature at the tube entrance.

Let there be stationary heat exchange before the nonstationary process commences in the tube. Then the temperature field at the initial time is described by the equation

$$\theta_{\text{Fo}=0}=\theta_0(X, Y, Z), \qquad (17\text{-}98)$$

where θ_0 is the solution of the problem,

$$\left.\begin{array}{l} W_x\,\dfrac{\partial\theta_0}{\partial X}=\dfrac{\partial^2\theta_0}{\partial Y^2}+\dfrac{\partial^2\theta_0}{\partial Z^2}, \\[2mm] \theta_0(0, Y, Z)=0, \ \theta_0(X, Y_c, Z_c)=\Phi_0, \end{array}\right\} \qquad (17\text{-}98a)$$

where Y_s and Z_s are the values of the Y and Z coordinates at the wall.

The fluid temperature at the tube entrance is assumed to be constant over the cross section and invariant in time, i.e.,

$$\theta(0, Y, Z, \text{Fo})=0. \qquad (17\text{-}99)$$

We confine the discussion to nonstationary processes resulting from the fact that beginning at time Fo = 0, the wall temperature, which is constant over the surface, changes with time in accordance with the law

$$\theta(X, Y_c, Z_c, \text{Fo})=\Phi(\text{Fo}). \qquad (17\text{-}100)$$

As to the function $\Phi(\text{Fo})$, we assume that it is differentiable a sufficient number of times, and that $\frac{d\Phi}{d\text{Fo}}>0$.[10]

Considering the existence and uniqueness of solutions to boundary-value problems for equations of the type (17-97), we see that in the region $|Y|\leqslant|Y_c|, |Z|\leqslant|Z_c|, \text{Fo}>0, X>0$, the solution of Eq. (17-97) is uniquely determined by Conditions (17-98)-(17-100).[11] We use the plane $X = W_m\text{Fo}$ (W_m is the maximum value of the fluid velocity W_x) to divide this region into two regions: $|Y|\leqslant|Y_c|, |Z|\leqslant|Z_c|, \text{Fo}>0, X>W_m\text{Fo}$ and $|Y|\leqslant|Y_c|, |Z|\leqslant|Z_c|, \text{Fo}>0, X<W_m\text{Fo}$. We note that $X = W_m\text{Fo}$ corresponds to the maximum distance traversed during time τ_0 by the fluid located, at the initial instant, in the entrance section to the heated tube segment. In the first region, the solution

of (17-97) is uniquely determined by just the initial condition (17-98) and the condition (17-100) at the tube wall. In the second region, the solution is determined by the condition (17-99) at the entrance, the condition (17-100) at the wall, and the condition at the boundary between the first and second regions:

$$(17-101)$$

where θ_1 and θ_2 are the fluid temperatures at $X \geqslant W_m \text{Fo}$ and $X < W_m \text{Fo}$, respectively.

1. The solution at $X \geqslant W_m \text{Fo}$ does not depend on the conditions at the entrance, and in the case considered $\left(\frac{\partial \Phi}{\partial X} = 0\right)$ reduces to solution of the heat-conduction equation. This solution has been obtained in [19]. To determine the time variation of Nu, however, it is more convenient to replace the exact solution by asymptotic estimates for the temperature field, which are valid for large Fo.[12]

As has been shown in [19], the limiting properties in time for the temperature field and, consequently, for Nu are determined by the limit of the logarithmic derivative of the function describing the change in tube wall temperature with time when Fo → ∞. Asymptotic estimates of the temperature field are obtained for two types of function $\Phi(\text{Fo})$. The functions of the first type include those functions $\Phi(\text{Fo})$ for which

$$\lim_{\text{Fo}\to\infty} \frac{d \ln \Phi}{d \text{Fo}} = 0;$$

while the functions of the second kind include those functions for which

$$\lim_{\text{Fo}\to\infty} \frac{d \ln \Phi}{d \text{Fo}} = K_* \ (K_* > 0).$$

When Fo is large, for functions of the first type

$$\theta_1 \approx \Psi(\text{Fo}) + V_1(Y, Z) \frac{d\Phi}{d \text{Fo}} - \Phi_* + \theta_* + o\left(\frac{d\Phi}{d \text{Fo}}\right), \qquad (17-102)$$

while for functions of the second type

$$\theta_1 \approx V_0(Y, Z)\Phi(\text{Fo}) + o(\Phi)^{*13}. \qquad (17-103)$$

The functions V_1 and V_0 are found from the solution to the following problems:

$$\frac{\partial^2 V_1}{\partial Y^2} + \frac{\partial^2 V_1}{\partial Z^2} = 1, \ V_1(Y_c, Z_c) = 0;$$

$$\frac{\partial^2 V_0}{\partial Y^2} + \frac{\partial^2 V_0}{\partial Z^2} - K_0 V_0 = 0, \ V_0(Y_c, Z_c) = 1.$$

Using Expressions (17-102) and (17-103), we can show that when X is sufficiently large (as large as the value of Fo at which the asymptotic estimates (17-102) and (17-103) become valid, which

happens when $X \geqslant W_m Fo$), the local value $Nu = \frac{\omega d_s}{\lambda}$ approaches the limit $Nu_{1\infty}$. If $\Phi(Fo)$ is a function of the first type, then

$$Nu_{1\infty} = -2 \frac{L \left(\frac{\partial V_1}{\partial N}\right)_{Y=Y_c, Z=Z_c} + \left(\frac{\partial \Theta_0}{\partial N}\right)_{Y=Y_c, Z=Z_c}}{\Phi_0 - \frac{L}{F}\int_F V_1 W_x df - \frac{1}{F}\int_F \Theta_0 W_x dF}, \qquad (17\text{-}104)$$

where $L = \lim\limits_{Fo \to \infty} \frac{d\Phi}{d\,Fo}$; $N = \frac{n}{d_s/2}$ is the dimensionless normal to the wall, directed toward the fluid; $F = \frac{4f}{d_s^2}$ is the dimensionless cross-sectional area.

Since for fixed X, the values of Fo are bounded in the region $X \geqslant W_m Fo$, Nu reaches values $Nu_{1\infty}$ only if $\frac{d\Phi}{d Fo}$ approaches L rapidly enough. Here, as we can see from (17-104), $Nu_{1\infty}$, depends on X, since Θ_0 depends on X. When $L = 0$, $Nu_{1\infty}$ coincides with the stationary values. If $\frac{d\Phi}{d Fo}$ rises without limit when Fo $\to \infty$, then

$$Nu_{1\infty} = - \frac{2F \left(\frac{\partial V_1}{\partial N}\right)_{Y=Y_c, Z=Z_c}}{\int V_1 W_x dF} \qquad (17\text{-}105)$$

and, consequently, it does not depend on X.

If $\Phi(Fo)$ is a function of the second type, then

$$Nu_{1\infty} = - \frac{2 \left(\frac{\partial V_0}{\partial N}\right)_{Y=Y_c, Z=Z_c}}{1 - \frac{1}{F}\int_F V_0 W_x dF}. \qquad (17\text{-}106)$$

The value of Fo at which Nu reaches values $Nu_{1\infty}$ depends on the tube geometry, the type of function that $\Phi(Fo)$ is, and the distance from the beginning of the heated segment (if there was stationary heat exchange prior to the beginning of the nonstationary process). It can be determined for each specific case by using the exact solution given in [19].

2. In the region of values $X < W_m Fo$, the temperature field depends on the conditions at the entrance, and is determined by the solution of Eq. (17-97) under Conditions (17-99), (17-100), and (17-101). Here also we can obtain an asymptotic representation for the temperature field that is valid for large Fo. It has the form

$$\Theta_1 \approx \sum_{i=0}^{\infty} U_i(X, Y, Z) x_i(Fo) + \Theta_0(X, Y, Z). \qquad (17\text{-}107)$$

The functions U_i are solutions of the problems

$$W_x \frac{\partial U_0}{\partial X} = \frac{\partial^2 U_0}{\partial Y^2} + \frac{\partial^2 U_0}{\partial Z^2} - K_0 U_0,$$
$$U_0(0, Y, Z) = 0, \ U_0(X, Y_c, Z_c) = 1; \qquad\qquad (17\text{-}108)$$

$$W_x \frac{\partial U_i}{\partial X} = \frac{\partial^2 U_i}{\partial Y^2} + \frac{\partial^2 U_i}{\partial Z^2} - K_i U_i - U_{i-1},$$
$$U_i(0, Y, Z) = 0, \ U_i(X, Y_c, Z_c) = 0. \qquad\qquad (17\text{-}109)$$

The functions X_i are determined by the relationships

$$X_0 = \Psi - \Phi_s; \ldots; \ X_i = \frac{dX_{i-1}}{d\text{Fo}} - K_{i-1} X_{i-1};$$

$$K_i = \lim_{\text{Fo} \to \infty} \frac{d \ln X_i}{d \text{Fo}}.$$

If for a certain $i = i_1 \frac{d \ln X_{i_1}}{d \text{Fo}} = K_{i_1}$, then Series (17-107) breaks off at term i_1, and we obtain the following asymptotic expression for θ_2:

$$\theta_2 = \sum_{i=0}^{i_1} U_i(X, Y, Z) \ X_i(\text{Fo}) + O\left[\exp(-\lambda_1 \text{Fo})\right].^{14}$$

where λ_1 is the first eigenvalue of the problem

$$\frac{\partial^2 \Psi}{\partial Y^2} + \frac{\partial^2 \Psi}{\partial Z^2} + \lambda \Psi = 0, \ \Psi(Y_c, Z_c) = 0.$$

Using (17-107), we can derive asymptotic equations for specific cases. These equations will be valid beginning at a certain Fo value that can be determined by numerical solution of the corresponding problem, or by the approximate method given in [19].

Using the asymptotic equations for the temperature field, we can obtain the corresponding expressions for Nu.

When $X < W_m \text{Fo}$, the limiting heat-exchange properties corresponding to large Fo values are determined, as in the case in which $X \cdot W_m \text{Fo}$, by the limit of variation for the logarithmic derivative of the function $\Phi(\text{Fo})$ describing the wall-temperature variation in time. If the function $\Phi(\text{Fo})$ is of the first or second type, then Nu is stabilized in time. While in the first case the limiting Nusselt number corresponds to a stationary value, in the second case it differs from the stationary value.

If $\Phi(\text{Fo})$ is a function of the second type, then

$$\text{Nu}_{2\infty} = \frac{2\left(\frac{\partial U_0}{\partial N}\right)_{Y = Y_c, \ Z = Z_c}}{1 - \frac{1}{F} \int_F U_0 W_x dF}. \qquad\qquad (17\text{-}110)$$

When $X \to \infty$, U_0 and, consequently, $Nu_{z\infty}$ will cease to depend on X, i.e., $Nu_{z\infty}$ becomes stabilized along the tube length.

TABLE 17-4

Values of Nu in Round Tube When the Wall Temperature Varies Linearly in Time

Fo	Nu			Fo	Nu		
	$X=0.5$	$X=1.0$	$X=2.0$		$X=0.5$	$X=1.0$	$X=2.0$
0.005	31.56	31.56	31.56	5.0	4.17	5.15	5.97
0.01	22.07	22.07	22.07	10	3.93	4.72	5.93
0.05	10.63	10.63	10.63	50	3.71	3.98	5.67
0.1	8.21	8.21	8.21	100	3.68	3.83	5.42
0.25	6.55	6.55	6.55	500	3.66	3.69	4.54
0.5	6.02	6.11	6.11	1 000	3.66	3.67	4.20
0.75	5.62	5.93	6.02	5 000	3.66	3.66	3.79
1.0	5.34	5.86	6.01	10 000	3.66	3.66	3.72

As an example, Table 17-4 shows the results of calculations for Nu in the case of nonstationary heat exchange in a round tube produced by a linear increase in wall temperature with time, under the condition that there is no heat exchange at the initial instant. When Fo = 0, Nu is infinite, while as Fo increases, it drops sharply, approaching the limit $Nu_{1\infty} = 6$. For values $X > 1.2$-

1.5, Nu reaches its limit, and with a further increase in Fo shows almost no variation up to Fo = $X/2$, when the fluid that had been at the entrance to the heated segment at the initial instant arrives at the cross section under consideration. Following this, Nu again drops, approaching the stationary value. For values $X < 1.2$, Nu varies in like manner, except that within the region $X \geq 2$Fo, it cannot reach the limit $Nu_{1\infty}$.

Manuscript Page No.

Footnotes

447   [1]See, for example [2].

450   [2]The first six roots are derived on page   . There they are represented by the symbol ε_n.

461   [3]This is the superposition method, based on utilization of the Duhamel principle; this is discussed, for example in [4].

466   corresponding stationary problems are considered in §§15-1 and 15-2.

456   [5]These problems have been solved by Siegel and Sparrow [6, 7].

467   [6]The temperature profile is approximated by quadratic relationship (17-49) for a stationary regime with an error of up to 14% of the exact-solution result. Utilization of a higher-order polynomial gives no noticeable improvement, however.

473   [7]The numerical values of the constants in this problem are the same as for the problem solved in §17-2, paragraph 2.

486   [8]This curve can be well described by the familiar solution to the problem of nonstationary heat conduction in an unbounded plate which was at first at a constant temperature t_0, and then experienced a temperature jump on its surface.

488   [9]The problem of heat exchange in flat and round tubes with stationary slug flow and a step variation in q_s

in time has been considered in [15].

492   [10]A similar approach can be used to investigate the case in which wall temperature decreases, as well as other nonstationary processes (time variation in heat flux at wall or in fluid temperature at entrance).

492   [11]For the references to the original studies, see [19].

493   [12]Estimates can be obtained by the same method as in the study referred to in §6-6 (see Reference [19] in the references for Chapter 6).

493   [13]The symbol $o(x)$ means that $o(x)$ is of lower order than x.

495   [14]The symbol $O(x)$ means that $O(x)$ is of the same order as x.

Manuscript Page No.   Transliterated Symbols

446   c = s = stenka = wall

479   кр = kr = kriticheskiy = critical

488   н = n = naruzhnyy = outside

492   э = e = ekvivalentnyy = equivalent

REFERENCES

Chapter 1

1. Landau, L.D. and Lifshits, Ye.M., Mekhanika sploshnykh sred [Mechanics of Continuous Media], Gos. izd. tekhniko-teoreticheskoy literatury, 1953.

2. Loytsyanskiy, L.G., Mekhanika zhidkosti i gaza [Mechanics of Liquids and Gases], Gos. izd. tekhniko-teoreticheskoy literatury, 1957.

3. Kochin, N.Ye., Kibel', I.A., and Roze, N.V., Teoreti-cheskaya gidromekhanika [Theoretical Fluid Mechanics], Part 2. Gos. izd. fiziko-matematicheskoy literatury, 1963.

4. Sovremennoye sostoyaniye aerodinamiki bol'shikh skorostey [High-Speed Aerodynamics: State of the Art], edited by Khouart, Vol. 1, Izd-vo inostrannoy literatury, 1955.

Chapter 3

1. Teplofizicheskiye svoystva veshchestv spravochnik [Thermophysical Properties of Matter, Handbook] edited by, N.B. Vargaftik, Gosenergoizdat, 1956.

2. Vargaftik, N.B., Spravochnik po teplofizicheskim svoystvam gazov i zhidkostey [Handbook on Thermophysical Properties of Gases and Liquids], Gos. izd. fiziko-matematicheskoy literatury, 1963.

3. Tables of Thermal Properties of Gases, U.S. NBS, Circular, 564, 1955.

4. Termodinamicheskiye svoystva individual'nykh veshchestv [Thermodynamic Properties of Individual Substances], Vol. 1 and 2, Izd-vo AN SSSR, 1962.

5. Golubev, I.F., Vyazkost' gazov i gazovykh smesey [Viscosity of Gases and Gas Mixtures], Fizmatgizdat, 1959.

6. Tsederberg, N.V., Teploprovodnost' gazov i zhidkostey [Thermal Conductivity of Gases and Liquids], Gosenergoizdat, 1957.

7. Teplotekhnicheskiy spravochnik [Heat-Engineering Handbook], Vol. 1, Gosenergoizdat, 1957.

8.   Spravochnik mashinostroitelya [Machine Designer's
        Handbook], Vol. 2, Mashgiz, 1961.

9.   Karapet'yants, M.Kh., Khimicheskaya termodinamika
        [Chemical Thermodynamics], Goskhimizdat, 1953.

Chapter 4

1.   Sedov, L.I., Metody podobiya i razmernosti v mekhanika
        [The Similarity and Dimensional Methods in Mechanics],
        Gos. izd. tekhniko-teoreticheskoy literatury, 1957.

2.   Voskresenskiy, K.D., Sbornik raschetov i zadach po tep-
        loperedache [Handbook of Heat-Transfer Calculations and
        Problems], Gosenergoizdat, 1959.

3.   Petukhov, B.S., Opytnoye izucheniye protsessov teploper-
        edachi [Experimental Study of Heat-Transfer Processes],
        Gosenergoizdat, 1952.

4.   Novikov, I.I. and Voskresenskiy, K.D., Prikladnaya
        termodinamika i teploperedacha [Applied Thermodynamics
        and Heat Transfer], Gosatomizdat, 1961.

Chapter 5

1.   Landau, L.D., and Lifshitz, Ye.M., Mekhanika sploshnykh
        sred [Mechanics of Continuous Media], Gos. izd. tekhniko-
        teoreticheskoy literatury, 1953.

2.   Loytsyanskiy, L.G., Mekhanika zhidkosti i gaza [Mechan-
        ics of Liquids and Gases], Gos. izd. tekhniko-teoret-
        icheskoy literatury, 1957.

3.   Marco, S.M., Han, L.S., A Note on Limiting Laminar Nus-
        selt Number in Ducts with Constant Temperature Gradient
        by Analogy to Thin-Plate Theory, Trans. ASME, 1955, Vol.
        77, pages 625-630.

4.   Eckert, E.R.G., Irvine, T.F., Yen, T.T., Local Laminar
        Heat Transfer in Wedge-Shaped Passages, Trans. ASME,
        1958, Vol. 80, pages 1433-1438.

5.   Tao, L.N., Nekotoryye zadachi o vynuzhdennoy konvektsii pri
        laminarnom techenii [Some Forced-Convection Problems in
        Laminar Flow], "Teploperedacha," [Heat Transfer], (Russian
        translation, Trans. ASME, Ser. C), 1961, No. 4, pages 96-
        103.

6.   Sparrow, E.M., Siegel, R.A Variational Method for Fully
        Developed Laminar Heat Transfer in Ducts, Trans. ASME,
        ser. C., 1959, Vol. 81, pages 157-167.

7.   Tao, L.N., Method of Conformal Mapping in Forced Convection
        Problems, International Developments in Heat Transfer,
        1961, International Heat Transfer Conference,Colorado,
        USA, rep. 61, page 598.

8. Eckert, E.R.G., Irvine, T.F., Trans. ASME, 1955, Vol. 77, No. 8.

9. Migay, V.K., Gidravlicheskoye soprotivleniye treugol'nykh kamalov v laminarnom potoke [Hydraulic Resistance of Triangular Channels in Laminar Flow], Izvestiya vuzov, xer. "Energetika," 1963, No. 5.

10. Sparrow, E.M. and Loeffler, Ir., Longitudinal Laminar Flow Between Cylinders Arranged in Regular Array, AIChE J., 1959, Vol. 5, No. 3, pages 325-330.

11. Laybenzon, L.S., Vil'ker, D.S., Shumilov, P.P. and Yablonskiy, V.S., Gidravlika [Hydraulics], Gos. nauchno-tekhn. gorno-geologo-neftyanoye izd., 1934.

12. Shiller, L., Dvizheniye zhidkosti v trubakh [Fluid Motion in Tubes], ONTI, 1936.

13. Shapiro, A.H., Siegel, R., Klein, S.I., Friction Factor in the Laminar Entry Region of a Round Tube, Proc. of the Second U.S. National Congress of Appl. Mechanics, ASME, 1954, pages 733-741.

14. Campbell, D., and Slattern, Ts., Techeniye v nachal'nom uchastke truby [Flow in the Initial Segment of a Tube] "Tekhnicheskaya mekhanika," [Engineering Mechanics], Russian translation, Trans. ASME, Ser. D., 1963, Vol. 85, No. 1, pages 51-57.

15. Sovremennoye sostoyaniye gidroaerodinamiki vyazkoy zhidkosti, [Hydro- and Aerodynamics of Viscous Fluids], edited by S. Gol'dshteyn, Vol. 1, Izd-vo inostrannoy literatury, 1948.

16. Targ, S.M., Osnovnyye zadachi teorii laminarnykh techeniy [Basic Problems in Laminar-Flow Theory], Gos. izd. tekhniko-teoreticheskoy literatury, 1948.

17. Langhaar, H.L., Steady Flow in the Transition Length of a Straight Tube, J. of Appl. Mechanics, Vol. 9; Trans. ASME, Vol. 64, 1942, pages A-55-58.

18. Punnis, B., Zur Berechnung der laminaren Einlaufstromung in Rohr, Bericht 47 P/03 Max Planck Inst. für Strömungsforschung, 1947. [Calculation of Laminar Inlet Flow in Tubes].

19. Tatsumi, T., Stability of the Laminar Inlet-Flow Prior to the Formation of Poiseuille Regime, J. Physic. Society of Japan, 1952, Vol. 7, No. 5, pages 489-495.

20. Prandtl, L. and Tit'yens, O., Gidro- i aeromekhanika [Hydro- and Aeromechanics], Vol. 2, ONTI, 1935.

21.   Reshotko, E., Experimental Study of the Stability of
Pipe Flow, 1. Establishment of an axially-symmetric
Poiseuille Flow, Progress Rep., No. 20, 364, Jet Pro-
pulsion Laboratory, California Inst. Technology, 1958.

22.   Leybenzon, L.S., Rukovodstvo po neftepromyslovoy mekhanike
[Handbook of Oil-Field Mechanics], Part, 1, Gidravlika,
GNTI, 1931.

23.   Sparrow, E.M., in book Knudsen, J.G. and Katz, D.L.,
Fluid Dynamics and Heat Transfer, 1958.

24.   Sugino Eitaro, Velocity Distribution and Pressure Drop
in the Laminar Inlet of a Pipe with Annular Space, Bull.
ISME, 1962, Vol. 5, No. 20, pages 651-655.

25.   Heaton, H.S., Reynolds, W.C., and Kays, W.M., Heat Trans-
fer in Annular Passages, Simultaneous Development of
Velocity and Temperature Fields in Laminar Flow, Inst.
of Heat and Mass Transfer, 1964, Vol. 7, pages 763-781.

26.   Sparrow, E.M., Lin S.H., The Developing Laminar Flow
and Pressure Drop in the Entrance Region of Annular
Ducts. Doklad 64-Fe-1 na konferentsii po gidrotekhnike,
ASME, Philadelphia, May 1964.

27.   Frankl', F and Baklanov, T., Trudy TsAGI, No. 176, 1939.

28.   Han, L.S., Hydrodynamic Entrance Lengths for Incompres-
sible Laminar Flow in Rectangular Ducts, J. of Appl.
Mech. (Trans. ASME, Ser. E), 1960, E27, pages 403-409.

29.   Developments in Heat Transfer, Academic Press, N.Y.
and London, 1963.

30.   Mori, Ya. and Nakayama, V., Issledovaniye teploobmena pri
vynuzhdennom techenii zhidkosti v izognutykh trubakh
[Investigation of Heat Exchange for Forced Fluid Flow
in Curved Tubes], Int. J. of Heat a. Mass Transfer, 1965,
Vol. 8, No. 1, pages 61-82.

31.   Dean, W.R., Note on the Motion of Fluid in Curved Pipe,
Phil. Mag., 1927, Vol. 4, pages 208-223; Phil. Mag.,
1928, Vol. 5, pages 673-695.

32.   Aronov, Z., O povyshenii kriticheskogo chisla Reynolds pri
dvizhenii zhidkosti v izognutykh trubakh [Increasing the
Critical Reynolds Number for Fluid Moving in Bent Tubes],
Izvestiya vuzov, ser. "Energetika," 1960, No. 4, page
127-132.

33.   Gromeka, I.S., K teorii dvizheniya zhidkosti v uzkikh
tsilindricheskikh trubkakh [Toward a Theory of Fluid
Motion in Narrow Cylindrical Tubes], Uchenyye zapiski
kazanskogo universiteta [Scientific Reports of Kazan
University], 1882; see also Sobraniye sochineniy, Izd-

Izd-vo AN SSSR, 1952, pages 149-171.

34. Szymanski, F., Quelques solutions exactes des equations
     de l'hydrodynamique de fluide vesqueux dans le cas d'un
     tube cylindreque, [Exact Solution for Hydrodynamic
     Equation of Fluid Flow in Cylindrical Tubes].
     J. de Mathem. pures et appliquees, 1932, Ser. 9, Vol. 11,
     pages 67-107.

35. Lup'ye, A.I., Operatsionnoye ischisleniye [Operational
     Calculus], ONTI, 1938.

36. Karslou, Kh., and Yeger, D., Operatsionnyye metody v
     prikladnoy matematike [Operational Methods in Applied
     Mathematics], Izd-vo inostranncy literature, 1948.

37. Perlmutter, M. and Siegel, R., Nestatsionarnoye laminar-
     noye techeniye v kanale s nestatsionarnym podvodom tepla,
     [Nonstationary Laminar Flow in a Channel with Nonstation-
     ary Supply of Heat], "Teploperedacha" [Heat Transfers],
     Russian Translation. ASME, Ser. C) 1961,No. 4, pages 52-63.

38. Lambosi, P., Vynuzhdennyye kolebaniya neszhimayemoy vyazkoy
     zhidkosti v zhestkoy gorizontalnoy trube [Forced Oscilla-
     tions of Incompressible Viscous Fluid in Rigid Horizontal
     Tube], Helvetica Physica Acta, 1952, 25, No. 4, see also
     Russian translation in collection "Mekhanika" [Mechanics],
     1953, No. 3, pages 67-77.

39. Uchida, Sh. The Pulsating Viscous Flow Superposed on the
     Steady Laminar Motion of Incompressible Fluid in a Circu-
     lar Pipe, ZAMP, 1956, Vol. 7, pages 403-422.

40. Siegel, R. and Perlmutter, M., Teplootdacha pri pul'sir-
     uyushchem laminarnom techenii v kanale [Heat Transfer
     for Pulsating Laminar Flow in a Channel], "Teploperedach,"
     Russian translation, Trans. ASME, Ser. C), 1962, No. 2,
     pages 18-32.

41. Karslou G. and Yeger D.,   Teploprovodnost' tverdykh
     tel, [Heat Conduction in Solids], Izd-vo "Nauka,"

42. El'perin, I.T., Galershteyn, D.M. and Levental', L.I.,
     Vliyaniye poverkhnostnykh effektov i nestatsionarnosti
     na protsessy perenosa v geterogennykh sistemakh [Influ-
     ence of Surface Effects and Nonstationarity on Trans-
     port Processes in Heterogeneous Systems. IFZh, 1964,
     Vol. VII, No. 8, pages 16-19.

43. Ladyzhenskaya, O.A., Matematicheskiye voprosy dinamiki
     vyazkoy zhidkosti [Mathematical Problems in the Dynamics
     of Viscous Fluids], Fizmatgiz, 1961.

Chapter 6

1. Graetz, L., Uber Warmeleitungsfahigheit von Flussigkeiten, [Heat Transfer Capacity of Fluids]. Ann. d. Physik, 1885, Vol. 25, pages 337-357.

2. Nusselt, W., Z. VDI. 1910, Vol. 54, pages 1154-1158.

3. Shumilov, P.P. and Yablonskiy, V.S., Issledovaniye peredachi tepla pri dvizhenii nefti i drugikh zhidkostey i gazov po trubam [Investigation of Heat Transfer for Petroleum and Other Fluids and Gases Moving Through Tubes], "Neftyanoye khozyaistvo," 1929, No. 5.

4. Jacob, M., Heat Transfer, Vol. 1, New York, 1949.

5. Lipkis, R., see discussion on article by W.M. Kays, Trans. ASME, 1955, Vol. 77, No. 8.

6. Brown, G.M., Heat or Mass Transfer in a Fluid in Laminar Flow in a Circular or Flat Conduit, AIChE J., 1960, Vol. 6, No. 2, pages 179-183.

7. Sellers, J.R., Tribus, M. and Klein, J.S., Heat Transfer to Laminar Flow in a Round Tube or Flat Conduit — the Graetz Problem Extended, Trans. ASME, 1956, Vol. 78, No. 2, pages 441-448.

8a. Grigull, U. and Tratz, H., Thermischer Einlauf in ausgebildeter laminarer Rohrströmung, [Thermal Influx in Developed Laminar Tube Flow]. Int. J. of Heat a. Mass Transfer, 1965, Vol. 8, No. 5, pages 669-678.

8b. Hausen, H., Z. VDI, Beiheft Verfahrenstechnik, 1943, No. 4, pages 91-98.

8. Rubinshteyn, Ya.M., Metod analogii s diffuziey i primeneniye yego dlya issledovaniya teploperedachi v nachal'nom uchastke truby [Diffusion Analogy Method and Its Application to Investigation of of Heat Transfer in Initial Segment of Tube], In collection. "Issledovaniye protsessov regulirovaniya, teploperedachi i obratnogo okhlazhdeniya," [Investigation of Control, Heat-Transfer, and Reverse-Cooling Processes], GONTI, 1938.

10. Nusselt, W., VDI, 1923, Vol. 67, page 206.

11. Norris, R.H., Streid, D.D., Trans. ASME, 1940, Vol. 62, page 525.

12. Leybenzon, L.S., K voprosu o teploperedache v nefteprovodnykh trubakh [The Problem of Heat Transfer in Petroleum Pipelines], "Neftyanoye khozyaystvo," 1928, No. 2.

13.   Mar'yamov, N.B., Analiticheskoye opredeleniye teplootdachi
       i gidravlicheskogo soprotivleniya maslyanykh radiatorov
       [Analytic Determination of Heat Transfer and Hydraulic
       Resistance of Oil Radiators], Trudy TsAGI, No. 444, 1939.

14.   Prins, J.A., Mulder, J., Schenk, J., Heat Transfer in
       Laminar Flow Between Parallel Plates, Appl. Scient. Res.,
       1951, Vol. A2, No. 5-6, pages 431-438.

15.   Siegel, R., Heat Transfer for Laminar Flow in Ducts with
       Arbitrary Time Variations in Wall Temperature, J. Appl.
       Mech. (Trans. ASME, Ser. E), 1960, E27, No. 2, pages
       241-249.

16.   Leveque, J., Ann. des Mines, 1928, Vol. 13, 12 serie.

17.   Shmushkevich, I.M., Teploperedacha v laminarnom potoke
       zhidkosti, protekayushchey v trubakh maloy dliny [Heat
       Transfer in Laminar Flow of Fluid Through Short Tubes],
       ZhTF, 1948, Vol. 18, No. 1.

18.   Schenk, J., A Problem of Heat Transfer in Laminar Flow
       Between Parallel Plates, Appl. Scient. Res., 1955, Vol. A5,
       No. 2-3, pages 241-244.

19.   Vilenskiy, V.D., Obshiye zakonomernosti stabilizatsii
       koeffitsienta teplootdachi pri techenii zhidkosti v
       kanale [General Laws Governing Stabilization of Heat-
       Transfer Coefficient for Fluid Flowing in Channel],
       "Teplofizika vysokikh temperatur," 1966, Vol. 4, No. 5.

20.   I. Auwerier, H.A. Appl. Scient. Res., 1950, Vol. A2,
       No. 3, page 184.

21.   Lauwerier, H.A., Appl. Scient. Res., 1951, Vol. A2, No. 1,
       page 58.

Chapter 7

1.   Leybenzon, L.S., O dvizhenii podogretoy vyazkoy zhidkosti
       [Motion of a Hot Viscous Fluid], "Azerbaydzhanskoye nef-
       tyanoye khozyaystvo," 1922, No. 2 (3) and 4 (5); 1924,
       No. 3 (27).

2.   Targ, S.M., Osnovnyye zadachi teorii laminarnykh techeniy,
       [Basic Problems in the Theory of Laminar Flows], Gos.
       izd. tekhnikoteoreticheskoy literatury, 1951.

3.   Mar'yamov, N.B., Analiticheskoye opredeleniye teplootdachi
       i gidravlicheskogo soprotivleniya maslyanykh radiatorov
       [Analytic Determination of Heat Transfer and Hydraulic
       Resistance for Oil Radiators], Trudy TsAGI, No. 444,
       1939.

4.   Lee, A., Nelson, W.O., Cherry, V.H. and Boelter, L.M.K.,
       Pressure Drop and Velocity Distribution for Incompres-

sible Viscous Nonisothermal Flow in the Steady State Through a Pipe, Proc. Fifth Int. Congress for Appl. Mech., 1939.

5. Boelter, L.M.K., Cherry, V.H., Johnson, H.A., and Martinelli, R.C., Heat Transfer Notes, University of California Press, Chapt. 10, 1948.

6. Yamagata, K., A Contribution to the Theory of Nonisothermal Laminar Flow of Fluids Inside a Straight Tube of Circular Cross Section, Memoirs of the Faculty of Engineering, Kyushu Imperial University, Fukuoka, Japan, 1940, Vol. 8, No. 6, pages 365-449.

7. Petukhov, B.S., Raschet teploobmena i gidravlicheskogo soprotivleniya pri laminarnom techenii zhidkosti peremennoy vyazkosti v ploskom kanale [Determination of Heat Exchange and Hydraulic Resistance for Laminar Flow of Fluid with Variable Viscosity in Flat Channel], "Teploenergetika," 1954, No. 7.

8. Petukhov, B.S., Raschet teploobmena i gidravlicheskogo soprotivleniya pri laminarnom techenii zhidkosti peremennoy vyazkosti v krugloy trube [Determination of Heat Exchange and Hydraulic Resistance for Laminar Flow of Fluid with Variable Viscosity in Round Tube], "Teploenergetika," 1954, No. 9.

9. Yang, Van-Tszu, Konvektivnyy teploobmen pri vynuzhdennom laminarnom techenii zhidkosti v trubakh v sluchaye peremennoy vyazkosti [Convective Heat Exchange for Forced Laminar Flow of Fluid in Tubes When the Viscosity Varies], "Teploperedacha," Russian translation. Trans. ASME, Ser. C), 1962, No. 4, pages 95-105.

10. Bradley, D., Developed Laminar Flow Heat Transfer from Air for Variable Physical Properties, Int. J. Heat a. Mass Transfer, 1965, Vol. 8, pages 621-638.

11. Worse-Schmidt, P.M., Leppert, G., Heat Transfer and Friction for Laminar Flow of Gas in a Circular Tube of High Heating Rate, Int. J. Heat a. Mass Transfer, 1966, Vol. 8, No. 10, pages 1281-1301.

12. Petukhov, B.S. and Krasnoshchekov, Ye.A., Issledovaniye teplootdachi pri vyazkostnom rezhime techeniya zhidkosti v pryamougol'nykh kanalakh i kruglykh trubakh [Investigation of Heat Transfer for Viscous Flow of Fluid in Rectangular Channels and Round Tubes], Izvestiya AN SSSR, OTN, 1953, No. 6.

13. Petukhov, B.S., Krasnoshchekov, Ye.A. and Nol'de, L.D., Issledovaniye mestnoy teplootdachi pri vyazkostnom techenii zhidkosti v krugloy trube [Investigation of Local Heat Transfer for Viscous Flow of Fluid in Round Tube], Trudy MEI, No. 25, Gosenergoizdat, 1955.

14.   Petukhov, B.S., Krasnoshchekov, Ye.A. anu Nol'de, L.D.,
      Teploobmen pri vyazkostnom dvizhenii zhidkosti v trubakh
      i kanalakh [Heat Exchange for Viscous Flow of Fluid in
      Tubes and Channels], "Teploenergetika," 1956, No. 12.

15.   Petukhov, B.S. and Krasnoshchekov, Ye.A., Teplootdacha pri
      vyazkostnom techenii zhidkosti v krugloy trube v usloviyakh
      sushchestvennogo izmeneniya vyazkosti [Heat Exchange for
      Viscous Flow of Fluid in Round Tube When There is Substan-
      tial Variation in Viscosity], In collection, "Teplopereda-
      cha i modelirovaniye," [Heat Transfer and Simulation],
      Izd-vo AN SSSR, 1958.

16.   Kraussold, H., Der Wärmeübergang bei zahen flüssigkeiten
      in Rohren, [Heat Transfer in Viscous Fluids in
      Tubes].   Forschungsheft, No. 351, 1931.

17.   Sieder, E.N. and Tate, G.E., Heat Transfer and Pressure
      Drop of Liquids in Tubes, Ind. Engng. Chem., 1936, Vol.
      28, No. 12.

18.   Böhm, J., Messungen des Wärmeübergangs im laminaren
      Strömungsgebiet mit Rizinusöl, [Measurements of Heat
      Transfer with Carter Oil in Laminar Flow Region].
      Die Wärme, 1943, No. 15.

19.   Magomedov, A.D., Issledovaniye teploobmena i gidravliches-
      kogo soprotivleniya pri dvizhenii vyazkoy i uprugo-vyazko-
      plasticheskoy zhidkosti i trubakh [Investigation of Heat
      Exchange and Hydraulic Resistance for Motion of Viscous
      and Elastic-Viscous-Plastic Fluid in Tubes], Candidate's
      dissertation, ENIN, 1954.

20.   Mikheyev M.A., In collection, "Materialy k soveshchaniyu
      po modelirovaniyu teplovykh ustroystv," [Materials for
      Conference on Simulation of Thermal Devices], Izd-vo
      AN SSSR, 1938.

21.   Mikheyev, M.A., Osnovy teploperedachi [Fundamentals of
      Heat Transfer], Gosenergoizdat, 1956.

22.   Petukhov, B.S. and Krasnoshchekov, Ye.A., Gidravlicheskoye
      soprotivleniye pri vyazkostnom neizotermicheskom dvizhenii
      zhidkosti i trubakh [Hydraulic Resistance for Viscous
      Nonisothermal Motion of Fluid in Tube], ZhTF, 1958, Vol. 28,
      No. 6, pages 1207-1214.

Chapter 8

1.   Eagle, A. and Ferguson, R.M., Proc. Roy. Soc., 1930, A,
      127, pages 540-566.

2.   Siegel, R., Sparrow, E.M. and Hallman, T.M., Steady
      Laminar Heat Transfer in a Circular Tube with Prescribed
      Wall Heat Flux, Appl. Scient. Res., 1958, Sect. A, Vol.
      7, No. 5.

3.   Sellers, J.R., Tribus, M. and Klein, J.S., Heat Transfer
     to Laminar Flow in Round Tube or Flat Conduit — the Graetz
     problem extended, Trans. ASME, 1956, Vol. 78, No. 2,
     page 441.

4.   Cess, R.D. and Shaffer, E.S., Heat Transfer to Laminar
     Flow Between Parallel Plates with a Prescribed Wall Heat
     Flux, Appl. Scient. Res., 1959, Vol. A8, No. 5, page 339.

5.   Cess, R.D., Shaffer, E.S., Laminar Heat Transfer Between
     Parallel Plates with an Unsymmetrically Prescribed Heat
     Flux at the Walls, Appl. Scient. Res., 1959, Vol. A9,
     No. 1, pages 64-70.

6.   Noyes, Zakonchennoye resheniye zadachi o laminarnom i
     turbulentnom techenii v trube dlya proizvol'nogo ras-
     predeleniya teplovogo potoka na stenke [Complete Solution
     for Laminar and Turbulent Flow in Tube for Arbitrary
     Distribution of Heat Flux at Wall], "Teploperedacha"
     (Russian translation, Trans. ASME, Ser. C), 1961, Vol.
     83, No. 1.

7.   Dzung, L.S., Heat Transfer in a Round Duct with Sinusoidal
     Heat Flux Distribution. Peacful Uses of Atomic Energy, Proc.
     of the Second Ind. Conference (Geneva), Vol. 7, Reactor
     Technology, pages 657-670.

8.   Dzung, L.S., Heat Transfer in a Flat Duct with Sinusoidal
     Heat Flux Distribution, Ibid, pages 671-675.

9.   Reynolds, W.C., Heat Transfer to Fully Developed Laminar
     Flow in a Circular Tube with Arbitrary Circumferential
     Heat Flux, J. of Heat Transfer, Trans. ASME, Ser. C,
     1960, Vol. 82, No. 2, pages 108-112.

10. Reynolds, W.C., Effect of Wall Heat Conduction on Convec-
     tion in a Circular Tube with Arbitrary Circumferential
     Heat Input, Int. J. of Heat and Mass Transfer, 1963,
     Vol. 6, No. 2, page 925.

11. Irvin, T.F., Shteyn, R.P. and Simon, G.A., Vliyaniye
     izlucheniya na konvektsiyu v ploskom kanale [Influence of
     Radiation on Convection in Flat Channel], Doklad na
     Vsesoyuznom soveshchanii po teplo- i masloobmanu, Minsk,
     5-9 May 1964.

Chapter 9

1.   Ma. Tun-uze, Razvitiye protsessa teplootdachi v trubakh
     pri laminarnom rezhime, dissertatsiya, Energeticheskiy
     institut imeni G.M. Krzhizhanovskogo

     1961; In collection "Teploperedacha," Izd-vo AN SSSR, 1962.

2.   Mikheyev, M.A. Filimonov, S.S. and Khrustalev, B.A., Is-
     sledovaniye teploobmena i gidravlicheskogo soprotivleniya

pri dvizhenii vody v trubakh [Investigation of Heat Exchange and Hydraulic Resistance for Water Moving in Tubes], In collection, "Konvektivnyy i luchistyy teploobmen" [Convective and Radiative Heat Exchange], Izd-vo AN SSSR, 1960.

3. Petukhov, B.S. and Popov, V.N., Teoreticheskiy raschet teploobmena i soprotivleniya treniya pri laminarnom techenii v trubakh neszhimayemoy zhidkosti s peremennymi fizicheskimi svoystvami [Theoretical Determination of Heat Exchange and Flow Resistance for Laminar Flow in Tubes by Incompressible Fluid with Variable Physical Properties], "Teplofizika vysokikh temperatur," [High-Temperature Thermophysics], 1963, Vol. 1, No. 2, pages 228-237.

4. Tepl tekhnicheskiy spravochnik [Heat-Engineering Handbook], Vol. 1, Gosenergoizdat, 1957.

5. Hilsenrath, J. et al., Tables of Thermodynamic and Transport Properties of Air, Argon, Carbon Dioxide, Carbon Monoxide, Hydrogen, Nitrogen, Oxygen, Steam, Pergamon Press, Oxford, London-New York-Paris, 1960.

6. Blais, N., Mann, J., The J. of Chem., Phys., 1960, Vol. 32, No. 5.

7. McAdams, V.Kh., Teploperedacha [Heat Transfer], Metallurgizdat, 1961.

8. Davenport, and Leppert, Vliyaniye poperechnykh temperaturnykh gradiyentov na teplostdachu i treniye v laminarnom potoke gaza [Influence of Transverse Temperature Gradients on Heat Transfer and Flow in Laminar Gas Stream], "Teploperedacha" (Russian translation, Trans. ASME, Ser. C), 1965, No. 2, pages 36-43.

9. Petukhov, B.S. and Popov, V.N., Teoreticheskiy raschet teplootdachi i soprotivleniya pri turbulentnom techenii v trube ravnovesno dissotsiiruyushchego vodoroda [Theoretical Determination of Heat Transfer and Resistance for Turbulent Flow in Tube by Hydrogen in Equilibrium Dissociation], "Teplofizika vysokikh temperatur," 1964, Vol. 2, No. 4, pages 599-611.

10. Popov, V.N. and Petukhov, B.S., Teoreticheskiy raschet teplootdachi i soprotivleniya treniya pri laminarnom techenii v trube ravnovesno dissotsiiruyushchego vodoroda, [Theoretical Determination of Heat Transfer and Friction Resistance for Laminar Flow in Tube by Hydrogen in Equilibrium Dissociation], "Teplofizika vysokikh temperatur," 1966, Vol. 4, No. 4, pages 531-539.

11. Popov, V.N., Teoreticheskiy raschet teplootdachi i soprotivleniya treniya dlya dvuokisi ugleroda v sverkhkriticheskoy oblasti pri laminarnom techenii v krugloy trube [Theoretical Determination of Heat Transfer and Friction Resis-

tance for Carbon Dio,ic, in Supercritical Region for Laminar Flow in Round Tube], "Teplofizika vysokikh temperatur," 1966, Vol. 4, No. 5, pages 689-697.

12. Michels, A., Appl. Sci. Res., 1948, Vol. Al, No. 2.

13. Teplofizicheskiye svoystva veshchestv [Thermophysical Properties of Matter], Edited by N.B. Vargraftik, Gosenergoizdat, 1956.

14. Tsederberg, N.V. and Morozova, N.A., "Teploenergetika," 1960, No. 1.

15. Golubev, I.F., Vyazkost' gazov i gazovykh smesey [Viscosity of Gases and Gas Mixtures], Fizmatgiz, 1959.

16. Connel Smith, Teplootdacha v laminarnom potoke s peremennymi fizicheskimi svoystvami [Heat Transfer in Laminar Flow with Variable Physical Properties], "Teploperedacha," (Russian translation, Trans. ASME, Ser. C), 1962, No. 2, pages 71-79.

17. Worse-Schmidt, P.M., Leppert, G., Int. J. Heat a. Mass Transfer, 1966, Vol. 9, No. 11, page 1291.

Chapter 10

1. Labuntsov, D.A., Nekotoryye voprosy teorii teploobmena pri laminarnom techenii zhidkosti v trubakh [Some Problems in the Theory of Heat Exchange for Laminar Flow of Fluids in Tubes], "Teploenergetika," 1958, No. 3.

2. Pahor, S. and Strand, J., Die Nusseltische Zahl für laminare Strömung im zylindrischen Rohr mit konstanter Wandtemperatur [The Nusselt Number for Laminar Flow in Cylindrical Tube at Constant Wall Temperature].
Z. f. Angew. Math. u. Phys., 1956, Vol. 7, Fasc. 6, page 536.

3. Pahor, S. and Strnad, J., A note on Heat Transfer in Laminar Flow Through a Gap, Appl. Scient. Res., 1961, Sec. A, Vol. 10, pages 81-84.

4. Petukhov, B.S. and Yushin, A.Ya., O teploobmene pri techenii zhidkogo metalla v laminarnoy i perekhodnoy oblastyakh [Heat Exchange for Flow of a Liquid Metal in the Laminar and Transition Regions], Doklady AN SSSR, 1961, Vol. 136, No. 6, pages 1321-1324.

5. Yushin, A.Ya., Sukomel, A.S. and Strigin, B.K., Issledovaniye teploobmena pri techenii rtuti v krugloy trube v oblasti malykh znacheniy chisla Pekle [Investigation of Heat Exchange for Mercury Flowing in Round Tube in Regions of Small Peclet Numbers], Izvestiya vuzov, ser. "Energetika," 1961, No. 7, pages 79-85.

6. Johnson, H.A., Hartnett, J.P. and Claybaugh, W.J., Teplootdacha pri techenii rtuti i splava svinets-vismut v laminarnoy i perekhodnoy oblastyakh [Heat Transfer in Flow of Mercury and Lead-Bismuth Alloy in Laminar and Transition Regions], Trans. ASME, 1954, Vol. 76, No. 4, page 513.

7. Deryugin, V.M. and Fedynskiy, O.S., O teplootdache pri perekhodnom rezhime techeniya zhidkikh metallov v trubakh [Heat Transfer for Transition Flow of Liquid Metals in Tubes], IFZh, 1959, No. 12, pages 3-10.

8. Petukhov, B.S. and Tsvetkov, F.F., Raschet teploobmena pri laminarnom techenii zhidkosti v trubakh v oblasti malykh chisel Pekle [Determination of Heat Exchange for Laminar Flow of Fluid in Tubes for Small Peclet Numbers], IFZh, 1961, No. 3, pages 10-17.

9. Agrawal, H.C., Heat Transfer in Laminar Flow Between Parallel Plates at Small Peclet Numbers, Appl. Scient. Res., 1960, Sec. A, Vol. 9, No. 2-3, pages 177-189.

Chapter 11

1. Leybenzon, L.S., Sobraniye trudov, [Collected Works], Vol. III, Izd-vo AN SSSR, 1955, page 31.

2. Lauverier, Pouseulle Functions, Appl. Sci. Res., 1951, Vol. A3, No. 1.

3. Schenk, J. and Dumore, Y.M., Heat Transfer in Laminar Flow Through Cylindrical Tubes, Appl. Sci. Res., 1953, Vol. A4, No. 1.

4. Rosen and Scott, Resheniye leveka dlya stenki s konechnym soprotivleniyem [Leveque Solution for Wall with Finite Resistance], "Teploperedacha" (Russian translation, Trans. ASME, Ser. C), 1961, No. 1.

5. Van der Does de Bye, J.A.W., Schenk, J., Heat Transfer in Laminar Flow Between Parallwl Plates, Appl. Sci. Res., 1952, Vol. A3, No. 4.

6. Schenk, J., A Problem of Heat Transfer in Laminar Flow Between Parallel Plates, Appl. Sci. Res., 1955, Vol. A5, No. 2-3.

Chapter 12

1. Lykova, A.V., Teoriya teploprovodnosti [Theory of Heat Conduction], Gos. izd. tekhniko-teoreticheskoy literatury, 1952.

Sadikov, I.N., Teploobmen v nachal'nykh uchastkakh ploskogo i pryamougol'nogo kanalov [Heat Exchange in Initial Segments of Flat and Rectangular Channels], IFZh, 1964, Vol. 7, No. 9.

3. Sadikov, I.N., Laminernyy teploobmen v ploskom kanale
    pri neravnomernom pole temperatur na vkhode [Insert
    Laminar Heat Exchange in Flat Channel for Nonuniform
    Temperature Field at Entrance], IFZh, 1965, Vol. 8, No. 3.

4. Sadikov, I.N., Laminernyy teploobmen v nachal'nom
    uchastke pryamougol'nogo kanala [Laminar Heat Exchange in
    Initial Segment of Rectangular Channel], IFZh, 1965,
    Vol. 8, No. 4.

5. Shneyder, Vliyaniye teploprovodnosti zhidkosti na tep-
    loperedachu vo vkhodnom uchastke parallel'nykh plastin
    i trub [Influence of Fluid Heat Conduction on Heat Trans-
    fer at Entrance Segment of Parallel Plates and Tubes],
    Trans. ASME, 1957, Vol. 79, No. 4, pages 765-773 (for
    translation see "Voprosy yadernoy energetiki" [Problems
    of Nuclear Power Engineering], 1958, No. 2).

6. Pirogov, M.S., Raspredeleniye temperatur v potoke zhid-
    kosti mezhdu parallel'nymi plastinami i v trube pri
    konechnoy dline obogrevayemogo uchastka i granichnykh
    usloviyakh vtorogo roda [Temperature Distribution in
    Fluid Flow Between Parallel Plates and in Tube with Fin-
    ite Length of Heated Segment and Boundary Conditions of
    the Second Kind], in collection "Zhidkiye metally,"
    [Liquid Metals], Gosatomizdat, 1963.

7. Brin, M.S., Friedman, S.J., Glukker, F.A., Pigford, R.L.,
    Teploperedacha k granulirovannomu materialu pri dvizhenii
    vniz po vertikal'nym trubam [Heat Transfer to Granulated
    Material for Downward Motion in Vertical Tubes], Ind.
    a. Engng Chem., 1948, Vol. 60, No. 6.

8. Nikolayev, P.N., Issledovaniye teploobmena pri dvizhenii
    granulirovannogo materiala v trube [Investigation of
    Heat Exchange for Granulated Material Moving in Tube],
    Dissertation, MIKhM, 1952.

9. Gorbis, Z.R., and Kalendar'yan, V.A., Teplootdacha sloya,
    prodol'no dvizhushchegosya v gladkikh tsilindricheskikh
    kanalakh [Heat Transfer of Layer Moving Longitudinally
    in Smooth Cylindrical Channels], "Teploenergetika,"
    1962, No. 1.

10. Kays, W.M., Numerical Solutions for Laminar-flow Heat
    Transfer in Circular Tubes, Trans. ASME, 1955, Vol. 77,
    Pages 1265-1274.

11. Ulrichson, D.L., Schmitz, R.A., Laminar-flow Heat Trans-
    fer in the Entrance Region of Circular Tubes, Int. J.
    of Heat a. Mass Transfer, 1965, Vol. 3, No. 2, pages
    253-258.

12. Stephan, K., Beitrag zur Berechnung des Wärmeüberganges und
    Druckabfalles laminarer Einlaufströmungen [Report on
    Calculation of Heat Transfer and Pressure Drop in Laminar Flow].
    Ing. Archiv, 1960, Vol. 29, No. 3, pages 176-186.

13. Sparrow, ".M., see the book, Knudsen, J.G. and Katz, D.L., Fluid Dynamics and Heat Transfer, 1958.

14. Van Pu-syuen', Teoretich skiy raschet teplootdachi pri laminarnom pogranichnom sloye vo vkhodnom uchastke krugloy truby [Theoretical Determination of Heat Transfer for a Laminar Boundary Layer at the Entrance Segment of a Round Tube], Trudy Politekhnicheskogo instituta Tsin Khua [Transactions of the Tsin Khua Polytechnical Institute], 1962, Vol. 9, No. 3. (in Chinese).

15. Petukhov, B.S., Krasnoshchekov, Ye.A. and Nol'de, L.D., Issledovaniye mestnoy teplootdachi pri vyazkostnom techenii zhidkosti v krugloy trube [Investigation of Local Heat Transfer for Viscous Flow of a Fluid in a Round Tube], Trudy MEI, No. 25, "Teploenergetika,", Gosenergoizdat, 1955.

16. Petukhov, B.S. and Chzhan Chzhen-yun, Teploobmen v gidrodinamicheskom nachal'nom uchastke krugloy truby pri laminarnom techenii zhidkosti [Heat Exchange in Hydrodynamic Initial Segment of Round Tube with Laminar Flow of Fluid], Teplo- i massoperenos, [Heat and Mass Transfer], Vol. 1, Konvektivnyy teploobmen v odnofaznoy srede [Convective Heat Exchange in a Single-Phase Medium], izd-vo "Nauka i tekhnika", Minsk, 1965.

17. Tribus, M. and Klein, J., Forced Convection from Nonisothermal Surfaces, Heat Transfer Symposium, University of Michigan, 1953, page 211.

18. Mikheyev, M.A., Filimonov, S.S. and Khrustalev, B.A., Issledovaniye teploobmena i gidravlicheskogo soprotivleniya pri dvizhenii vody v trubakh [Investigation of Heat Exchange and Hydraulic Resistance for Water Flowing in Tube], In collection "Konvektivnyy i luchistyy teploobmen," [Convective and Radiant Heat Exchange], Izd-vo AN SSSR, 1960.

19. Deisler, R.G. and Presler, A.F., Analysis of Developing Laminar Flow and Heat Transfer in a Tube for a Gas with Variable Properties, Proc. of the Third International Heat Transfer Conference, Chicago, Illinois, 1966, Vol. 1, paper No. 24, page 250.

20. Siegel, R., Sparrow, E.M., Simultaneous Development of Velocity and Temperature Distributions in a Flat Duct with Uniform Wall Heating, AIChE J., 1959, Vol. 5, No. 1, pages 73-75.

21. Heaton, H.S., Reynolds, W.C., and Kays, W.M., Heat Transfer in Annular Passages, Simultaneous Development of Velocity and Temperature Fields in Laminar Flow, Int. J. of Heat and Mass Transfer, 1964, Vol. 7, pages 763-781.

  . Han, L.S., Simultaneous Developments of Temperature and Velocity Profiles in Flat Ducts, International Heat Trans-

fer Conference, 1961, rep. 70.

Chapter 13

1. Reichardt, H., Die Wärmeübertragung in turbulenten Reibungsschichten, [Heat Transfer in Turbulent Friction Layers]. Z. angew. Math. u. Mech., 1940, Vol. 20, pages 297-328.

2. Elser, K., Der Stationäre Wärmeübergang bei laminarer Strom- ung, [Steady Heat Transfer in Laminar Flow]. Schweiz, Bau- zeitung, 1951, Vol. 69, No. 46, pages 641-642.

3. Hartmann, H., Wärmeübergang bei laminarer Strömung durch Ringspalte [Heat Transfer in Laminar Flow through Circular Orifices]. Chem.-Ing.-Technik, 1961, 35, Jahrgang, Heft 1.

4. Hatton, A.P., Quarmby, A., Heat Transfer in the Thermal Entry Length with Laminar Flow in an Annulus, Int. J. of Heat a. Mass Transfer, 1962, Vol. 5, pages 973-980.

5. Petukhov, B.S. and Royzen, I..I., Teploobmen v trubakh kol'tsevogo secheniya [Heat Exchange in Annular Tubes], IFZh, 1963, No. 3, pages 3-11.

6. Jacob, M. and Rees, K.A., Trans. Am. Inst. Chem. Eng., 1941, Vol. 37, page 619.

7. Jacob, M., Heat Transfer, Vol. 1, 1949.

8. Lyon, R.N., Chem. Eng. Progress, 1951, Vol. 47, pages 75-79.

9. Krischer, O., Wärmeaustausch in Ringspalten bei laminaren und turbulenten Strömung, [Heat Transfer in Circular Orifices with Laminar and Turbulent Flow] Chem.-Ing.-Technik, 1961, 33, Jahrgang, Heft 1.

10. Heaton, H.S., Reynolds, W.C., Kays, W.M., Heat Transfer in Annular Passages. Simultaneous Development of Velocity and Temperature Fields in Laminar Flow, Int. J. of Heat a. Mass Transfer, 1964, Vol. 7, pages 763-781.

Chapter 14

1. Migay, V.K., Teploobmen v treugol'nom kanale pri laminar- nom techenii [Heat Exchange in Triangular Channel with Laminar Flow], IFZh, 1958, No. 7.

2. Kantorovich, L.V. and Krylov, V.I., Priblizhennyye metody vysshego analiza [Approximate Methods of Higher Analysis], Gos. izd. tekhniko-teoreticheskoy literatury, 1952.

3. Dennis, S.C.R., Mercer, A. McD., Poots, G., Forced Heat Convection in Laminar Flow Through Rectangular Ducts, Quarterly Appl. Math., 1959, Vol. 17, No. 3, pages 285-297.

4. Migay, V.K., Issledovaniye teplootdachi i gidravlicheskogo soprotivleniya poverkhnostey nagreva vrashchayushchikhsya regeneratorcv [Investigation of Heat Transfer and Hydraulic Resistance for Heating Surfaces of Rotating Regenerators], Author's abstract of dissertation, Leningradskiy politekhnicheskiy institut, 1959.

5. Clark, S.H., Kays, W.M., Trans. ASME, 1953, Vol. 75, pages 859-866.

5a. Montgomery, S.R. and Wibulswas, P., Laminar Flow Heat Transfer in Ducts of Rectangular Cross-section. Proc. of the Third International Heat Transfer Conference, Chicago, Illinois, 1966, Vol. 1, paper No. 10, page 104.

6. Danvudi, N.T., Teploobmen pri vynuzhdennoy konvektsii v trubakh ellipticheskogo secheniya [Heat Exchange Under Forced Convection in Tubes of Elliptical Cross Section], "Prikladnaya mekhanika" (Russian translation, Trans. ASME, Ser. E), 1962, Vol. 29, No.1, pages 184-189.

7. Petukhov, B.S. and Krasnoshchekov, Ye.A., Issledovaniye teplootdachi pri vyazkostnom rezhime techeniya zhidkosti v pryamougol'nykh kanalakh i kruglykh trubakh [Investigation of Heat Transfer for Viscous Flow of Fluid in Rectangular Channels and Round Tubes], Izv. AN SSSR, OTN, 1953, No. 6.

8. Timoshenko, S.P., Theory of Plates and Shells, McGraw-Hill Book Company, Inc., New York, 1940.

9. Marco, S.M., Han, L.S., A Note on Limiting Laminar Nusselt Number in Ducts with Constant Temperature Gradient by Analogy to Thin-Plate Theory, Trans. ASME, 1955, Vol. 77, pages 625-630.

10. Eckert, E.R.G., Irvine, T.F., Yen, J.T., Local Laminar Heat Transfer in Wedge-Shaped Passages, Trans. ASME, 1958, Vol. 80, pages 1433-1438.

11. Tao, L.N., Nekotoryye zadachi o vynuzhdennoy konvektsii pri laminarnom techenii [Some Problems of Forced Convection in Laminar Flow], "Teploperedacha" (Russian translation, Trans. ASME, Ser. C), 1961, No. 4, pages 96-103.

12. Sparrow, E.M., Siegel, R., A Variational Method for Fully Developed Laminar Heat Transfer in Ducts, J. of Heat Transfer, Trans. ASME, 1959, Vol. 81, Ser. C, pages 157-167.

13. Sparrow, E.M. and Khadzhi-Sheykh A., Teplootdacha i padeniye
davleniya pri laminarnom techenii v kanalakh s popa echnym
secheniyem v vide ravnobedrennogo treugol'nika, pryamougol'-
nogo treugol'nika i sektora kruga [Heat Transfer and Pres-
sure Drop for Laminar Flow in Channels with Cross Section
in Form of Equilateral Triangle, Right Triangle, and Sector
of Circle], "Teploperedacha" (Russian translation, Trans.
ASME, Ser. C), 1965, No. 3, pages 121-122.

14. Han, L.S., Laminar Heat Transfer in Rectangular Channels,
J. of Heat Transfer, Trans. ASME, 1959, Vol. 81, Ser. C,
pages 121-128.

15. Tao, L.N., Method of Conformal Mapping in Forced Convec-
tion Problems, Int. Developments in Heat Transfer, 1961,
Int. Heat Transfer Conference, Colorado, U.S.A., rep.
71, page 598.

15a. Cheng, K.C., Laminar Flow and Heat Transfer Characteris-
tics in Regular Polygonal Ducts, Proc. of the Third In-
ternational Heat Transfer Conference, Chicago, Illinois,
1966, Vol. 1, paper No. 6, page 64.

16. Sparrow, Loeffler and Hubbard, Teploobmen pri prodol'nom
obtekanii tsilindrov laminarnym potokom [Heat Exchange
for Longitudinal Laminar Flow at Cylinders], "Teploperedacha"
(Russian translationHeat Transfer, Trans. ASME, Ser. C),
1961, No. 4, pages 31-40.

17. Savino, J.M., Siegel, R., Laminar Forced Convection in
Rectangular Channels with Unequal Heat Addition on Adja-
cent Sides, Int. J. of Heat a. Mass Transfer, 1964,
Vol. 7, No. 7, pages 733-741.

18. Sparrow, E.M. and Siegel, R., Application of Variational
Methods to the Thermal Entrance Region of Ducts, Int. J.
of Heat a. Mass Transfer, 1960, Vol. 1, pages 161-172.

19. Siegel, R. and Savino, D., Analiticheskoye resheniye zad-
achi o vliyanii periferiinoy teploprovodnosti stenok na
vynuzhdennuyu konvektsiyu pri laminarnom techenii v
pryamougol'nykh kanalakh [Analytic Solution to Problem
of Influence of Peripheral Wall Heat Conduction on Forced
Convection in Laminar Flow in Rectangular Channels],
"Teploneredacha" (Russian translation Trans. ASME, Ser.C),
1965, No. 1, pages 71-81.

20. Mori, Ya. and Nakayama, V., Issledovaniye teploobmena pri
vynuzhdennom dvizhenii zhidkosti v izognutykh trubakh
[Investigation of Heat Exchange for Forced Motion of Fluid
in Curved Tubes], Int. J. of Heat a. Mass Transfer, 1965,
Vol. 8, No. 1.

21. Fastovskiy, V.G. and Rovinskiy, A.Ye., Issledovaniye
teplootdachi v spiral'nom kanale [Investigation of Heat
Transfer in Spiral Channel], "Teploenergetika," 1957,
No. 1, pages 39-41.

22.   Seban, A. and McLanghlin, E.F., Heat Transfer in tube coils with laminar and turbulent flow, Int. J. of Heat a. Mass Transfer, 1963, Vol. 6, pages 387-395.

Chapter 15

1.   Hausenblas, H., Neizotermicheskoye laminarnoye techeniye vyazkoy zhidkosti v uzkoy shcheli i v kapillyarakh [Non-isothermal Laminar Flow of Viscous Fluid in Narrow Slot and in Capillaries], Ing.-Arch., 1950, Vol. 18, pages 151-166.

2.   Regirer, S.A., Nekotoryye termogidrodinamicheskiye zadachi ob ustanovivshemsya odnomernom techenii vyazkoy kapel'noy zhidkosti [Certain Thermohydrodynamic Problems of Steady One-Dimensional Flow of a Viscous Liquid], P.M.M., 1957, Vol. 21, No. 3, pages 424-430.

3.   Kaganov, S.A., Ob ustanovivshemsya laminarnom techenii neszhimayemoy zhidkosti v ploskom kanale i krugloy tsilin-dricheskoy trube s uchetom teploty treniya i zavisimosti vyazkosti ot temperatury [Steady Laminar Flow of Incom-pressible Fluid in Flat Channel and Round Cylindrical Tube with Allowance for Heat of Friction and Temperature-Dependence of Viscosity], PMTF, 1962, No. 3, pages 96-99.

4.   Schlichting, H., Nekotoryye tochnyye resheniya dlya ras-predeleniya temperatury v laminarnom potoke [Some Exact Solutions for Temperature Distribution in Laminar Flow], Z. d. Angew. Math. u. Wech., 1951, Vol. 31, pages 78-83.

5.   Topper, L., Vynuzhdennaya teplovaya konvektsiya v tsilindri-cheskikh kanalakh: nekotoryye zadachi, vklyuchayushchiye potentsial'noye i parabolicheskoye raspredeleniye sko-rosti [Forced Thermal Convection in Cylindrical Channels: Some Problems Including the Potential and Parabolic Velo-city Distributions], Chem. Eng. Sci. 1956, Vol. 5, page 13.

6.   Toor, H.L., Heat Transfer in Forced Convection with Inter-nal Heat Generation, AIChE J., 1958, Vol. 4, No. 3, pages 319-323.

7.   Kudryashov, L.I. and Golovin, V.M., Vliyaniye dissipatsii mekhanicheskoy energii na teploobmen pri laminarnom dvizhenii zhidkosti v krugloy tsilindricheskoy trube [Influence of Mechanical-Energy Dissipation on Heat Exchange in Laminar Flow of Fluid in Round Cylindrical Tube], In collection "Teplo- i massoperenos," [Heat and Mass Transfer], Vol. 5, Izd-vo AN BSSR, 1963.

8.   Petukhov, B.S., Genin, L.G. and Mal'ter, V.L., Teploobmen v trubakh pri nalichii v potoke zhidkosti vnutrennikh istochnikov tepla [Heat Exchange in Tubes When There are Internal Heat Sources in Fluid Flow], IFZh, 1960, Vol. 3, No. 9.

9.   Poppendiek, H.F., Chem. Eng. Progress Symposium, 1954,
        50, No. 11, pages 93-104.

10.   Voskresenskiy, K.D. and Turilina, Ye.S., O vliyanii na
        teplootdachu v trube vnutrennikh istochnikov tepla, dey-
        stvuyushchikh v potoke zhidkosti [Influences of Internal
        Heat Sources Acting in Fluid Flow on Heat Transfer in Tube],
        In collection, "Konvektivnyy i luchistyy teploobmen" [Con-
        vective and Radiant Heat Exchange], Izd-vo AN SSSR, 1960.

11.   Sparrow, E.M., Siegel, R., Laminar Tube Flow with Arbi-
        trary Internal Heat Sources and Wall Heat Transfer,
        Nuclear Sci. a. Engng, 1958, Vol. 4, No. 2, pages 239-254.

12.   Juman, R.M., Experimental Study of Temperature Distribu-
        tion in Laminar Tube Flow of a Fluid with Internal Heat
        Generation, Int. J. of Heat a. Mass Transfer, 1962, Vol.
        5, pages 1053-1058.

13.   Tao, Nekotoryye zadachi vynuzhdennoy konvektsii pri lami-
        narnom techenii [Some Problems in Forced Convection Dur-
        ing Laminar Flow], "Teploperedacha," (Russian transla-
        tion, Trans. ASME, Ser. C), 1961, No. 4, pages 96-103.

Chapter 16

1.   Ostroumov, G.A., Svobodnaya konvektsiya v usloviyakh
        vnutrenney zadachi [Free Convection Under the Conditions
        of the Internal Problem], Gos. izd. tekhniko-teoreticheskoy
        literatury, 1952.

2.   Watzinger, A., Jonson, D., Wärmeübertragung von Wasser an
        Rohrwand bei senkrechter Stromung in Übergangsgebiet zwis-
        chen laminarer und turbulenter Strömung, [Heat Transfer
        between Water and Tube Wall with Vertical Flow in Transi-
        tion Region between Laminar and Turbulent Flow].
        Forschung, 1939, Vol. 10, No. 4, pages 182-196.

3.   Scheele, G.F., Rosen, E.M., Hanratty, T.J., Effect of Na-
        tural Convection on Transition Turbulence in Vertical
        Pipes, Canadian J. of Chem. Engng, 1960, Vol. 38, No. 3,
        page 67.

4.   Petukhov, B.S. and Nol'de, L.D., Teploobmen pri vyazkostno-
        gravitatsionnom techenii zhidkosti v trubakh [Exchange for
        Viscous-Gravitational Flow of Fluid in Tubes], "Teplo-
        energetika," 1959, No. 1.

5.   Martinelli, R.S. and Boelter, L.M.K., The Analytical
        Prediction of Superposed Free and Forced Viscous Convec-
        tion in a Vertical Pipe, University of California Publica-
        tions in Engng, 1942, Vol. 5, No. 2, pages 23-58.

6.   Martinelli, R.C., Southwell, C.J., Alves, G., Carig, H.L.,
        Weinberg, E.G., Lansing, N.F. and Boelter, L.M.K. Heat
        Transfer and Pressure Drop for a Fluid Flowing in the Vis-

cous Region Through a Vertical Pipe, Trans. ASME, 1942, Vol. 38, No. 3, pages 493-530.

7a. Pigford, R.L., Chem. Engng Progress, Symposium Series, 1955, Vol. 51, No. 17.

7b. Rosen, E.M. Hanratty, T.J., A.I. Ch. E. Journal, 1961, Vol. 7, No. 1, pages 112-123.

8. Petukhov, B.S., Eksperimental'noye issledovaniye teplootdachi pri laminarnom techenii zhidkosti v krugloy trube [Experimental Investigation of Heat Transfer for Laminar Flow of Fluid in Round Tube], Izv. AN SSSR, OTN, 1948, No. 7, pages 1055-1065.

9. Alad'yev, I.T., Mikheyev, M.A. and Fedynskiy, O.S., Zavisimost' teplootdachi v trubakh ot napravleniya teplovogo potoka i yestestvennoy konvektsii [Heat Transfer in Tubes as Function of Direction of Heat Flux and Natural Convection], Izd. AN SSSR, OTN, 1951, No. 1, pages 53-67.

10. Kern, D.Q. and Othmer, D.F., Effect of Free Convection on Viscous Heat Transfer in Horizontal Tubes, Trans. Amer. Inst. Chem. Eng., 1943, Vol. 39, No. 4, pages 517-55, No. 5, page 579.

11. Kirshbaum, E., Neues zum Wärmeübergang mit und ohne Anderung des Aggregatzustandes, [Recent Developments in Heat Transfer with and without Variation of Overall State]. Chem.-Ing.-Technik, 1952, 24, No. 7, pages 391-400.

12. Wetjen, K.A. Wärmeübergang bei strömenden Flüssigkeiten im senkrechten Rohr mit und ohne Eigenkonvektion [Heat Transfer in Flowing Fluids in Vertical Tube, with and without convection]. Chem.-Ing.-Technik, 1954, 26, No. 8-9, pages 454-460.

13. Kirpichev, M.V., Mikheyev, M.A. and Eygenson, L.S., Teploperedacha [Heat Transfer], Gosenergoizdat, 1940.

14. Ostroumov, G.A., Matematicheskaya tecriya ustanovivsheysya teploperedachi v krugloy vertikal'noy skvazhine pri superpozitsii vynuzhdennoy i svobodnoy laminarnoy konvektsii [Mathematical Theory of Steady Heat Transfer in Round Vertical Well With Superposition of Force and Free Laminar Convection], ZhTF, 1950, Vol. 20, No. 6, pages 750-757.

15. Hallman, T.M., Combined Forced and Free-Laminar Heat Transfer in Vertical Tubes with Uniform Internal Heat Generation, Trans. ASME, 1956, Vol. 78, pages 1831-1841.

16. Hanratty, T.J., Rosen, E.M. and Kabel, R.L., Effect of Heat Transfer on Flow Field at Low Reynolds Numbers in Vertical Tubes, Ind. Engng Chem., 1958, Vol. 50, No. 5, pages 815-820.

17. Brown, W.G., Die Uberlagerung von erzwungener und natürlicher Konvektion bei niedrigen Durchsatzen in einem lo-

trechten Rohr, [Super.os.tion of Forced and Natural Convection with Low Throughput in Horizontal Tube]. VDI-Forschungsheft, 1960, Vol. 26, No. 480, pages 1-31.

18. Morton, B.R., Laminar Convection in Uniformly Heated Vertical Pipes, J. Fluid Mech., 1960, Vol. 8, No. 2, pages 227-240.

19. Tao, L.N., Heat Transfer of Combined Free and Forced Convection in Circular and Sector Tubes, Appl. Scient. Res., 1960, Vol. A9, No. 5, pages 357-368.

20. Tao, L.N., On Combined Free and Forced Convection in Channels, J. of Heat Transfer (Trans. ASME, Ser. C), 1960, Vol. 82, No. 3, pages 233-238.

21. Ostrach, S., On the Flow, Heat Transfer and Stability of Viscous Fluids Subject to Body Forces and Heated From Below in Vertical Channels, In collection "50 Jahre Grenzschichtforschung," , Braunschweig, 1955.

22. Han, L.S., Laminar Heat Transfer in Rectangular Channels, J. of Heat Transfer (Trans. ASME, Ser. C), 1959, Vol. 81, No. 2, pages 121-128.

23. Lu Pan-Chang, Combined Free and Forced-Convection Heat-Generating Laminar Flow Inside Vertical Pipes with Circular Sector Cross Sections, J. of Heat Transfer (Trans. ASME, Ser. C), 1960, Vol. 82, No. 3, pages 227-232.

24. Morton, B.R., Laminar Convection in Uniformly Heated Horizontal Pipes at low Rayleigh Numbers, Quart. J. Mech. a. Appl. Math., 1959, Vol. 12, No. 4, pages 410-420.

25. Ikbol, M., and Stakhevich, D.V., Vliyaniye oriyentatsii truby na teploperedachu pri sovmestnom deystvii svobodnoy i vynuzhdennoy laminarnoy konvektsii [Influence of Tube Orientation on Heat Transfer With Combined Action of Free and Forced Laminar Convection], Teploperedacha [Heat Transfer], (Russian translation, Trans. ASME, Ser. C), 1966, No. 1, pages 119-126.

26. Petukhov, B.S. and Polyakov, A.F., Eksperimental'noye issledovaniye teploobmena pri vyazkostno-gravitatsionnom techenii zhidkosti v gorizontal'noy trube [Experimental Investigation of Heat Exchange in Viscous-Gravitational Flow of Fluid in Horizontal Tube], Teplofizika vysokikh temperatur," 1967, Vol. 5, No. 1.

27. Petukhov, B.S. and Polyakov, A.F., O vliyanii svobodnoy konvektsii na teplootdachu pri vynuzhdennom techenii v gorizontal'noy trube [Influence of Free Convection on Heat Transfer with Forced Flow in Horizontal Tube], Teplofizika vysokikh temperatur, 1967, Vol. 5, No. 2.

28. Mori, Y., Futagami,K., Tokuda, S. and Nakamura, M., Forced Convective Heat Transfer in Uniformly Heated-Horizontal Tubes, Int. Heat Mass Transfer, 1966, Vol. 9, No. 5, pages 453-463.

29. Mikhaylov, A.I., Kalinin, E.K. and Yarkho, S.A., Issoedovaniye teplootdachi i gidravlicheskogo soprotivleniya pri vyazkostno-gravitatsionnom techenii vody v horizontal'noy trube pri q_s = const [Investigation of Heat Transfer and Hydraulic Resistance for Viscous-Gravitational Flow of Water in Horizontal Tube with q_s = const]. IFZh, 1966, Vol. 10, No. 2, pages 158-163.

Chapter 17

1. Siegel, R., Heat Transfer for Laminar Flow in Ducts with Arbitrary Time Variations in Wall Temperature, J. Appl. Mech. (Trans. ASME, Ser. E), 1960, Vol. 27, No. 2, pages 241-249.

2. Courant, R. and Hilbert, D., Metody matematicheskiye metody v inzhenernom, dele [Methods of Mathematical Physics], Gostekhizdat, 1951.

3. Lykov, A.V., Teoriya teploprovodnosti [Theory of Heat Conduction], Gosenergoizdat, 1952.

4. Karman, T. and Biot, M., Matematicheskiye metody v inzhenernom dele [Mathematical Methods in Engineering Practice], Gostekhizdat, 1948.

5. Sadikov, I.N., Tochnyye resheniya uravneniya energii dlya techeniya vyazkoy neszhimayemoy zhidkosti v trubakh [Exact Solutions of Energy Equation for Flow of Viscous Incompressible Fluid in Tube], IFZh, 1963, No. 4, pages 40-45.

6. Siegal, R., Sparrow, E.M., Transient Heat Transfer for Laminar Forced Convection in the Thermal Entrance Region of Flat Ducts, J. of Heat Transfer (Trans. ASME, Ser. C), 1959, Vol. 81, February, pages 29-31.

7. Sparrow, E.M. and Siegel, R., Thermal Entrance Region of a Circular Tube Under Transient Heating Conditions, Proceedings of the Third U.S. National Congress for Applied Mechanics, Brown University Providence, R.I., June, 1958.

8. Siegel, R., Perlmutter, M., Two-Dimensional Pulsating Laminar Flow in a Constant Wall Temperature, Int. Developments in Heat Transfer, 1961, Int. Heat Transfer Conference, Colorado, U.S.A., rep. 61.

9. Siegel, R. and Perlmutter, M., Teplootdacha pri pul'siruyushchem laminarnom techenii v kanale [Heat Transfer for Pulsating Laminar Flow in Channel], "Teploperedacha" (Russian translation, Trans. ASME, Ser. C), 1962, No. 2, pages 18-32.

10. Linke, W. and Hufschmidt, W., Gidravlicheskoye sopro-
     tivleniye i peredacha tepla v pul'siruyushchem laminar-
     nom i turbulentnom potokakh [Hydraulic Resistance and
     Heat Transfer in Pulsating Laminar and Turbulent Flow],
     Die Chem. Fabrik, 1958, Vol. 30, No. 3, pages 159-165.

11. Darling, G.B., Heat Transfer to Liquids in Intermittent
     Flow, Petroleum, Vol. 22, May, 1959, pages 177-178.

12. Perlmutter, M., Siegel, R., Two-Dimensional Unsteady In-
     compressible Laminar Duct Flow with a Step Change in Wall
     Temperature, Int. J. of Heat and Mass Transfer, 1961,
     Vol. 3, No. 2, pages 94-107.

13. Mayer, E., Heat Flow in Composite Slabs, J. Amer. Rocket
     Soc., 1952, Vol. 22, Page 150.

14. Perlmutter, M. and Siegel, R., Nestatsionarnoye laminar-
     noye techeniye v kanale s nestatsionarnym podvodom tepla
     [Nonstationary Laminar Flow in Channel with Nonstationary
     Heat Supply], "Teploperedacha," (Russian translation,
     Trans. ASME, Ser. C), 1961, No. 4, pages 52-63.

15. Siegel, R., Transient Heat Transfer for Laminar Slug Flow
     in Ducts, J. of Appl. Mech., 1959, Vol. 26, Ser. E,
     No. 1, pages 140-142.

16. Siegel, R. and Perlmutter, M., Teploperedacha pri lami-
     narnom neustanovivshemsya techenii v kanale s proizvol'no
     izmenyayushchimsya teplovym potokom na stenke [Heat Trans-
     fer for Unsteady Laminar Flow in Channel with Arbitrarily
     Varying Heat Flux at Wall], "Teploperedacha" (Russian
     translation, Trans. ASME, Ser. C), 1963, No. 4, pages
     83-92.

17. Zayberg, S.L. and Myuller, V.K., Neustanovivshiysya
     laminarnyy potok v kanale pri sovmestnom deystvii svobodnoy
     i vynuzhdennoy konvektsii [Unsteady Laminar Flow in Chan-
     nel with Joint Action of Free and Forced Convection],
     "Teploperedacha" (Russian translation, Trans. ASME, Ser.
     C), 1962, No. 2, pages 53-61.

18. Tao, L.N., O nestatsionarnoy teplootdache pri sovmestnom
     deystvii svobodnoy i vynuzhennoy konvektsii [Nonstationary
     Heat Transfer Under Joint Action of Free and Forced Con-
     vection], "Prikladnaya mekhanika" (Russian translation,
     Trans. ASME, Ser. E), 1963, No. 2, pages 112-118.

19. Vilenskiy, V.D., Nekotoryye obshchiye zakonomernosti nes-
     tatsionarnogo teploobmena pri laminarnom techenii zhid-
     kosti v kanale [Some General Laws Governing Nonstationary
     Heat Exchange in Laminar Flow of Fluid in Channel], "Tep-
     lofizika vysokikh temperatur," [High-Temperature Thermo-
     physics], 1966, Vol. 4, No. 6, pages 838-845.